

Water quality risk assessment of carp biocontrol for Australian waterways



THE UNIVERSITY OF
**WESTERN
AUSTRALIA**



THE UNIVERSITY
of **ADELAIDE**

OCTOBER 19

**The University of Adelaide &
The University of Western Australia**

Edited by: *Justin D. Brookes & Matthew R. Hipsey*



NATIONAL CARP CONTROL PLAN
RESTORING NATIVE BIODIVERSITY

Citation: Justin D. Brookes and Matthew R. Hipsey (2019). Water quality risk assessment of carp biocontrol for Australian waterways. Unpublished Client Report for the Fisheries Research and Development Corporation. Environment Institute, University of Adelaide, Adelaide, South Australia.

Front cover photo: Carp mortality trial in Little Duck Lagoon, South Australia.
© University of Adelaide and The University of Western Australia

Disclaimer

This publication has been prepared with all efforts to ensure accuracy and may be of assistance to you but the authors do not guarantee that the publication is without flaw of any kind or is wholly appropriate for your particular purposes and therefore disclaims all liability for any error, loss or other consequence which may arise from you relying on any information in this publication.

Water quality risk assessment of carp biocontrol for Australian waterways

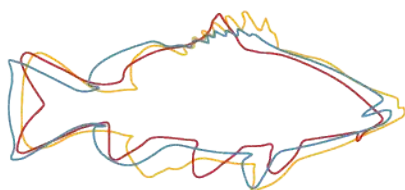
Edited by : *Justin D. Brookes and Matthew R. Hipsey*

Authors (alphabetical):

Justin D. Brookes¹, Brendan Busch², Phillip Cassey¹, Matthew R. Hipsey², Mark Laws¹, Sanjina Upadhyay¹, Richard Walsh¹

¹ School of Biological Science, The University of Adelaide, South Australia, 5005

² Aquatic Ecodynamics, UWA School of Agriculture & Environment, The University of Western Australia, Perth, Western Australia



University of Adelaide Environment Institute

Report for the Fisheries Research and Development Corporation

FINAL REPORT

Rev 2 – 18 Oct 2019.

Executive Summary

While proposed biological control agents to reduce carp numbers may have positive impacts to aquatic ecosystems, it is possible that wide-spread carp mortality may present considerable risks to the quality of water in Australian wetlands and waterways that need to be managed. Specifically, large-scale carp mortality in aquatic systems will lead to generation of:

- High oxygen demand
- A pulse of fish-derived nutrients

There is a concern that these impacts will generate water quality risks for humans and ecosystems associated with persistent low oxygen (hypoxia and anoxia), excessive levels of ammonia, and the build-up of cyanobacteria blooms, including the associated challenges of cyano-toxin release, and further deoxygenation during bloom collapse.

Empirical studies

To determine how mass carp mortality would affect nutrient and oxygen dynamics a suite of experiments were firstly undertaken at scales ranging from bucket to mesocosm to whole-wetland scale. Dead carp were added to buckets and the rate of nutrient flux and oxygen decrease were measured. The mean maximum Total Phosphorus (TP) leached from carp carcasses was 2106.7 (± 180.98) mg/kg. Maximum TP was then used to calculate maximum TP load and potential chlorophyll-*a* concentration from each biomass at each depth. At a biomass of 3144, 696 and 265 kg/ha, the estimated TP loading from carp carcasses is 6.67, 1.48 and 0.56 kg/ha, respectively. At the highest biomass (3144 kg/ha) and water depths of 1, 2 and 3 m, carp carcasses may result in TP concentrations of 0.667, 333 mg/L and 222 mg/L respectively. It was estimated that these TP concentrations have the potential to cause chlorophyll-*a* concentrations of upto 0.131, 0.066 and 0.045 mg/L, respectively. Recent biomass estimates from the NCCP program are an order of magnitude lower than the biomass used in this experiment, and consequently the TP and chlorophyll -a concentrations would also be proportionally lower.

The mean oxygen demand of carp carcasses in warm (18°C) and cold ponds (12°C) was 1.022 and 0.496 mg/kg/min, respectively. The rate of nutrient release and oxygen demand from decaying carp highlights the degree to which oxygen demand from decaying carp is dependent on carp biomass and water temperature; this information was incorporated into the biogeochemical model described below.

A whole of wetland study was then conducted and had dead carp added at a density of approximately 2400kg/ha. This high carp biomass caused notably poor water quality throughout the wetland. Limited accessibility during the carp addition meant they were not evenly distributed throughout the wetland, although strong winds and water movement aided distribution and provided a carp carcass density gradient across the wetland. Six sites were established along the length of the wetland. DO concentrations

were recorded every 10 minutes for the seven week experiment. Nitrogen and phosphorus concentrations reached very high levels commensurate with the extremely high carp biomass loading used in this experiment. The nutrient flux from carp carcasses fuelled algal growth and all sites showed steady increase of chlorophyll-*a* over the course of the experiment, with the exception of a small dip on Day 14. A maximum concentration of 1854 mg/L was recorded. The resultant nutrient concentrations were scaled to lower biomass densities to add in impact assessment.

Modelling assessments

This study developed a modelling platform able to account for the hydro-biogeochemical processes shaping water quality to ascertain the conditions under which poor water quality would develop, the time scale of the impacts, and the types of environments and conditions where risks would be most likely to manifest. The underlying question to answer has been whether the carp biomass densities reported for Australian waterbodies are high enough to lead to long-term water quality degradation.

The analysis combined a hydrodynamic model with a biogeochemical model and carp mortality model. The coupled model system was applied in high resolution to four “representative domains”, each with a diverse range of habitats and geomorphological complexity spanning geographically isolated through to well-flushed regions. A carp mortality model was developed by linking habitat-specific carp biomass estimates to a particle release and decay model. Each domain was subjected to a range of hydrological conditions, and alternate biomass loading rates were also simulated to account for uncertainty in biomass estimates and epidemiological dynamics. In addition, the chosen domains spanned different hydro-climatological conditions, and we therefore used the findings to generalise more broadly about water quality responses within the range of environments likely to be impacted.

In essence, for any given aquatic environment, there is a balance between biomass loading and hydrologic flushing; that is, the relationship between water quality response and biomass loading depends on the extent of water mixing and flow. For most sites within the domains tested, the anticipated biomass levels following release of the carp virus (based on the associated NCCP biomass and epidemiological project estimates), did not lead to excessive water column deoxygenation. There were some exceptions such as large, shallow areas with poor levels of hydrologic connectivity with the main flow (e.g., off channel wetlands and lake systems), and anticipated biomass levels exceeding ~300 kg/Ha. Where oxygen “sag” was noted, it was rarely persistent at these biomass levels due to re-aeration associated with wind and/or water flow. Anticipated biomass levels in the Moonie River study domain were the lowest of all tested and showed minimal impacts at these levels. Simulations run to test (hypothetical) higher biomass loading did however begin to display more pronounced levels of oxygen sag. For sites with anticipated biomass amounts of >200 kg/Ha, once the decaying biomass levels exceeded this by 2-5×, periods of low oxygen

were predicted to become more prominent, lasting for periods of weeks. In some cases, this did lead to more complete deoxygenation consistent with the wetland experiment reported above.

The levels of nutrient accumulation were also examined, due to the high levels of bioavailable N and P released by carp biomass on decay. Increases in levels of bioavailable nutrients (PO_4 , NO_3 and NH_4) were all predicted, though in most areas this was within the range of observed variability in these parameters for the anticipated biomass levels. As for oxygen, there were some exceptions to this with build-up of PO_4 in particular in shallow and poorly connected lakes and wetlands. In most sites, NH_4 build-up did not exceed thresholds associated with ammonia toxicity, except in some areas of the highest-biomass domain (Chowilla), where shallow waters and lake environments started to display very high levels that did not dissipate over the month-long simulation time scale. When biomasses that were by 2-5 \times higher than the anticipated amount were simulated, very high accumulations of PO_4 and NH_4 were reported in some sites that would be difficult to manage.

Cyanobacterial bloom formation relies on the coalescence of not just high nutrients but also warm temperatures and generally still (low flow) hydrodynamic conditions. Nonetheless, in line with the above findings, the cyanobacterial risk also followed trends described above for oxygen and nutrients.

The lowest risk to water quality is when the carp biomass is evenly distributed over the system when mortality occurs, but due to preferred habitats and aggregation behaviour it is likely biomass will be unevenly distributed. The spatial patterns of accumulation of carp biomass were also explored, with shallow and deeper water environments compared, and the results did highlight accumulation “hotspots” are likely to occur and that there will be areas of concentrated water quality risk in poorly connected embayment’s and “dead-end” flow paths. This analysis may still underestimate the extent of the biomass focusing into hotspots prior to decay, and this should be considered. The higher, hypothetical, biomass simulations can be used as a guide for what may be expected at these sites of high biomass focusing.

At the biomass levels anticipated based on the NCCP biomass and epidemiological projects (~50-1000 kg/Ha and ~60% knockdown rate, respectively), and under the hydro-climatological conditions tested, the likelihood of water quality impacts were varied, but generally modest, at the broad-scale. Areas of biomass >300 kg/Ha are predicted to show signs of water quality decline, particularly in areas with poor hydrologic connectivity, though they appear to be relatively short lived when considered in the context of existing water quality conditions (e.g., periods of blackwater or cyanobacterial blooms) experienced already in many Australian waterways. This suggests that river hydrologic conditions should be considered in any release strategy, not just from the point of view of virus epidemiology, but also as a lever to mitigate the emergence of water quality risks. Hydrologic conditions suitable for virus transmission are potentially in tension with hydrologic conditions required to mitigate water quality impacts, and it is recommended high flows following release should be considered to enhance river flushing, dilute biomass, and prevent poorly

connected areas becoming hotspots of biomass accumulation. Whilst oxygen conditions can recover over reasonable time-frames due to reaeration, the long-term accumulation and persistence of nutrients will lead to a longer-term management challenge, and therefore enhancing downstream (and ultimately oceanic) nutrient export following release is recommended. In tandem, clean-up strategies focused on areas of high accumulation are also recommended to reduce and remove carp carcasses before extensive decay can release nutrients to the system.

Acknowledgements

The authors gratefully acknowledge the staff from DEWNR in South Australia who helped with wetland trial and Will Zacharin and John Virtue from Biosecurity SA who supported early work on water quality risk from carp mortality. The authors also thank FRDC staff Matt Barwick, Toby Piddock, Jennifer Marshall, Pamela Milnes, Jamie Allnut and Peter O'Brien for their assistance in framing and undertaking the research and the Scientific Advisory Group for the National Carp Control Program. Jarod Lyon and Ivor Stuart provided biomass estimate data which formed the basis of our calculations. We appreciate modelling support by Casper Boon and Peisheng Huang from UWA for managing the extensive simulations required.

Table of Contents

EXECUTIVE SUMMARY	5
ACKNOWLEDGEMENTS	9
TABLE OF CONTENTS	11
INTRODUCTION	15
METHODS	17
POND EXPERIMENTS	17
PHOSPHORUS AND CHLOROPHYLL-A CONCENTRATIONS.....	17
MESOCOSM EXPERIMENT	18
WETLAND EXPERIMENT	19
RESULTS	20
POND EXPERIMENTS – THE EFFECT OF TEMPERATURE	20
PHOSPHORUS AND CHLOROPHYLL-A CONCENTRATIONS.....	21
MESOCOSM EXPERIMENTS.....	23
WETLAND EXPERIMENT	24
<i>Dissolved Oxygen</i>	24
<i>Nutrients</i>	25
DISCUSSION	28
CONCLUSION	31
CHAPTER 2: CRITICAL FLOW ESTIMATION TO DETERMINE CYANOBACTERIAL RISK FOLLOWING MASS MORTALITY OF CARP FOLLOWING RELEASE OF PROPOSED CYHV-3 CARP BIOCONTROL	33
INTRODUCTION	35
METHOD	37
MIXING CRITERION MODEL	37
FLOW ANALYSIS	38
RESULTS	39
MIXING CRITERION MODEL	39
FLOW ANALYSIS – ANNUAL	42
FLOW ANALYSIS - SUMMER.....	46
DISCUSSION	52
<i>Management implications</i>	53

CHAPTER 3: A MODEL ASSESSMENT OF WATER QUALITY RISK OF CARP BIOCONTROL FOR AUSTRALIAN WATERWAYS.....	55
INTRODUCTION	57
BACKGROUND	57
AIMS & SCOPE	58
CARP MODEL BASIS AND RATIONALE	60
CONCEPTUAL MODEL	60
APPROACH TO IMPLEMENTATION	62
STUDY SITES	63
SITE SELECTION.....	63
MODEL SETUP AND VALIDATION	68
GENERAL APPROACH AND SIMULATION FRAMEWORK	68
RIVER AND LAKE ECOHYDROLOGICAL MODELS	69
<i>Model platform</i>	69
<i>Water quality model validation summary</i>	69
CARP MORTALITY MODEL	78
<i>Homogenised carp (HC)</i>	78
<i>Decaying carp particles (DCP)</i>	80
MODEL SETUP AND SCENARIO MATRIX APPROACH	85
WATER QUALITY RISK ASSESSMENT	87
ASSESSMENT METRICS	87
<i>Oxygen</i>	87
<i>Nutrients and cyanobacteria</i>	87
HYPOXIA AND ANOXIA ASSESSMENT	89
NUTRIENT RELEASE AND ACCUMULATION.....	105
CYANOBACTERIA ASSESSMENT	122
DISCUSSION	127
REFERENCES	131
APPENDIX A: MODEL SETUP INFORMATION	135
APPENDIX B : DOMAIN SUB-REGIONS.....	138
APPENDIX C : MODEL SIMULATION OUTPUT SUMMARY	142

Chapter 1: **Oxygen dynamics and nutrient flux during carp decay**

Richard Walsh, Sanjina Upadhyay, Matthew R. Hipsey, Mark Laws, Phillip Cassey, Justin D. Brookes

Introduction

The common carp (*Cyprinus carpio*) is widely considered the worst aquatic pest throughout the Murray-Darling Basin (MDB). Altered water regimes, reproductive advantages and high tolerance to poor water quality have facilitated the invasion by and establishment of large common carp (hereafter 'carp') populations (Harris and Gehrke 1997; Koehn 2004). Large carp populations are associated with poor water quality, habitat destruction, and detrimental effects to macrophyte, invertebrate and zooplankton communities (King *et al.* 1997; Koehn *et al.* 2000; Vilizzi *et al.* 2014). Furthermore, increasing carp populations have coincided with reductions in native fish populations, although alterations to water regimes are likely to be larger contributors to this reduction (Clunie and Koehn 1997; Reid *et al.* 1997). Carp are now the dominant fish species in many of Australia's freshwater ecosystems and have extensive distribution throughout the MDB. Without intervention, carp populations are expected to grow and continue expanding into the upper reaches of the MDB, the remaining south-east coastal river systems, and throughout the Tasmanian river systems (Koehn 2004).

The cyprinid herpesvirus 3 (CyHV-3) is currently being considered as a carp biocontrol agent for implementation in Australia. CyHV-3 causes rapid and significant morbidity and mortality in carp and has endangered carp populations in other countries (Hara *et al.* 2006; Gotesman *et al.* 2013). While CyHV-3 may reduce carp populations and facilitate positive ecological outcomes in the long term, little knowledge of the short-term environmental impacts exists.

Of particular concern is the effect of decomposing carp carcasses on dissolved oxygen (DO) concentrations in the water column and the potential for hypoxic or anoxic conditions to occur. High levels of microbial activity associated with decomposition of organic matter are a key driver of hypoxic or anoxic conditions in the River Murray (King *et al.* 2012). Water temperature plays an important role in this process due to its key role in the development, growth and respiration of microbial communities and its influence on the metabolic demand of aquatic organisms (Howitt *et al.* 2007). Crucially, the effect of oxygen depletion on aquatic organisms is exacerbated at high temperatures when both the metabolic demand for oxygen is increased and the solubility of oxygen in water is reduced (Lewis 1970). Table outlines the estimated DO thresholds of four Australian lowland river predatory fish species (Small *et al.* 2014). While vegetation-derived anoxia has been well studied (e.g. Gehrke *et al.* 1993; McMaster and Bond 2008), and the effect of temperature on this process has been investigated (Whitworth *et al.* 2014), the deoxygenation potential of carp carcasses and the effect of temperature on this process are both largely unquantified for Australian freshwater systems.

Table 1: Generalised Linear Mixed Model (GLMM) estimates of lethal dissolved oxygen (DO) concentrations for four Australian lowland river predatory fish (Small et al. 2014), also indicating the standard error (SE).

Fish species	DO threshold estimate (mg/L)	SE
Murray cod <i>Maccullochella peelii</i>	4.80	0.74
Golden perch <i>Macquaria ambigua</i>	1.72	0.63
Silver perch <i>Bidyanus bidyanus</i>	2.65	0.60
Eel-tailed catfish <i>Tandanus tandanus</i>	1.85	0.53

Another key concern is the magnitude of carp-derived nutrient enrichment, the fate of these nutrients, and the potential for the occurrence of harmful algal blooms. Harmful algal blooms impact directly on native fish and other aquatic organisms, with a suite of side-effects including water toxicity and food-web alterations (Paerl et al. 2001). Cyanobacteria genera such as *Anabaena*, *Aphanizomenon* and *Microcystis* are highly productive in warm, turbid waters and frequently form harmful algal blooms throughout the MDB. The cyanotoxins produced by cyanobacteria are hazardous to both aquatic and terrestrial biota, including humans and livestock (Chorus and Bartram 1999). Symptoms include gastrointestinal disorders, fever and irritations of the skin, ears, eyes, throat and respiratory tract, liver damage, neurotoxicity and tumour promotion (World Health Organization 2011). Further, cyanobacteria are a relatively inadequate food source for zooplankton, being nutritionally poor and physically problematic for most grazers, and therefore are a poor pathway for carbon flow to aquatic foodwebs (Lampert 1987). Nutrient enrichment has been identified as a key driver of freshwater algal blooms, and although nutrient enrichment associated with fish mortality has been explored (e.g. Stevenson and Childers 2004; Schoenebeck et al. 2012; Killberg-Thoreson et al. 2014), no such study exists for carp in Australian freshwater systems.

To address this dearth of information, this study will determine the effect of carp carcass decomposition on DO concentrations and nutrient loading with a series of field and laboratory experiments, culminating in a wetland-scale experiment in the lower River Murray, South Australia.

Methods

Pond experiments

Cold water ponds

Six large plastic ponds were filled with 712.65 litres of tap water and left for five days to facilitate diffusion of chlorine from the water. Following this, a 1% inoculum (7.13 litres) of river water taken from Torrens Lake, South Australia was added to make a total volume of 720 litres. Three ponds were left as controls, while three ponds received a treatment of one carp carcass each. Carp were obtained from fish nets in Lake Alexandrina, SA. Carp carcass weights for replicates 1, 2 and 3 were 3.68, 3.89 and 2.56 kg respectively, giving an average of 3.38 kg. Ponds were left outside at ambient temperature of approximately 12°C. DO concentrations, temperature and pH were measured every 5 minutes with D-Opto Optical DO sensors.

Warm water ponds

Five large plastic ponds were filled with 712.65 litres of tap water and left for five days to facilitate diffusion of chlorine from the water. Following this, a 1% inoculum (7.13 litres) of river water taken from Torrens Lake, South Australia was added to make a total volume of 720 litres. Two ponds were left as controls, while three ponds received a treatment of one carp carcass each. Carp were obtained from a Williams' Cage at Lock 1, Blanchetown, South Australia. Carp carcass weights for replicates 1, 2 and 3 were 2.89, 2.07 and 3.29 kg respectively, giving an average of 2.75 kg. Ponds were left in a temperature controlled room set at 20°C, although actual water temperature was 18°C. DO concentrations, temperature and pH were measured every 5 minutes with D-Opto Optical DO sensors.

Phosphorus and chlorophyll-*a* concentrations

Phosphorus (P) flux into surrounding water was measured in a controlled laboratory experiment, conducted in buckets containing 15 L of RO water. Filtered reactive phosphorus (FRP) and total phosphorus (TP) concentrations were measured intermittently over a 45-day period. A carp carcass treatment and control treatment were each replicated five times. For each carp carcass replicate, a single whole carp was added to the bucket. Control buckets received no fish. The carp used were electro-fished from the River Torrens on 9th June 2016. Buckets were placed in a controlled temperature room, where an ambient temperature of 20°C was maintained throughout the experiment. Sampling occurred on days 0, 1, 2, 4, 7, 14, 23, 30, 37 and 45. Prior to collecting samples, the water in each bucket was homogenised by mixing. Samples were collected using a 50 mL syringe and FRP samples were obtained using 0.45 µm syringe filters. Samples were immediately frozen in 50 mL cryogenic vials. The FRP and TP concentration of multiple samples was determined on days 30 and 45. A Biochrom Libra S22 UV/Vis Spectrophotometer was used to determine FRP and TP concentrations in mg/L, following the ascorbic acid colorimetric method outlined in *Water Analysis: Some Revised Methods for Limnologists* (Mackereth *et al.* 1978). For both occasions when P

was determined, standards of known P concentration were prepared to develop a model for P concentration and absorbance.

To estimate the maximum chlorophyll-*a* concentration that could result from the P release from fish, the relationship between maximum TP and chlorophyll-*a* for Myponga Reservoir was used (Linden *et al.* 2004):

- $\text{Chl } a \text{ (}\mu\text{g L)} = 195.57 * \text{TP (mg L)} + 1.71$

Biomass estimates used were determined following a literature review of carp biomass estimates in Australia. The following estimates were all derived from a calibration experiment on the Bogan River where catch efficiency was 21% (Gehrke *et al.* 1995). The same catch efficiency was assumed at the following sites and used to calculate total biomass:

- 'Low' - 265 kg/ha in MDB regulated lowland (altitude <300 m) (Driver *et al.* 2005)
- 'Moderate' - 696 kg/ha in MDB reach (altitude 300-700 m) (Driver *et al.* 2005)
- 'High' - 3144 kg/ha in Lachlan River reach (altitude 460 m) (Driver *et al.* 1997)

Mesocosm experiment

Nine 3.9 m² mesocosms were constructed in a River Murray wetland near Swan Reach, South Australia. The mesocosms were left to settle for seven days before the commencement of the experiment. At this point, three mesocosms were left with no fish (control), three mesocosms received a single dead whole carp weighing approximately 500g (low biomass), and three mesocosms received a single dead whole carp weighing approximately 1000g (high biomass). Carp carcasses were tied to a steel pole, which was used to keep them submerged. Low biomass treatment fish weights had a mean of 495 g (SD = 34). High biomass fish treatments had a mean of 1084 g (SD = 119). DO concentrations were measured for 14 days every 10 minutes using a D-Opto Oxygen Sensor that was installed in each mesocosm 10cm above the sediment surface.

Wetland experiment

Little Duck Lagoon (LDL) is a 2.5 ha, 10 ML managed wetland approximately 4 km south of the township of Berri, South Australia. It is part of the *Causeway Wetland Complex* that forms the larger Gurra Gurra Wetland Complex. Little Duck Lagoon was selected as a suitable site for the carp wetland experiment based on its size, volume and distance from residential/recreational areas. Importantly, the wetland was due for a managed drawdown phase via closing of the sluice gate between Little Duck Lagoon and Gurra Gurra Creek, which was organised to coincide with the carp wetland experiment. Closing the sluice gate and allowing the wetland to completely dry out would limit post-experiment environmental impacts such as poor quality water being flushed into the rest of the system.

Six tonnes of dead carp were procured from the Williams' Cage at Lock 1, South Australia and frozen for storage before being added to the south eastern end of Little Duck Lagoon with a front end loader. Carp biomass was 2400 kg/ha. Limited accessibility meant that carp were not evenly distributed throughout the wetland, although strong winds and water movement aided distribution and provided a carp carcass density gradient across the wetland. Six sites were established along the length of the wetland, starting in the south-eastern end and moving north-west. DO concentrations were recorded every 10 minutes at Sites 1-5 using D-Opto Loggers (ZebraTech) for the duration of the experiment. DO data was downloaded periodically and D-Opto Loggers were recalibrated mid-experiment. On Days 0, 2, 4, 7, 14, 21, 28 and 42 water samples were taken from each of the 6 sample sites. Water samples were iced for transport back to the laboratory, where they were processed and/or frozen, as appropriate. Samples for total nutrients (phosphorus, nitrogen), dissolved nutrients (ammonia, phosphate, nitrate, nitrite) and dissolved organic carbon were sent to Environmental Analysis Laboratory (EAL) for analysis. Biological oxygen demand (BOD) samples were processed using the standard 5 day BOD method outlined in *Standard Methods for the Examination of Water and Wastewater* (Water Environmental Federation and American Public Health Association 2005). Chlorophyll-*a* was analysed in-house at the University of Adelaide using standard methods outlined in *Standard Methods for the Examination of Water and Wastewater* (Water Environmental Federation and American Public Health Association 2005). Lipids were analysed using standard methods outlined in Bligh and Dyer (1959).

Results

Pond experiments – the effect of temperature

Comparison between warm (18°C) and cold (12°C) ponds indicates that rate of oxygen demand is positively correlated with increased temperature. Carp carcasses in warm ponds (W1 – W3) displayed a higher BOD than those in cold ponds (C1 – C3), and anoxia occurred twice as quickly in warm ponds as cold ponds (Figure 1). The mean oxygen demand of carp carcasses in warm and cold ponds was 1.022 and 0.496 mg/kg/min, respectively (Table 2).

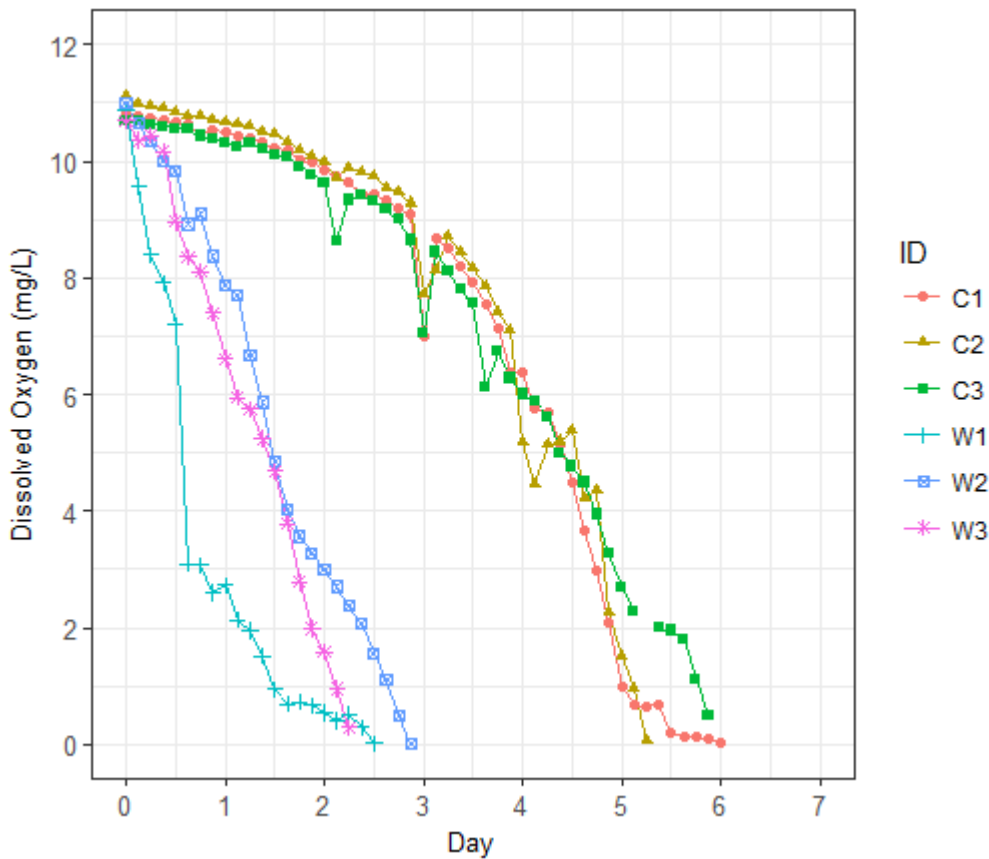


Figure 1: Dissolved oxygen concentrations over time for warm pond replicates (W1 - W3) and cold pond replicates (C1 - C3).

Table 2: Mean BOD for warm ponds and cold ponds with standard deviation.

Temperature	O2 Demand (mg/kg/min)	SD
Cold (12°C)	0.496	0.029
Warm (18°C)	1.022	0.239

Phosphorus and chlorophyll-*a* concentrations

Total phosphorus (TP) and filtered reactive phosphorus (FRP) liberation from carp carcasses increased over time at 20°C (Figure 2). TP flux commenced immediately and continued to increase until day 14. After day 14 TP concentrations were relatively stable, which indicates complete breakdown of carp tissue and liberation of the nutrients into the water column. TP was comprised entirely of FRP, which is the most bioavailable fraction.

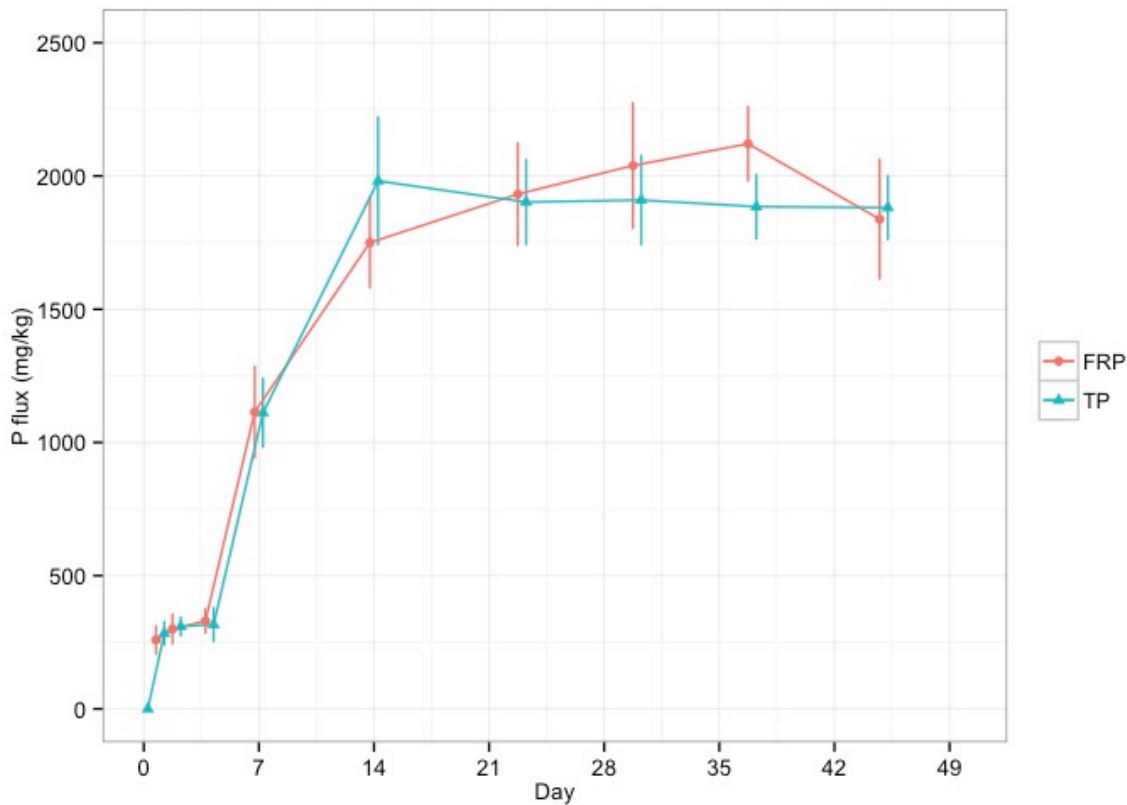


Figure 2: Filtered reactive phosphorus (FRP) and total phosphorus (TP) flux from carp carcasses in mg/kg car. Error bars represent standard deviation.

The mean maximum TP leached from carp carcasses was 2106.7 (± 180.98) mg/kg on day 37. Maximum TP was then used to calculate maximum TP load and potential chlorophyll-*a* concentrations from each biomass at each depth. At a biomass of 3144, 696 and 265 kg/ha, the estimated TP loading from carp carcasses is 6.67, 1.48 and 0.56 kg/ha, respectively (Table 3). At the highest biomass (3144 kg/ha) and water depths of 1, 2 and 3 m, carp carcasses may result in TP concentrations of 0.667, 333 mg/L and 222 mg/L respectively. These TP concentrations have the potential to cause chlorophyll-*a* concentrations of 0.131, 0.066 and 0.045 mg/L, respectively.

Table 3: Maximum TP loading and chlorophyll-a concentrations for three different biomasses (265, 696 and 3144 kg/ha) and assumed depths (1, 2, 3 m).

Max TP = 2106.7 mg/kg					
Biomass (kg/ha)	TP Load (kg/ha)	TP Load (mg/m ²)	Assumed Depth (m)	TP Load (mg/L)	Chl a (mg/L)
265	0.56	56.21	1	0.056	0.013
			2	0.028	0.007
			3	0.019	0.005
696	1.48	147.63	1	0.148	0.030
			2	0.074	0.016
			3	0.049	0.011
3144	6.67	666.87	1	0.667	0.131
			2	0.333	0.066
			3	0.222	0.045

This study reported TP flux of 6.67 kg/ha from carp biomass of 3144 kg/ha. While N was not measured in this study, it may be estimated using the findings of a previous study. Schoenebeck *et al.* (2012) reported P and N flux of 0.5 kg/ha and 4.3 kg/ha, respectively, from a carp biomass of 177 kg/ha. Extrapolating these findings out to 3144 kg/ha gives an estimated P and N loadings of 8.9 kg/ha and 76.7 kg/ha, respectively. Using the proportional difference between the P concentrations reported in this experiment (6.67 kg/ha) and the previous study (8.9 kg/ha) allows us to estimate an N flux of 57.5 kg/ha.

Mesocosm experiments

Figure 3 shows low and high biomass treatments compared to control treatments. Considerable algal growth had occurred in the mesocosms before the carp were added and consequently there were large diel fluctuations of the oxygen concentrations due to phytoplankton photosynthesis and respiration. Both biomass treatments showed lower minimum overnight DO concentrations than controls. Minimum overnight DO concentrations for control, low biomass and high biomass treatments were 0.308, 0.009 and 0.010 mg/L, respectively. High biomass treatments experienced overnight anoxia (DO <0.1 mg/L) more frequently than low biomass treatments. High biomass treatments went anoxic on eleven of the fourteen nights (nights 2, 3, 5, 6, 7, 8, 9, 10, 11, 12 and 13). Low biomass treatments went anoxic on six of the fourteen nights (nights 6, 7, 8, 9, 12 and 13). Control treatments did not reach anoxia, although hypoxic conditions were recorded for nights 12, 13 and 14. An increase in algal biomass was also observed across all treatments and replicates.

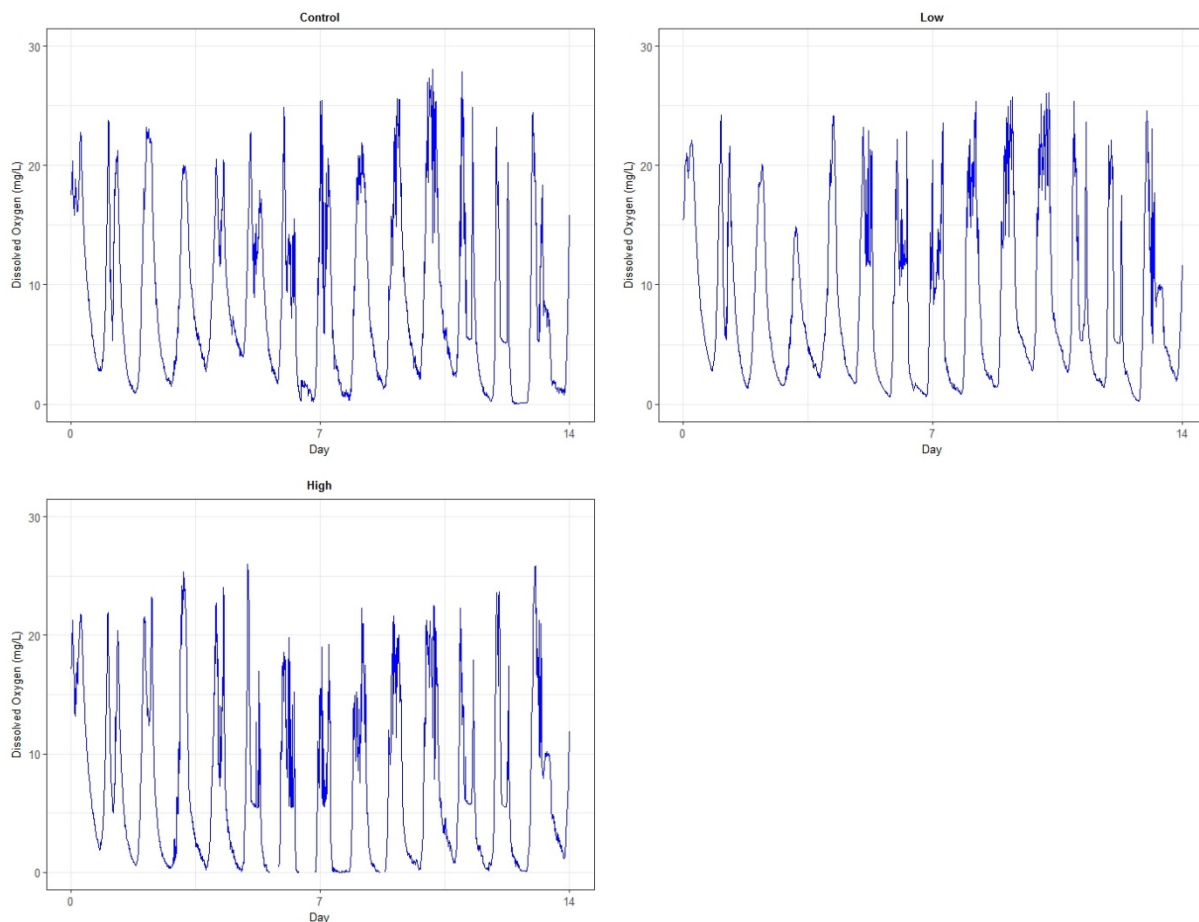


Figure 3: Dissolved oxygen concentrations for control, low and high biomass treatments for the duration of the mesocosm experiment.

Wetland experiment

Dissolved Oxygen

Similar to what was observed in the mesocosm experiments, overnight anoxia was ubiquitous across all sites (Figure 4). The instances and severity of anoxia decreased with distance from where the dead carp were initially added. During the first two weeks, Site 1 experienced severe and protracted anoxic conditions.

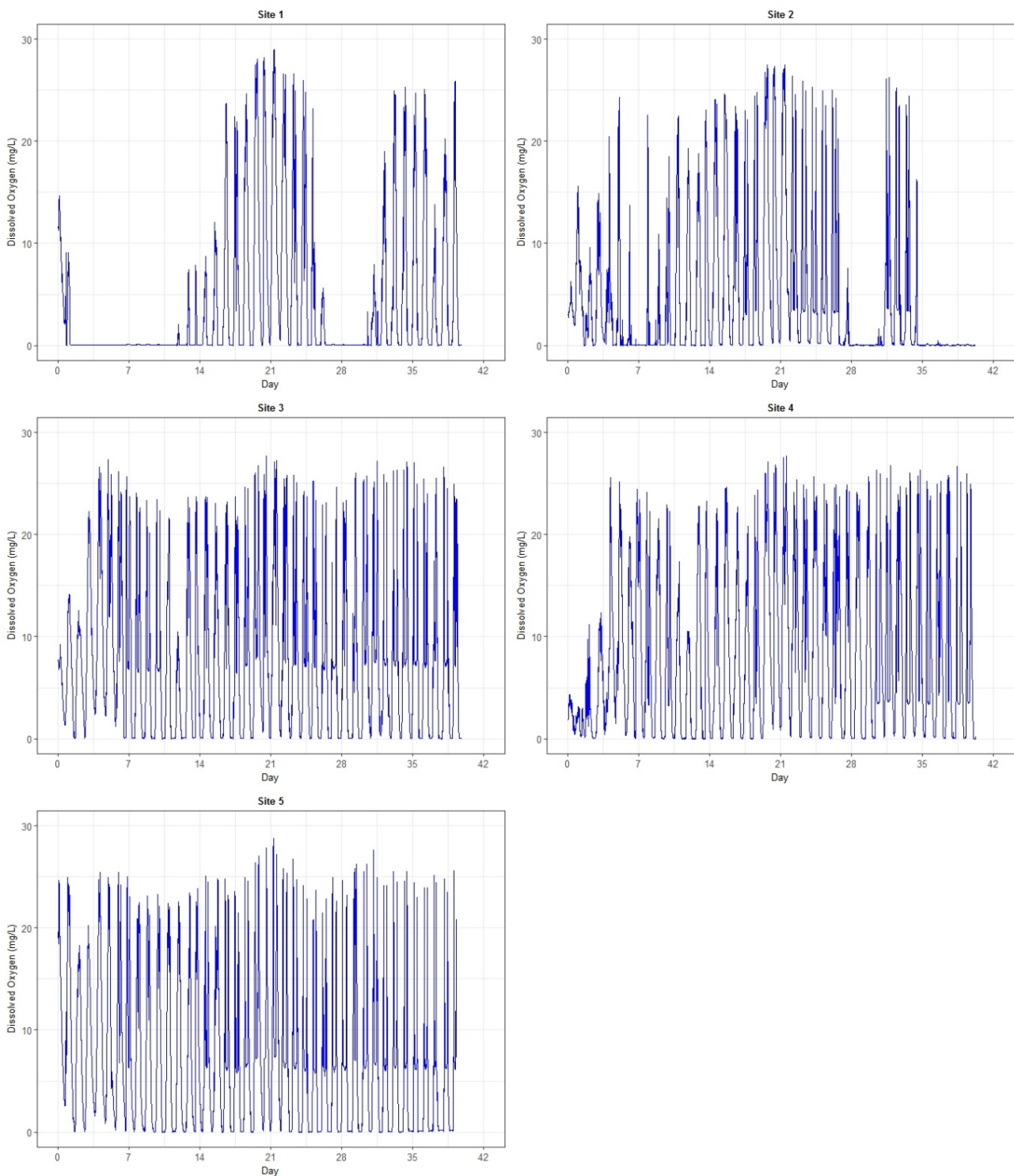


Figure 4: Dissolved oxygen concentrations for Sites 1 - 5 for the duration of the wetland experiment.

Nutrients

Nutrient concentrations in the wetland experiment increased rapidly as carp decayed (Figure 5). The maximum concentrations detected in the wetland experiment all exceed the relevant freshwater trigger values outlined the Australia and New Zealand Guidelines for Fresh and Marine Water Quality (Australian and New Zealand Environment and Conservation Council and Agriculture and Resource Management Council of Australia and New Zealand 2000).

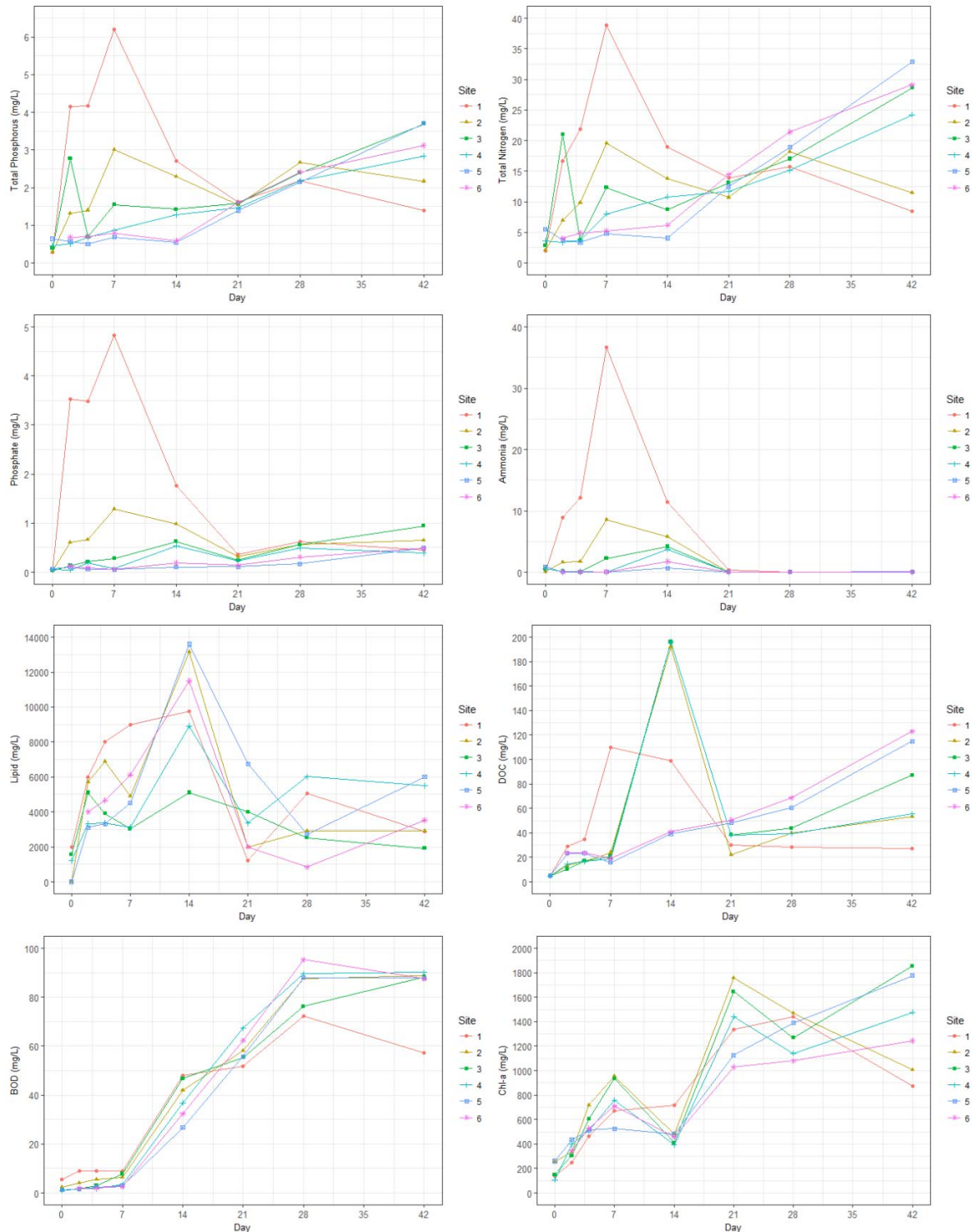


Figure 5: Nutrient concentrations for the duration of the wetland experiment. TP = total phosphorus, TN = total nitrogen, DOC = dissolved organic carbon, BOD = biological oxygen demand, Chl-a = chlorophyll-a. Nitrate and nitrite concentrations were not plotted as many concentrations were below detectable levels.

Table 4: Maximum concentrations detected during wetland experiment and default trigger values for south central Australia for slightly disturbed systems. DOC = dissolved organic carbon, BOD = biological oxygen demand, Chl-a = chlorophyll-a. Taken from Australia and New Zealand Guidelines for Fresh and Marine Water Quality (Australian and New Zealand Environment and Conservation Council and Agriculture and Resource Management Council of Australia and New Zealand 2000). All default trigger values are for lowland river systems of south central Australia unless otherwise specified.

	Max concentration detected (mg/L)	Default trigger values (mg/L)
Total Phosphorus	6.2	0.1
Total Nitrogen	38.9	1
Phosphate	4.8	0.04
Ammonia	36.7	0.9 a
Nitrate	0.07	0.1
Nitrite	0.03	0.1
DOC	196.0	-
BOD	95.3	15 b
Chl-a	1854	0.005 c
Lipid	13600	-

a: General trigger value for freshwater (95% species protected) at pH 8
b: Aquaculture recommended guidelines
c: South eastern Australia lowland river guidelines

Table 5: Mean concentrations (with standard deviation) detected during wetland experiment at actual biomass (2400 kg/ha) and calculated concentrations at lower biomasses (1000, 500 and 150 kg/ha). DOC = dissolved organic carbon, BOD = biological oxygen demand, Chl-a = chlorophyll-a.

Nutrient (mg/L)	Biomass (kg/ha)			
	2400	1000	500	150
Total Phosphorus	2.82 (±0.90)	1.18 (±0.38)	0.59 (±0.19)	0.18 (±0.06)
Total Nitrogen	22.46 (±10.11)	9.36 (±4.21)	4.68 (±2.21)	1.40 (±0.63)
Phosphate	1.10 (±1.89)	0.46 (±0.79)	0.23 (±0.39)	0.07 (±0.12)
Ammonia	7.92 (±14.48)	3.30 (±6.03)	1.65 (±3.02)	0.50 (±0.90)
Nitrate	0.030 (±0.032)	0.013 (±0.013)	0.006 (±0.007)	0.002 (±0.002)
Nitrite	0.017 (±0.017)	0.007 (±0.007)	0.004 (±0.004)	0.001 (±0.001)
DOC	127.15 (±77.02)	52.98 (±32.09)	26.49 (±16.05)	7.95 (±4.81)
BOD	84.80 (±8.70)	35.33 (±3.63)	17.67 (±1.81)	5.30 (±0.54)
Chl-a	1389.23 (±285.03)	578.84 (±118.76)	289.42 (±59.38)	86.83 (±17.81)
Lipid	10336.67 (±3154.66)	4306.94 (±1314.44)	2153.47 (±657.22)	646.04 (±197.17)

Total phosphorus, total nitrogen, ammonia and phosphate

A rapid spike in total and dissolved nutrients was recorded within the first two weeks for Sites 1, 2 and 3. The strength of this spike was generally proportionate to the distance from the dump site, with Site 1 reporting the highest TP, TN, phosphate and ammonia concentrations followed by Site 2 and 3 in turn. Maximum reported concentrations for TP, TN, phosphate and ammonia were 6.2, 38.9, 4.8 and 36.7 mg/L, respectively. Following this initial spike TP and TN concentrations fell temporarily, before steadily increasing towards the end of the experiment. Ammonia and phosphate concentrations dropped considerably following the initial spike and remained low throughout the remainder of the experiment.

Presumably this was due to phytoplankton uptake and oxidation of ammonia to nitrate. Sites 4, 5 and 6 showed steady increase over the course of the experiment as water from sites with higher carp density was exchanged across the wetland.

DOC, Lipid, BOD and Chl-a

Sites 1, 2, 3 and 4 showed a peak in DOC concentrations within the first two weeks, with maximum concentration of 196 mg/L recorded for Site 3 and 4 on Day 14. DOC concentrations fell towards Day 21 before steadily increasing throughout the remainder of the experiment. Sites 5 and 6 showed steady increase over the course of the experiment. The release of carbon from carp and the decaying carcasses all contribute to increase biological oxygen demand. BOD for all sites increased over the course of the experiment, with Site 6 recording the highest concentration of 95.3 mg/L on Day 28. Lipid concentrations peaked on Day 14, with a maximum concentration of 13600 mg/L recorded at Site 5. The nutrient flux from carp carcasses fuelled algal growth and all sites showed steady increase of Chl-*a* over the course of the experiment, with the exception of a small dip on Day 14. A maximum concentration of 1854 mg/L was recorded at Site 3 on Day 42.

Scaling to lower biomass

Table 5 shows mean concentrations (with standard deviation) detected during wetland experiment at actual biomass (2400 kg/ha) and calculated concentrations at lower biomasses (1000, 500 and 150 kg/ha). Even at the lowest biomass estimates of 150 kg/ha, Chl-*a*, TP, TN, phosphate and ammonia concentrations exceeded the default trigger values set out for lowland river systems of south central Australia in the Australian and New Zealand guidelines for fresh and marine water quality (Australian and New Zealand Environment and Conservation Council and Agriculture and Resource Management Council of Australia and New Zealand 2000). BOD fell below its default trigger value at 150 kg/ha, although biomass of 500 kg/ha saw the default trigger value exceeded. Nitrate and nitrite trigger values were not exceeded at any biomass.

Discussion

This series of experiments has highlighted several important factors that should be considered prior to implementing the CyHV-3 as a biocontrol agent in Australia. These include the potential for the decomposition of carp carcass to result in deoxygenation of the water column, and increased algal productivity in response to carp-derived nutrient loading.

The pond experiments show that temperature is a significant regulator of the rate of onset of hypoxia and anoxia following carp mortality. This is due in part to its influence on the development, growth and respiration of microbial communities (Stevenson and Childers 2004). Ponds that were 18°C went anoxic 66% faster than the ponds at 12°C. This is consistent with existing literature, which states that a 10°C increase in temperature results in a two-fold increase in oxygen demand (Howitt *et al.* 2007). Thus, in areas where high water temperatures and high carp biomass coincide, such as wetland systems, there is increased potential for the development of hypoxic and anoxic conditions. This is particularly true in areas of low-flow and/or where woody debris has collected, where post-mortality aggregation of carp carcasses may lead to a biomass accumulation significantly higher than current estimates (Monaghan and Milner 2008). Such conditions were simulated in the wetland experiment, where a carp biomass of 2400 kg/ha was, for reasons of accessibility, added from a single dump site. While effort was made to distribute the carp across the wetland, the prevailing winds meant carp were not evenly distributed which resulted in a carp carcass density gradient across the sample sites. At the highest carp carcass density, anoxic conditions were maintained for a period of 13 days. Additionally, overnight anoxic conditions were common throughout the wetland experiment. Overnight DO concentrations regularly fell below 0.1 mg/L, even at lower densities. This pattern of overnight anoxia was also observed in the mesocosm experiments, which implicated carp biomass in the duration and severity of anoxia.

Dissolved oxygen concentrations below 4 mg/L can cause stress in Australian native fish and other aquatic organisms, and DO concentrations below 2 mg/L can cause mortality (Gehrke 1988). Recent findings suggest these general tolerance limits may be too low for some sensitive species (Gilmore *et al.* 2015). While most fish are adapted to cope with fluctuations in oxygen concentrations, even short periods below critical oxygen thresholds can lead to mortality in some native fish and exotic species. For example, populations of Rainbow trout (*Oncorhynchus mykiss*) and Australian smelt (*Retropinna retropinna*) have been found to suffer 50% mortality after being exposed to 1 mg/L for less than 1 hour (Dean and Richardson 1999). Murray crayfish (*Euastacus armatus*) are particularly susceptible to hypoxic conditions due to their low mobility. Murray crayfish emergence occurs at approximately 2 mg/L and prolonged periods of hypoxia can drastically reduce their abundance due to increased predation and desiccation (McKinnon 1995; King *et al.* 2012). Population recovery after mass mortality events is slow due to their slow growing, late maturing and poorly dispersing life histories, leaving them vulnerable to local extinction (McCarthy *et al.* 2014). Additionally, high mortality of some freshwater shrimp (*Macrobrachium spp.*) and

yabbies (*Cherax spp.*) has been observed at DO concentrations of 2 mg/L (King *et al.* 2012). As an important link in the River Murray food-web, reductions in the populations of these species will affect higher trophic levels, including direct and indirect impacts on native fish and invertebrate populations (Usio and Townsend 2004). The wetland experiment has confirmed that the microbial decomposition of carp carcasses following a mass mortality event has the potential to reduce DO concentrations with a severity and duration that precludes the survival of local native aquatic biota and has the potential to disrupt food web stability.

The bucket and wetland experiments suggest the majority of nutrients are liberated from carp carcasses within the first two weeks. This pattern was also observed in the wetland experiment, where nutrient concentrations showed an initial spike over the first two weeks as carp-derived nutrients entered the water column. This spike was followed by a more gradual increase as a result of evaporative concentration and sediment leaching under hypoxic and anoxic conditions (Oliver and Ganf 2000). Chl-*a* also increased over the course of the experiment, and we observed extensive and increasingly conspicuous algal blooms across Little Duck Lagoon.

The relationship between excess nutrients in the water column and an increase in algal biomass is well documented (e.g. Correll 1998). Phosphorus is usually the limiting nutrient in freshwater systems, and algal blooms can occur at phosphorus concentrations as small as 0.02-0.05 mg/L (Wasson *et al.* 1996). The bucket experiment reported phosphorus concentrations ranging from 0.02 mg/L for low biomass/deep water conditions to 0.67 mg/L for high biomass/shallow water conditions, while the wetland experiment reported maximum phosphorus and nitrogen concentrations of 6.2 and 38.9 mg/L, respectively. These concentrations are well in excess of the default trigger values for lowland rivers of south central Australia, which are of 0.1 mg/L and 1 mg/L for phosphorus and nitrogen, respectively (Australian and New Zealand Environment and Conservation Council and Agriculture and Resource Management Council of Australia and New Zealand 2000).

Nutrients derived from carp carcasses combined with those leached from the sediment under anoxic conditions resulted in nutrient concentrations well above those necessary to cause algal blooms. Harmful algal blooms, such as cyanobacteria, can have detrimental effects on the health of both aquatic and terrestrial organisms, and the health and integrity of the ecosystem in general (Landsberg 2002). Cyanobacteria genera such *Anabaena*, *Aphanizomenon* and *Microcystis* are highly productive in warm, turbid waters (Paerl 2008). Such conditions as those common throughout the Murray-Darling Basin. Additionally, algal blooms that are not incorporated into the food web can form a large proportion of sedimented organic matter upon die-off, the decomposition of which can increase the potential for oxygen depletion (Paerl 2008). Such an event may have caused the extended period of anoxia recorded at Sites 1 and 2 around day 28. Further, sedimentation of nutrients in algal biomass may have a strong positive feedback on future events, particularly in systems with long residence time, such as wetlands, where this

legacy nutrient may stay in sediment for some time. Hence, when considering nutrient release from carp carcasses, it is not just the ambient hydrodynamics at the time of implementation of the CyHV-3 biocontrol that need to be considered, but also the flow and hydrodynamics in subsequent years, when these legacy nutrients may support blooms.

Algal blooms are not the only concern when considering nutrient enrichment following carp decomposition. During the wetland experiment a secondary fish-kill event occurred between Day 14 and Day 21. Approximately 150 large (>40 cm) floating carp carcasses were discovered evenly distributed along the length of the wetland. As carp is a hardy species with high tolerance to poor water quality, the mortality of the resident carp population is of particular significance. High ammonia concentrations were recorded during this period and could have contributed to the mortality event. The toxicity of ammonia is primarily attributed to the un-ionised ammonia (NH_3) and is dependent on factors such as DO concentrations, pH and temperature (Randall and Tsui 2002). Ammonia is toxic to freshwater organisms at concentrations (uncorrected for temperature and pH) ranging from 0.5 to 23 mg/L NH_3 for 19 invertebrate species and from 0.88 to 4.6 mg/L NH_3 for 29 fish species (Stephan *et al.* 1985). The maximum ammonia concentration recorded during the wetland trial was 36.7 mg/L NH_3 . These ammonia concentrations, compounded by low DO concentrations and high water temperatures, could be considered sufficient to cause such a fish-kill event.

The carp wetland trial provided a partial demonstration of a 'worst case scenario' following the implementation of CyHV-3 as a carp biocontrol. While the biomass of 2400 kg/ha used in this experiment may be representative of parts of the system, it is not representative of the whole system. Carp biomass density in Australian waters is highly variable, and estimates for mean lowland and mid-slope biomasses are 265 to 3144 kg/ha, respectively (Harris and Gehrke 1997; Driver *et al.* 2005; Gehrke *et al.* 2010; Thwaites *et al.* 2010). There is also potential for carp carcasses to aggregate in slow flowing wetlands and backwaters, which may increase biomass by a full order of magnitude (Monaghan and Milner 2008). As such, using the findings of this study alone to assess the risk of deoxygenation, nutrient loading and potential for harmful algal blooms across the whole system may misestimate the likelihood and severity of such events. While most default trigger values were exceeded even at the lowest biomass concentration, these calculations assume 100% mortality of carp biomass and do not consider mortality of other aquatic biota. Real-world mortality rates will likely be lower, and a secondary mortality event of carp and other aquatic biota due to poor water quality is a possibility. Actual mortality will affect the pool of nutrients available and thus the magnitude of side-effects. Similarly, different habitat types will have different carp biomasses, and each habitat will each have different hydrodynamic characteristics which will affect factors such as water temperature, residency times and the instances of eutrophication, which can in turn act as controls on the rate of oxygen drawdown, nutrient liberation and algal growth. Only when all these factors

are fully understood and considered can we begin to accurately predict the short and long-term effects of carp mortality following the release of the proposed CyHV-3 biocontrol.

Conclusion

Decomposing carp carcasses can exert a considerable oxygen demand and fuel algal growth through nutrient enrichment of the water column. The magnitude of the biological oxygen demand and the nutrient enrichment is dependent upon the carp density, which is known to vary between habitats. The rate of decay is rapid with nutrient release being mostly complete within two weeks. This has implications for the clean-up strategy if CyHV-3 was to be used as a biocontrol agent. Dead carp would need to be removed within several days to prevent flux of nutrients and dissolved organic carbon into the water column. The nutrients from decomposing carp are likely to be bioavailable and fuel considerable algal growth, but the species of algae may vary depending upon the season and prevailing hydrodynamics. The pool of nutrients currently in carp in Australian waterways is likely to be considerable and, upon carp mortality, will be incorporated into algal biomass and contribute to nutrient concentrations in the sediment. These legacy nutrients may be available to support algal growth for a considerable period following a mass mortality event. The magnitude and implications of increased biological oxygen demand and nutrient enrichment following carp mortality can only adequately predicted when there is a better understanding of carp density and distribution.

Chapter 2: Critical flow estimation to determine cyanobacterial risk following mass mortality of carp following release of proposed CyHV-3 carp biocontrol

Richard Walsh, Justin D. Brookes, Sanjina Upadhyay

Introduction

The cyprinid herpesvirus 3 (CyHV-3) is being considered as a biocontrol agent for common carp (*Cyprinus carpio*) in Australia. CyHV-3 causes rapid and significant morbidity and mortality in common carp (hereafter “carp”) and has endangered carp populations in other countries (Hara et al. 2006; Gotesman et al. 2013). While CyHV-3 may reduce carp populations and facilitate positive ecological outcomes in the long term, little knowledge of the short-term environmental impacts exists. Of particular concern is the magnitude of carp-derived nutrient enrichment, the fate of these nutrients, and the potential for the occurrence of harmful algal blooms (HABs) in the Murray-Darling Basin (MDB).

HABs impact directly on native fish and other aquatic organisms, with a suite of side-effects including water toxicity and food-web alterations (Paerl *et al.* 2001). Cyanobacteria genera such as *Anabaena*, *Aphanizomenon* and *Microcystis* are highly productive in warm, turbid waters and frequently form HABs throughout the MDB. The cyanotoxins produced by cyanobacteria are hazardous to both aquatic and terrestrial biota, including humans and livestock (Chorus and Bartram 1999). Symptoms include gastrointestinal disorders, fever and irritations of the skin, ears, eyes, throat and respiratory tract, liver damage, neurotoxicity and tumour promotion (World Health Organization 2011). Furthermore, cyanobacteria are a relatively inadequate food source for zooplankton, being nutritionally poor and physically problematic for most grazers, and therefore are a poor pathway for carbon flow to aquatic foodwebs (Lampert 1987).

While many cyanobacteria are known to produce potent toxins, toxicological data with which to derive guideline values for cyanotoxins is inadequate, and, to date, Microcystin-LR is the only cyanobacterial toxin to have a guideline value set for drinking water (World Health Organization 2011). The provisional guideline value for Microcystin-LR is 0.001 mg/L (1 µg/L) (World Health Organization 2003). As such, cyanotoxin monitoring is most effectively based on surveillance of source water for evidence of cyanobacterial blooms or bloom-forming potential.

There is a suite of approaches to the prevention, suppression or termination of cyanobacteria bloom events. Chemical approaches, such as the use of algicides, can pose dangers to human and ecosystem health, and are not environmentally sustainable on the scale necessary to prevent or treat cyanobacteria blooms as a result of carp-derived nutrient enrichment across the MDB. Other approaches aim to decrease the incidence or duration of cyanobacteria blooms by addressing one or more of the four stimulatory factors; light, warmth, nutrients and temperature stratification. Light and warmth are impractical intervention targets in some cases, but limiting light by mixing has proved to be effective. Similarly, the control of cyanobacteria blooms through nutrient input reduction is a long-term process, and unlikely to be effective in this instance. Even if nutrient inputs could be drastically reduced in the near term, nutrient concentrations in sediments would remain elevated due to prior inputs. Further, assuming carp carcasses

are left to decompose *in situ*, a considerable pulse of carp-derived nutrients following mortality is expected (Walsh *et al.* 2018).

More promisingly, the use of hydrologic manipulations to prevent temperature stratification is a demonstrated method of controlling cyanobacteria blooms. Increased flow has been shown to reduce cyanobacteria blooms even in nutrient-rich freshwaters, due to the controlling influence of flow on river stratification and phytoplankton population dynamics (Sherman *et al.* 1998; Oliver and Ganf 2000; Paerl 2008). This has been demonstrated in Australian freshwater systems, where correlations between flow and cyanobacterial abundance have been demonstrated in the Murrumbidgee River (Jones 1993; Sherman *et al.* 1998), the lower River Murray (Bormans *et al.* 1997; Baker *et al.* 2000), and the Darling River (Mitrovic *et al.* 2003).

Hydrological manipulations offer a promising ecological strategy for preventing, suppressing and terminating cyanobacteria blooms following nutrient enrichment from decomposing carp carcasses in the MDB. As such, the estimation of critical flows for disrupting the formation of cyanobacteria blooms throughout this region forms a fundamental aspect of the management strategy following the release of the proposed CyHV-3 carp biocontrol in the MDB. The critical flow velocity necessary to disrupt temperature stratification as been determined in a number of rivers through both deployment of thermistors and by modelling the hydrodynamics. Current estimations of discharge and critical flow required to disrupt thermal stratification are outlined in Table 6.

Table 6: Discharge and critical flow velocity that leads to a change between stratified and mixed conditions.

Site	Discharge (ML/d)	Critical velocity (m/s)	Reference
Lower River Murray at Lock 1	4000	0.1	Bormans <i>et al.</i> , 1997: Baker <i>et al.</i> , 2000
Murrumbidgee at Maude Weir	1000	0.06	Sherman <i>et al.</i> , 1998
Darling River at Bourke	500	0.053	Mitrovic <i>et al.</i> 2003
Namoi River at Walgett	100	0.041	Mitrovic <i>et al.</i> 2003
Darling River at Wilcannia	200	0.046	Mitrovic <i>et al.</i> 2003

This study estimates the critical flow required to disrupt thermal stratification in key regions of the MDB and its tributaries using a mixing criterion model, and compares results with the minimum flow targets used by the Murray Darling Basin Authority (MDBA) for managing flows in selected rivers within MDB. Additionally, this study analyses existing flow rate data and water column temperature data to calculate the critical flow threshold necessary to disrupt thermal stratification and stave off cyanobacterial blooms for five key sites of the lower River Murray.

Method

Mixing criterion model

The mixing criterion developed by Bormans and Webster (1997) was used to estimate the critical flow required to disrupt the thermal stratification, and is given by:

$$R = \frac{U^3}{H(Q_{net} - \frac{2Q_I}{K_d H}) \frac{\alpha g}{\rho C_p}}$$

where, U is the depth-averaged velocity, H is the water depth, Q_{net} is the net surface heat flux into the water column, Q_I is the net shortwave radiation, K_d is the light attenuation coefficient (m^{-1}), α is the thermal expansion coefficient ($2.10 \times 10^{-4} \text{ } ^\circ\text{C}^{-1}$), g is the gravitational acceleration (9.81 ms^{-2}), ρ is the density of water (1000 kg m^{-3}) and C_p is the specific heat capacity of water ($4180 \text{ J kg}^{-1} \text{ } ^\circ\text{C}^{-1}$). The parameter R is only relevant when the factor in parenthesis is positive; otherwise the water column is losing heat, and stratification will not build up even under low discharge (Maier *et al.* 2001). In order to use the above equation as a predictive tool, an estimate of Q_{net} in terms of easily available parameters is needed. Q_{net} can be expressed as the sum of the radiative (short- and long-wave radiation), evaporative and sensible heat fluxes as follows:

$$Q_{net} = Q_I + Q_b + Q_e + Q_s$$

where, Q_I is the net short-wave radiation, Q_b is the net long-wave radiation, Q_e is the latent heat flux due to evaporation and Q_s is the sensible heat flux. The data on Q_I for each site was obtained from Bureau of Meteorology (BOM). Q_b was derived using an equation from Hodges (1998), and is given by:

$$Q_b = Q_{emitted} + Q_{absorbed}$$

$Q_{emitted}$ and $Q_{absorbed}$ were estimated as:

$$Q_{emitted} = -\varepsilon_{(water)} \sigma (273.2 + T_{(water)})^4$$

and,

$$Q_{absorbed} = \varepsilon_{(air)} \sigma (1 + 0.17 C_{(cloud)}^2) (273.2 + T_{(air\ 2)})^4 (1 - R_{t(lw)})$$

where, $\varepsilon_{(water)}$ is the emissivity of the water, a non-dimensional constant (0.96), $\varepsilon_{(air)}$ is the emissivity of air derived using formula from Hodges (1998). C_{cloud} is the fractional cloud cover, $T_{(water)}$ is the water surface temperature, $T_{(air\ 2)}$ is the air temperature (in Celsius degrees) measured two meters above the water surface, and $R_{t(lw)}$ is the total reflectivity of the water surface for long wave radiation.

The parameters Q_e and Q_s were estimated using the equation from Bormans and Webster (1997), and are given as:

$$Q_e = L_v \rho_a C_E W (q_s - q_a)$$

where, L_v is the latent heat of evaporation, ρ_a is the density of air, C_E is a dimensionless exchange coefficient for evaporative heat exchange, q_s and q_a are the specific humidities estimated from surface water temperatures, air temperature and humidity using the functional form of Kimball *et al.* (1982).

In a similar way, Q_s is estimated as:

$$Q_s = C_p \rho_a C_H W (T_s - T_a)$$

where, C_H is a dimensionless exchange coefficient for sensible heat exchange, W is the wind speed (m s^{-1}), T_s is the water surface temperature ($^{\circ}\text{C}$) and T_a is the air temperature ($^{\circ}\text{C}$).

Meteorological data required for the model has been imported online for the closest meteorological station of each sites from Bureau of Meteorology (BOM) website. The information on the flow and water temperature have been obtained from the River Murray Data (<https://riverdata.mdba.gov.au/system-view>). Sites were chosen based on availability of adequate hydrological data on flow. The data for the cross-sectional areas of water channel at different flow conditions typical for summer months (October-March) has been obtained from Murray Darling Basin Authority (MDBA).

Flow analysis

Thermistor data was acquired from SAWater for five locations along the lower River Murray; Renmark, Holder Bend, Morgan, Nildotti and Tailm Bend. Water temperature data was logged every 10 minutes.

Flow data was obtained from WaterConnect (waterconnect.sa.gov.au) for the nearest upstream flow monitoring station for periods matching thermistor data. Due to analysis limitations posed by once-daily flow data points, a linear weighted moving average function was applied to allow better comparison to water temperature data.

Well-mixed conditions were distinguished from stratified conditions based on thermistor measurements - a temperature difference of $<0.1^{\circ}\text{C}$ between the epilimnion and hypolimnion was selected to identify well-mixed conditions in the water column. For each instance of well-mixed conditions in water column a corresponding flow rate was extracted from the data.

Results

Mixing criterion model

Critical flows required to disrupt thermal stratification in the River Murray and its key tributaries are presented in Table 7. For comparison with the values estimated by using mixing criterion model, minimum flow targets set by MDBA for selected rivers along the Murray Darling Basin has also been summarized (Table 8).

Table 7: Critical flow (ML/d) for different sites along the River Murray and its key tributaries during summer months (October to March) estimated using the mixing criterion model.

Site	River	Critical flow (ML/d)
Balranald	Murrumbidgee	990
Colemans	Mitta Mitta	1195
Doctors Point	Murray	1974
Gulpa Offtake	Edward	1784
Heywoods	Murray	5476
Kerang	Loddon	304
McCoy Bridge	Goulburn	438
Swan Hill	Murray	2604
Weir 32	Darling	283
Wilcannia	Darling	1226
Yarrowonga	Murray	756
Renmark	Murray	2962
Holder Bend	Murray	2386
Morgan	Murray	2792
Nildottie	Murray	1387
Tailem Bend	Murray	2969

Table 8: MDBA minimum flow targets (ML/d) for selected rivers along the Murray Darling Basin.

Site	River	Period	Minimum flow (ML/d)
Balranald	Murrumbidgee	January	186
		February	180
		March	180
		October	1030
		November	568
		December	254
Colemans	Mitta Mitta	All times	200
		Dart. storage 60% - 70%	Average of 200 – 300
		Dart. storage 70% - 80%	Average of 200 – 400
		Dart. storage > 80%	Average of 200 – 500
Doctors Point	Murray	All times	1,200
Gulpa Offtake	Edward	All times	80
Heywoods	Murray	All times	600
Kerang	Loddon	All times	No minimum
McCoy Bridge	Goulburn	November to June	Minimum 300. An average <u>monthly</u> minimum flow of 350 ML/day.
		July to October	Minimum 350. An average <u>monthly</u> minimum flow of 400 ML/day.
Swan Hill	Murray	All times	1,600 - 1,900
Weir 32	Lower Darling	January to March	350
		April, November and Dec	300

		May to October	200
		Whenever storage above FSL	500
Yarrawonga	Murray	All times	1,800
SA Border (Entitlement Flow)	Murray	December entitlement	7000
		January entitlement	7000
		February entitlement	6900
		March entitlement	6000

Flow analysis – Annual

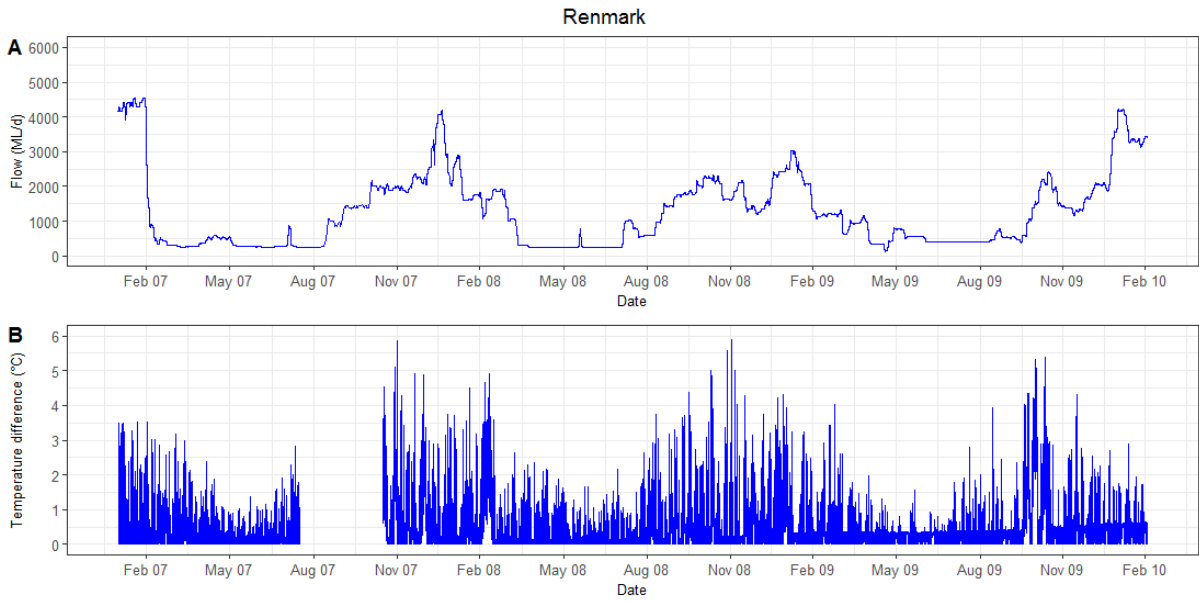
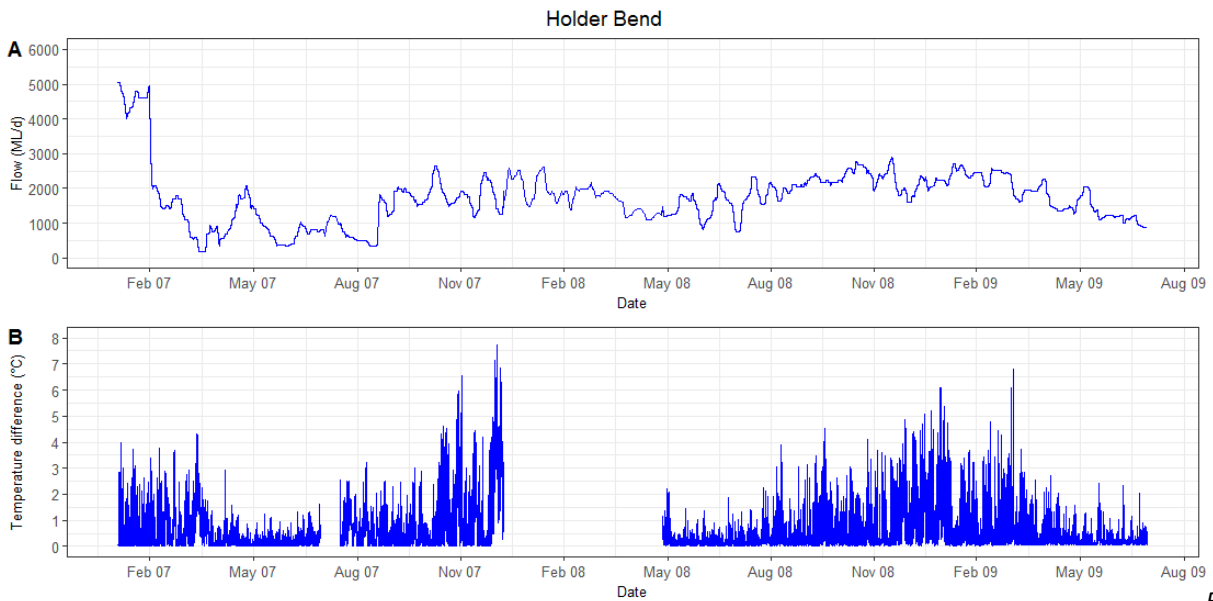


Figure 6: Flow (A) and water temperature difference between epilimnion and hypolimnion (B) for Renmark, South Australia.



Figure

7: Flow (A) and water temperature difference between epilimnion and hypolimnion (B) for Holder Bend, South Australia.

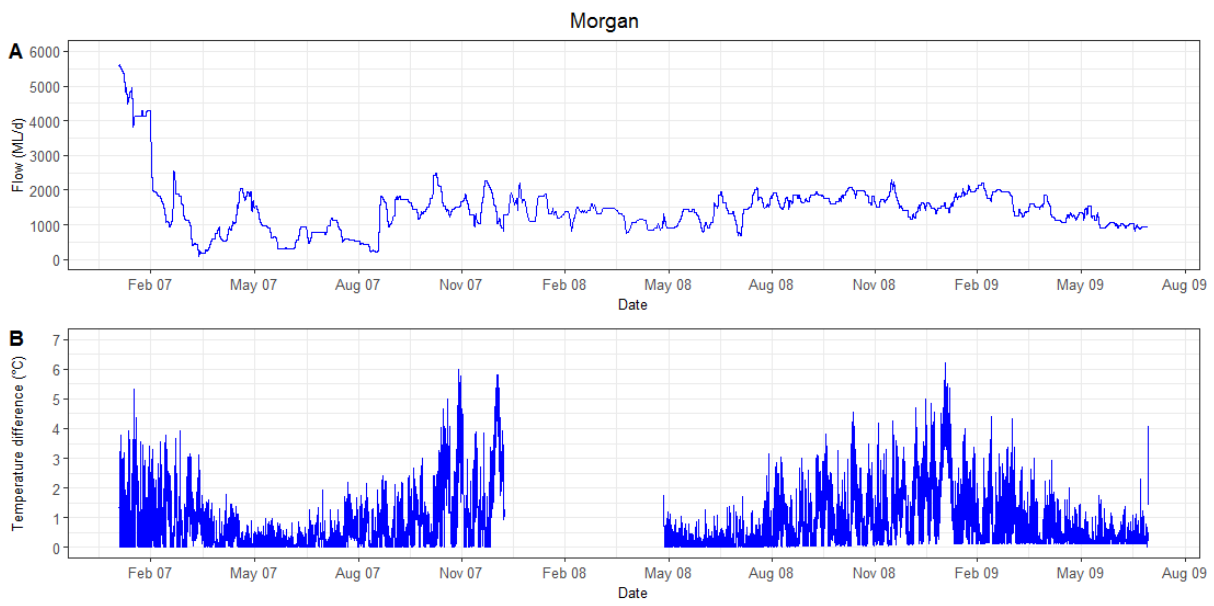
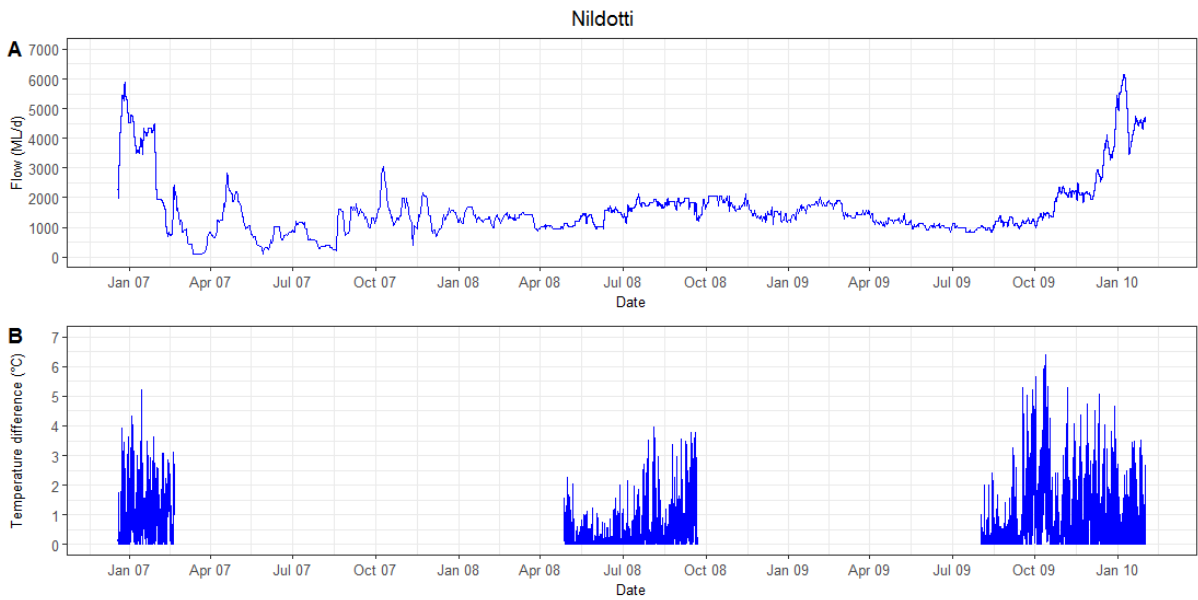


Figure 8: Flow (A) and water temperature difference between epilimnion and hypolimnion (B) for Morgan, South Australia.



Figure

9: Flow (A) and water temperature difference between epilimnion and hypolimnion (B) for Nildotti, South Australia.

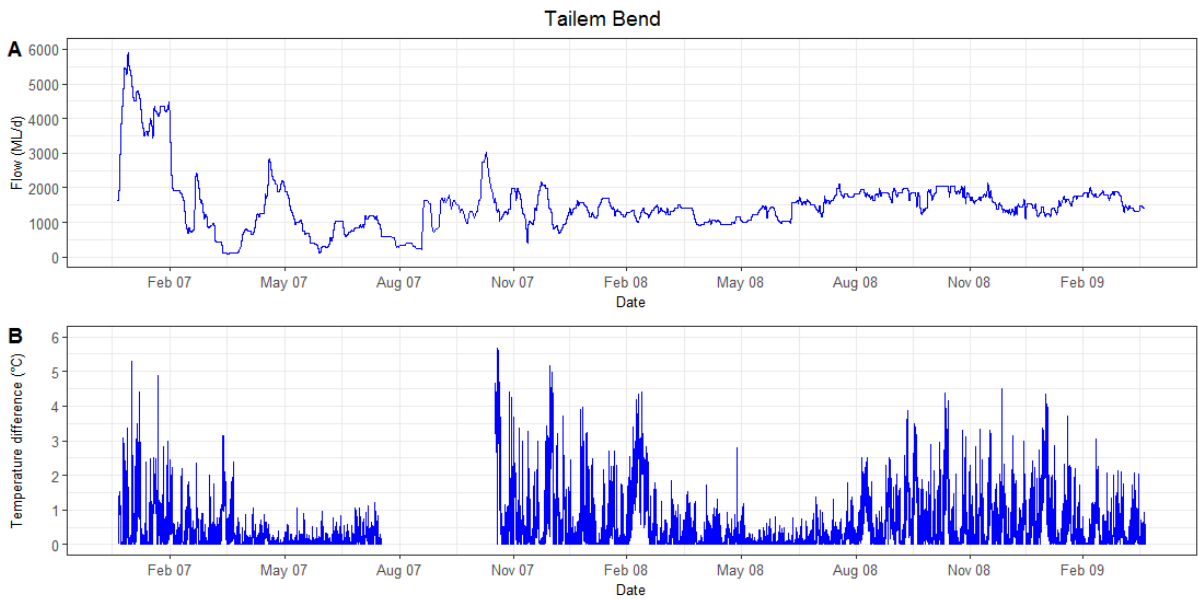


Figure 10: Flow (A) and water temperature difference between epilimnion and hypolimnion (B) for Taillem Bend, South Australia.

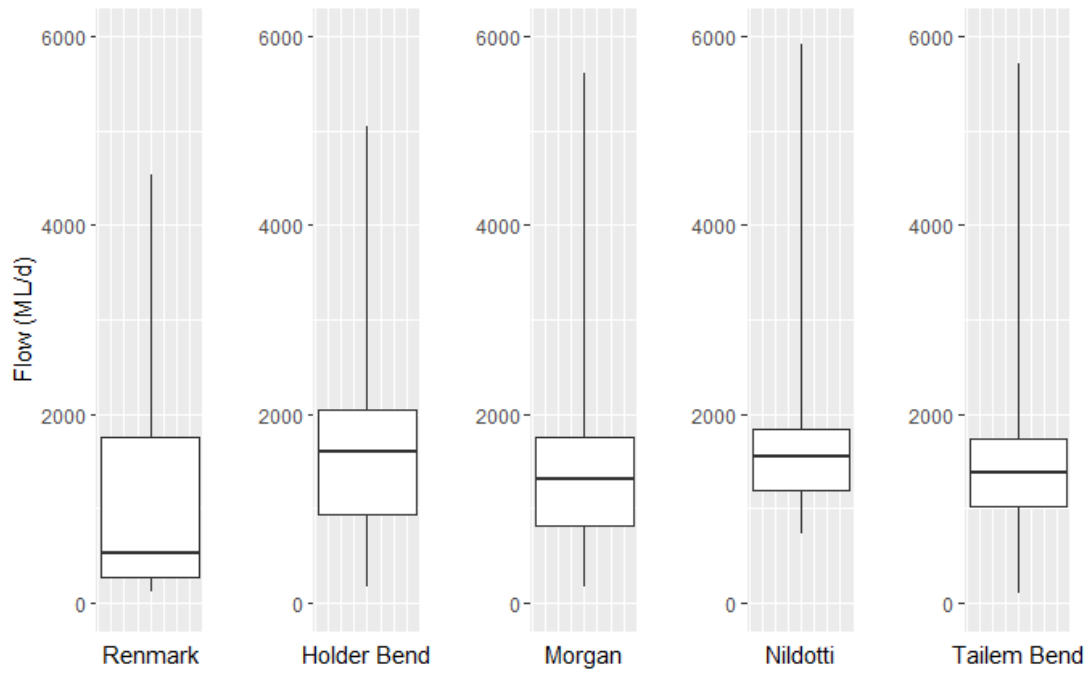


Figure 11: Flow (ML/d) resulting in a temperature difference of $<0.1^{\circ}\text{C}$ between the epilimnion and hypolimnion for all record for all sites.

Flow analysis - Summer

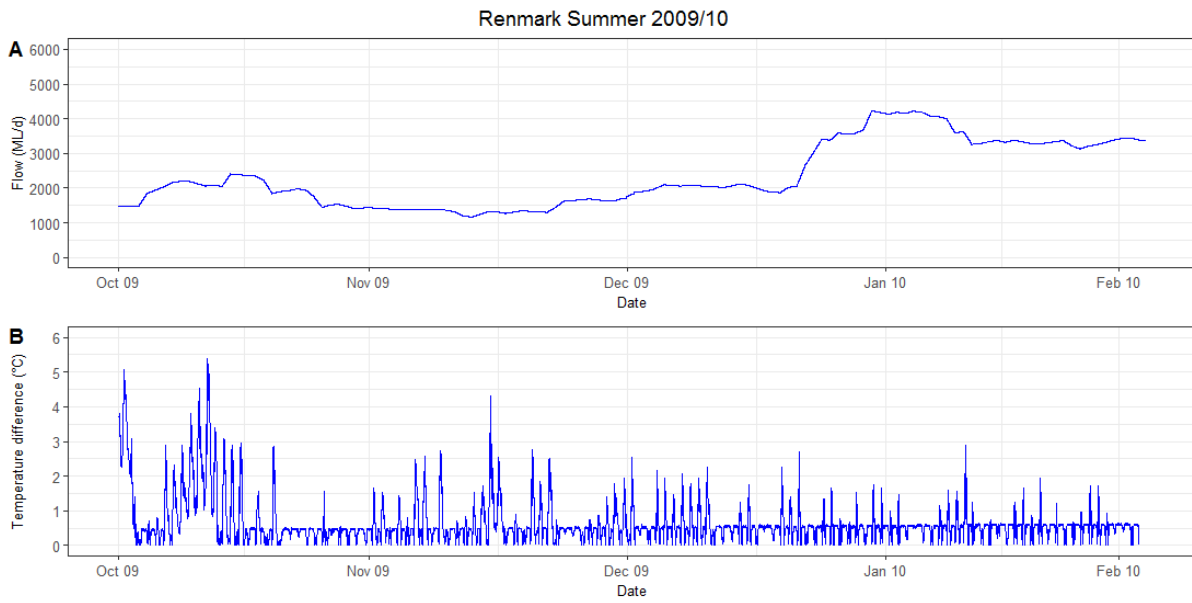
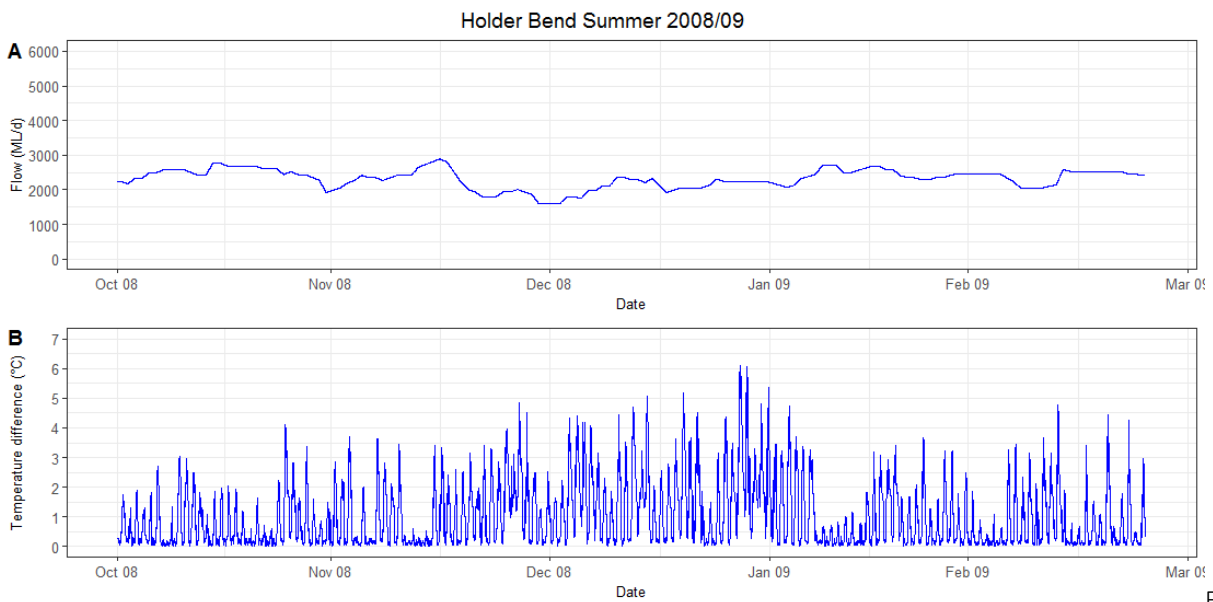


Figure 12: Flow (A) and water temperature difference between epilimnion and hypolimnion (B) for Renmark, South Australia over summer 2009/10.



Figure

13: Flow (A) and water temperature difference between epilimnion and hypolimnion (B) for Holder Bend, South Australia over summer 2008/09.

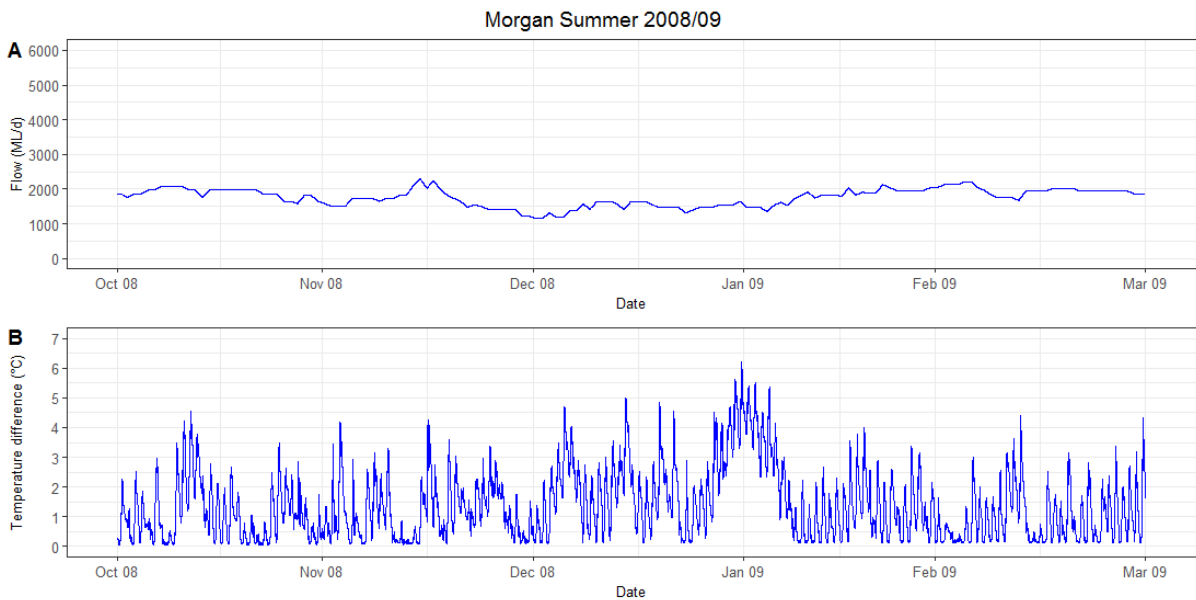
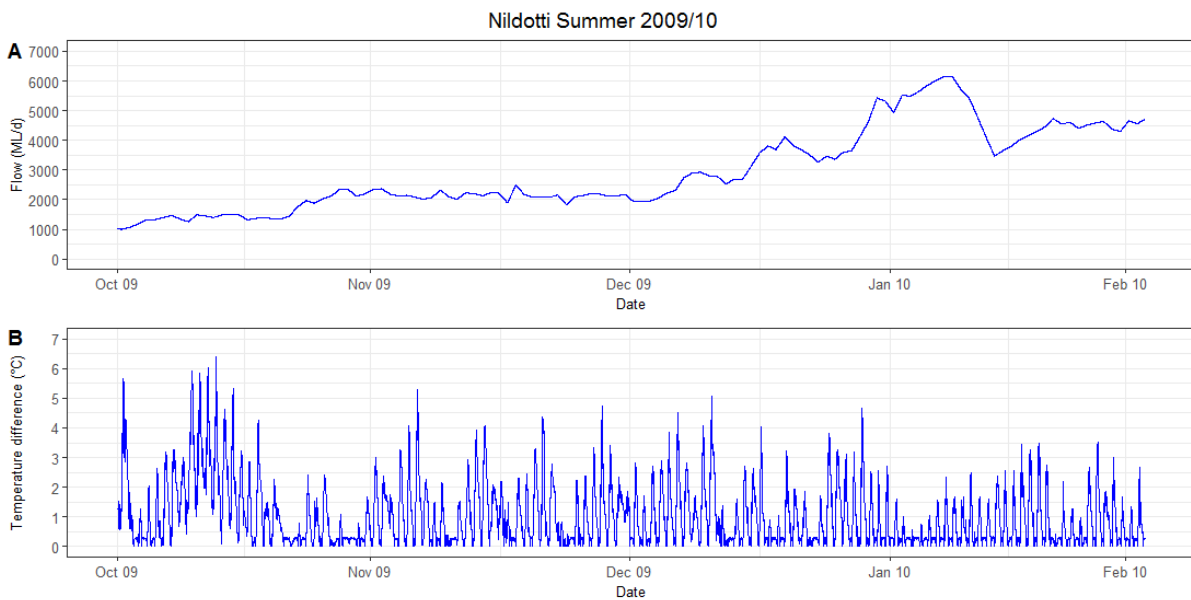


Figure 14: Flow (A) and water temperature difference between epilimnion and hypolimnion (B) for Morgan, South Australia over summer 2008/09.



Figure

15: Flow (A) and water temperature difference between epilimnion and hypolimnion (B) for Nildotti, South Australia over summer 2009/10.

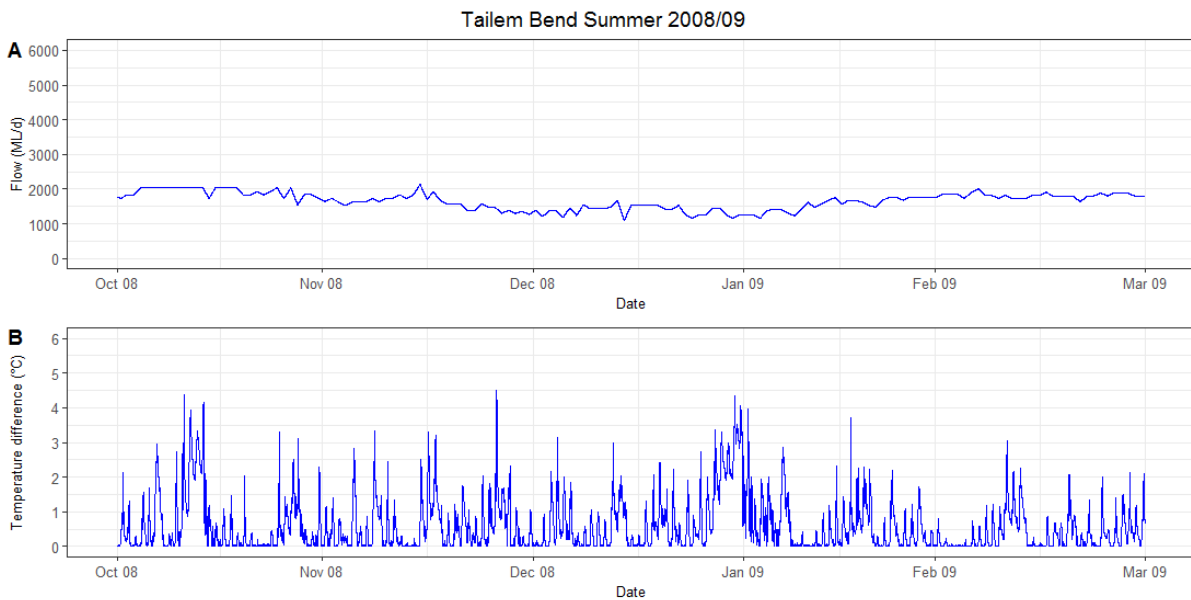


Figure 16: Flow (A) and water temperature difference between epilimnion and hypolimnion (B) for Tailem Bend, South Australia over summer 2008/09.

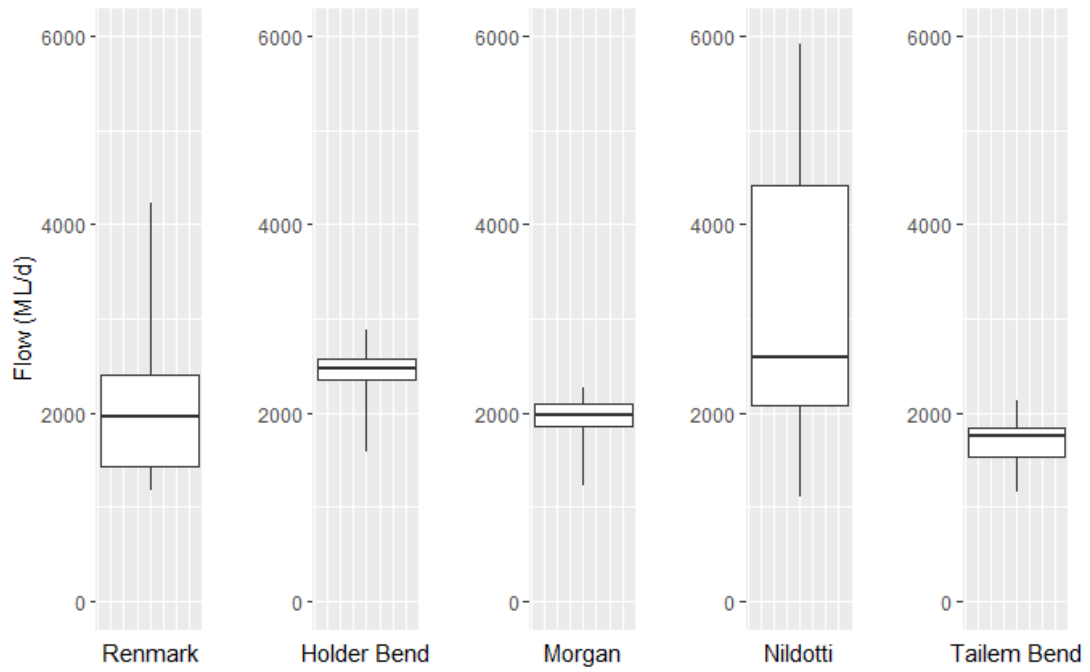


Figure 17: Flow (ML/d) resulting in a temperature difference of $<0.1^{\circ}\text{C}$ between the epilimnion and hypolimnion for summer period for all sites.

Flow required to create a water column temperature difference of $<0.1^{\circ}\text{C}$ were significantly lower (p -value $<2.2\text{e-}16$) for whole record than for summer period for all sites. This is because cool air temperatures induce convective cooling of the water column and mixing results. Additionally, there was a weak positive correlation between flow and epilimnion/hypolimnion temperature difference for whole record data, whereas summer period data returned weak or moderate negative correlations, with the exception of Renmark.

Table 9: Location of flow data, depth range, mean flow required to create a temperature difference of $<0.1^{\circ}\text{C}$ between the epilimnion and hypolimnion with standard deviation, and correlation coefficient (Spearman's) for flow and temperature data for selected sites for all record.

Site	Flow data	Depth (m)	Mean flow (ML/d)	Median flow (ML/d)	Correlation coeff.
Renmark	Lock 6	0.5 – 4.5	1116.75 (1150.58)	523.25	0.265
Holder Bend	Lock 3	0.5 – 6	1658.84 (964.36)	1610	0.124
Morgan	Lock 2	0.5 – 6	1390.22 (931.72)	1310	0.220
Nildotti	Lock 1	0.5 – 6.9	1848.07 (1150.58)	1560	0.211
Tailem Bend	Lock 1	0.5 – 9.7	1465.54 (796.43)	1380	0.119

Table 10: Location of flow data, depth range, mean flow required to create a temperature difference of $<0.1^{\circ}\text{C}$ between the epilimnion and hypolimnion with standard deviation, and correlation coefficient (Spearman's) for flow and temperature data for selected sites over summer period.

Site	Flow data	Depth (m)	Mean flow (ML/d)	Median flow (ML/d)	Correlation coeff.
Renmark	Lock 6	0.5 – 4.5	2155.31 (825.35)	1965.89	0.144
Holder Bend	Lock 3	0.5 – 6	2445.44 (231.98)	2475.96	-0.316
Morgan	Lock 2	0.5 – 6	1943.62 (142.5)	1970	-0.310
Nildotti	Lock 1	0.5 – 6.9	3186.06 (1383.38)	2667.95	-0.216
Tailem Bend	Lock 1	0.5 – 9.7	1691.08 (223.95)	1749.73	-0.146

Table 11: Site, location of flow data, and river distance.

Site	Flow data	River distance (km)
Renmark	Lock 6	49.8
Holder Bend	Lock 3	48.4
Morgan	Lock 2	42.1
Nildotti	Lock 1	55.3
Tailem Bend	Lock 1	187.3

Discussion

The critical flow estimated using the mixing criterion model in this study is comparable to the minimum flow target set by MDBA and with the values proposed in the literature for some rivers. The values were similar to the flow target set by MDBA for sites in the Goulbourn (McCoy Bridge) and Darling (Weir 32) rivers. The minimum flow target estimated at site Balranald of the lower Murrumbidgee River (990 ML/d) in this study is comparable to the threshold value (1000 ML/d) proposed by Sherman *et al.* (1998) at the Maude Weir pool of the lower Murrumbidgee River. In their study, flows less than 1000 ML/d corresponded to persistent stratification with a very shallow, but strong thermocline layer, whereas greater flows caused complete mixing of the water column. A similar approach was used to determine the average critical flow we estimated for different sites within the River Murray is comparable to the minimum flow target proposed by Bormans *et al.* (1997) for the lower section of the River Murray.

There were some differences the values we estimated in this study and the targeted flow values proposed by MDBA for select rivers. For example, the minimum flow target set by MDBA for Yarrawonga, in the River Murray, is significantly higher than the flow target we estimated in this study. The difference may be attributed to the target being developed for other ecological outcomes or to overcome operational constraints. In this study, the objective was to estimate critical flows to minimise the development of cyanobacterial blooms under worst case scenario for summer month (highest average air and water temperature and very low wind speed), whereas the flow target set by MDBA may include considerations for achieving ecological outcomes for birds, fish and vegetation communities, or flow required to avoid stranding irrigator pumps.

The normal entitlement flow over South Australian border will not necessarily correspond to flow at the South Australian sites analysed. In all cases, however, the critical flow estimated by the mixing criterion model was exceeded by entitlement flow over the South Australian border. During dry periods the Normal Entitlement Flow over the South Australian border may be decreased, and the potential for thermal stratification to occur may increase in these cases.

The critical flow estimated using flow analysis suggests the average flow rate required to mix the water column ranges between 523.25 and 1610 ML/d for the five key sites of the lower River Murray. The required flow rate is higher for summer period only, when it ranges from 2667.95 and 1749.73 ML/d. The weak and moderate negative correlation between flow and water column temperature difference between epilimnion and hypolimnion during the summer period suggests a moderate correlation between increased flows and increased mixing. This pattern was not seen for all record data, possibly due to the prevalence of other mixing dynamics during winter, such as convective mixing. An obvious limitation of using flow data collected a considerable distance upstream from where temperature data is collected is the lag between changes in flow rates upstream and corresponding changes in flow rates downstream. Water travel time is

complex and dynamic, dependent on myriad factors such as flow, tributary inflows, extractions, topography, and weather conditions. An estimate can be achieved by considering the water travel time from Albury, NSW to the South Australian border. During times of regulated flow, water released from Albury takes approximately one month to reach the South Australian border, 1600 km away, which is approximately 57 km a day. Most sites had a river distance of between 42 and 55 km from where their flow data was collected (except Tailem Bend, which was 187 km), so it is not unreasonable to expect most sites to be experiencing changes in flow as little as a day after the corresponding change in flow upstream. Collecting flow rate data in the same area as water column temperature data would enable more accurate analysis of the relationship between flow and mixing, and allow calculation of an accurate and reliable critical flow threshold.

There has been substantial increases in phytoplankton counts across the River Murray over the period 1994-2008, with significant cyanobacteria bloom events in 1983, 1991, 2009, 2010 and 2016 (Croome et al. 2011; Murray Darling Basin Authority 2016). While the first four events were related to conditions of low flow, the bloom in 2016 was related to elevated water temperature. Hence, while the controlling influence of flow may help to mitigate cyanobacteria blooms in the MDB under current conditions, future climate scenarios may influence the occurrence and duration of cyanobacteria blooms in the MDB. Similarly, it is important to consider the influence of a carp-derived nutrients fluxing into the system following mass mortality. There is a considerable pool of nutrients in carp biomass that will become available following carp mortality. These nutrients may fuel rapid considerable algal growth, although the species of algae may vary depending upon the season and prevailing hydrodynamics.

Nutrients not taken up into algal biomass will contribute to nutrient concentrations in the sediment, and these legacy nutrients may flux into the water column under certain conditions, providing fuel for algal growth for a considerable period following a mass mortality event. These legacy nutrients are of particular concern in Australia, where water available for hydrological manipulation strategies is limited resource. Carp-derived nutrients may stay in sediment for much longer than hydrological manipulations remain a feasible treatment option. As such, contingency strategies to combat cyanobacteria blooms as a result of flux of legacy nutrient into the water column should be developed.

Management implications

Temperature stratification tends to be a pre-condition for cyanobacteria to bloom and reach problematic concentrations in rivers. The analysis for river reaches in the Murray Darling Basin where there are existing flow targets predicts that these targets should be sufficient to disrupt stratification. While reducing the temperature stratification will reduce the likelihood of blooms it does not guarantee that high numbers of cyanobacteria will not occur. Mixing of the water column mean that on average phytoplankton will be exposed to less light than if they are with a stratified surface layer. However, depending upon the depth of

mixing and the light attenuating properties of the water (turbidity and dissolved organic matter), cells may still experience sufficient light to grow.

Oxbow lakes, billabongs and connected lakes may also host cyanobacterial populations. These ecosystems are typically shallower than the main river channels and have longer water residence time, creating conditions more conducive to cyanobacterial growth. These wetlands can act as nursery sites where cyanobacterial populations establish and seed the main river channel.

In Australian lakes and reservoirs temperature stratification is observed during the warm months. A range of techniques have been employed to reduce cyanobacterial risk in lake and reservoirs. Notable amongst these is the use of artificial destratification with bubble plume aerators. These mixers act to weaken temperature stratification so the water column is more readily mixed with wind driven and convective mixing. The risk from mass carp mortality can be mitigated in lakes and reservoirs because they can essentially be operated as closed systems and the carp populations can be fished to reduce risks associated with nutrients and low DO following mass carp mortality.

Managing the physical conditions is only one part of managing cyanobacterial risk. Nutrients determine the phytoplankton carrying capacity of lakes and reservoirs. The bioavailable nutrients will increase with mass carp mortality and this may fuel phytoplankton growth and/or contribute to a legacy pool of nutrients, which will become bioavailable later. Removing dead carp would be the only management technique to reduce impacts from elevated nutrient concentrations.

Toxins and cyanobacterial blooms can present an unacceptable risk to recreational use of infested waterways. Exposure and contact with blooms should be avoided. Cyanobacterial risks in reservoirs can be mitigated by 'fishing-down' carp populations and ensuring optimised coagulation and sufficient contact chlorination contact time destroy any residual toxins. Cyanobacteria also produce compounds that taint the odour and taste of water. These compounds can be removed with activated carbon but this comes at considerable cost.

Chapter 3: A model assessment of water quality risk of carp biocontrol for Australian waterways

Matthew R. Hipsey, Brendan Busch, Justin D. Brookes

Introduction

Background

The common carp (*Cyprinus carpio*) is widely considered the worst aquatic pest throughout the Murray-Darling Basin (MDB). Altered water regimes, reproductive advantages and high tolerance to poor water quality have facilitated the invasion by and establishment of large common carp (hereafter 'carp') populations (Harris and Gehrke 1997; Koehn 2004). Large carp populations are associated with poor water quality, habitat destruction, and detrimental effects to macrophyte, invertebrate and zooplankton communities (King *et al.* 1997; Koehn *et al.* 2000; Vilizzi *et al.* 2014). Furthermore, increasing carp populations have coincided with reductions in native fish populations, although alterations to water regimes are likely to be larger contributors to this reduction (Clunie and Koehn 1997; Reid *et al.* 1997). Carp are now the dominant fish species in many of Australia's freshwater ecosystems and have extensive distribution throughout the MDB. Without intervention, carp populations are expected to grow and continue expanding into the upper reaches of the MDB, the remaining south-east coastal river systems, and throughout the Tasmanian river systems (Koehn 2004). The biomass distribution of carp throughout the diverse waterbodies of Australia has been recently quantified (Stuart *et al.* 2019), highlighting the variability in carp densities from ~50 to >1000 kg/Ha.

The cyprinid herpesvirus 3 (CyHV-3) is currently being considered as a carp biocontrol agent for implementation in Australia. CyHV-3 causes rapid and significant morbidity and mortality in carp and has endangered carp populations in other countries (Hara *et al.* 2006; Gotesman *et al.* 2013). While CyHV-3 may reduce carp populations and facilitate positive ecological outcomes in the long term, little knowledge of the short-term environmental impacts exists.

Of particular concern is the effect of decomposing carp carcasses on dissolved oxygen (DO) concentrations in the water column and the potential for hypoxic or anoxic conditions to occur. High levels of microbial activity associated with decomposition of organic matter are a key driver of hypoxic or anoxic conditions in the River Murray (King *et al.* 2012). Water temperature plays an important role in this process due to its key role in the development, growth and respiration of microbial communities and its influence on the metabolic demand of aquatic organisms (Howitt *et al.* 2007). Crucially, the effect of oxygen depletion on aquatic organisms is exacerbated at high temperatures when both the metabolic demand for oxygen is increased and the solubility of oxygen in water is reduced (Lewis 1970).

Another key concern is the magnitude of carp-derived nutrient enrichment, the fate of these nutrients, and the potential for the occurrence of harmful algal blooms. Harmful algal blooms impact directly on native fish and other aquatic organisms, with a suite of side-effects including water toxicity and food-web alterations (Paerl *et al.* 2001). Cyanobacteria genera such as *Anabaena*, *Aphanizomenon* and *Microcystis*

are highly productive in warm, turbid waters and frequently form harmful algal blooms throughout the MDB. The cyanotoxins produced by cyanobacteria are hazardous to both aquatic and terrestrial biota, including humans and livestock (Chorus and Bartram 1999).

In the associated study, the decay of dead carp was monitored in the lab, in mesocosms, and within a small wetland. The data generated from these studies has supported our understanding of how carp mortality will lead to deoxygenation and the extent of nutrient release. However, to fully assess the risks on water quality at the scale of a river reach, or a lake network requires the development of an appropriate model able to connect the biomass data and the above decay rate information, whilst also resolving how key environmental conditions change over space and time. These include flow, water temperature and hydro-biogeochemical processes controlling water column oxygen concentrations. The range of environments and habitats likely to be impacted by carp mortality are also quite varied, and therefore we need confidence the model approach can capture the variety of conditions, before we can assess the potential impacts of carp mortality.

Aims & scope

The aim of this work was therefore to understand the potential effects of mass carp mortality on water quality in Australian rivers and associated water bodies. Of particular concern was the impact on oxygen consumption (water column deoxygenation), and other water quality impacts were also explored, including the extent of nutrient release, and its potential to subsequently promote the development of local cyanobacteria blooms where the light and stratification conditions may also be favourable.

Within the National Carp Control Program (NCCP) this research had the following objectives to:

1. identify the loadings of carp that could negatively impact water quality, considering:
 - i. a range of geomorphological and aquatic habitat settings
 - ii. temperature variability
 - iii. the hydrologic flow regime
2. identify conditions where hotspots of accumulation may occur
3. provide rules for assessing risk of hypoxia, anoxia and cyanobacterial blooms.

The approach used in this analysis was to employ a spatially distributed simulation approach, using a coupled hydrodynamic-biogeochemical model. Whether carp mortality will lead to adverse conditions will be highly context dependent, and in any given water body will ultimately be dependent on the balance between oxygen consumption and oxygen replenishment. The model was therefore designed to generically capture the interactions between physical and chemical processes that are relevant to the problem.

The nature of the problem has meant that no “off-the-shelf” model was available to assess the carp transport and breakdown following mortality. This project has therefore driven the development of a new approach to assess the risks, involving integration of a carp “particle” model with the river ecohydrology models. This new model approach is guided by the related NCCP research program outputs (Figure 1).

The comprehensive nature of the model approach does however mean that it cannot be applied universally across all the waterways of Australia. Therefore, a selection of sites spanning different hydrologic and geomorphological contexts were chosen in consultation with the NCCP stakeholders. Learnings from these intensively studied sites were then used to generalise about types of the environments and typical conditions that would be required to lead to unacceptable water quality risks.

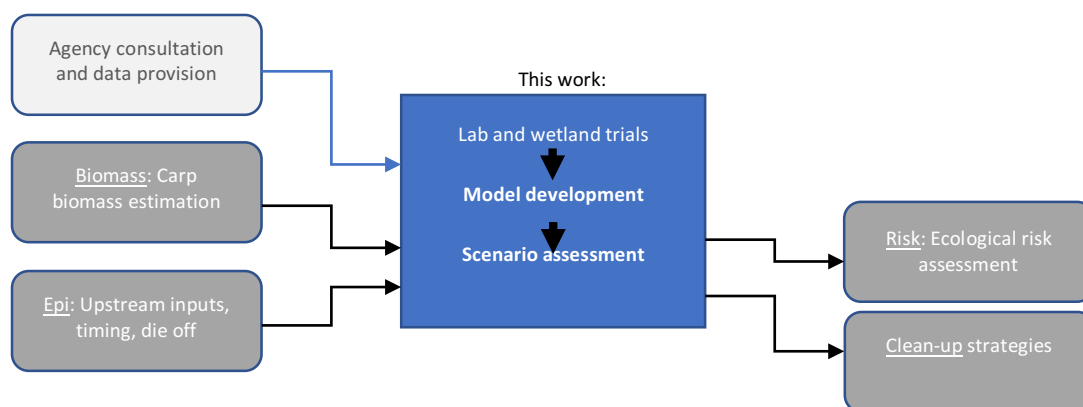


Figure 18: Scope of this project in relation to the broader NCCP research projects being undertaken.

The outcomes from this work allow us to consider what we might expect to happen to water quality with different carp loadings for a variety of water body conditions, which is critical to inform an assessment of risk to ecological, economic, and social assets due to potential biocontrol. Identification of accumulation hotspots is also instrumental for strategic planning development for both release and clean-up. The model can also be used to prioritise future monitoring activities and be further applied to specific sites to assess local risk.

Carp Model Basis and Rationale

Before describing the specific model applications and setup parameters of the models, we explore in this section the basis and general approach to capturing the impacts of carp mortality.

Conceptual model

A conceptualisation of the carp – anoxia link is depicted in the below diagram (Figure 2). This accounts for sources, redistribution mechanisms and decay processes, which need to be considered in the modelling approach. Since the largest risks are likely to occur where carp accumulate, rather than uniformly through an area, it is necessary to understand where the likely accumulation “hotspots” are, and it is expected these will be highly context specific, depending on local bathymetry and hydrologic conditions.

The problem is broken into five key steps, from problem to impact:

1. Addition of carp biomass to a region

- Most domains of concern are fed by one or more upstream rivers, and these will carry carp that may be in various stages of decomposition. This incoming carp mass will then be subject to local hydrodynamics and distributed through the domain.

2. Carp mortality within a region of interest

- Within a given region, carp will become infected and die – this may occur randomly through time and anywhere within the domain. Clustering of fish deaths may also occur where there is preferential habitat, or the likely formation of large aggregations.

3. Mobilisation of dead carp by various mechanisms

- Once carp die they will move depending on the hydrology of the region and the size and density of the fish. Factors to be considered include:
 - a) advection – flow with the current
 - b) buoyancy/flotation – when fish initially die they accumulate gas and rise to the surface
 - c) sedimentation – once fish begin to saturate they become dense and sink to the bottom
 - d) resuspension and bed-transport – once fish are dense enough to sit on the bed they may still roll along with the current.

4. Carp accumulation

- Where the flows become slow then carp “particles” will deposit in deeper holes, stagnant areas, or they may beach at the water’s edge. Understanding trends in the final accumulation densities is important to understand the local impacts in these regions.

5. Water quality impacts, including water column oxygen and nutrients, and sediment enrichment.

- Whether the dead carp are in transit or accumulated, they will be rapidly decaying. This entails consuming oxygen, and releasing nutrients. The rate of decay will largely depend on the temperature of the water. Deposited carp may also contribute to the long-term accumulation of organic material within the sediment and have an ongoing effect by enhancing the sediment-water interactions.

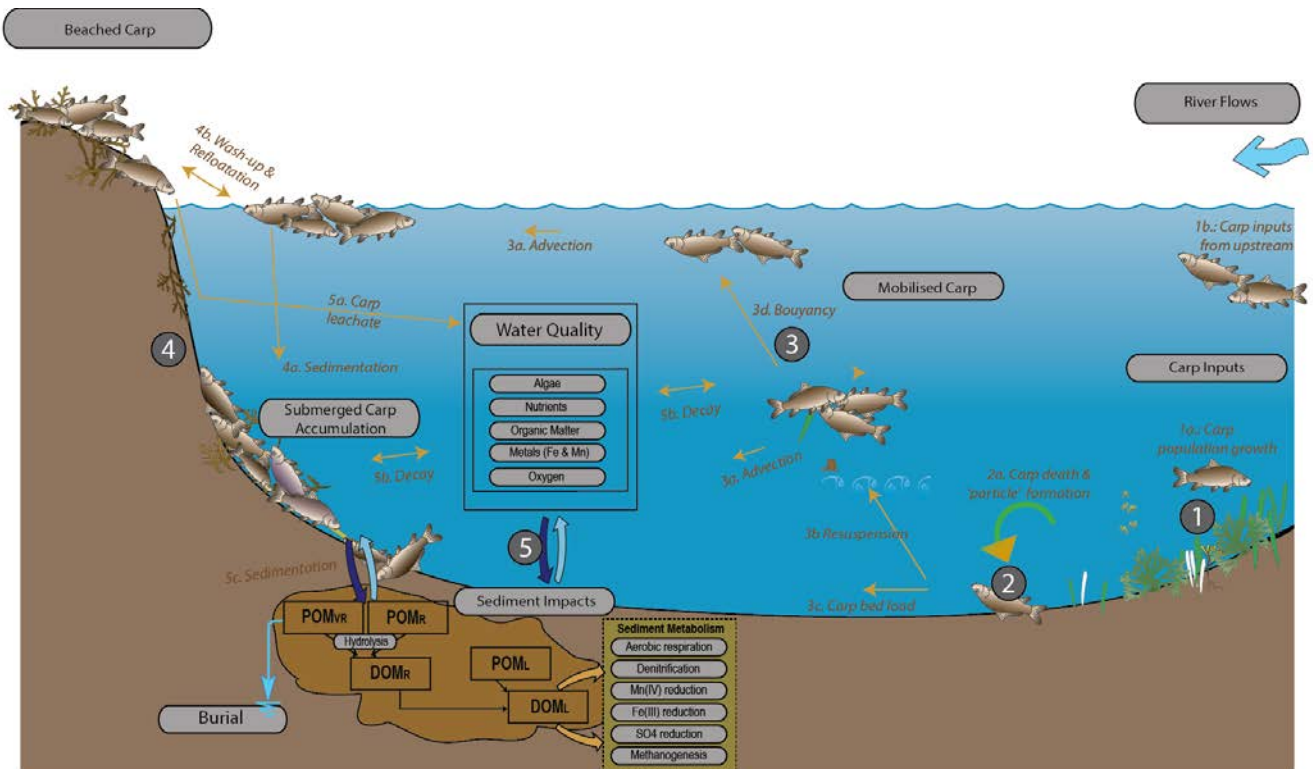


Figure 2: Conceptual model of process influencing carp mortality impacts on water quality.

The processes described above are superimposed on a dynamic hydro-biogeochemical environment. Processes 3 and 4, for example, are highly linked to the hydrodynamic conditions, affected by winds and currents. Process 5 is linked with oxygen and nutrient cycling processes, by contributing to oxygen demand and nutrient release. The oxygen metabolism in river, lake or wetland is controlled by wind, currents, light & benthic conditions, which alter primary productivity, community respiration, re-aeration and sediment demand (Figure 3).

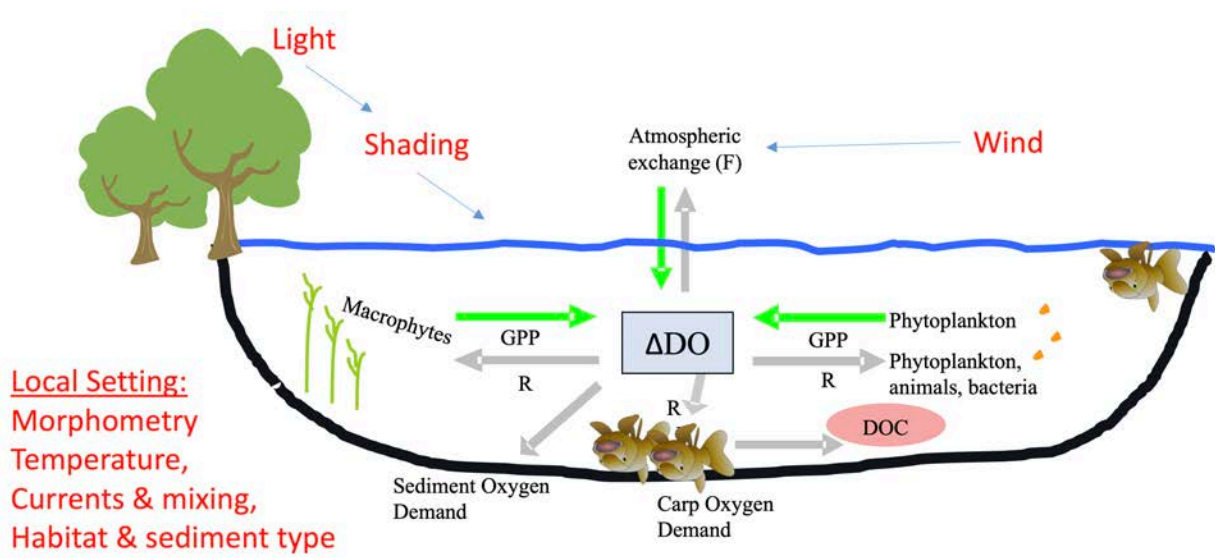


Figure 3: Processes influencing oxygen metabolism within waterways impacted by carp. The processes manifest in an oxygen balance which is governed by the local setting characteristics.

Approach to implementation

To ascertain and the impacts of different carp biomass under different flow conditions, there are two methods to capture the Carp Oxygen Demand indicated in Figure 3. The most simple method is to compute the total carp biomass within a domain, based on its area, and to assume this biomass is spread over the domain evenly. This mass then can be broken down at a defined rate, consistent with the breakdown experiments, and removing oxygen and releasing nutrients over this period.

This approach is useful for screening however it does not account for the redistribution, accumulation and potentially varied carp densities within a domain. The more comprehensive model therefore requires a particle tracking model embedded within the regional model in order to trace the population of decaying carp particles (DCP), and resolving the 5 steps described in the above section. The spatial mapping of biomass provides the opportunity for carp to be added to a domain based on its underlying habitat type, and therefore biomass can be aggregated into high density hotspots. Once particles enter the domain they are subject to floating and deposition, and decay, and they may disperse or accumulate depending on the hydrodynamics.

The different approaches to assess impacts are depicted in Figure 4. Regardless of the method used above, it is important to also acknowledge the potential for cumulative effects. The simulations reported subsequently describe loading at an individual site based on the internal generation of biomass, but any given site may also be impacted by the upstream delivery of poor water quality. This process is described in a given domain as external inputs.

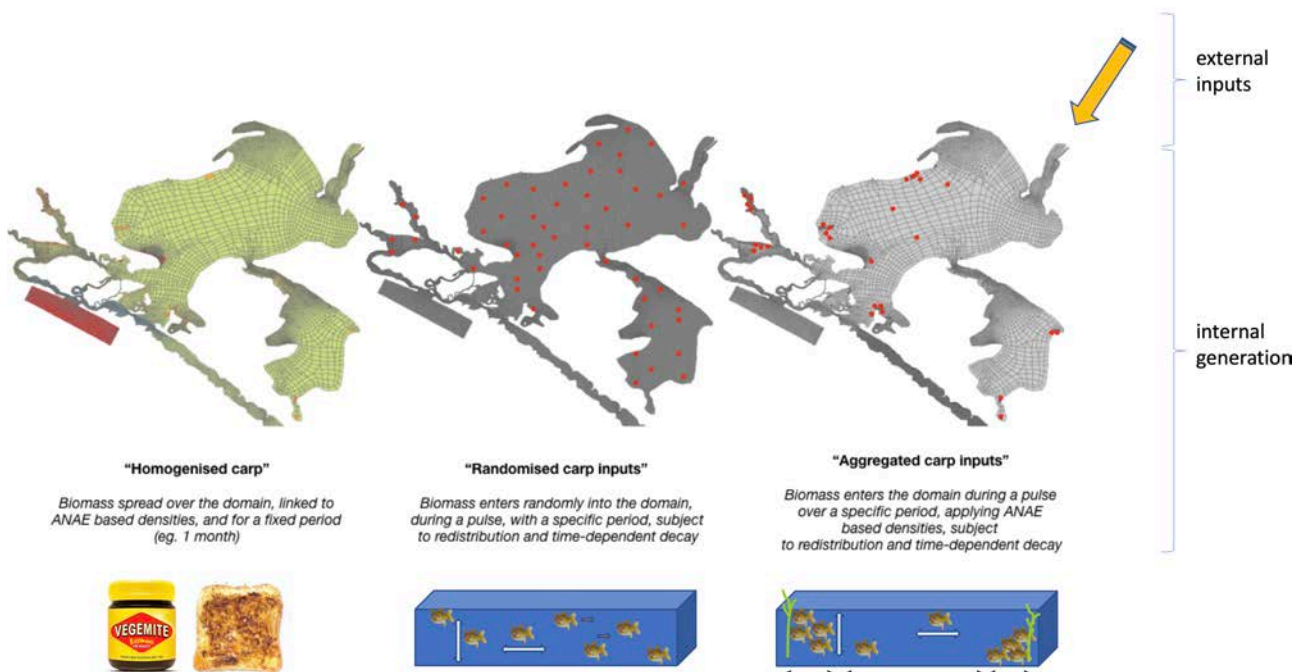


Figure 4: Conceptualisation of how biomass related to carp decay can be included in the spatially resolved model. The simplest "Homogenised Carp" approach evenly spreads the biomass over the domain, whereas the other options require the active particle dynamics. In the right-most example, the carp particles are added into the domain based on the known variability in carp biomass density, according to habitat type.

Study Sites

Site selection

Following the NCCP initial PI workshop and subsequent discussions on the areas to be impacted by the NCCP, a list of potential focus sites for high resolution anoxia risk assessment was suggested (Table 1). Following further discussion and initial simulations this list has been refined/adjusted based on considerations of data availability, and also to ensure the assessment will provide a range of differing contexts.

For each of the chosen sites (Figure 5), a detailed mesh was created ([Surface-water Modeling System](#) (SMS) version 12), spanning the main river and lakes, and the associated floodplains and adjacent wetland systems. The chosen sites each exhibit a heterogenous range of habitats, which were classified according to the Australian National Aquatic Ecosystem ([ANAE](#)) Classification Framework. The ANAE habitat IDs, were mapped to SMS “material zone” IDs for use in the TUFLOW-FV-AED2 modelling system, as shown in Figure 5. These domains represent a variety of conditions likely to be impacted, including shallow and deep environments, and areas with low and high degrees of hydrologic connectivity (and therefore flushing potential).

Table 1. Overview of sites being simulated to assess factors influencing carp mortality risk.

Site	State	Rationale
Selected sites chosen for detailed model assessment		
Lock 1 – Swan Reach (Lower Murray River)	SA	An important river channel reach with extensive connections to shallow wetlands with periodic connectivity. Downstream site in the MDB, likely to experience very high mortality loads.
Tailem Bend – Murray Bridge (Lower Murray River)	SA	As above, including several sites of concern to water utility WTP offtakes.
Chowilla	SA	A geo-morphologically and hydrologically complex system with regulated flows and locks likely to exhibit complex patterns of carp accumulation. Important biodiversity context, and high biomass region.
Lower Lakes	SA	Shallow lake/wetland system of regional significance. Existing data and model calibration make this site a safe test-case. Potential for accumulation in Lake Albert or shallow areas around barrages.
Moonie River (portion)	QLD	Inland northern river system subject to seasonal reductions in river pool connectivity, and warm temperatures.
Considered but not included due to data limitations for model setup, or perceived low risk		
Yarrawonga Reservoir	NSW	Large MDB storage and river reach with high value ecological assets downstream
Lachlan River (portion)	NSW	Typical MDB “wet” river reach with overlap to CSIRO modelling
Woods Lake	TAS	Lacustrine system of high value to recreational fishing community with cooler climate and potential for wind induced circulation and carp redistribution
Vasse-Wonnerup wetland system	WA	A highly seasonal drain-river-lagoon system in southern WA that experiences a wide range of temperatures, salinities and flow extremes, plus gate operation where stratification and hypoxia risk exists.

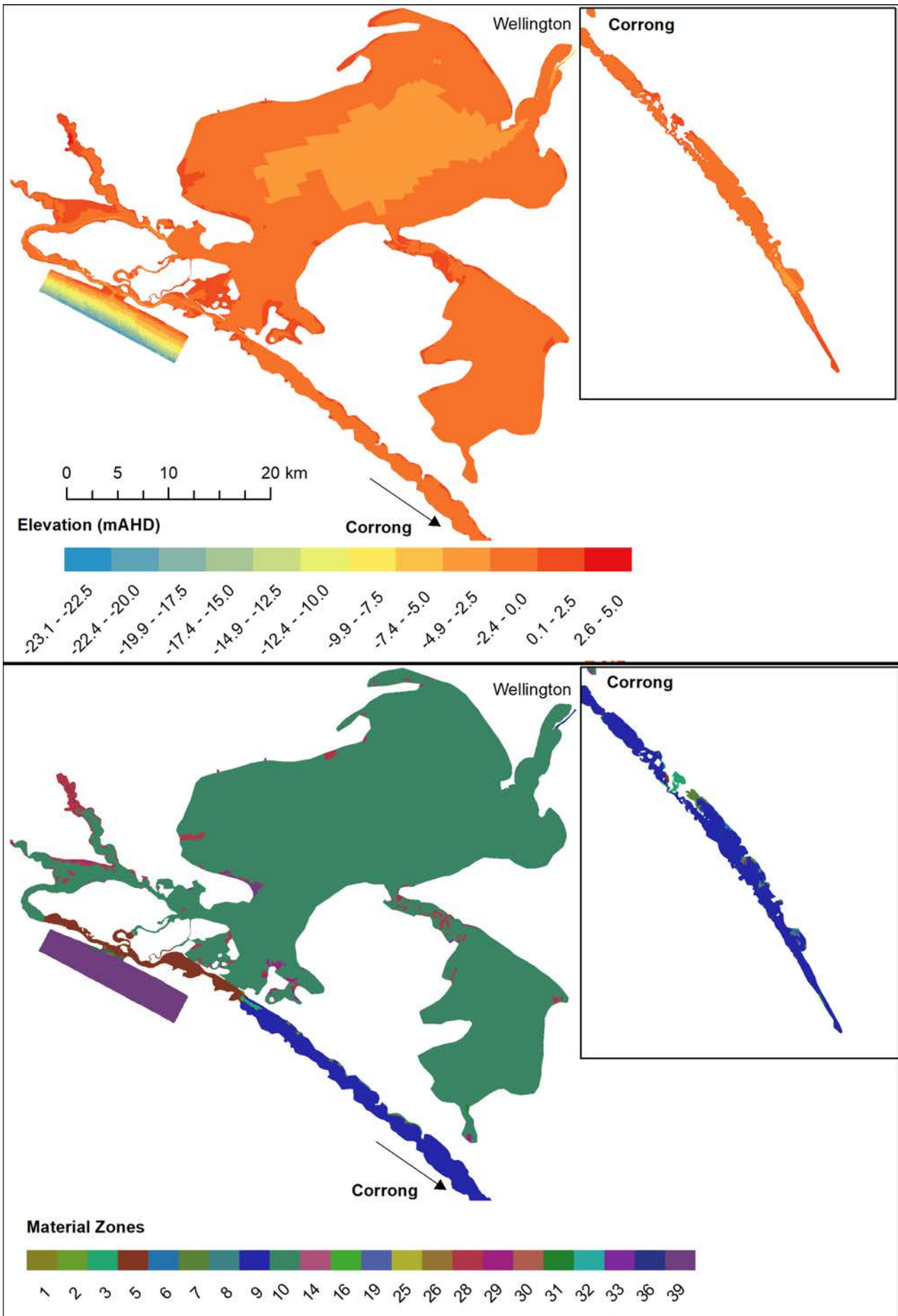


Figure 5a: Lower Lakes simulation domain showing the bathymetry (top) and ANAE based material zones (bottom).

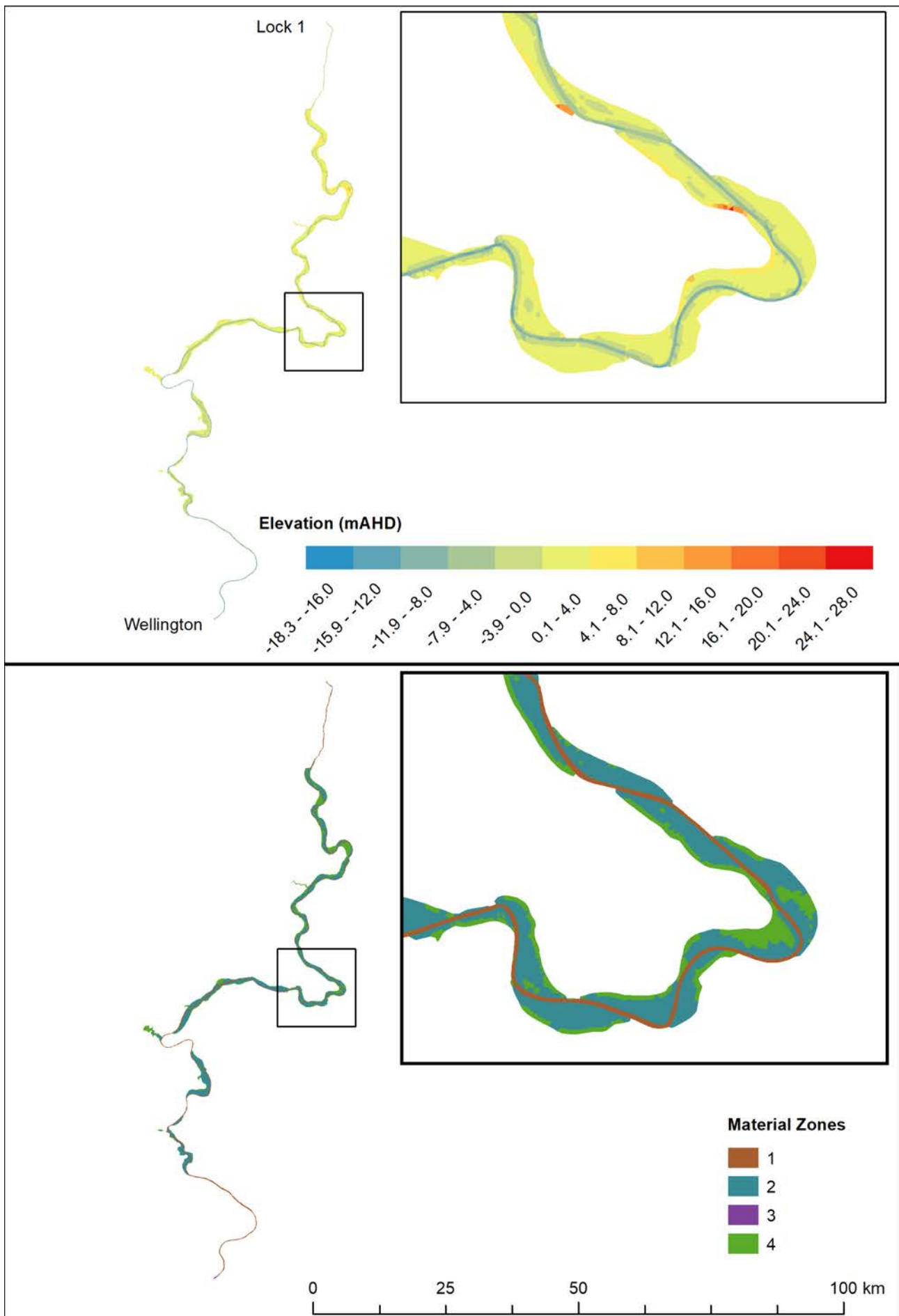


Figure 5b: Lower Murray simulation domain showing the bathymetry (top) and ANAE based material zones (bottom).

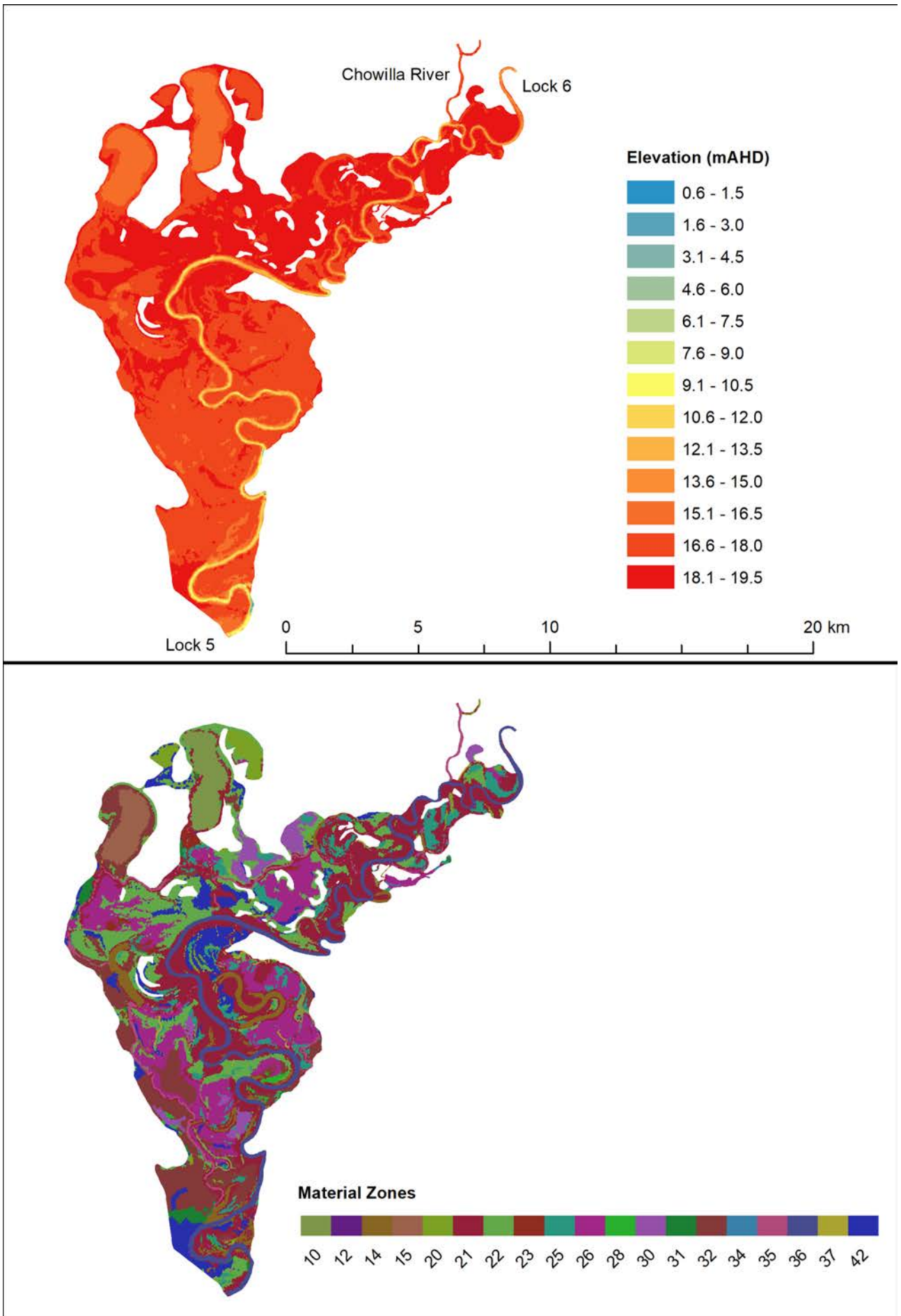


Figure 5c: Chowilla simulation domain showing the bathymetry (top) and ANAE based material zones (bottom).

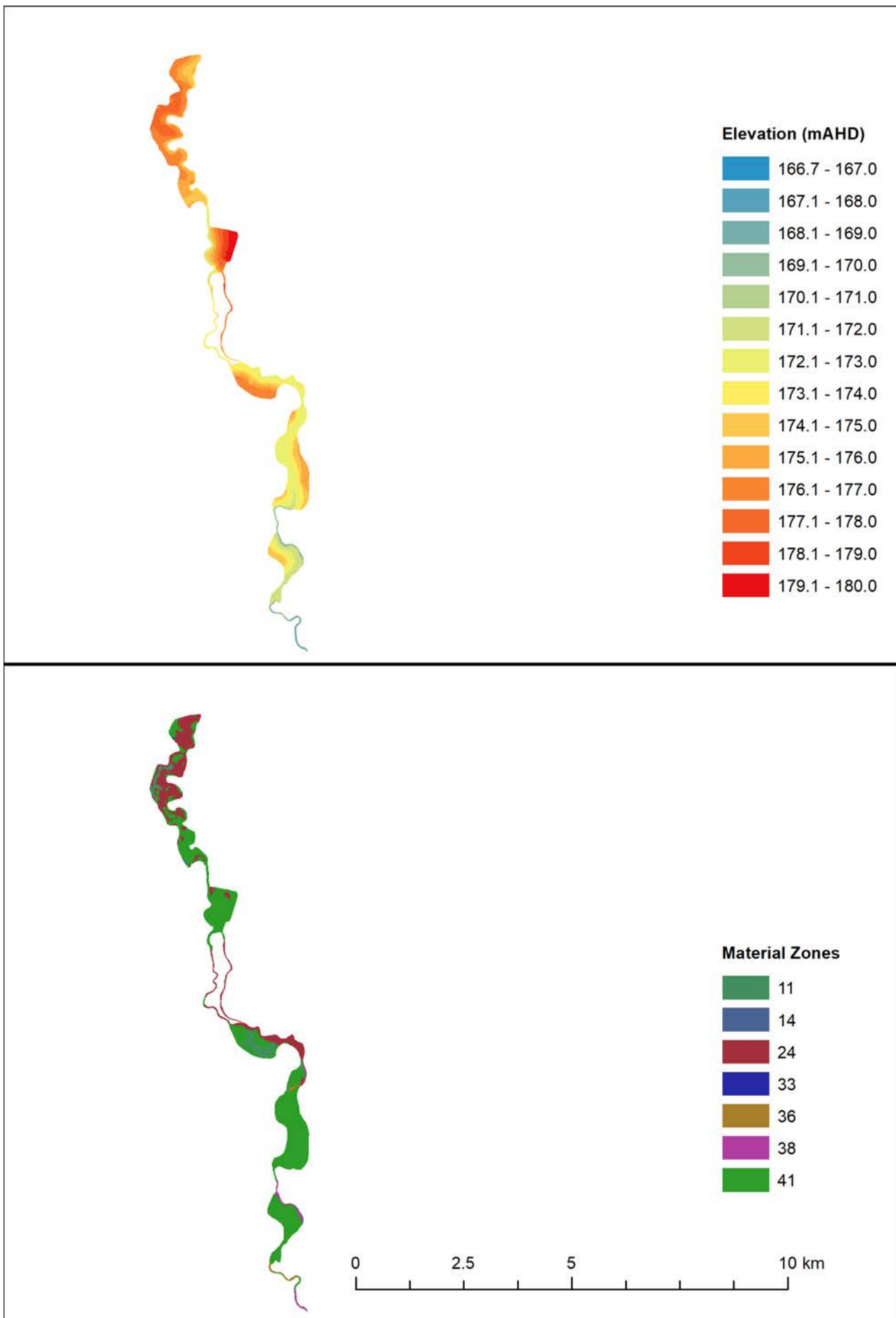


Figure 5d: Moonie River simulation domain, showing the bathymetry (top) and ANAE based material zones (bottom).

Model Setup and Validation

General approach and simulation framework

The approach to the assessment (Figure 6) involved multiple steps to a) first ensure the environmental models were suitable for simulation of water flow, temperature and water quality, and b) then assess the impacts of carp mortality over a wide range of conditions.

In this first step, key questions we were considering during the validation included:

- Can the model adequately capture seasonal differences, and differences associated with variable flow regimes (eg, low flow, normal flow and flood conditions)?
- How well does the model capture temperature heterogeneity? For example, the difference between vegetated floodplain conditions vs open-water systems, or the difference between a deep river channel and a shallow wetland environment?
- Does the model accurately portray drivers of (background) oxygen metabolism? For example, can the model capture the balance of primary productivity and respiration, and how this balance is impacted by hydro-meteorological conditions, and occurrences such as blackwater events.

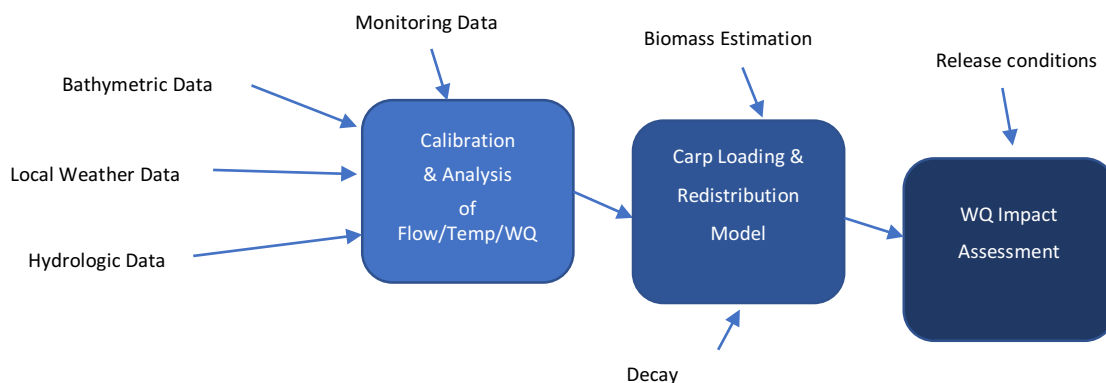


Figure 6: Overview of modelling approach, covering the initial setup and assessment of the environmental model, the loading and decay model, and then the subsequent water quality risk assessment.

In the second step, due to the uncertainty in the biomass, release conditions and how these manifest under different hydrologic scenarios, a “scenario matrix” approach was adopted spanning alternate conditions that may arise, allowing us to identify thresholds of loading where water quality risks become high.

Questions include:

- Is there a critical level of biomass that depletes oxygen below accepted thresholds?
- At what biomass does nutrient release from the carp biomass create a concern for algal bloom risks, or ammonium toxicity?
- Does accounting for particle accumulation change the risk profile, relative to evenly distributed biomass?
- Can we generalise about certain hydrologic settings where risks need to be prioritised?

River and lake ecohydrological models

Model platform

The base model platform for the assessment is the three-dimensional (3D) coupled model TUFLOW-FV (hydrodynamics) and AED2 (water quality). The model adopts an unstructured mesh and a finite volume numerical approach to predict the water flow, and includes extensions to simulate temperature and salinity, and is therefore able to capture stratification where relevant. The model links with AED2, which includes numerous modules for simulating water quality processes, such as oxygen, organic matter, nutrients and algae (Hipsey et al., 2019). See Appendix A for a summary of data sources used to setup and drive the models.

Water quality model validation summary

This task required the setup of the model to cover a range of hydrologic conditions, and was therefore run over drought, normal and flood periods. It also looked at seasonal differences in sites, and differences between habitat areas (e.g. main river vs wetland responses). To achieve this, we setup the model using available geo-spatial, hydrologic and meteorological data. We then compiled field monitoring data from all available collection campaigns that have been conducted in the region, to assess and calibrate the model, with a particular focus on temperature and oxygen. The model also simulates other factors, but the focus was on assessing the capability of the model to capture key processes and dynamics relevant to temperature and oxygen.

To cover off on the above questions we took the complex network of aquatic systems below Lock 1 as our focus since we had access to a wide variety of monitoring data. This is combining the separate domains to improve the range of conditions considered by our model assessment: the lower River Murray and Lower Lakes. As such, the site extent covered numerous types of aquatic habitats, including the main river channel, wetlands, floodplains, tributaries, shallow lakes and the estuary/lagoon at the Murray Mouth. We ran this for several years, thereby capturing conditions of drought, post-drought flooding, and subsequent “normal” flow conditions.

Overall, the model performance has been very good. Generally, the model was able to capture the seasonal changes in temperature across different conditions including flood and drought, the diurnal changes in temperature and oxygen metabolism, and differences between different habitat types. Some discrepancies occurred in very shallow waters during drought conditions, where the model under-predicted temperatures. However, based on the extensive analysis across many sites, the model is considered to now be competent in being used as a base platform, from which we can now start assessing carp loading scenarios. A summary of the model setup and predictions are presented below.

The initial validation effort focused on the Lower Lakes model domain (Figure 7, see also Figure 3a), where a large volume of historical (observed) water quality data was available spanning the 2008-2013. In particular there was a range of data spanning the main water column and the shallow tributary and wetland areas.

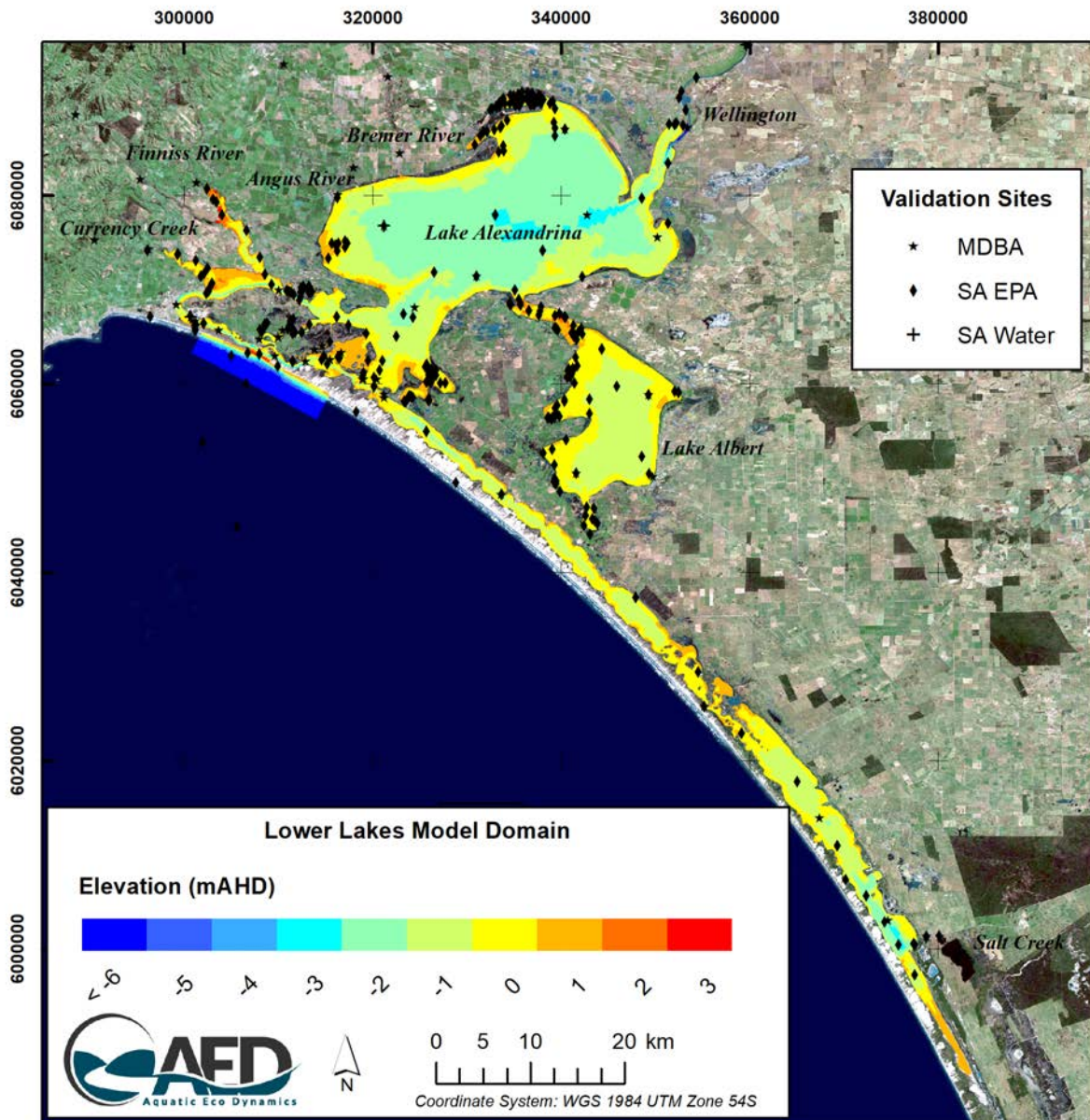


Figure 7: Overview of modelling approach, covering the initial setup and assessment of the environmental model, the loading and decay model, and then the subsequent water quality risk assessment.

The model setup is driven by sub-daily inputs from the main river and the side tributaries, and the weather forcing (including wind and solar heating etc), and oceanic conditions at the river mouth. The model is run in 3D with several cells resolving the vertical profiles of water conditions. The temperature and oxygen validation plots are shown below (Figure 8). Other water quality variables (TN, TP, Chl-a and TSS) were also validated.

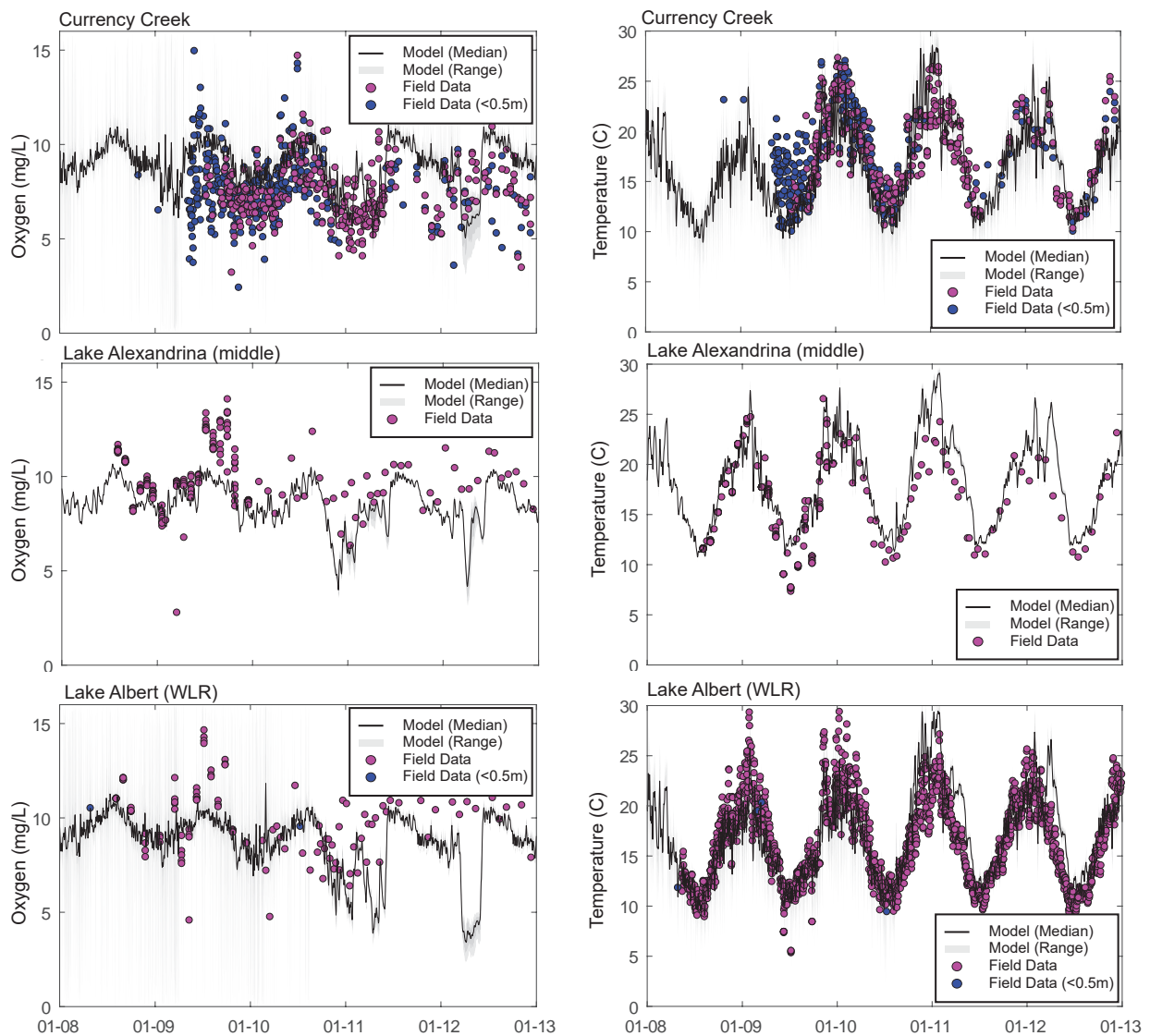


Figure 8: Five years of temperature (right) and oxygen (left) for three different regions within the lakes domain. Data is separated between shallow (<0.5m) and deeper waters.

A map of the Lower Murray River model domain, and sources of observational data is shown below (Figure 9), highlighting the resolution of the main river channel, with the curvilinear profile cells, and the wetland and floodplain cells on the margin.

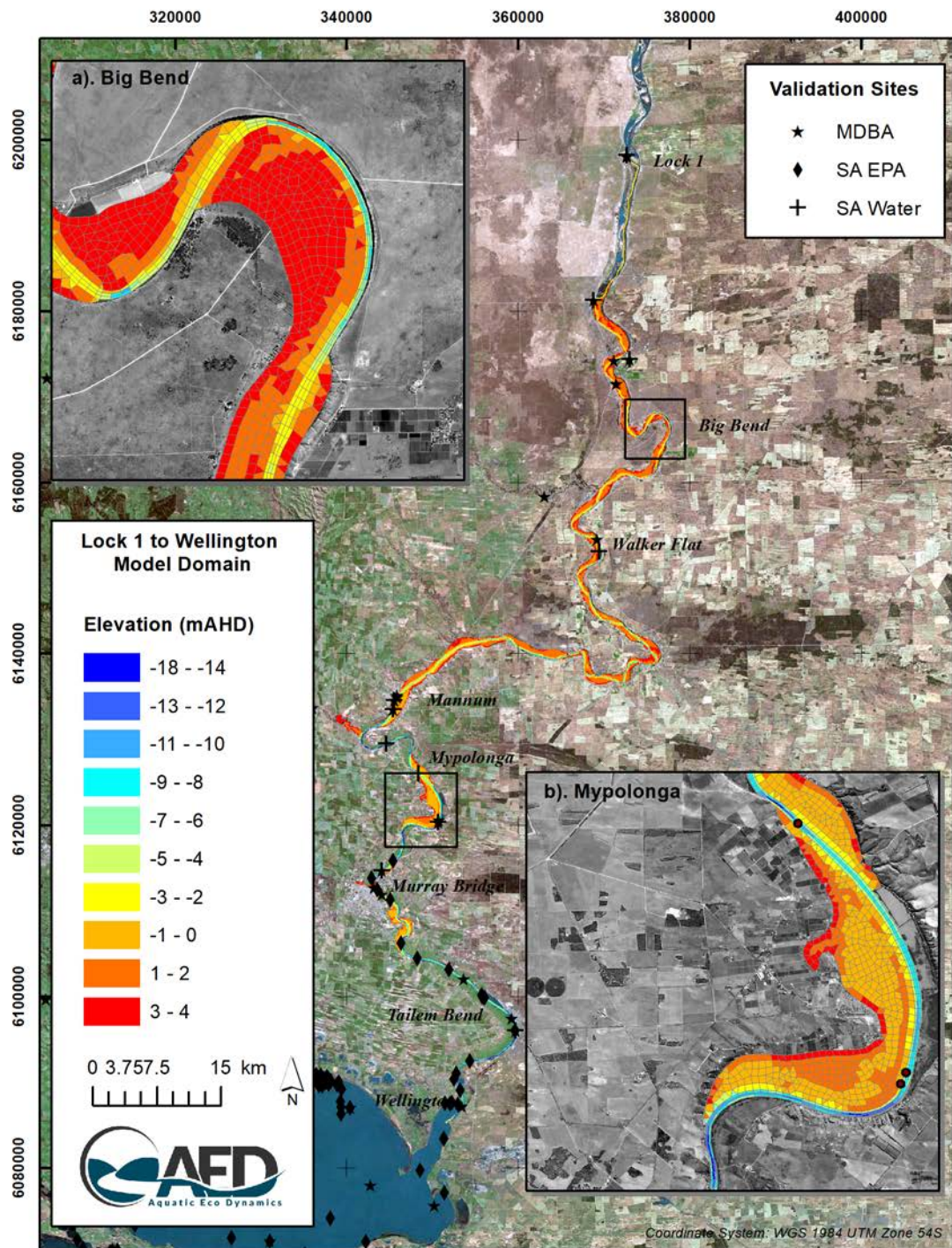


Figure 9: The Lower Murray River model domain.

In the case of the river reaches of the basin, there is a significant difference from the lakes in that the vegetation density overlaps with the hydrodynamic domain and the extent of vegetation can provide shading, and impact flow velocities (e.g. contributing to more stagnant areas). A map of the Lower Murray River model vegetation distributions is shown in Figure 10, which were derived from a remotely sensed image classification process.

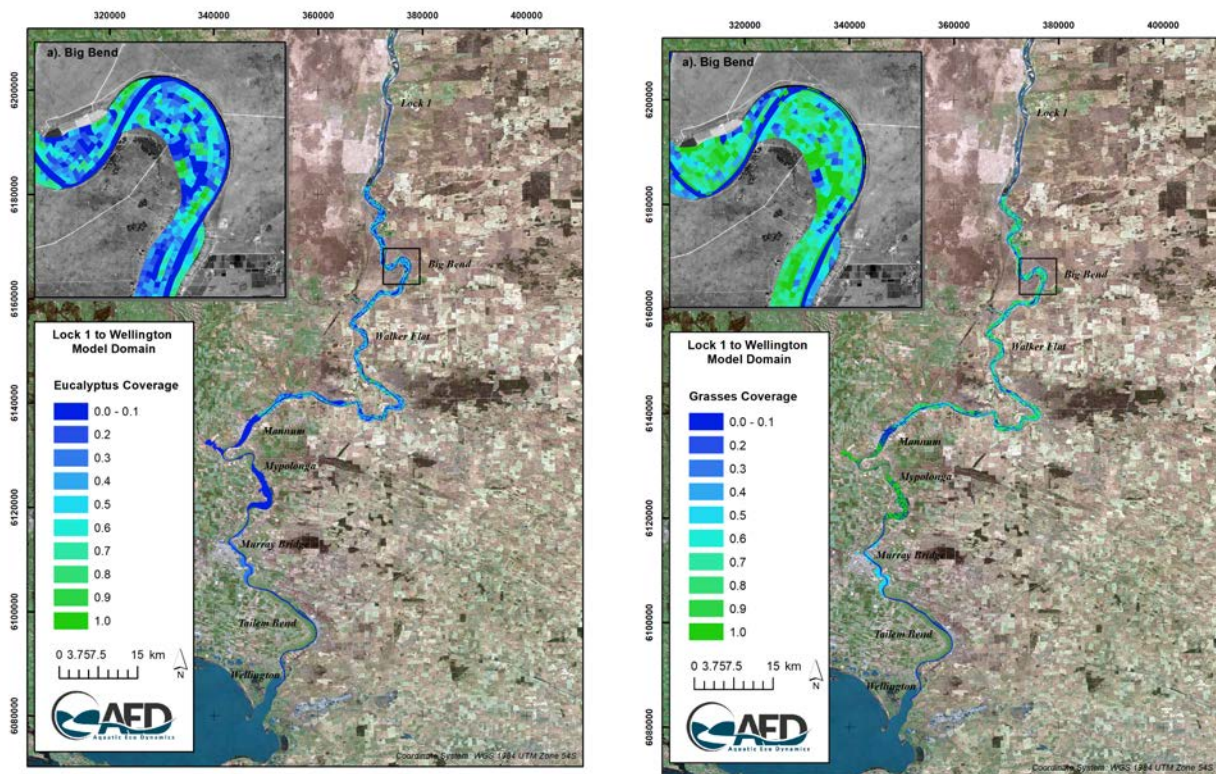


Figure 10: Vegetation density of the overstorey (top) and understorey (bottom) for the Lower River Murray study region.

This simulation was setup in a similar fashion to the Lower Lakes simulation, driven by river inflow forcing at Lock 1, and weather forcing from regional data available from the SA government (Appendix A), and offtake extractions were from the SA Water dataset. Two years of temperature and oxygen for three different regions within the Lower Murray River domain are shown in Figure 11, compared with available data collected within the river. Note that in this simulation, 2009 is a drought year, and flood waters are received in 2010 (note the oxygen declining in the latter part of the simulation due to blackwater inputs).

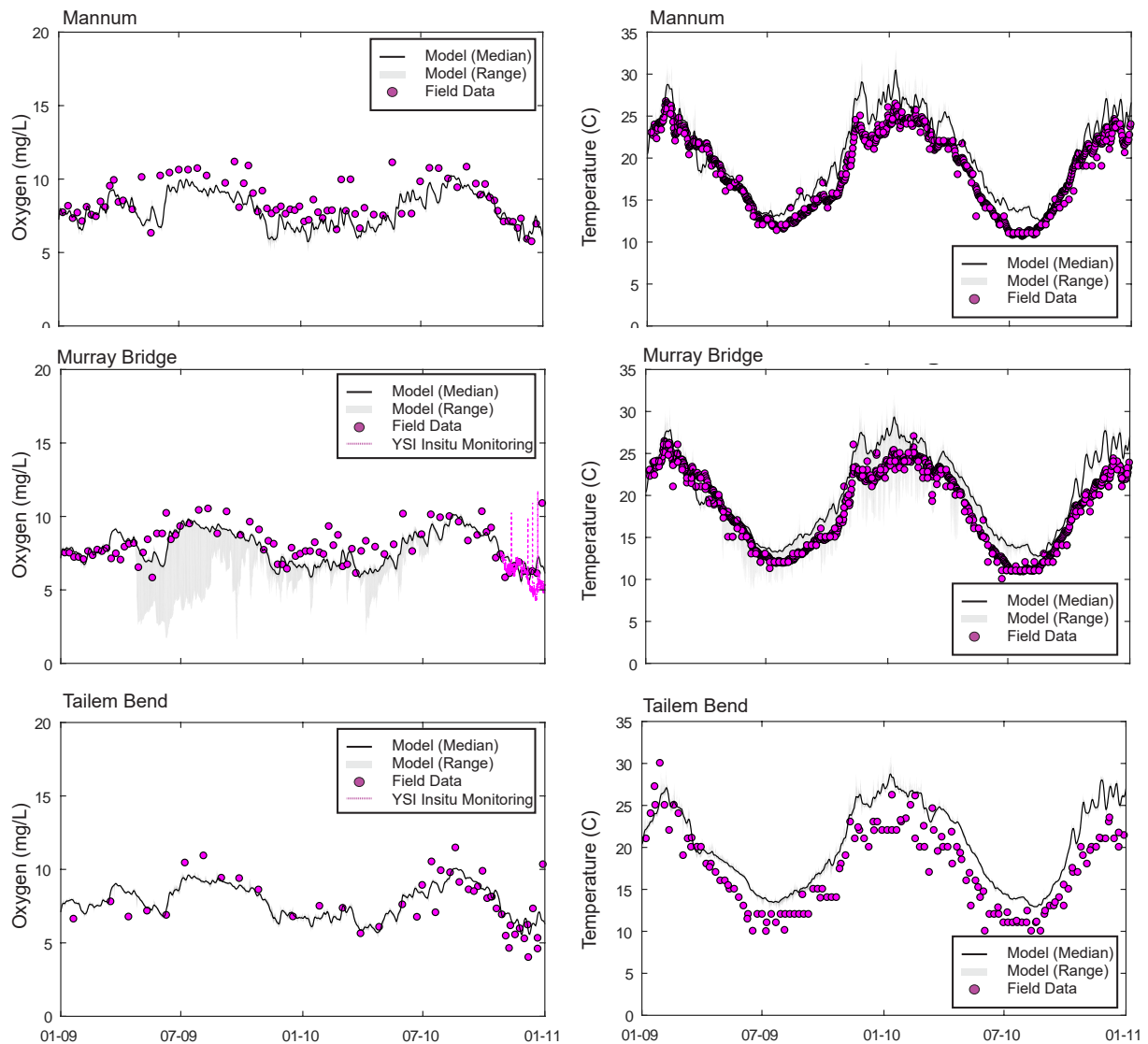


Figure 11: Two years of temperature (right) and oxygen (left) for three different regions within the river domain.

Because the river dynamics are highly dependent on flow conditions the domain is quite variable in terms of its underlying oxygen metabolism in wet and dry conditions. Figure 12 shows difference in temperature and oxygen separated between the side wetlands and the main river channel (for a region near Murray Bridge); note the patterns responding to changes in flow connectivity that occurred when the flow exceeded $600 \text{ m}^3/\text{s}$.

In order to ensure the model was reasonably capturing the “background” controls on oxygen metabolism and primary productivity, Figure 12 also highlights the diurnal and seasonal balance between oxygen creation (GPP) and sediment oxygen demand (SOD), and response to a notable increase in carbon loading (TOC) during the flood period. Figure 13 looks more closely at this by zooming in to see the river flow and oxygen dynamics during a post-drought flooding phase (late 2010), and the post-flood recovery phase (mid 2011).

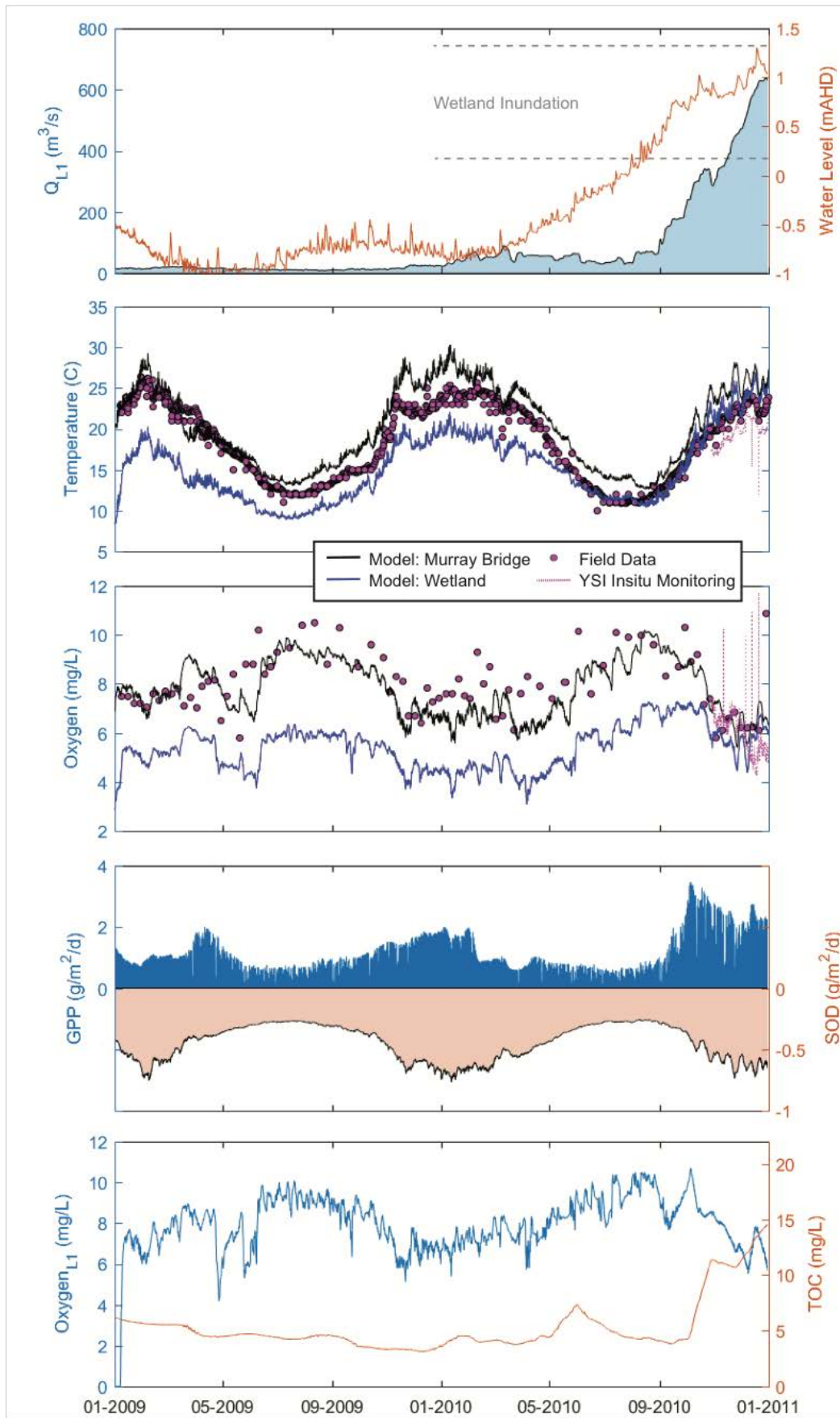


Figure 12: River domain temperature and oxygen near Murray Bridge, separating the main channel and wetland regions, and exploring the controls on oxygen metabolism (GPP and SOD) in response to upstream loading of carbon (TOC), bottom panel.

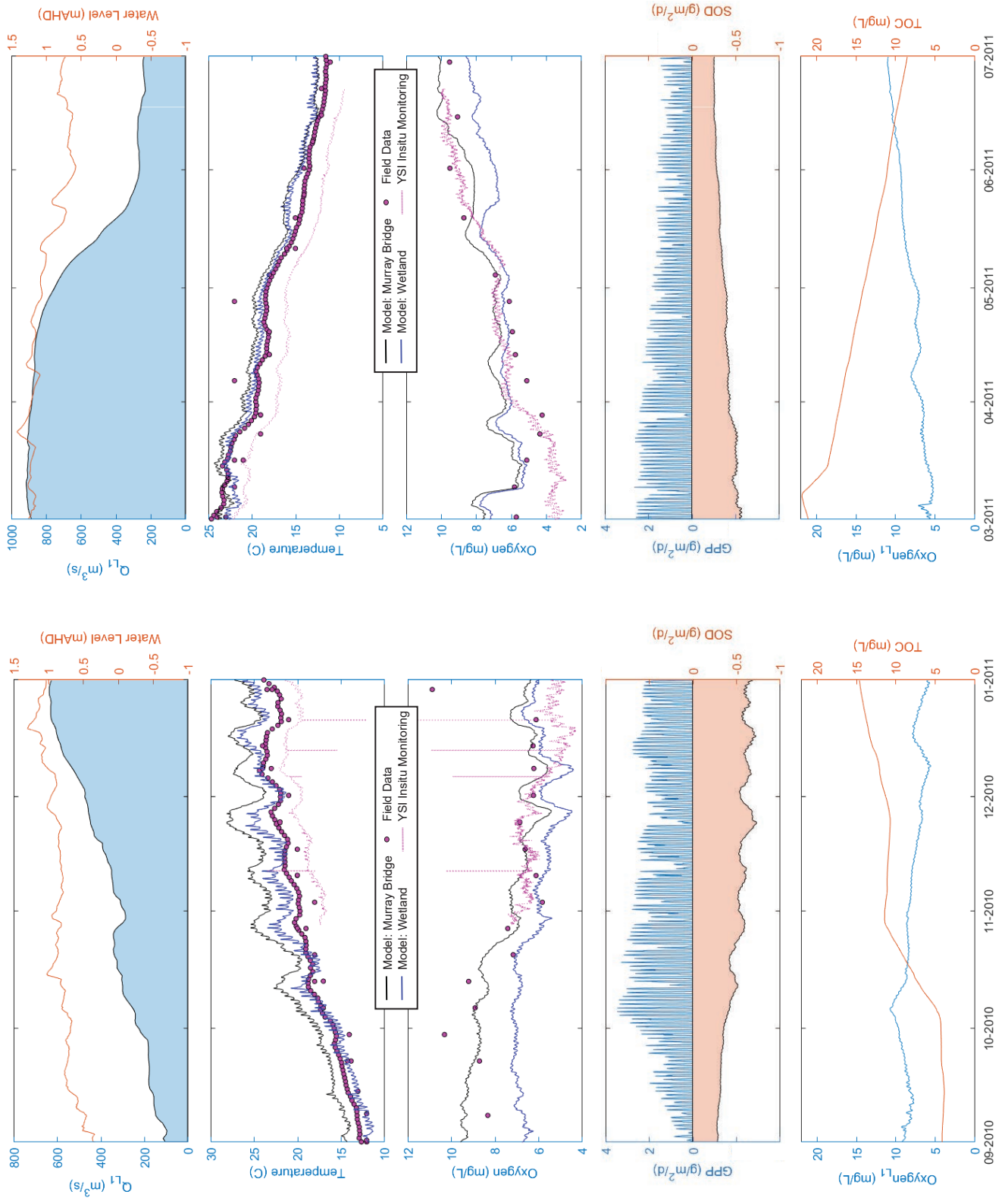


Figure 13: As for Figure 12, but zoomed into the flood and post flood period.

Temperature and oxygen validation of the ecohydrological model was not conducted within the Chowilla and Moonie River as it was not within the scope of the project. For the Chowilla domain, it is conceptually similar to the previous domains and was setup to have similar flow and weather forcing (except sourced from local sites). The Moonie domain however was slightly different in that it is a system more typical of the periodically drying systems in the North of the Basin. Whilst no data was available to validate in depth the pool dynamics, we did however undertake a stratification analysis of pools in the Moonie to examine the frequency of pool stratification and to ensure we were capturing the typical diurnal cycle of oxygen metabolism that occur under normal conditions. An example of this is shown in Figure 14.

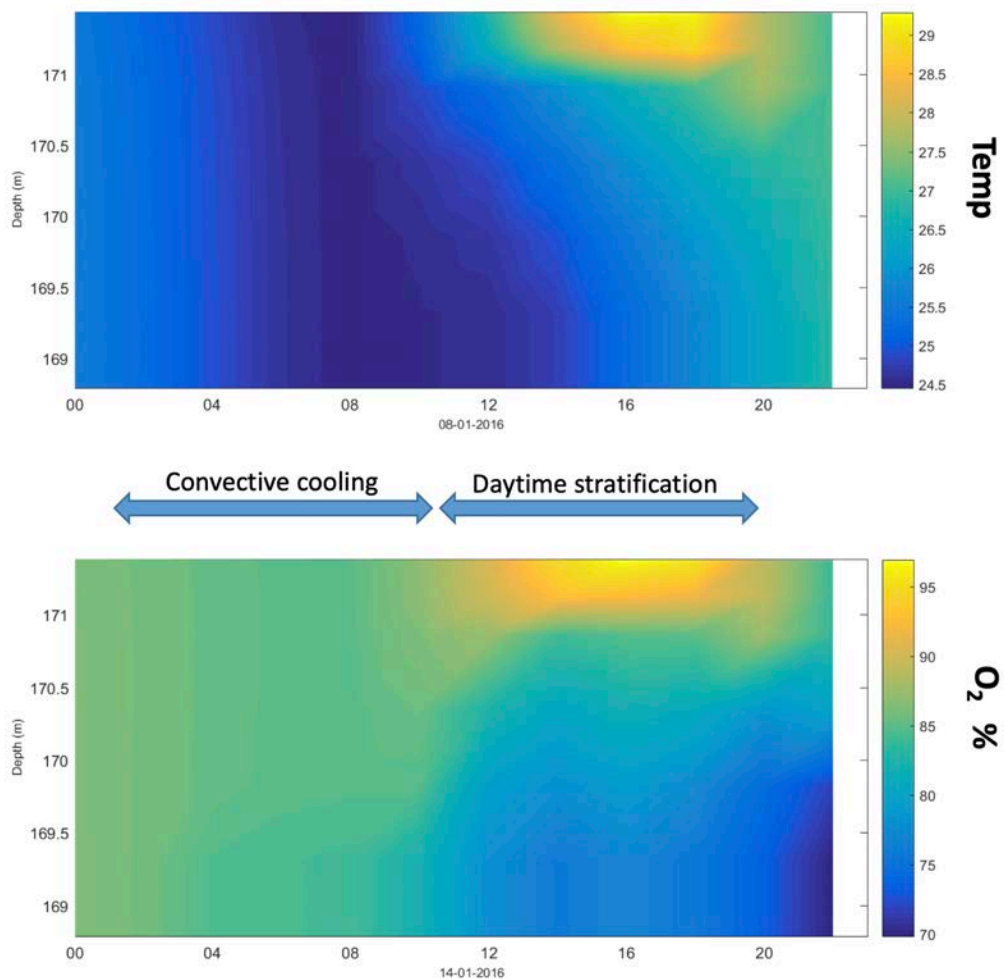


Figure 14: Stratification of temperature and oxygen predicted within a pool of the Moonie River domain.

Carp Mortality Model

The rationale and core processes relevant for the carp mortality model is presented in the previous section. Below we outline the details of two approaches adopted to assess mortality, HC and DCP, and how these are setup in relation to data collected by the biomass project, the epidemiological project and the decay experiments.

Homogenised carp (HC)

For the first approach, the carp biomass is spread over the domain. Biomass shape files (polygons) from the NCCP biomass project were interpolated onto the model meshes, so each cell of the model domain had an indicative carp density (kg fish / Ha), see Figure 15. The fish biomass was then converted into an equivalent mass of C per square metre, and associated N and P, based on an assumed fish stoichiometry. A time frame for the biomass to decay over was then assumed based on the decay rate of fish from the water quality experiments. The parameters associated with this approach are listed in Table 3, which were then used, in conjunction with the biomass density to work out the cell specific oxygen demand and nutrient release. In this case the material zone definitions in TUFLOW-FV mesh were used for AED2 to assign input release rates.

Table 3: Approach to convert fish biomass density to oxygen demand and nutrient release rates.

Variable	Value	Units	Comment
Carp biomass conversion to dry weight equivalent	1	kg WW / Ha	
	3	g WW/ g DW	χ_{DW}
	0.33	kg DW/Ha	
	333333.33	mg DW/Ha	
	33.33	mg DW /m2	
Assumed stoichiometry of carp biomass	0.47	g C /g DW	Guo et al., 2018
	0.1	g N /g DW	
	0.019	g P /g DW	
	80%	% decomp	
Carbon availability for respiration	12.53	mg C /m2	
	1.04	mmol C /m2	
Time scale of carp decay	14	days	
Areal carbon/nutrient flux rate	0.075	(mmol C /m ² /day) / kg fish	
	0.016	(mmol N /m ² /day) / kg fish	
	0.003	(mmol P/m ² /day) / kg fish	
Area flux partitioned into O ₂ consumption	-0.052	(mmol O ₂ /m ² /day) / kg fish	Note: used for HC carp simulation only.
Area flux partitioned into DOC leachate	0.022	(mmol C /m ² /day) / kg fish	
Area flux partitioned into DON leachate	0.005	(mmol N /m ² /day) / kg fish	
Area flux partitioned into NH ₄ release	0.011	(mmol N /m ² /day) / kg fish	
Area flux partitioned into DOP leachate	0.001	(mmol P/m ² /day) / kg fish	
Area flux partitioned into PO ₄ release	0.002	(mmol P/m ² /day) / kg fish	

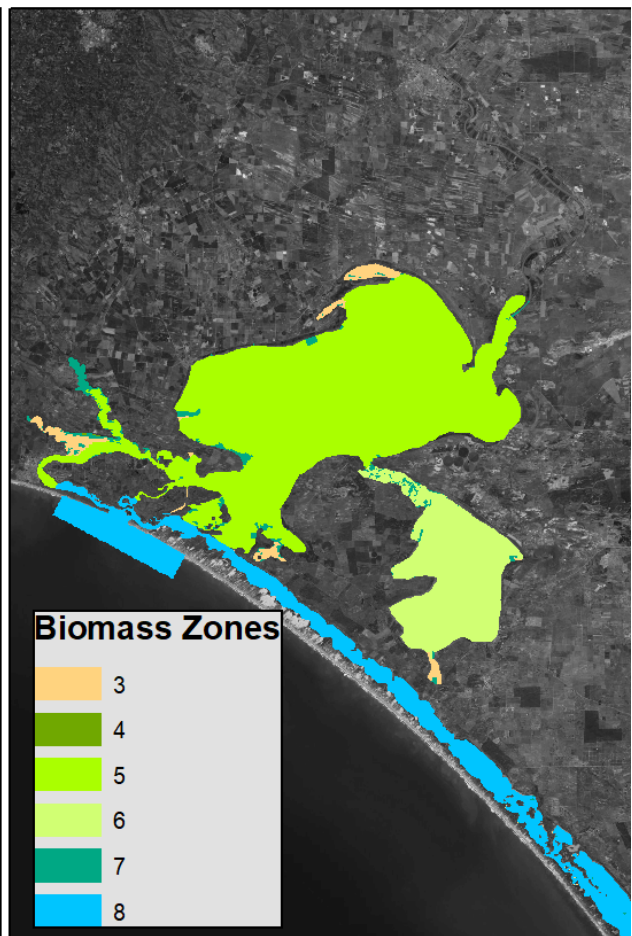
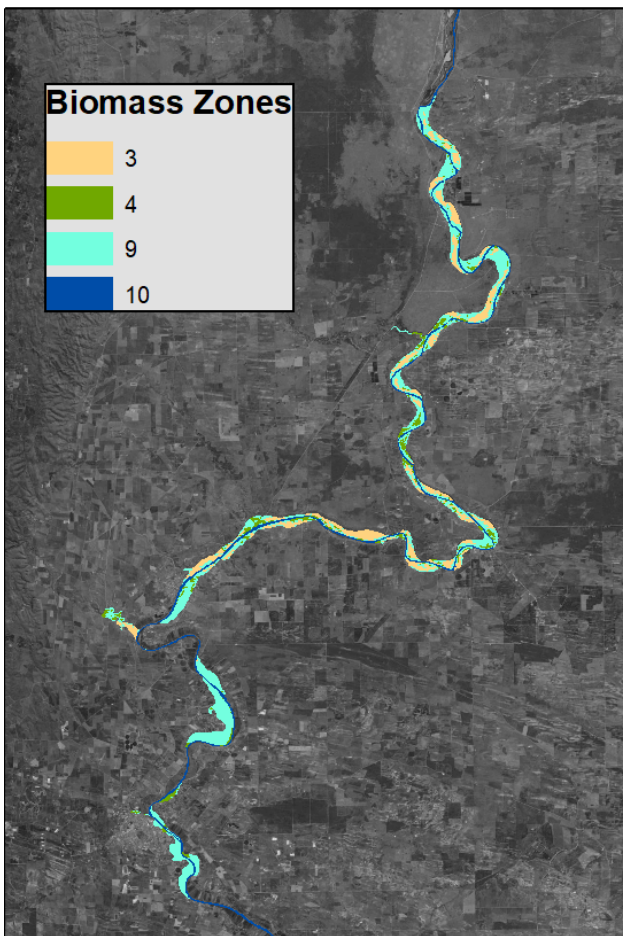
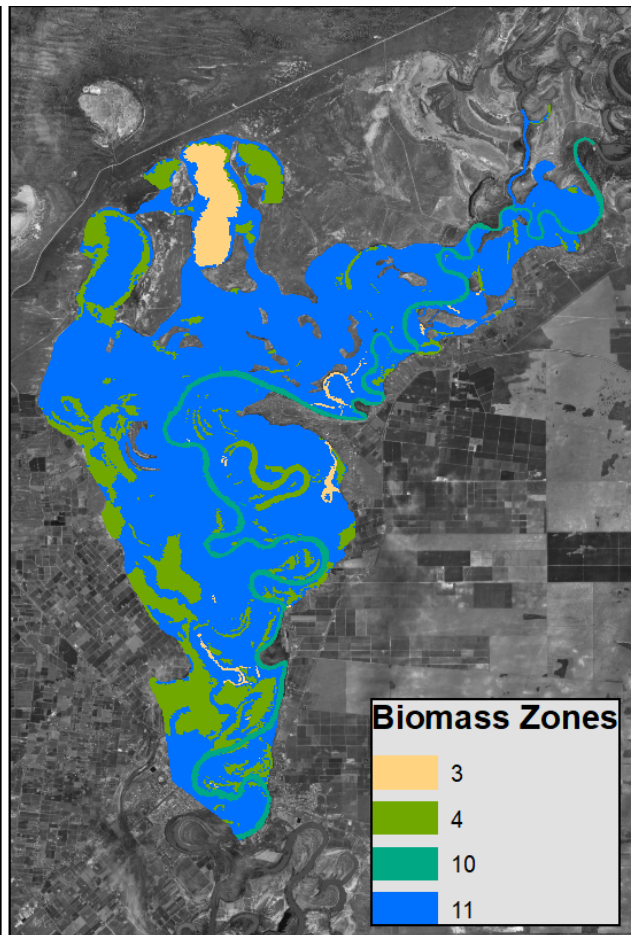
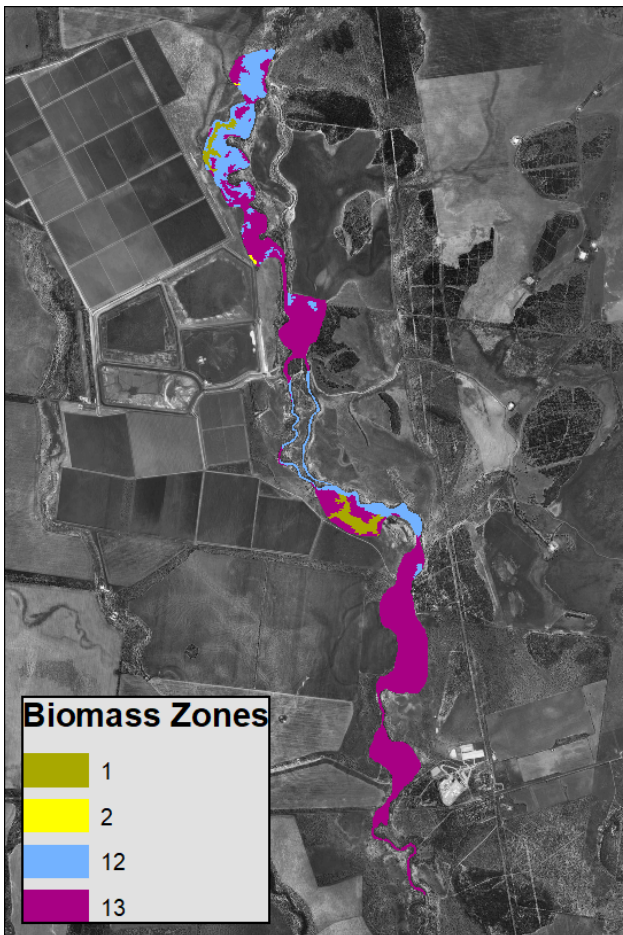


Figure 15: Biomass zones used in the 4 regional sub-domains. See Table B1 for biomass values.

Decaying carp particles (DCP)

In this model approach, the dead carp mass are treated as a set of Lagrangian “particles”, which move through the model domain based on interpolation of the velocities predicted within the model cells. In addition, the particles are configured to be able to float or sink. The particles do not necessarily reflect an individual fish, but rather a “representative” set of fish, with an assigned mass. This model approach utilises the TUFLOW-FV Particle Transport Model (PTM) functionality.

Based on the predicted distribution of modelled particles, the AED2 oxygen and nutrient modules were configured to be updated based on the rate of decay assigned to the particles. In this way, cells that have a large number of particles resting within them, also experience a large oxygen demand and nutrient release, and these impacts will subsequently affect neighbouring cells as the low oxygen conditions are mixed to the hydrodynamic processes.

Model parameterisation and setup:

Step 1: Carp particle inputs

Each focus site was modelled over a range of flow conditions, and depending on the flow, the water circulation with the river and wetland will develop. Within the model carp particles could enter at the inflow boundary and progress into the domain.

Assigning the number of particles, $N_{P_{in}}$, and the rate at which they enter, $n_p(t)$ provides the inflowing timeseries. The total particles entering over a time period, T , is:

$$N_{P_{in}} = \sum_{i=0}^I \int_{t=0}^T n_p(t) dt$$

where t is time and I is the number of inflow boundaries. The total mass of dead fish material entering the domain is therefore $N_{P_{in}} \chi_{DW}$, where χ_{DW} is the dry-weight of the representative particle before it begins to decay. Defining the function $n_p(t)$ is relatively uncertain, and for this application a random function is adopted that serves to introduce particles randomly through time, with varying numbers. Initial trials with a uniform distribution were used, however, a more complex distribution could also be implemented, to allow clustering of fish inputs, for example, to represent entry the of dense accumulations.

Step 2: Internal carp particle generation

The main source of carp mortality within the simulated domains was the internal generation of new carp particles (DCPs). These were assumed to occur randomly throughout time, and anywhere within the extent of the model mesh. As above, the total number of generated particles was computed, based on a generation rate:

$$\underbrace{\sum_{a=1}^A \frac{B_a A_a}{P_{DW_0}}}_{\text{biomass density used to estimate total mass of fish in domain}} = N_{P_{gen}} = \underbrace{\sum_{c=0}^{N_c} \int_{t=0}^T n_G(t)_c dt}_{\text{multiple time-series of DCPs being added into cells across the domain}}$$

where c = cell index, N_c = total number of cells in mesh, t = time, T = duration of delivery (days), a = ANAE habitat index class, B_a = biomass in habitat “a” (kg/Ha) (see Figure 15), A_a = area of habitat unit (Ha) within the simulated domain, A = number of habitat areas active within the domain, P_{DW_0} = average fish mass prior to decay (kg), and $n_G(t)$ = delivery time-series (kg/day) at a given point in the domain.

The particles created at any given time must be assigned to a cell where they enter the domain (i.e., their point of mortality). This is based on a sample of the all the available cell centroids. A non-uniform random probability function was implemented to allow certain geographic locations to develop particles at a different rate, based on where the biomass project identified higher levels. Or this could be adapted, for example, to account for preferential habitat where carp congregate. The timeseries functions at the DCP input positions, denoted by $n_G(t)$ on the RHS, were randomised, but constrained to ensure that the integrated total number of particles, matches the total on the LHS, as estimated by the NCCP biomass project. An example check of the input biomass to the Lower Lakes domain is shown below in Figure 16a.

Step 3: Carp particle transport

The total number of carp particles in the domain varies over time as particles are added (or removed), $N_p(t)$; the total number is the sum of $N_{P_{gen}}$ and $N_{P_{in}}$, at the time $T = t$. Each particle, P , is assigned a location on entry, $[P_x, P_y]$, and then is subject to transport with the currents generated within the model. Full description of the particle transport model is beyond the scope of this document, and readers are referred to the documentation describing the Lagrangian particle transport numerical scheme within TUFLOW-FV.

In addition to transport within the water, the vertical position in the water column depends on the density of the particle relative to the water, according to Stoke’s Law. The vertical velocity is computed as:

$$P_w = \frac{d_p^2 g (P_\rho - \rho_w)}{18\mu}$$

where d_p is the particle “diameter” and P_ρ is the density of particle P . This is applied in each time-step to track the vertical position, denoted P_z . The density of the dead fish particle is known from anecdotal evidence to change over time. For new particles the density is set to be low, due to buoyancy provided by gases that accumulate within the fish during its initial decomposition phase. Over time, the fish becomes waterlogged and eventually heavier than the water, allowing it to sink. This is capture based on the age of any particular particle, P_{age} :

$$P_p = \begin{cases} 980, & P_{age} \leq 2 \\ 980 + \frac{P_{age} - 2}{8} (1020 - 980), & 2 < P_{age} < 10 \\ 1020, & P_{age} \geq 10 \end{cases}$$

Once a particle hits the bottom, its status, P_s is logged as being sedimented. It can become resuspended when the bottom shear stress, τ , exceeds a user defined critical value, P_τ , and re-enter the bottom cell of the water column.

An example test of the DCP transport for the Lower River Murray is shown in Figure 16b. Note this does not include the random carp inputs across the domain (Step 2) but is specifically demonstrating post input transport and deposition position after entry from a discrete site.

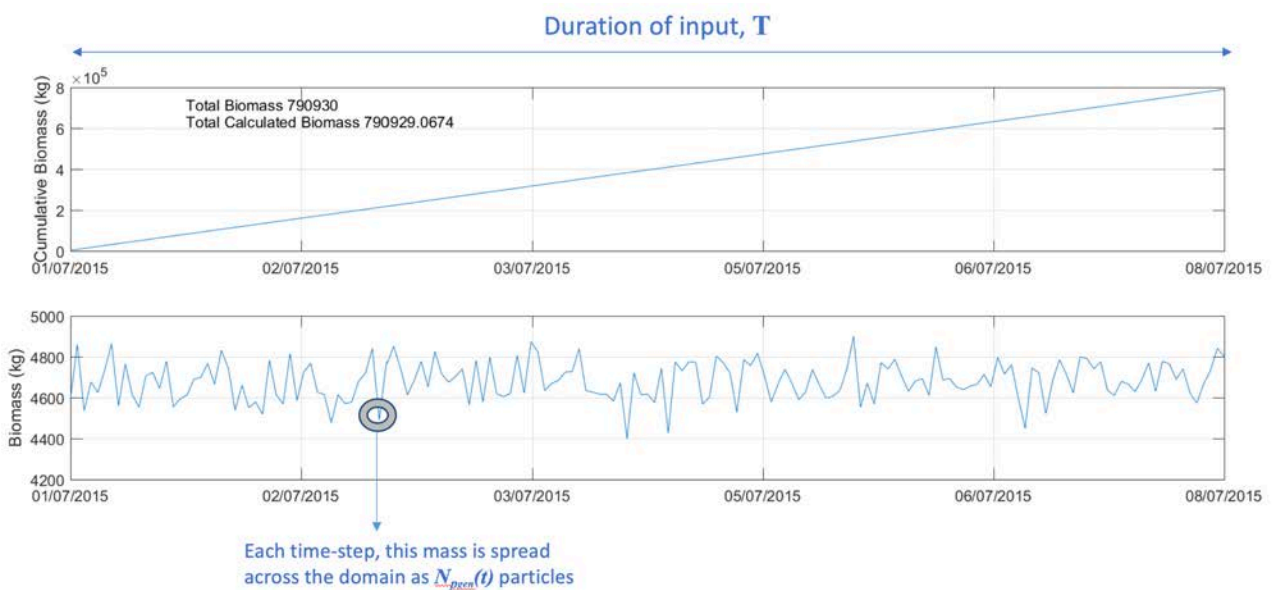


Figure 16a: Checking process of the biomass introduction into a domain, highlighting how random inputs in the domain over the time period, T , cumulate to contribute to the total available biomass.



Figure 16b: Example output from the DCP model showing carp particle transport after input at two discrete locations in the lower River Murray domain.

Step 4: Carp accumulation

Carp accumulation is not a specific modelled process but an outcome that emerges based on circulation and particle properties, within the context of a domain's bathymetry. It could manifest as particles tending to move along the bottom to deeper holes within the bathymetry, or on the water's edge if blown by the wind, during a falling water level, for example. Sensitivity tests were conducted with the model to understand the importance of DCP "sticky-ness" (as determined by the critical shear stress for remobilisation after deposition). To help visualise the accumulation outputs on the model Figure 17 shows a graphic representation of how particles can preferentially build up in areas of the domain where flows are reduced.

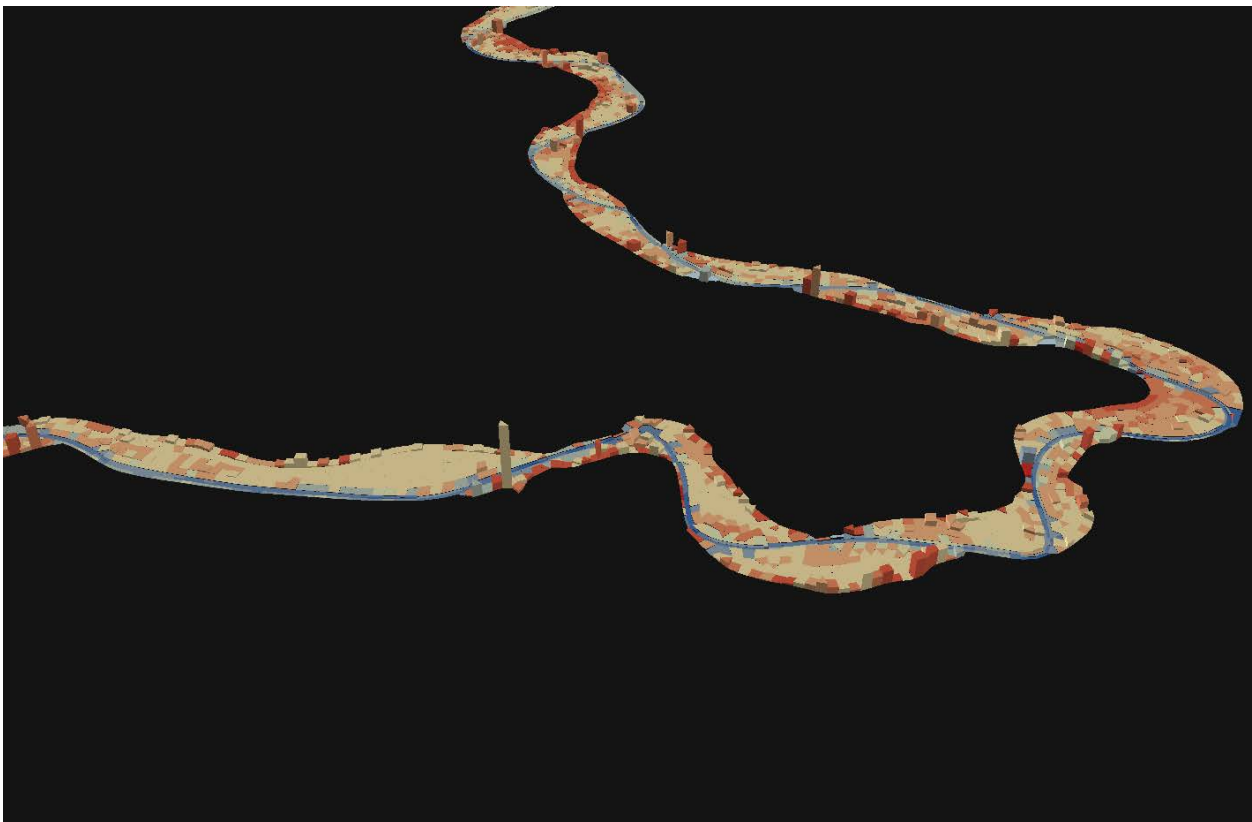


Figure 17: Hotspot densities of carp accumulation in two reaches of the lower Murray River. The colour indicates the cell bathymetry (i.e., water depth), and the vertical height indicates the relative mass of accumulated particles.

Step 5: Carp decay and water quality impacts

As particles move through the domain they can interact with the water column properties, such as oxygen. The rate of oxygen consumption in a cell, c , for an individual particle can be calculated based on the particle mass, such that:

$$\frac{d[O_2]_c}{dt} = \frac{P_{DW}(t) \chi_{C:DW} \chi_{O:c} r_{BOD}[T, P_{age}(t), P_S]}{A_c \Delta z_c}$$

where $\chi_{C:DW}$ is the dry-weight to carbon ratio, and $\chi_{O:C}$ is the carbon to oxygen stoichiometry associated with microbial respiration. The cell, c , that a particle is contained within is computed by comparing the cell outline with the co-ordinates $[P_x, P_y]$ each water quality model time-step (generally 15mins), and this is stored as P_c . The mass of the particle decays from the initial mass: $P_{DW}(t) = \chi_{DW}(1 - r_{BOD}[P_{age}]\Delta t)$. The rate of fish particle decay, r_{BOD} , adopts a two-stage decay rate depending on the particle age, P_{age} , (up to a decay limit), the particles status, P_S , and the water temperature.

Similar expressions are solved for NH_4 , PO_4 , DOC, DON and DOP release into the water.

Little Duck Lagoon DCP validation test:

Given the release of the carp virus and associated mortality is proposed it is not possible to fully validate the model. However, we made an attempt at checking the mass balance assumptions and indicative response by simulating the Little Duck Lagoon experiment (Figure 17). The model is overly simplified relative to the real conditions in that it did not have the high settings seen for benthic oxygen metabolism in the field data, and it had assumed depth profile and weather forcing conditions.

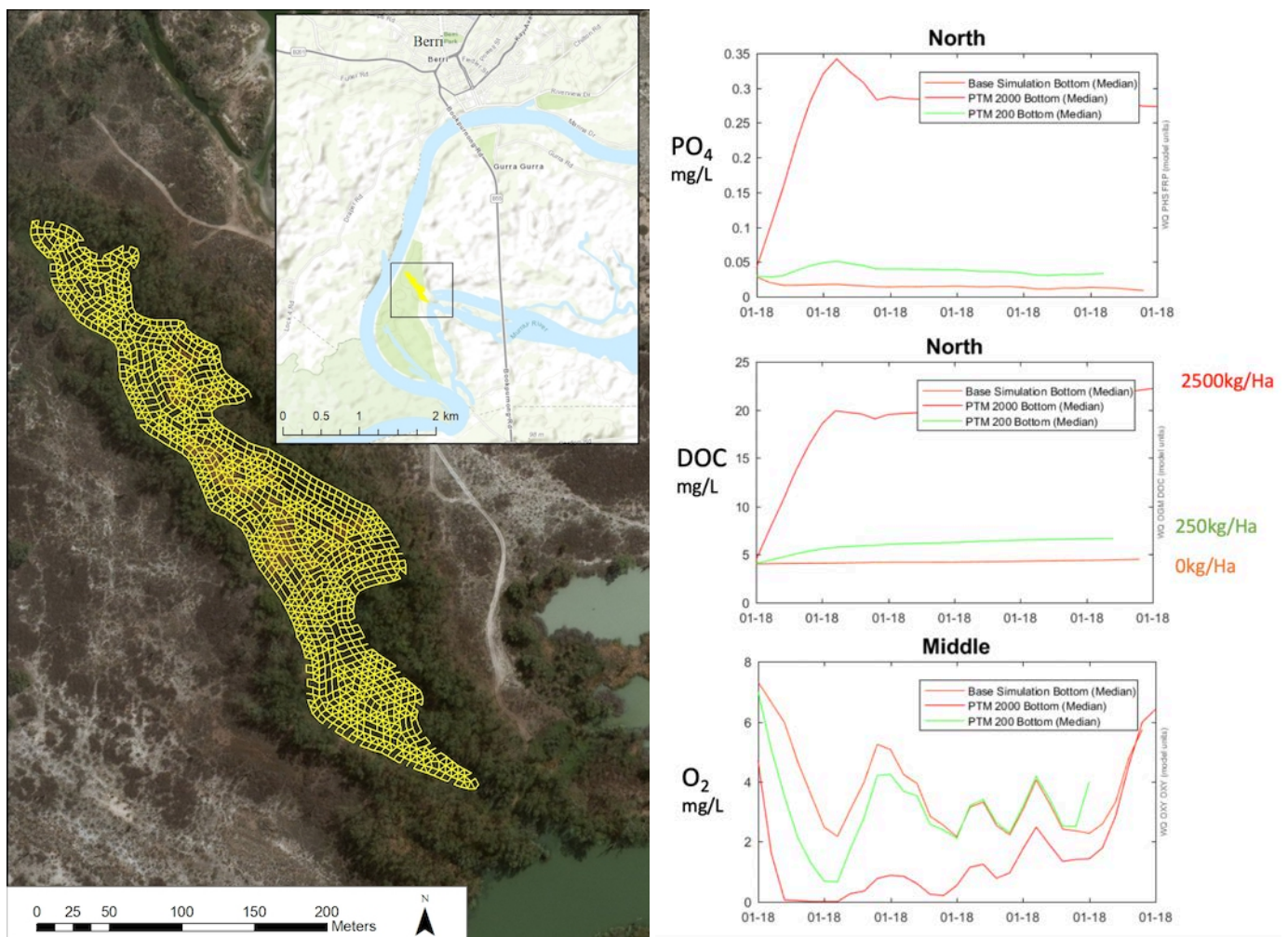


Figure 18: Setup of the Little Duck Lagoon “idealised” model, left, and comparison of PO_4 , DOC and O_2 under base conditions (orange) and under two DCP loading scenarios ($B=2500$ kg/Ha and 250 kg/Ha; red and green, respectively), right.

Nonetheless the accumulation of leachate products and the length of the oxygen drawdown period could be examined relative to the observed changes. A summary table of the end concentrations in the observed data and from the model, show some discrepancy, but overall the predicted effects are consistent with the observations (Table 4).

Table 4: Comparison of mean concentrations water quality parameters from the end of the Little Duck Lagoon carp loading experiment at actual biomass (2400 kg/ha) with modelled equivalents.

Water attribute	quality	Observed (Biomass 2400 = kg/ha)	Max (min) concentration reported	Modelled concentration	Default trigger values (mg/L)
Total Phosphorus		2.5	6.2		0.1
Total Nitrogen		20	38.9		1
Phosphate		0.6	4.8	0.275	0.04
Ammonia		0	36.7		0.9 ^a
Nitrate			0.07		0.1
DOC		60	196.0	22	-
Chl- <i>a</i>		1.4	1.854		0.005 ^c
BOD			95.3		15 ^b
O ₂	location dependent	(0)	(0)	(0)	

a: General trigger value for freshwater (95% species protected) at pH 8

b: Aquaculture recommended guidelines

c: South eastern Australia lowland river guidelines

Model setup and scenario matrix approach

As there remains a high level of uncertainty as to the specific biomass loading and conditions that may be experienced at a given site, the above HC and DCP approaches to modelling a domain are not just run for a single set of conditions, but for many permutations of flow and biomass amount. The following steps were undertaken with each of the simulation domains:

- i. Identify the time period to test the simulation, based on the suitable temperatures for virus activity (17-25C, Graham et al. 2019)
- ii. Identify the typical flow conditions, to work out the base case hydrologic conditions
- iii. Set a range of alternate flow conditions, described as a multiplier of the base-case values.
- iv. Run a base-case simulation set of all the different flows assuming no carp biomass was active.
- v. Set a range of potential biomass values that could enter the domain, described as a multiplier of the default values obtained by the NCCP biomass project. The multipliers were adopted to account for mortality efficiency of the virus, and also to identify where the threshold's for loads to impact water quality would sit.
- vi. Carp particle accumulation hotspots and water quality response were then assessed for each simulation and summarised for specific reporting sub-regions within the domains.

For step (i) of the assessment, Figure 19 below shows the suitability windows of virus activity, based on simulated temperatures, which were used to identify the simulation time periods to run the assessment.

Fore step (ii), the flow duration curves (FDC) from the available data are shown in Figure 20. The flow conditions during the chosen assessment period (i.e., the base-case conditions) are shown on this plot to give context as to the conditions experienced in these domains.

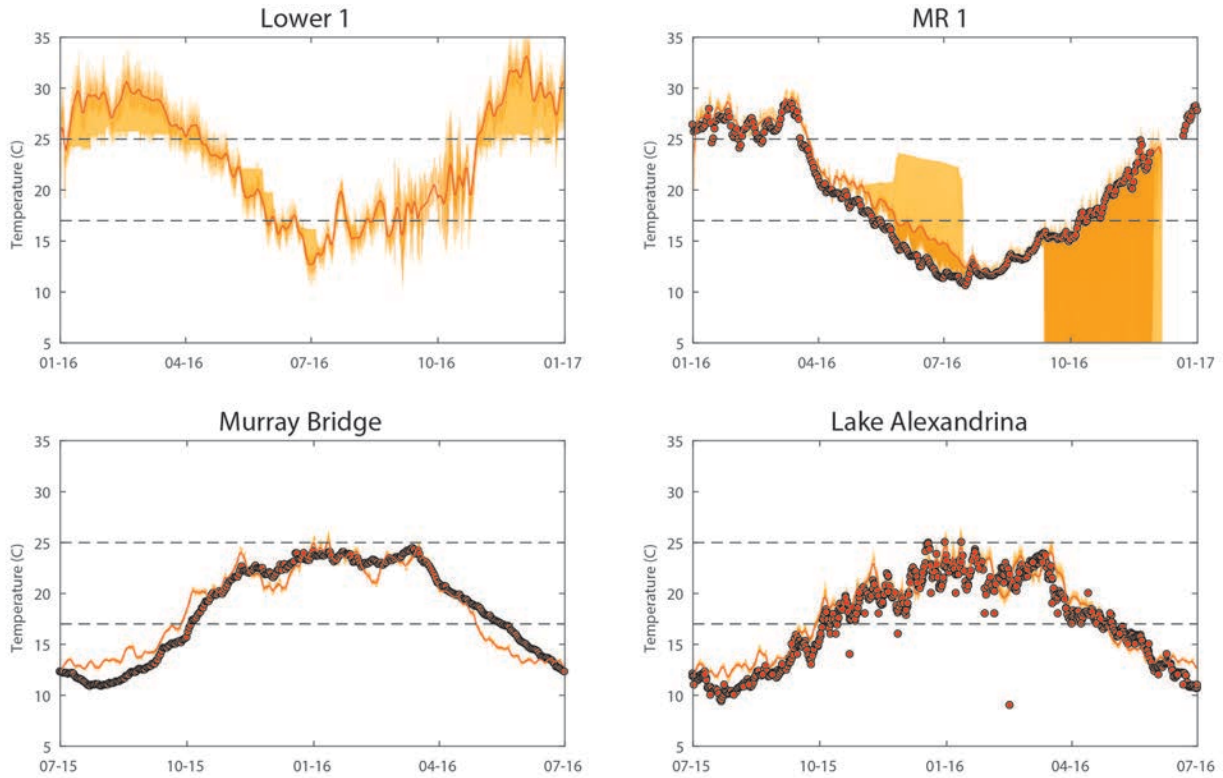


Figure 19: Modelled temperature outputs (orange line is median and orange shading is the range) of the 4 model domains moving down river from top-left to bottom-right, with the suitability periods of virus transmission (17-25C) indicated. These time-periods in the suitable range were adopted as the simulation time-periods in the model assessment simulations (see also Appendix A). Where available, field data are also shown.

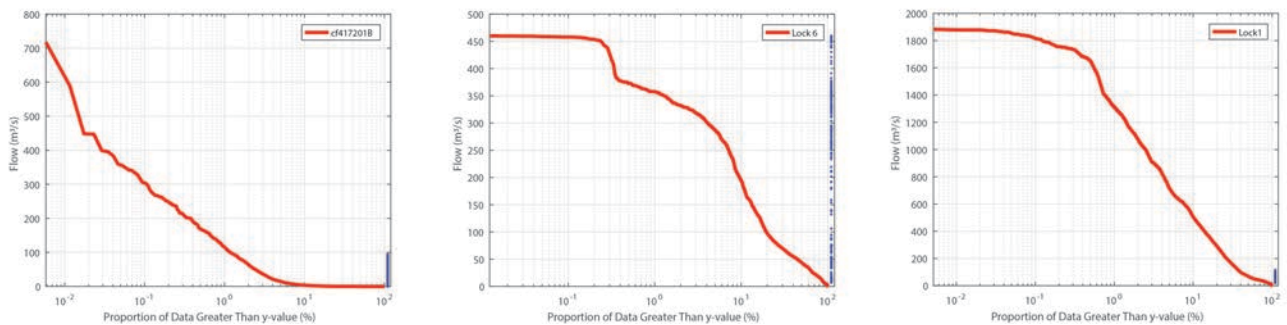


Figure 20: Flow duration curves computed from the raw flow data within the Moonie River (cf417201B) and the Murray River (@ Lock 6 and Lock 1). Note Lock 1 data was assumed for both the Lower River Murray and Lower Lakes domain since their hydrologic regime is similar in this regard. The blue dots on each panel summarise the range of conditions covered during the chosen simulation period.

Water Quality Risk Assessment

Assessment metrics

Oxygen

To assess the impact of carp mortality on oxygen we computed the oxygen “sag” over the mortality period as:

$$\overline{\Delta DO}_{q,b} = \frac{1}{A_{AR} N_c} \sum_{c=0}^{N_c} (DO_{q,b}^c - DO_{q,0}^c) A_c$$

where N_c is the number of active (wet) cells within the assessment polygon/region and q and b represent the scenario indices for flow and biomass, respectively. This metric is therefore the oxygen sag in a region relative to the mean oxygen that region would experience, in mg/L.

Additionally, we computed the likelihood of a cell within the region exceeding an acceptable threshold for low oxygen exposure. Table outlines the estimated DO thresholds of four Australian lowland river predatory fish species (Small *et al.* 2014). We set a conservative threshold value, DO^{crit} , of 4 mg/L which we assessed for each domain sub-region to compute $P(DO | DO < DO^{crit})$.

Table 5: Estimates of lethal dissolved oxygen (DO) concentrations for four Australian lowland river predatory fish.

Fish species	DO threshold estimate (mg/L)	SE
Murray cod <i>Maccullochella peelii</i>	4.80	0.74
Golden perch <i>Macquaria ambigua</i>	1.72	0.63
Silver perch <i>Bidyanus bidyanus</i>	2.65	0.60
Eel-tailed catfish <i>Tandanus tandanus</i>	1.85	0.53

Nutrients and cyanobacteria

To assess the impact of carp mortality nutrients we adopt a similar approach, by computing the mean concentration increase over the mortality period:

$$\overline{\Delta DP}_{q,b} = \frac{1}{A_{AR} N_c} \sum_{c=0}^{N_c} (DP_{q,b}^c - DP_{q,0}^c) A_c$$

$$\overline{\Delta DN}_{q,b} = \frac{1}{A_{AR} N_c} \sum_{c=0}^{N_c} (DN_{q,b}^c - DN_{q,0}^c) A_c$$

where $DP = DOP + PO_4$ and $DN = DON + NH_4 + NO_3$ (all in mg/L).

The frequency of NH_4 exceeding the tolerable limit of 0.5 mg/L was also quantified, $P(NH_4|NH_4 > NH_4^{crit})$, as an indicator of potential ammonia toxicity to biota.

Rather than simulating the bloom formation dynamics of cyanobacteria, we instead adopt a ‘‘HAB Score Index’’ (HSI) approach which is calculated in order to provide a semi-quantitative measure of whether conditions for cyanobacteria are favourable. The index is designed to consider temperature, T , light I , water velocity v , and the degree of vertical stratification, $\Delta\rho$, and the level of bioavailable nutrients, (NO_3, NH_4, PO_4) . As with the other metrics, the base conditions may already be susceptible to cyanobacteria blooms, and so the ΔHSI is reported as a measure of how carp mortality has increased the risk.

$$\overline{\Delta HSI}_{q,b} = \frac{1}{A_{AR}N_c} \sum_{c=0}^{N_c} (HSI_{q,b}^c - HSI_{q,0}^c)A_c$$

The HSI in any individual cell is computed as :

$$HSI^c[T, \Delta\rho, N, P] = f(\Delta\rho)f(T) \min[f(N), f(P)]$$

where $\Delta\rho = \rho_{bottom} - \rho_{surface}$, and T, N & P are temperature, light intensity, bioavailable nitrogen and phosphorus, respectively, representing conditions the cell c . The limitation functions are set as:

$$f(\Delta\rho) = \begin{cases} 0, & T_{surface}^c - T_{bottom}^c < 0.1 \\ \max \left[\frac{4 - (T_{surface}^c - T_{bottom}^c)}{4}, 0 \right], & T_{surface}^c - T_{bottom}^c \geq 0.1 \end{cases}$$

$$f(T) = \vartheta^{T^c-20} - \vartheta^{k(T^c-a)} + b$$

where $\vartheta = 1.08$, $a = 35.062$, $b = 0.107$ and $k = 4.110$; these fit a curve which corresponds to an optimum temperature of 34 and maximum tolerable temperature of 40°C. The nutrient limitation functions were assessed according to:

$$f(N) = \frac{NO_3 + NH_4}{NO_3 + NH_4 + K_N}$$

$$f(P) = \frac{PO_4}{PO_4 + K_P}$$

where $K_N = 4$, and $K_P = 0.15 \text{ mmol/m}^3$.

Hypoxia and anoxia assessment

Figure 21 summarises visually how the impacts on oxygen manifest, as demonstrated most clearly in the Lower Lakes domain. For this domain, assuming 100% biomass mortality contribution, the average oxygen deficit is 0.2-1 mg/L, with the main impact observed around the lake perimeter and in the shallow tributaries and lagoons. The other domains show relatively complex accumulation patterns and therefore hotspot areas where impacts are focused.

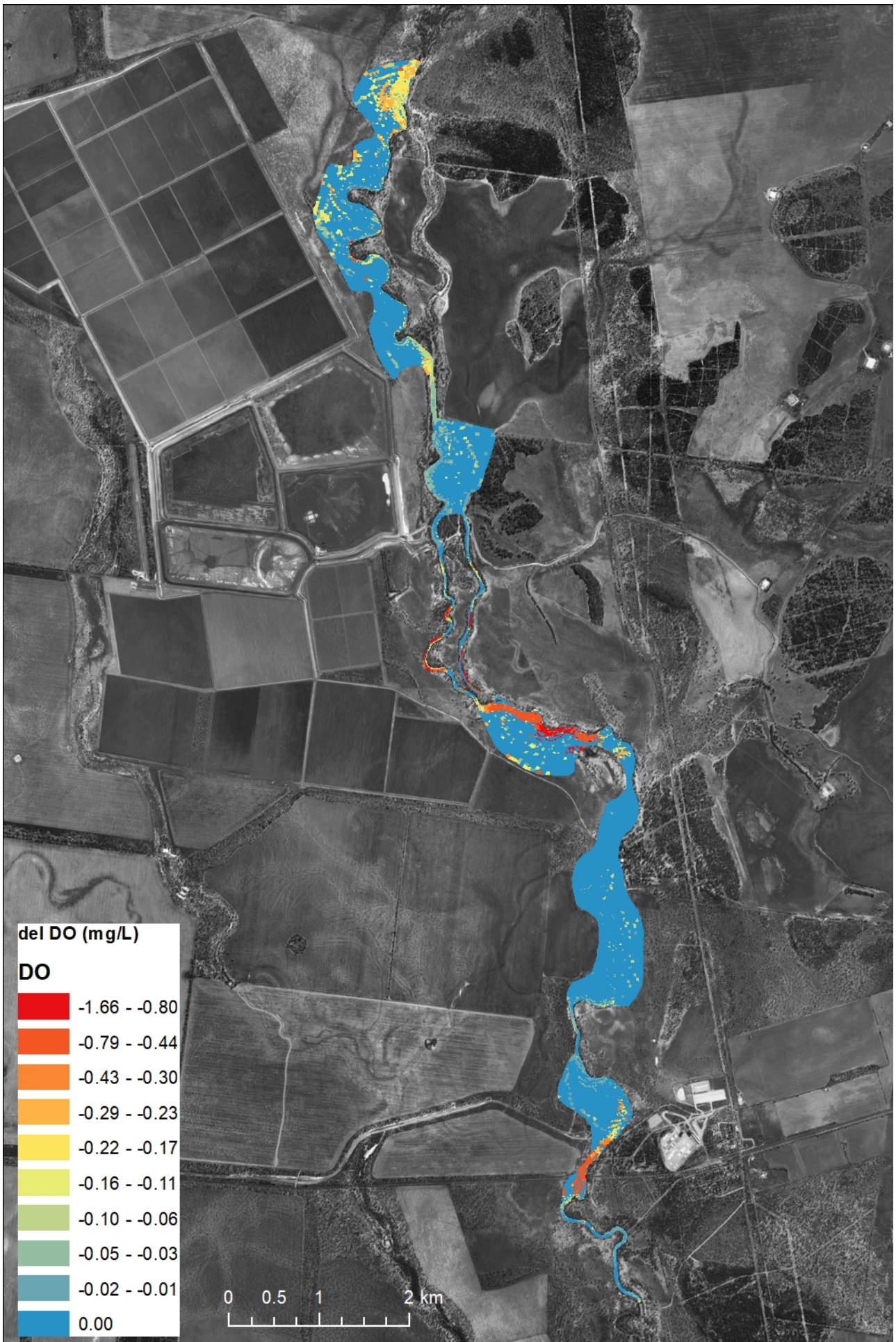
Over the four domains, a total of 30 sub-regions were chosen for assessment (Appendix B). Within each of these sub-regions the change in oxygen concentrations is shown in Figure 22, organised from north to south within the MDB. Comparison of the numerous sites over the 4 domains shows the relatively large range of conditions that were able to manifest, even under the base-case conditions (for each site). This figure also compares the HC versus DCP carp mortality model, which serves as a useful cross-check of model results, with the difference attributable to the movement and accumulation of particles. Generally, the DCP approach highlights more intense impacts in some regions since the risk is focused in certain locations.

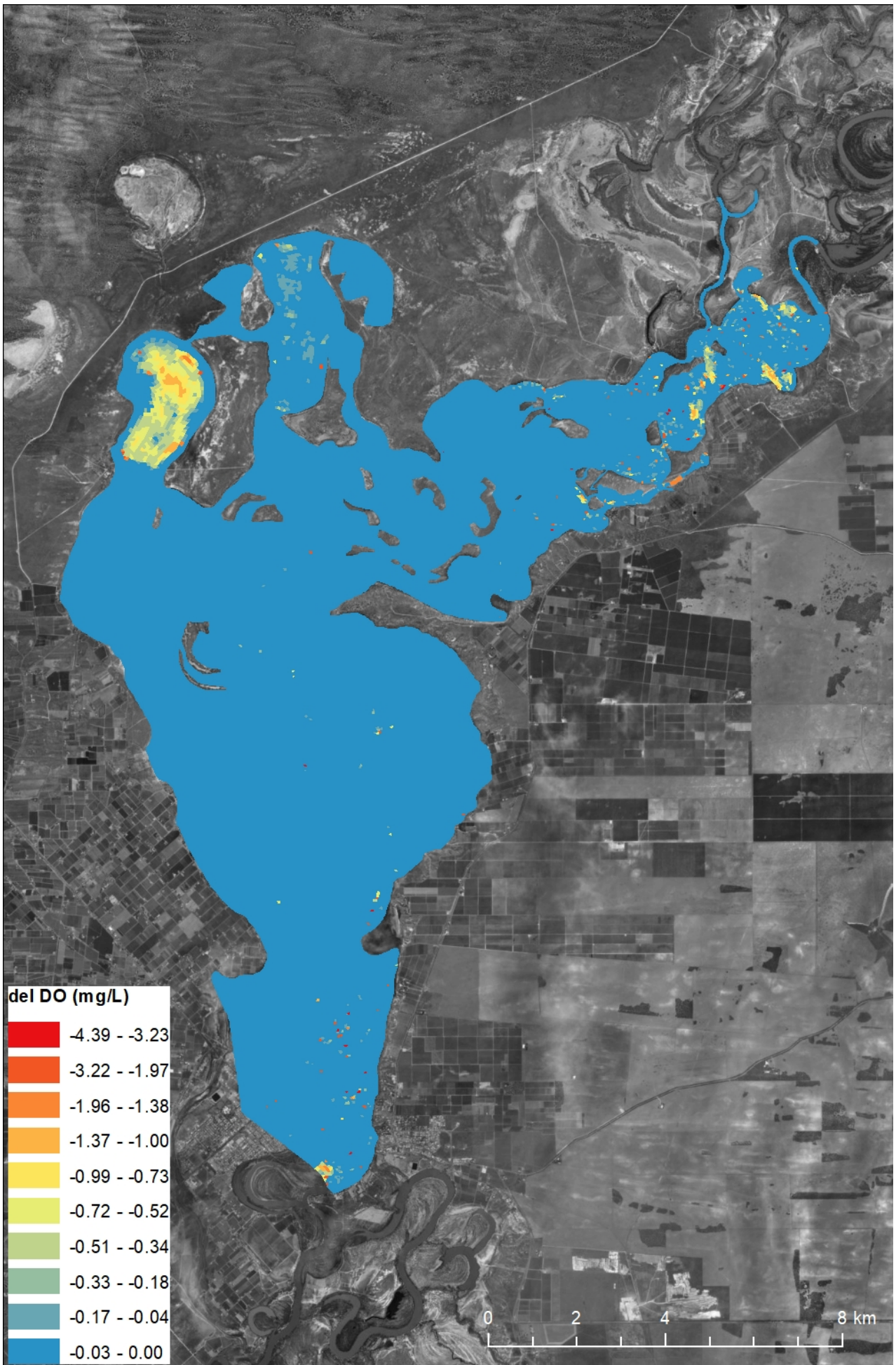
The highest risks were noted in the Chowilla domain, which is consistent with the higher biomass densities estimated for this region. Note some of the areas in this domain naturally experience complex histories of oxygen concentrations. The region is hydrologically complex with large areas of poorly connected waters which allow for accumulation of oxygen demand. Nonetheless, the large impacts relatively short-lived, over the life of the mortality event.

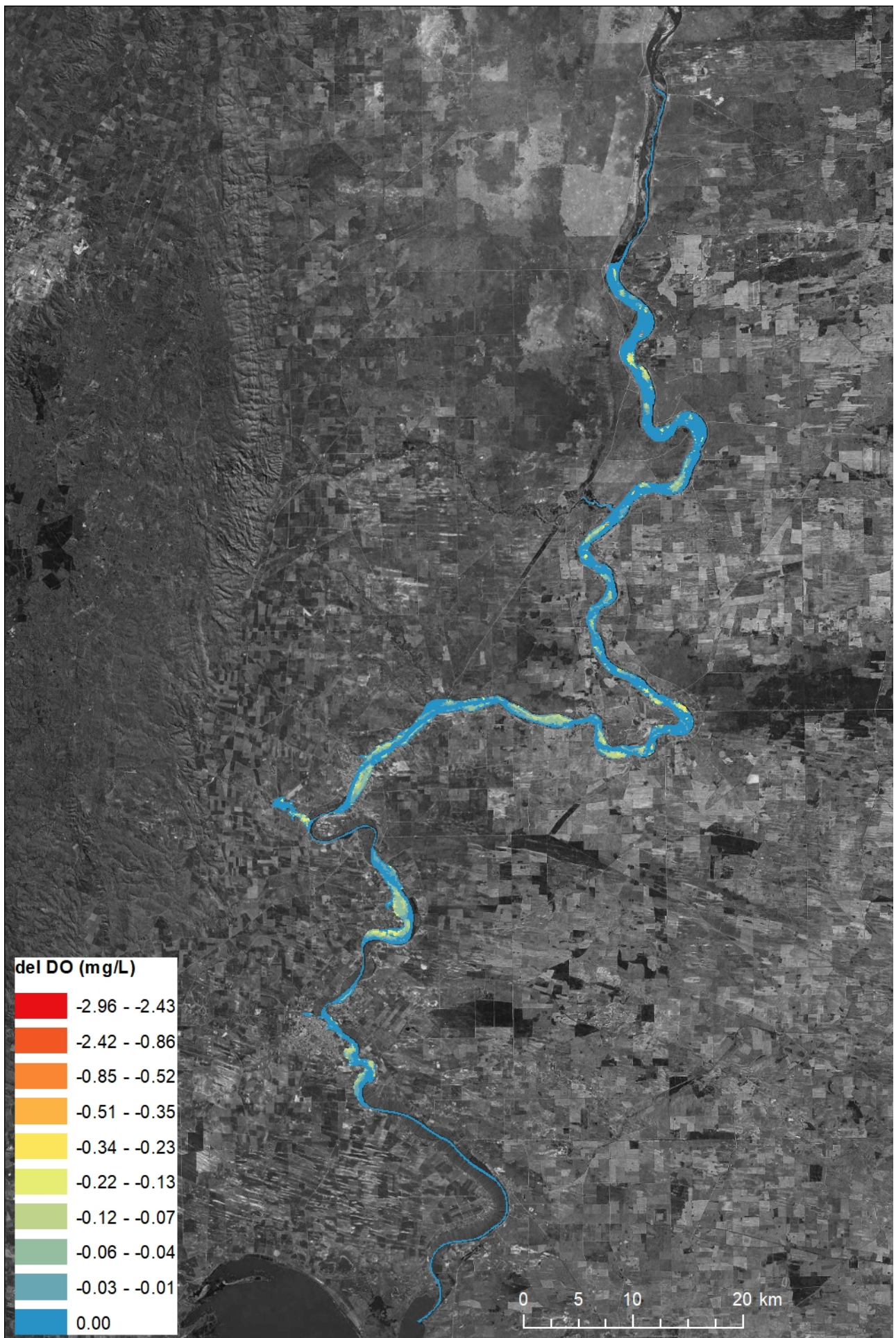
Exploring the sensitivity of the domain to flow and biomass loading highlights that at 2x Stuart et al. (2019) biomass level, oxygen sag of >1mg/L start to manifest (Figure 23). Some of these plots demonstrate two surfaces, which is where the sub-region is partitioned into shallow (largely littoral) zones and the main “deeper” water. This highlights the higher impacts on the water body margin, which, due to its lower water volume, will display a focussing of risk. In the Moonie domain, the modelled oxygen sag was low and in some cases the fish derived nutrients promoted photosynthesis and led to slightly elevated oxygen levels. The risk of hypoxia in this region and the Lower Lakes was low, even at higher biomass loading factors.

Overall, the results from these 30 sub-regions highlight the diversity in water body response, with some areas more susceptible than others. In general, the oxygen sag predicted at the anticipated biomass loads however is not catastrophic, though there may be regions of high biomass accumulation that show localised impacts. The risk from low-oxygen at considerably higher biomasses also appears manageable in all but several of the Chowilla sub-regions. It is clear in several sub-regions that higher flows can also reduce the increased risk of larger biomass. A numerical summary of this data is available in Appendix C.

Figure 21 (overpage): Average oxygen sag (ΔDO , mg/L) in the four simulated domains, assuming 100% carp biomass mortality over the simulation period (and no upstream carp inputs).







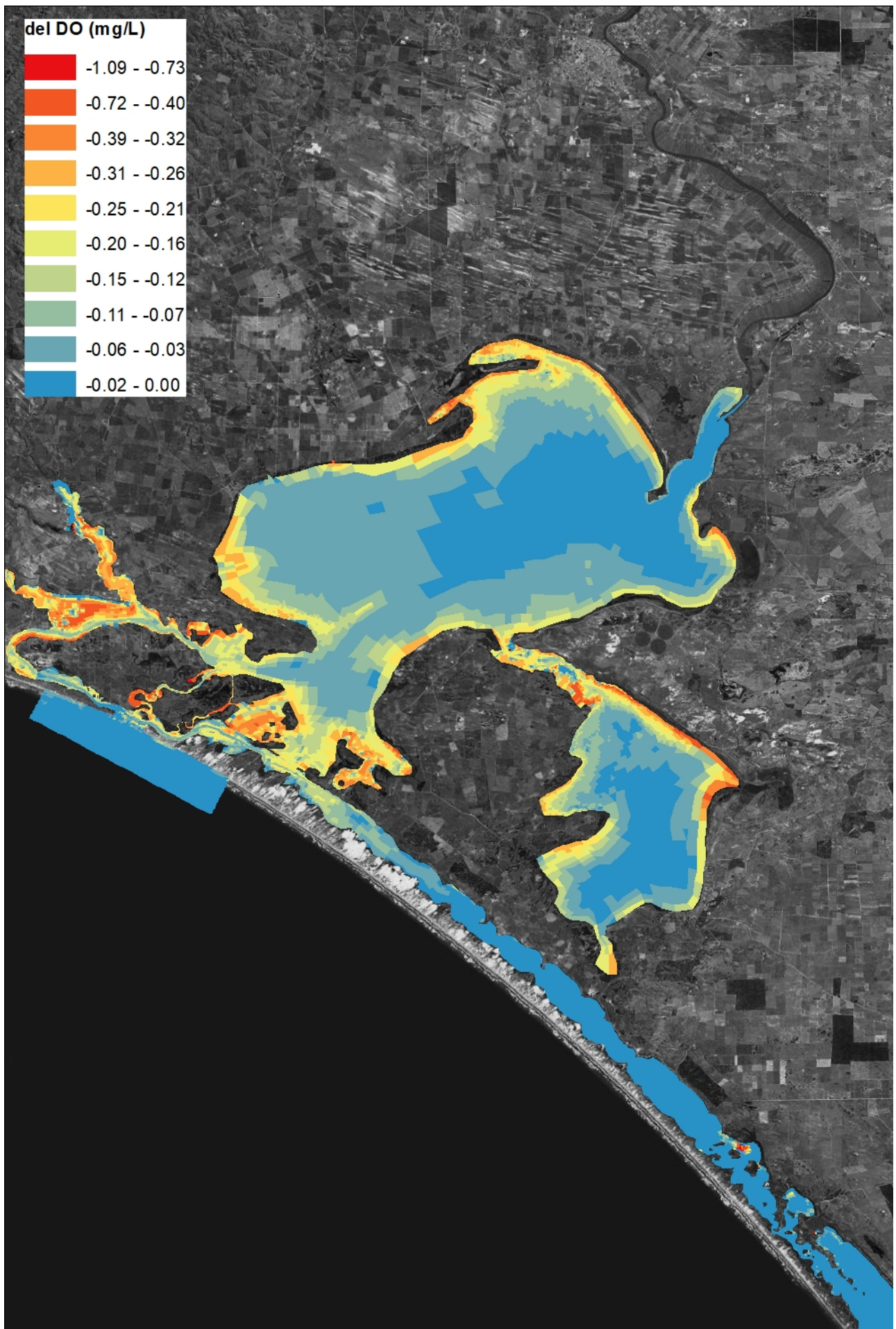
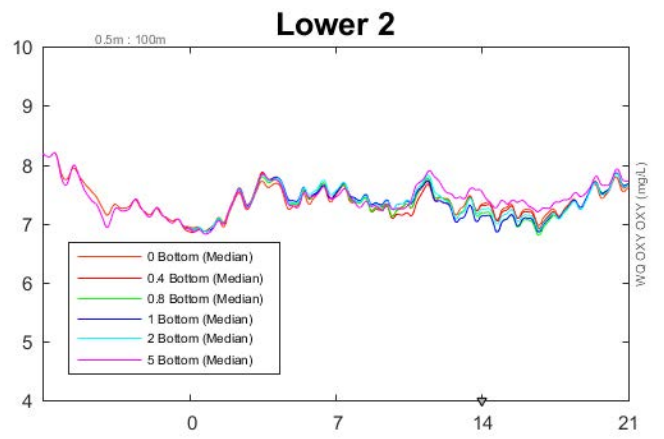
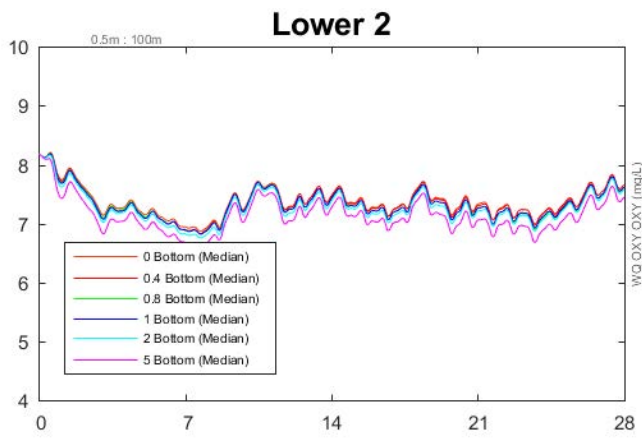
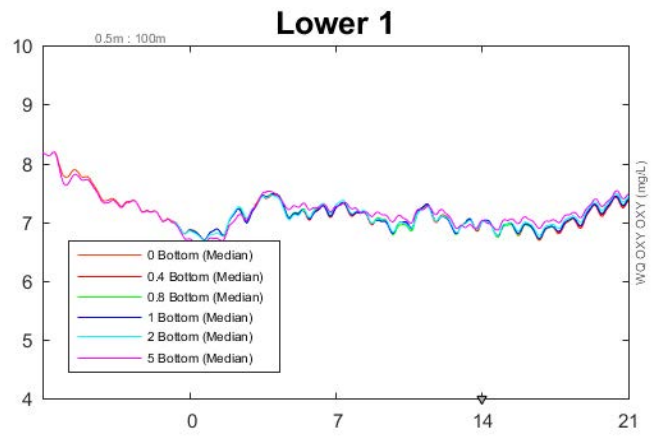
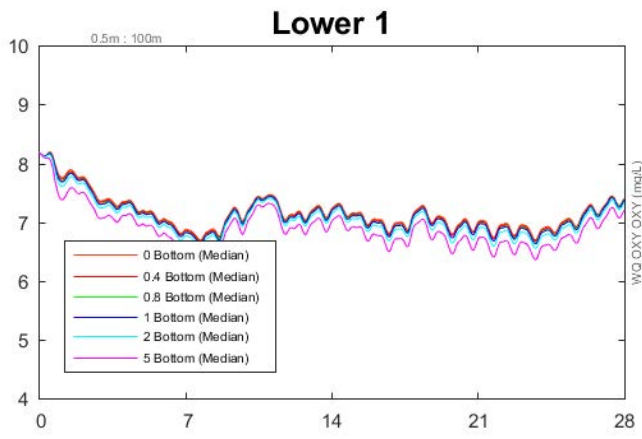
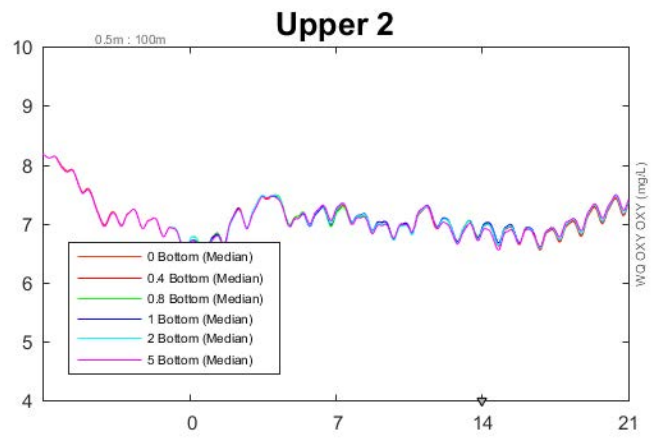
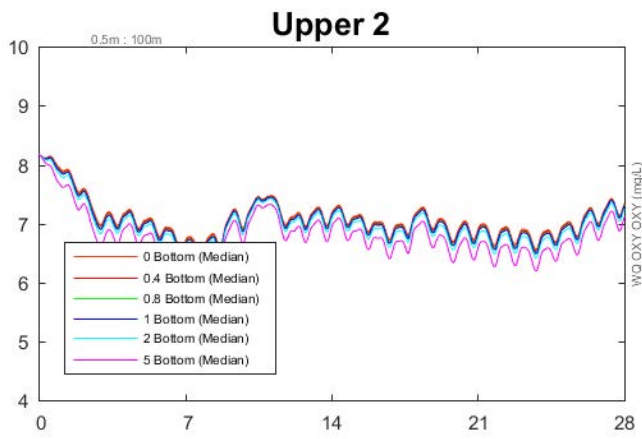
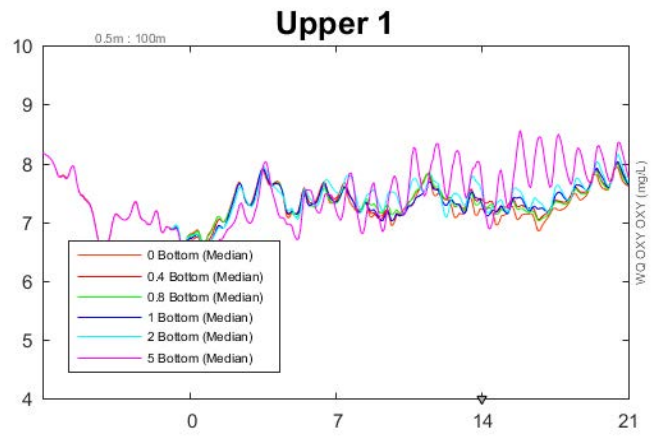
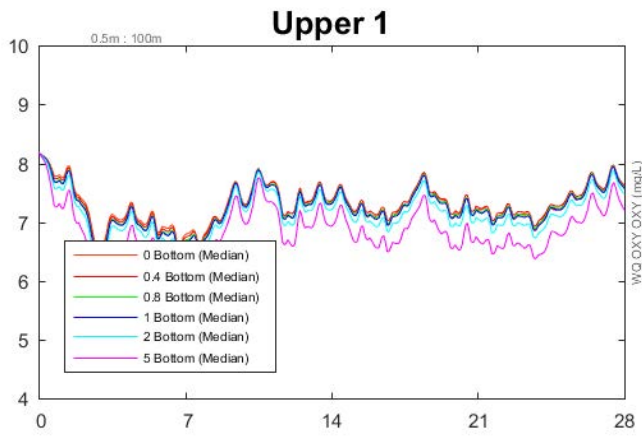
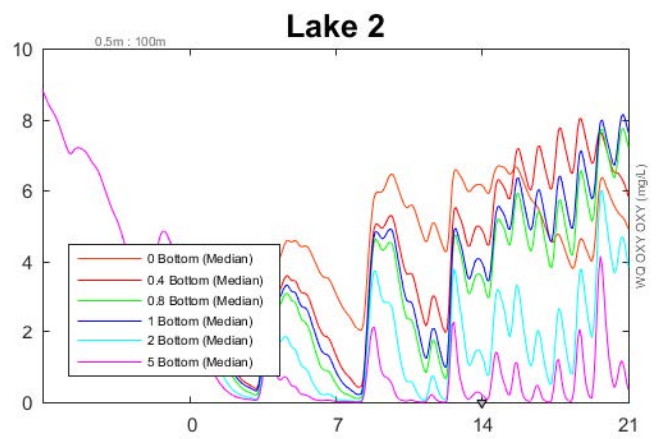
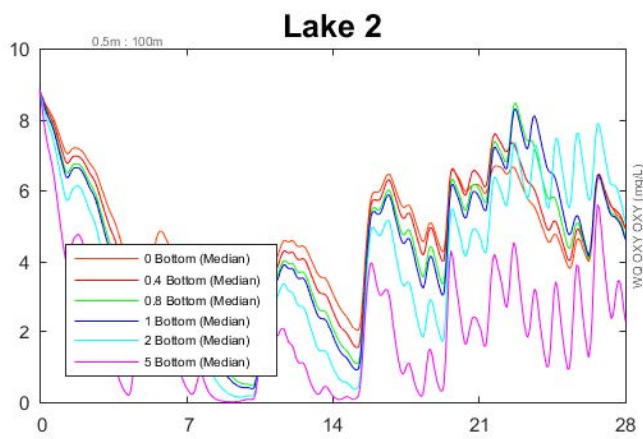
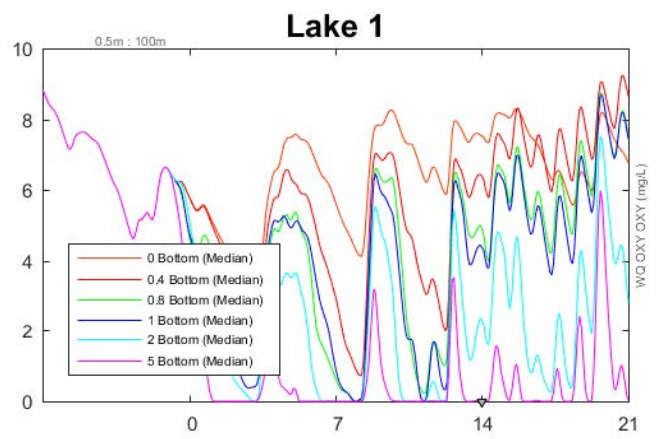
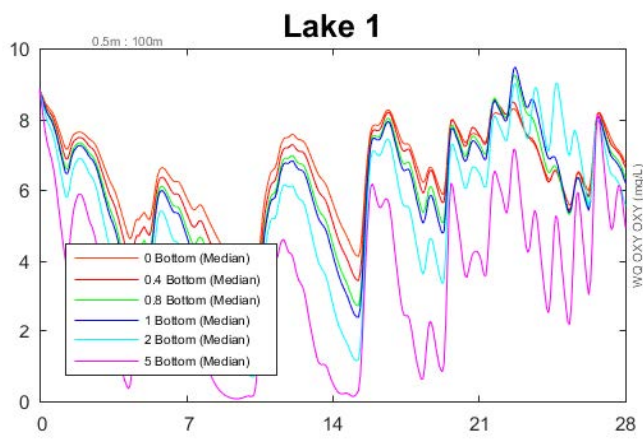
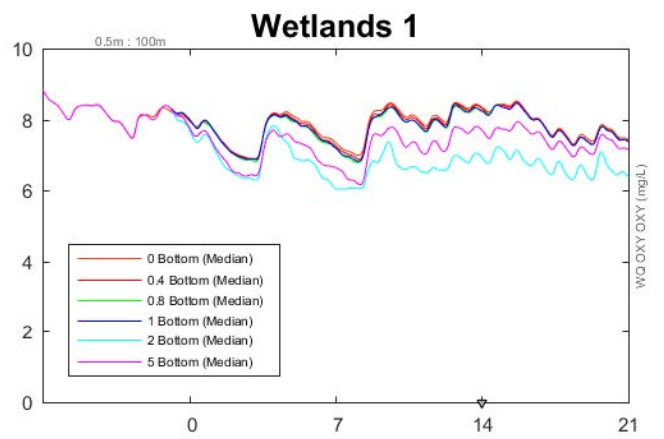
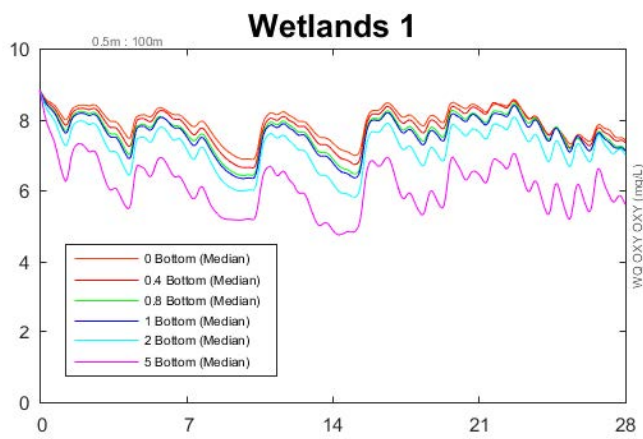
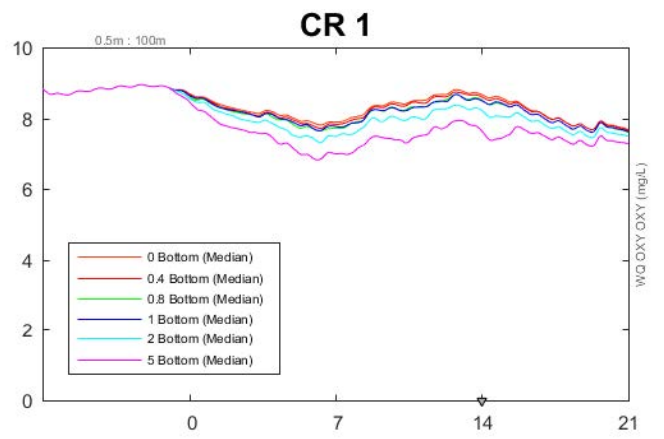
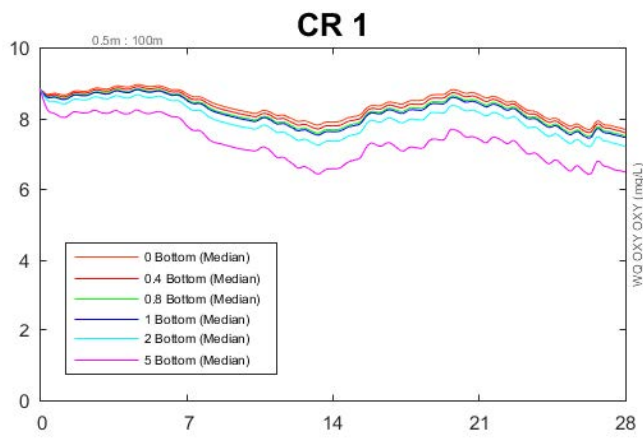
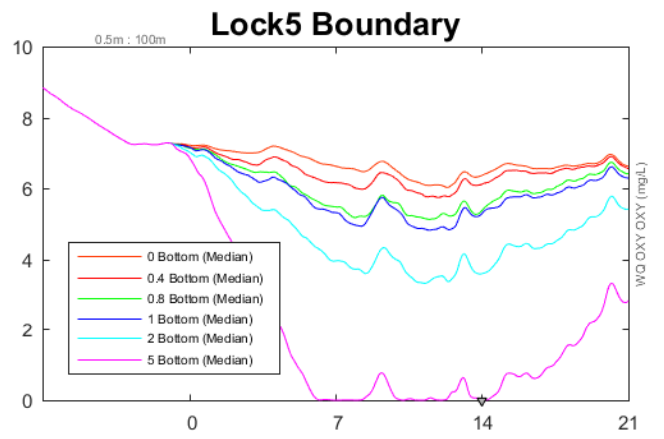
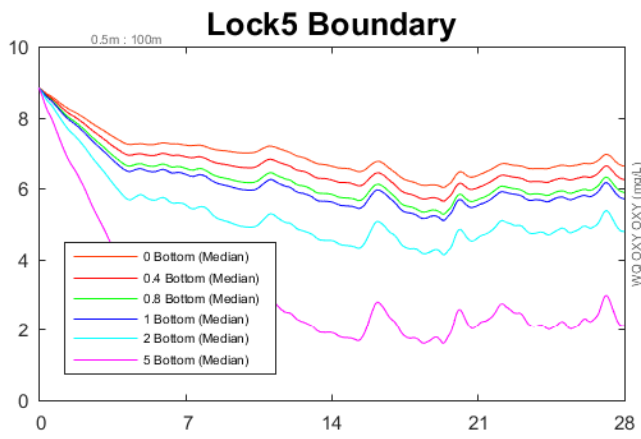
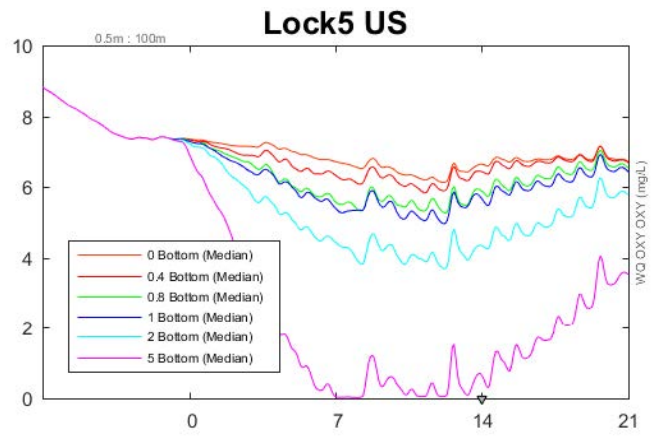
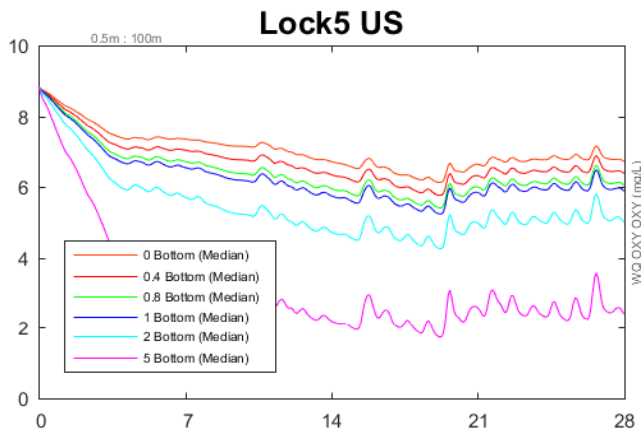
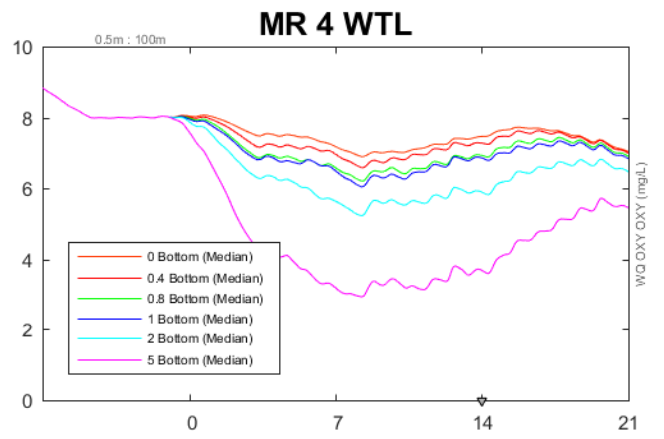
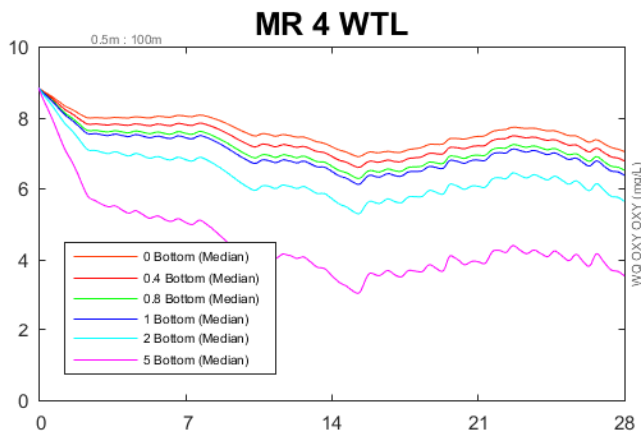
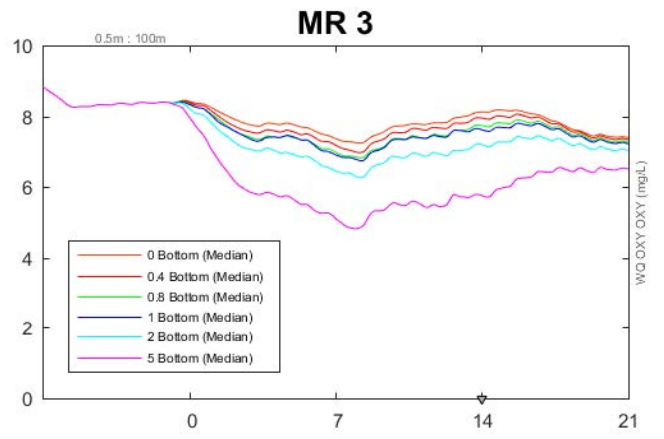
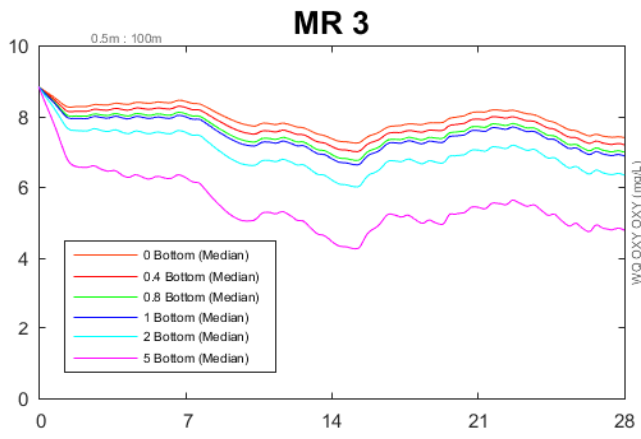
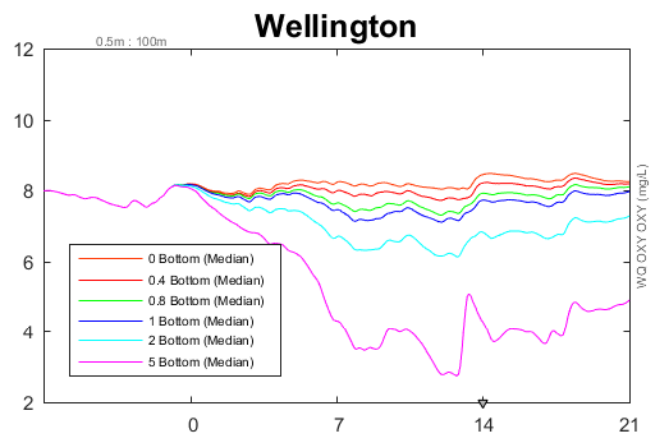
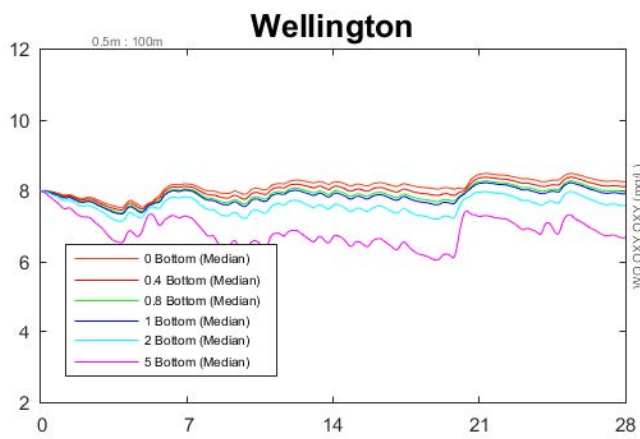
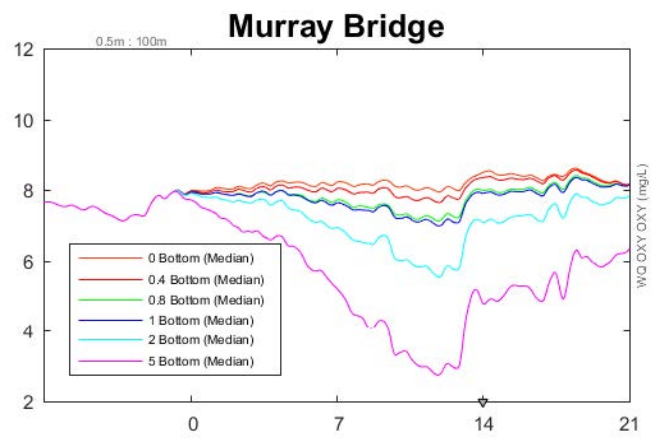
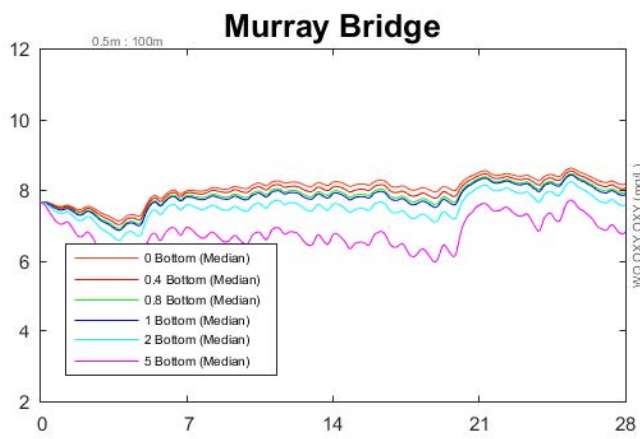
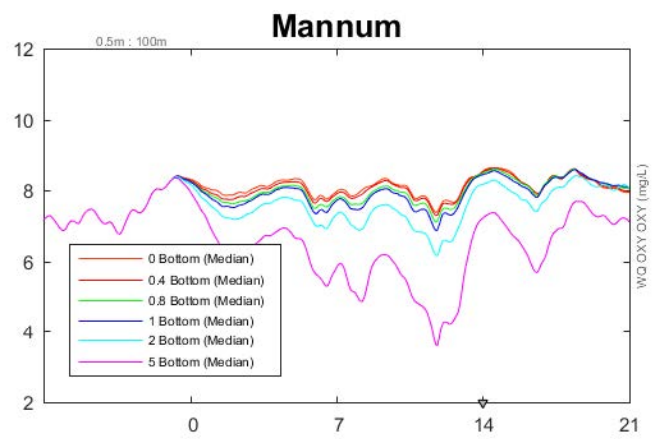
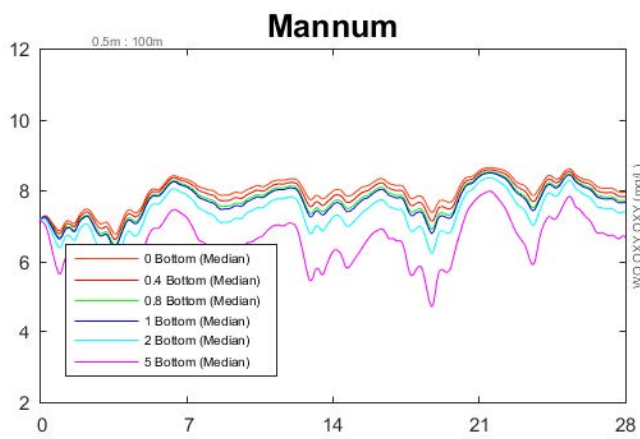
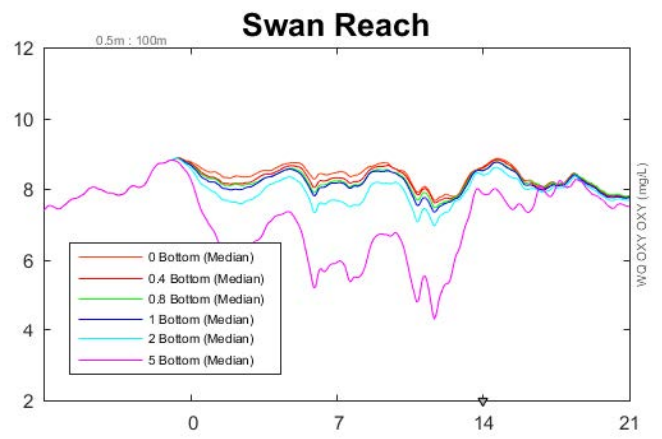
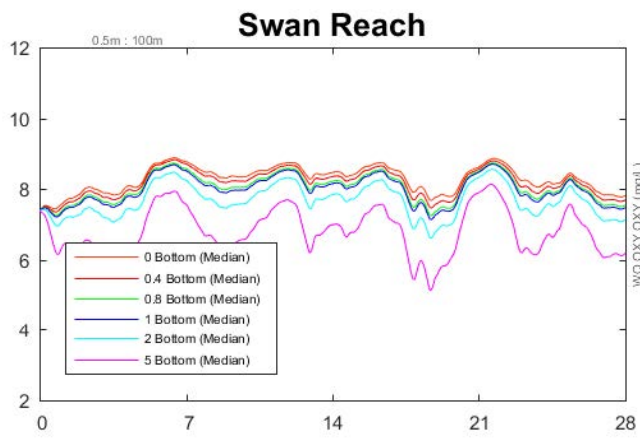


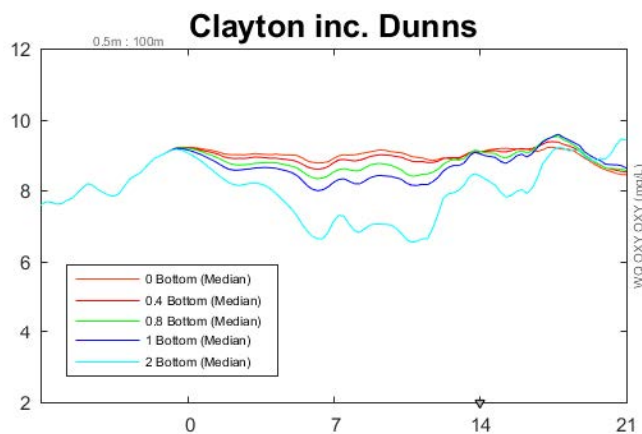
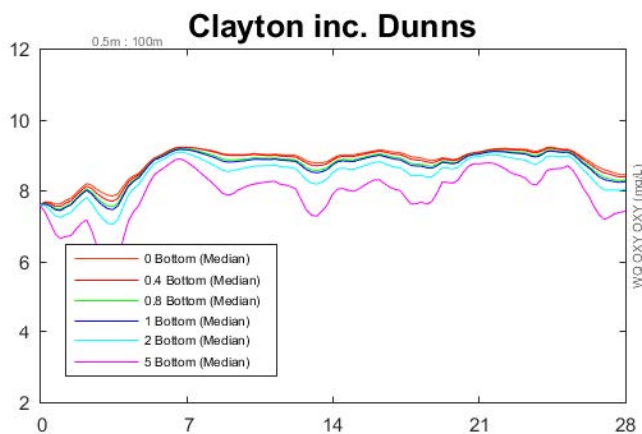
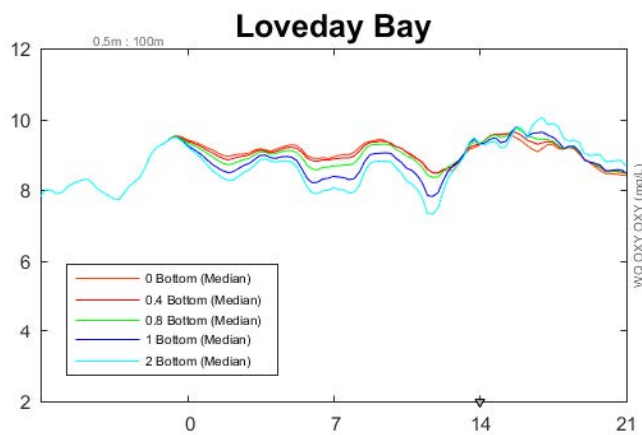
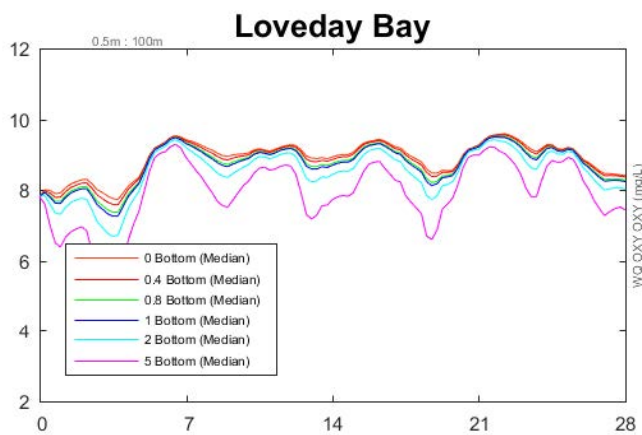
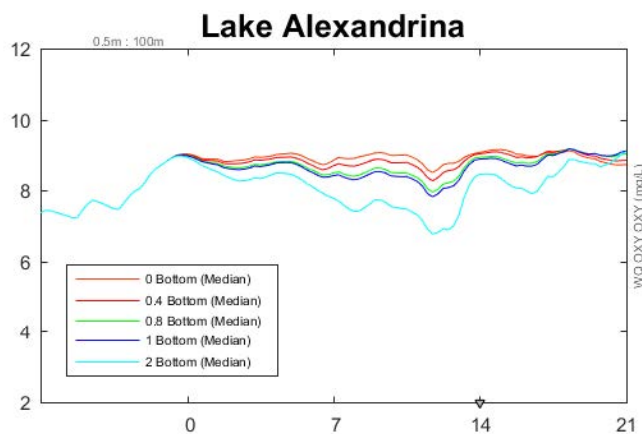
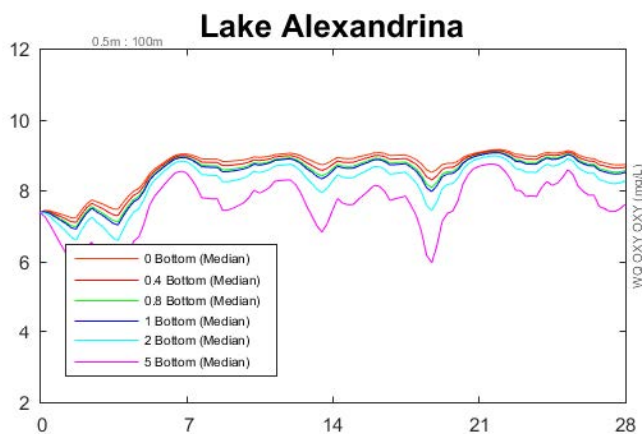
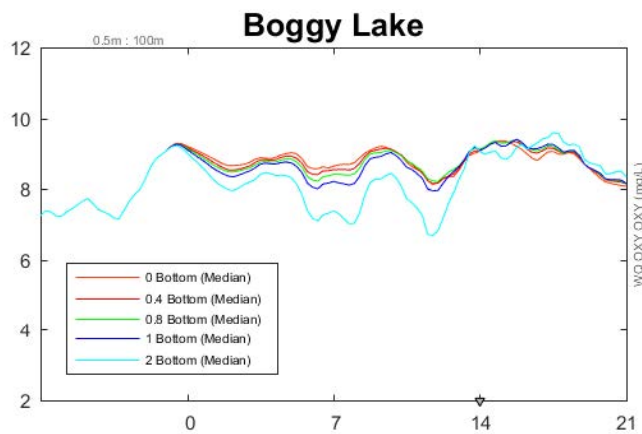
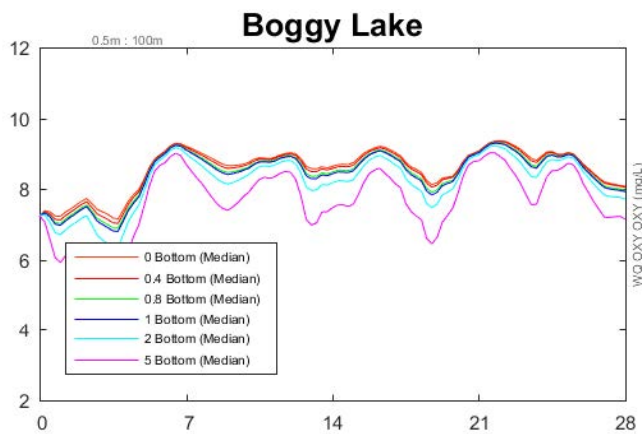
Figure 22 (overpage): Time series of oxygen concentrations from 1-month simulations assessing carp biomass loading. The left column are simulations run with constant biomass spread over the domain (HC), and the right column are similar simulations but with dynamic carp particles (DCP) subject to transport, accumulation and decay over the period from 0 days. Results for flow factor 1× are shown. Legend entries refer to the biomass loading factor, where 1× is the biomass according to Stuart et al. (2019). The sites are moving north to south through the four domains, starting at the top of the Moonie River and ending near the Murray Barrages (see Appendix B for site locations).











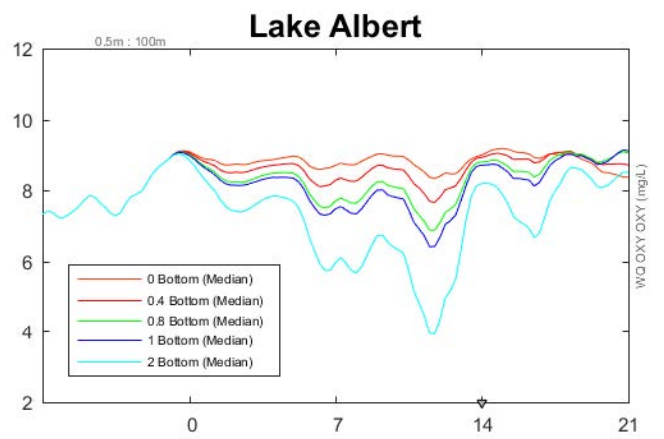
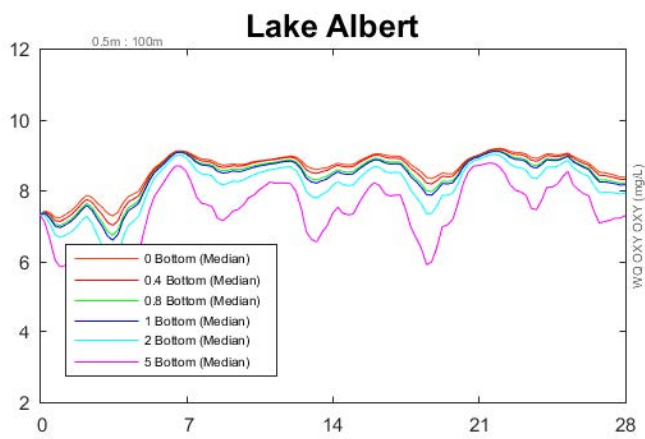
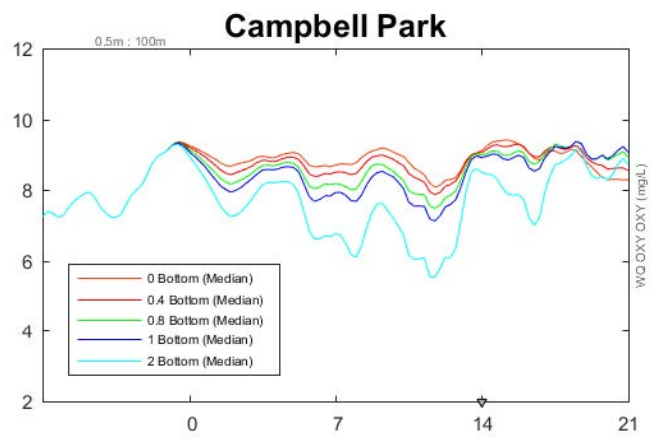
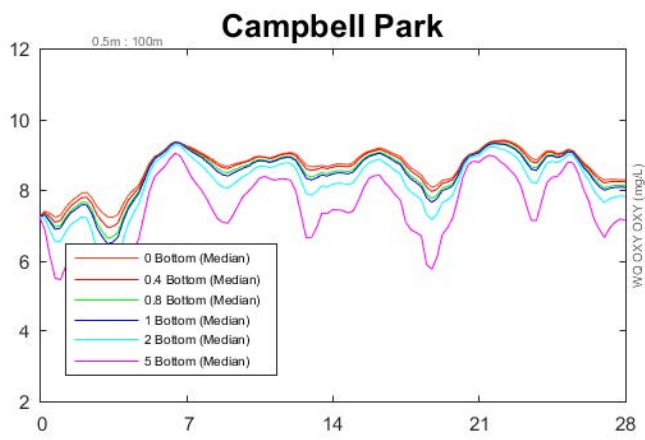
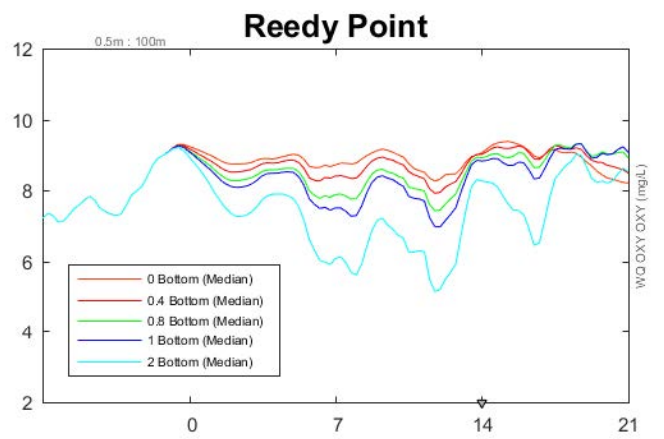
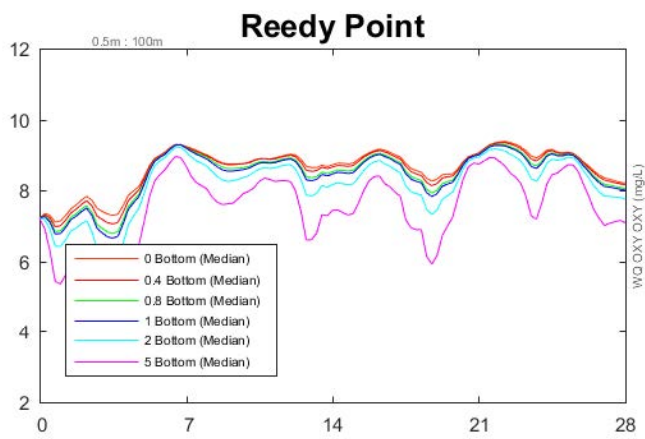
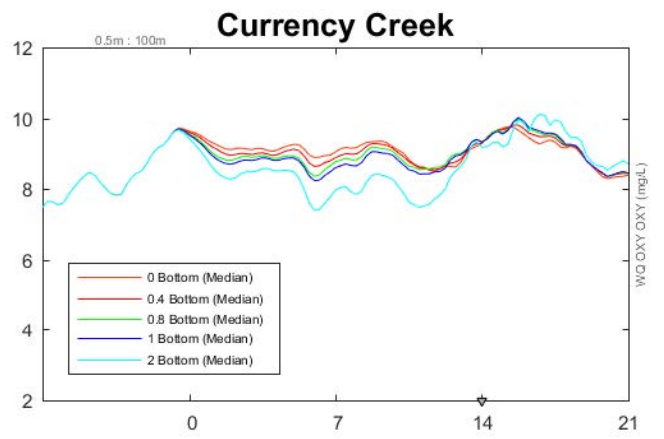
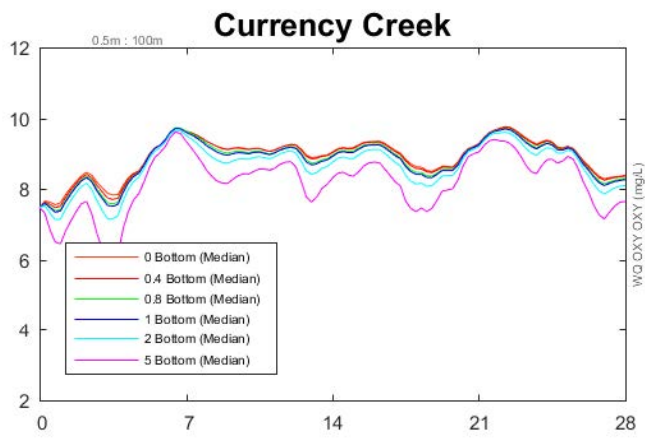
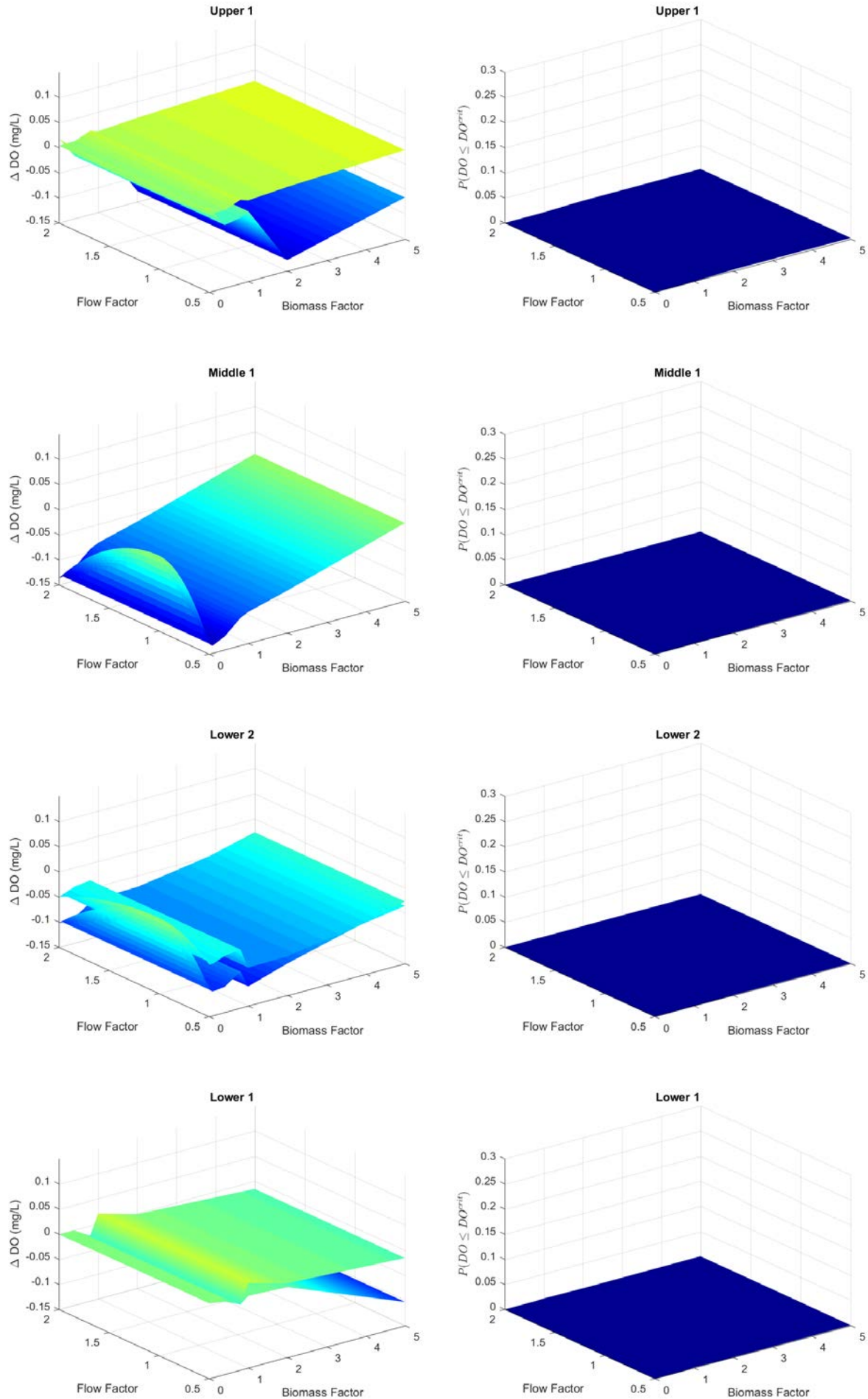
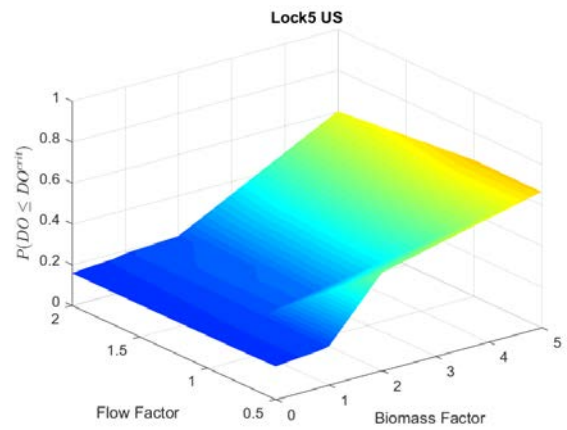
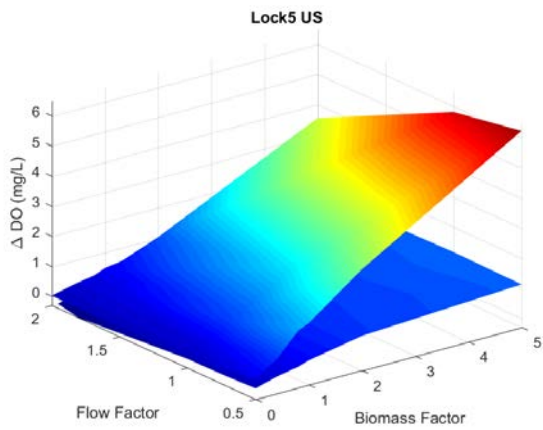
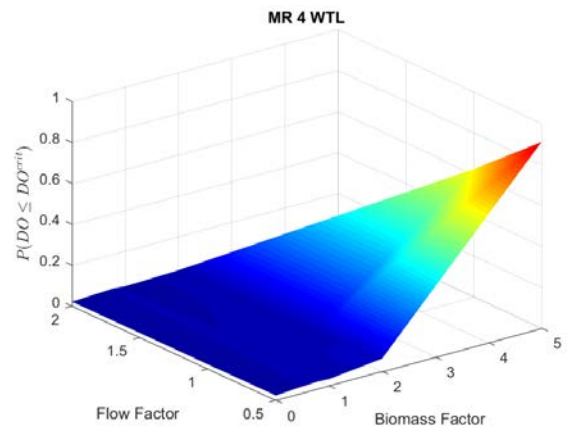
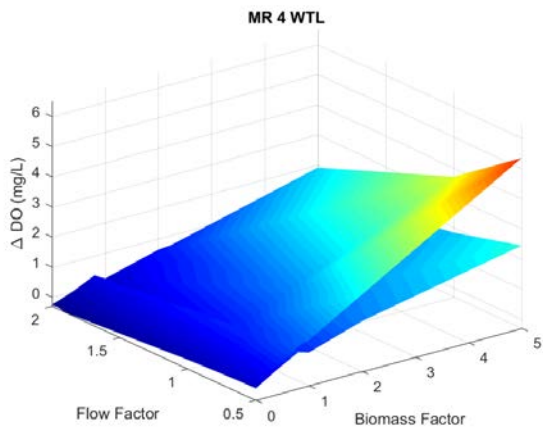
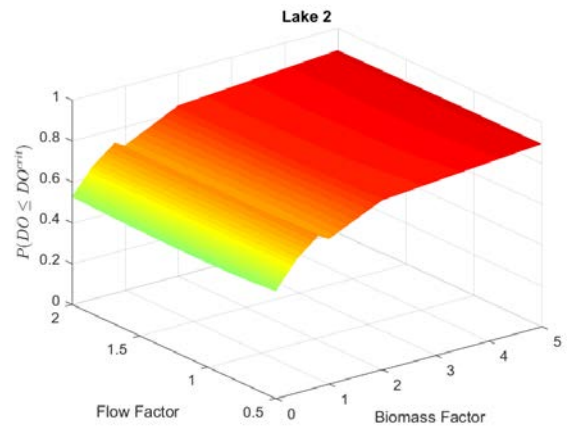
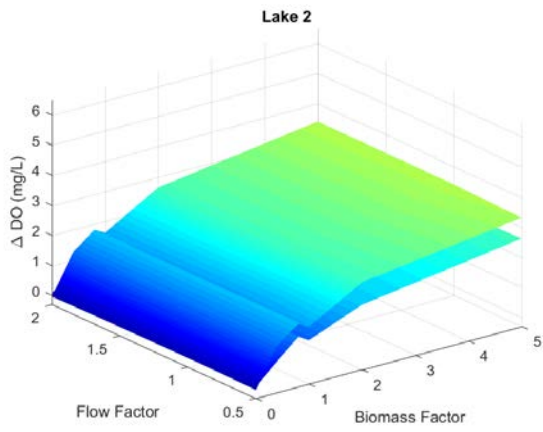
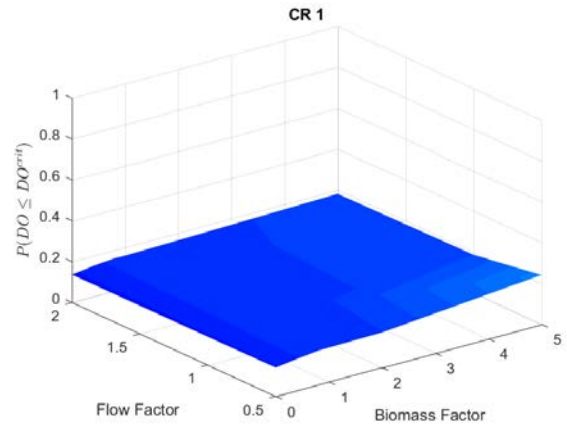
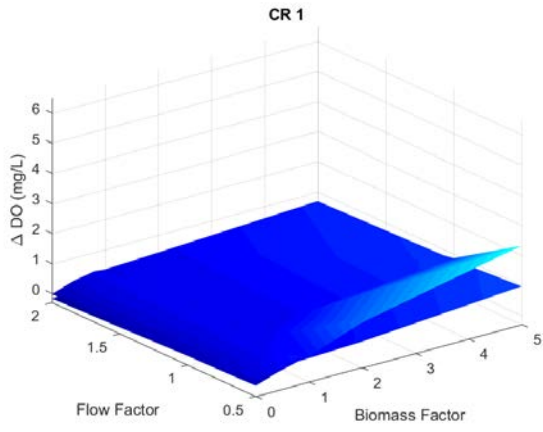
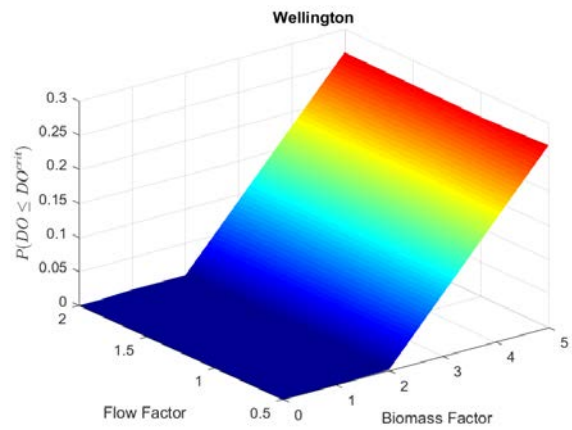
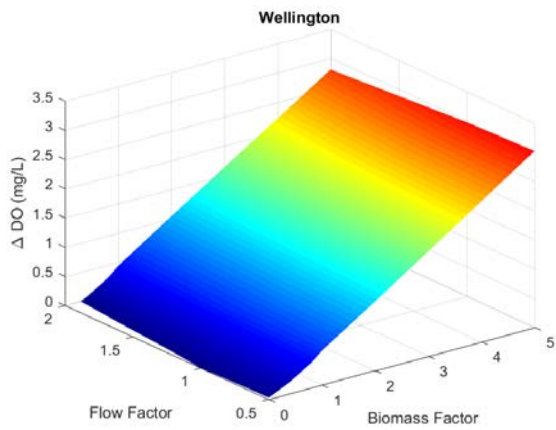
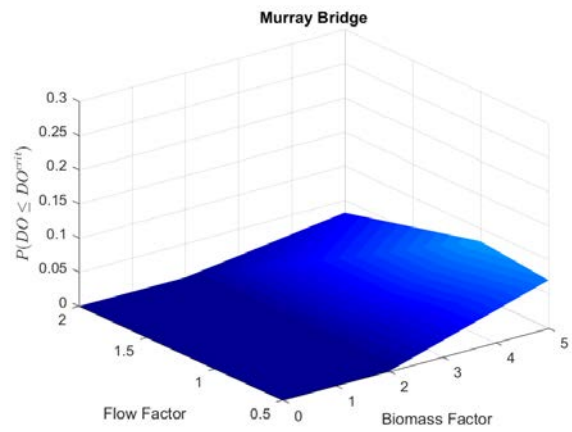
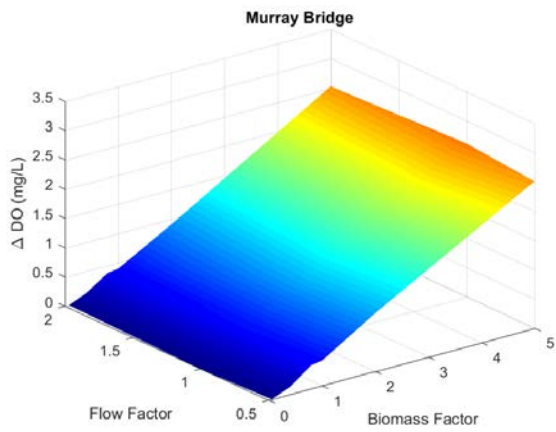
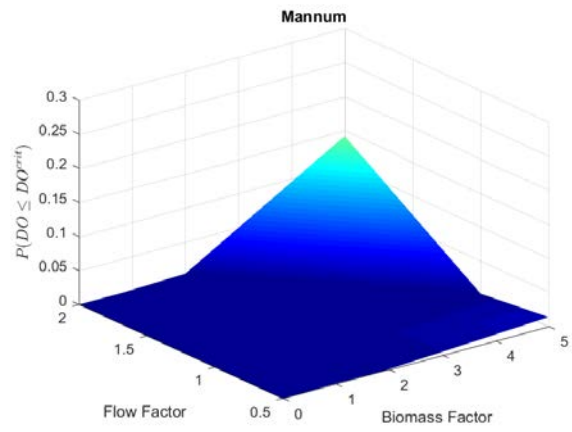
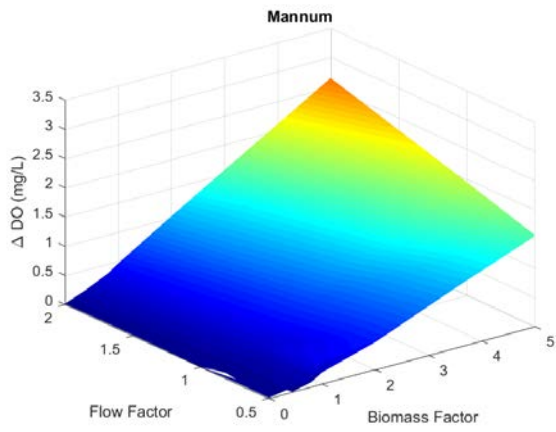
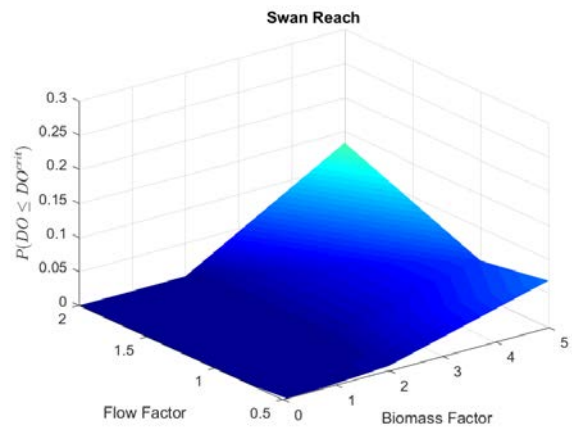
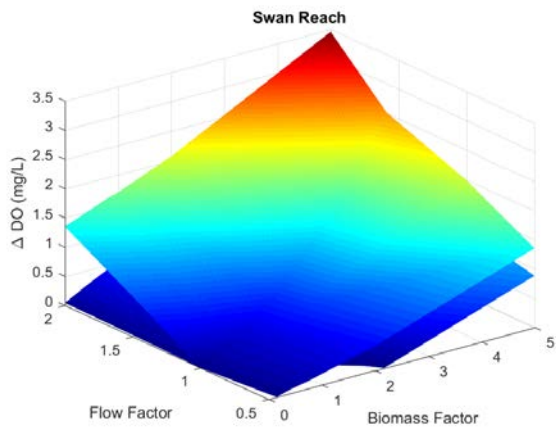
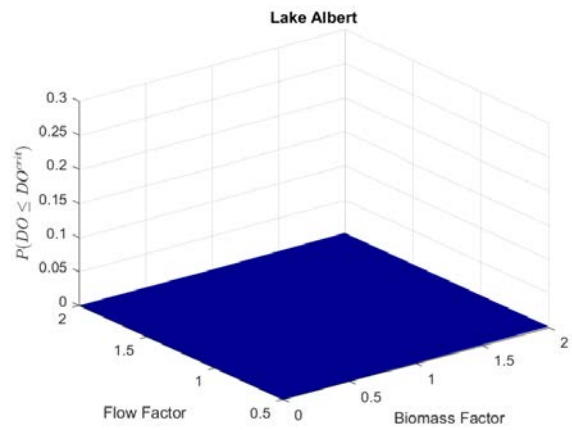
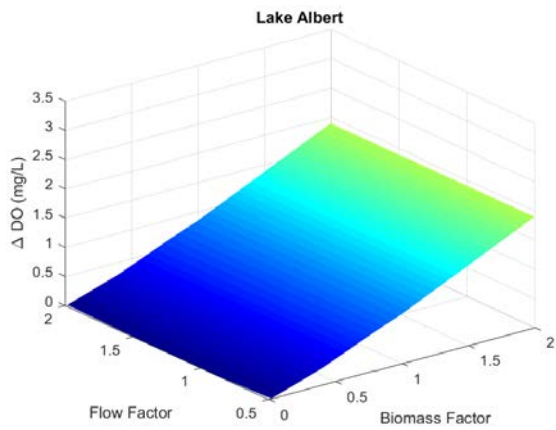
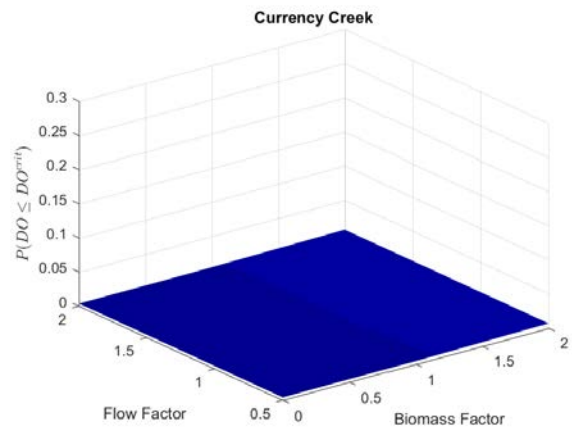
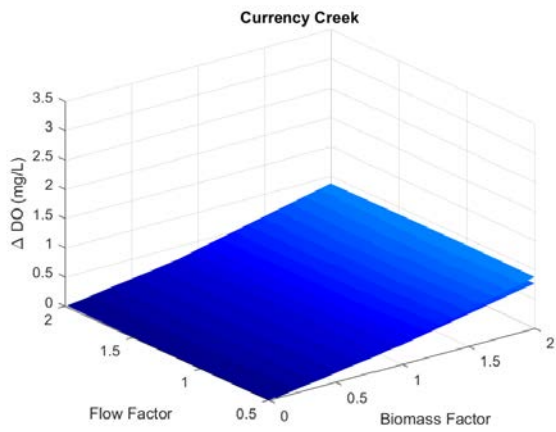
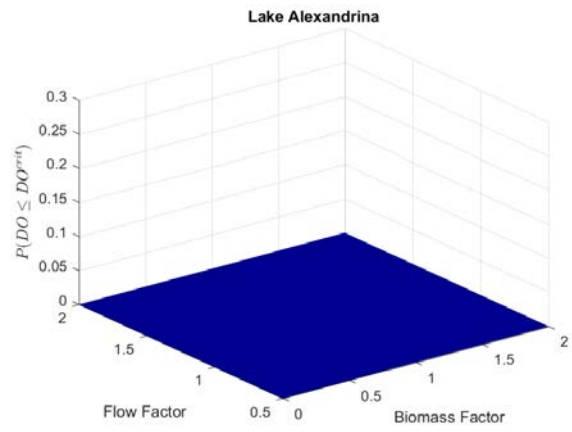
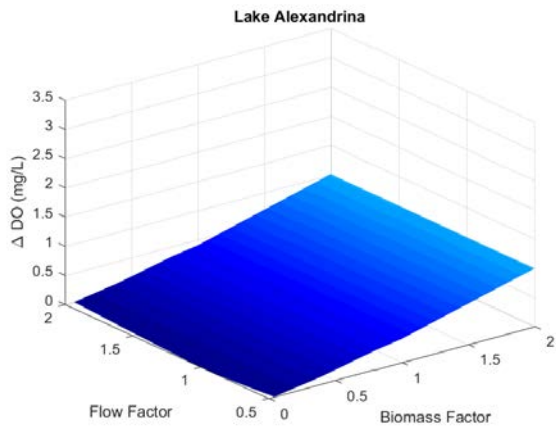
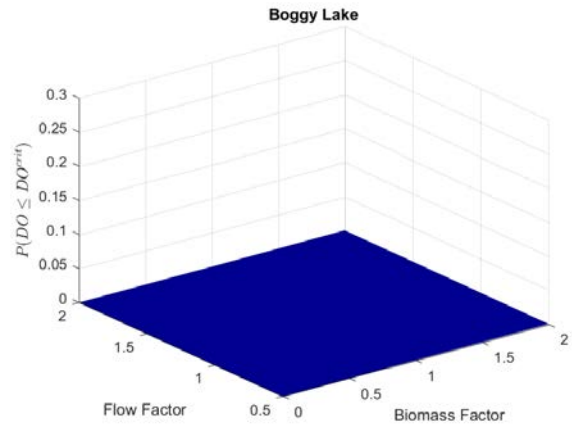
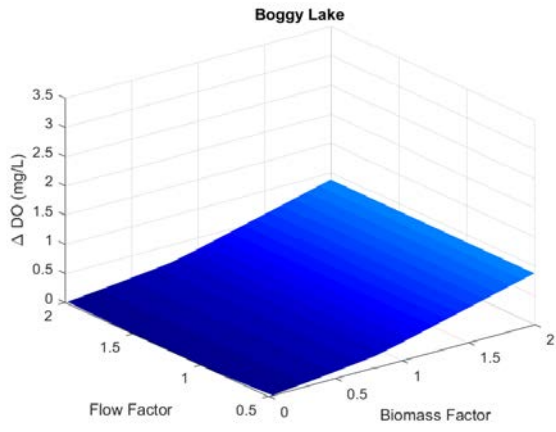


Figure 23 (continues overpage): Response surfaces of relative oxygen sag (left) and hypoxia risk (right) caused by carp mortality (DCP), for different flow conditions and biomass loading factors. The biomass factor of 1 represents the biomass values reported in Stuart et al., (2019), and a flow factor of 1 is as in Figure 20. Negative ΔDO indicates an increase in oxygen. For panels with 2 surfaces, the upper layer reflects water less than 50cm deep.









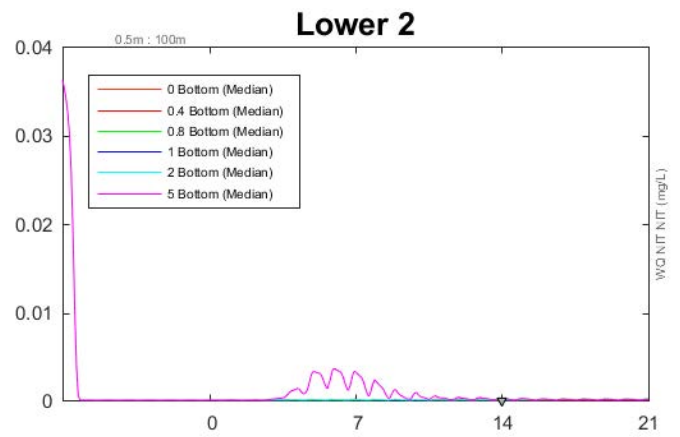
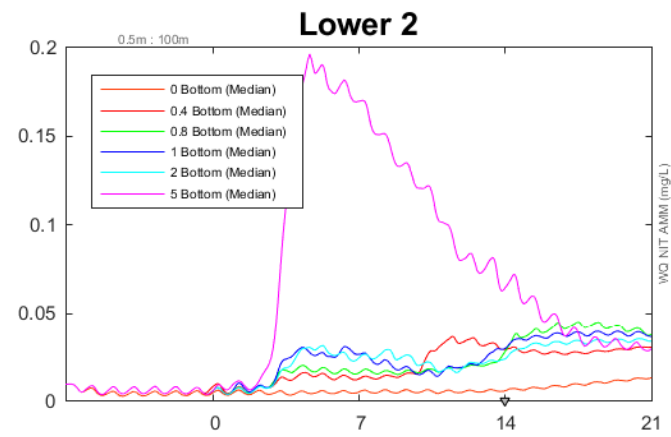
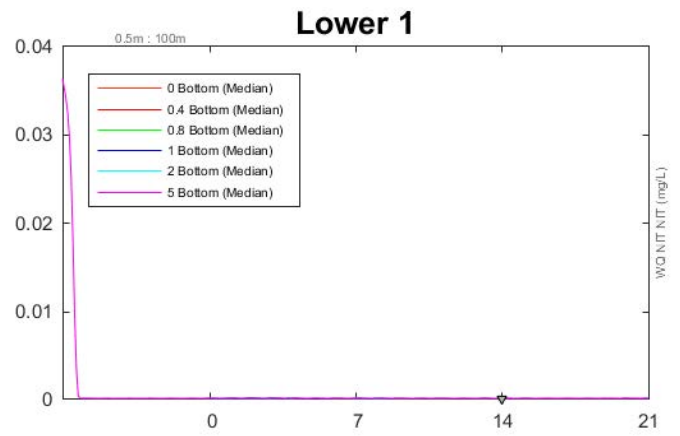
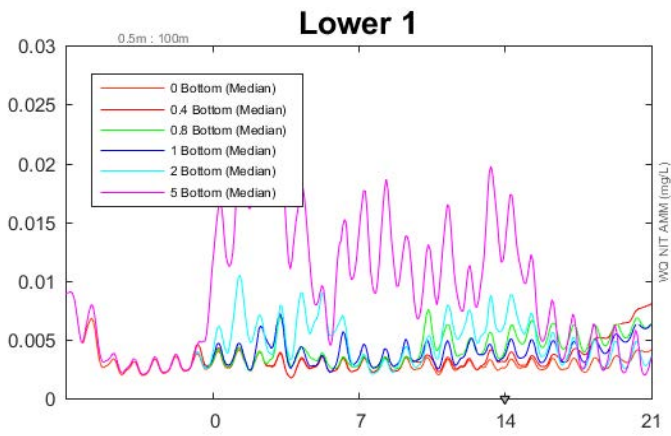
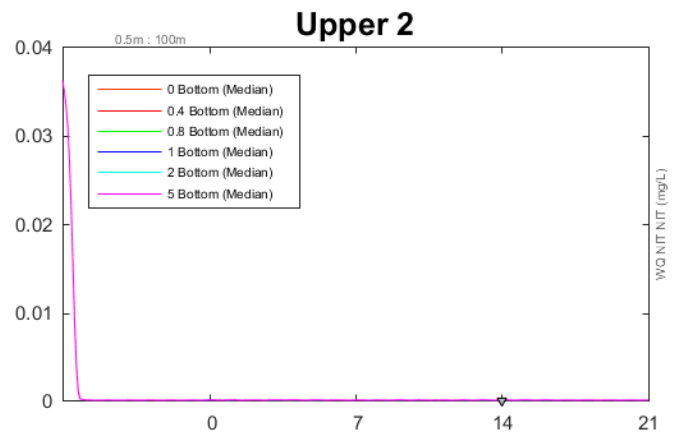
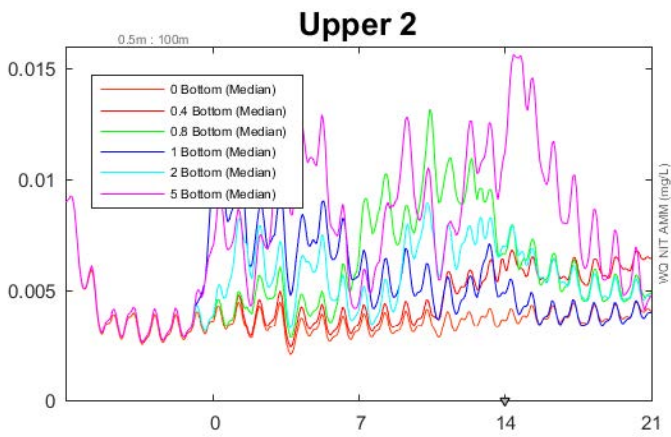
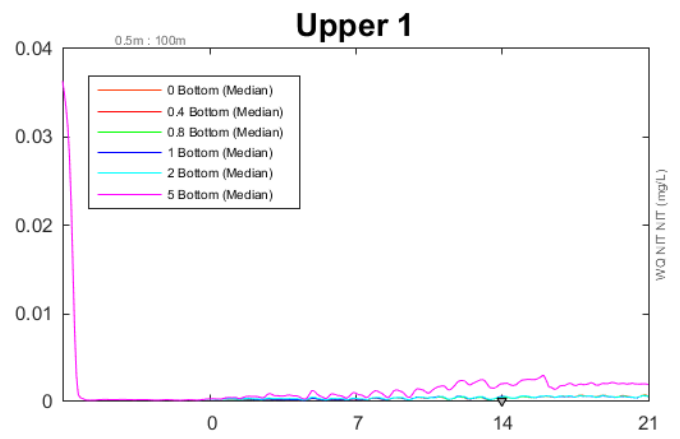
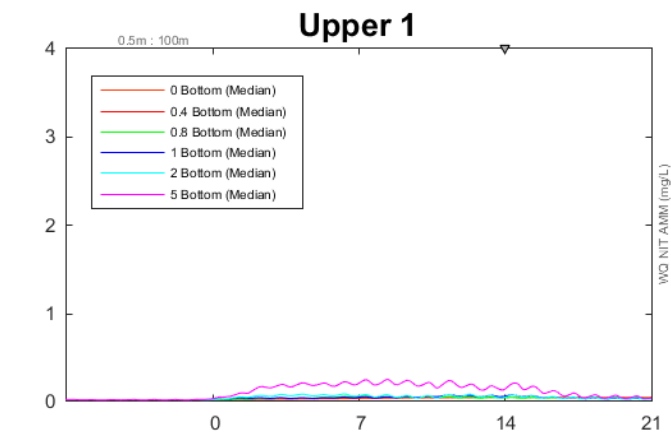
Nutrient release and accumulation

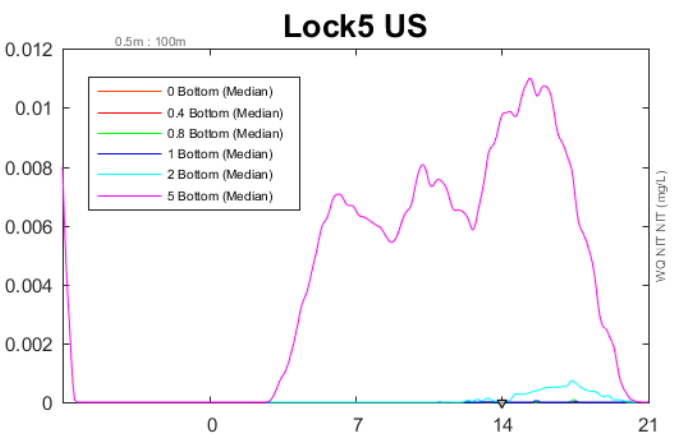
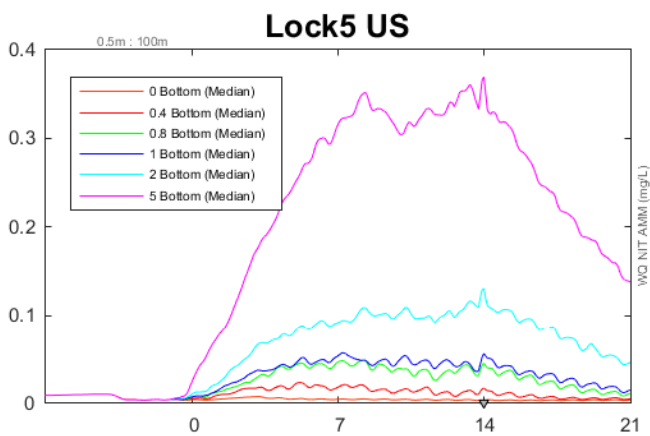
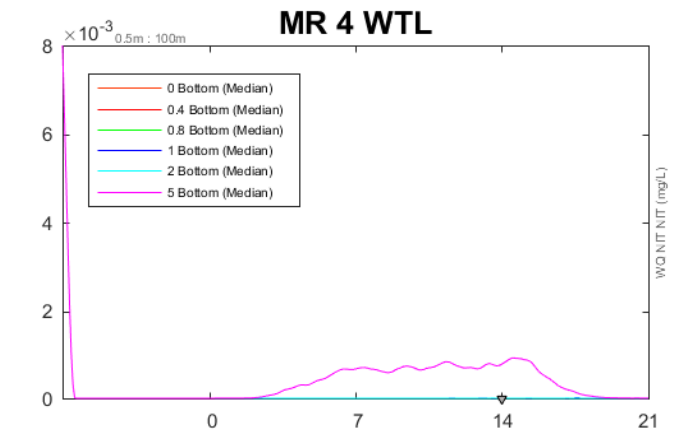
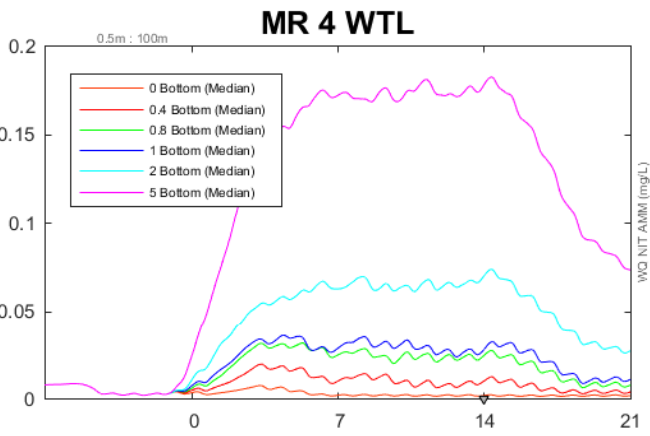
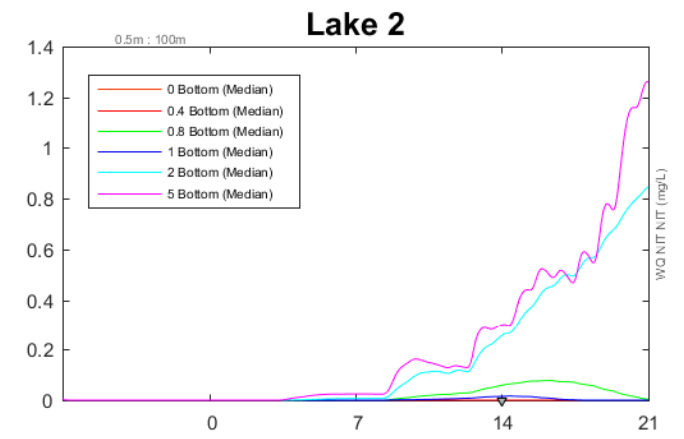
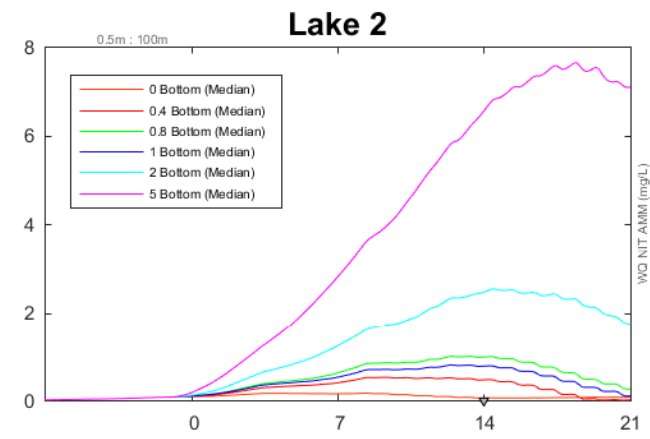
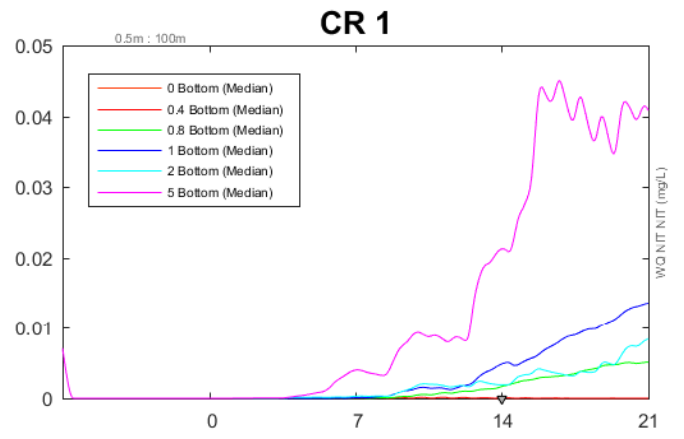
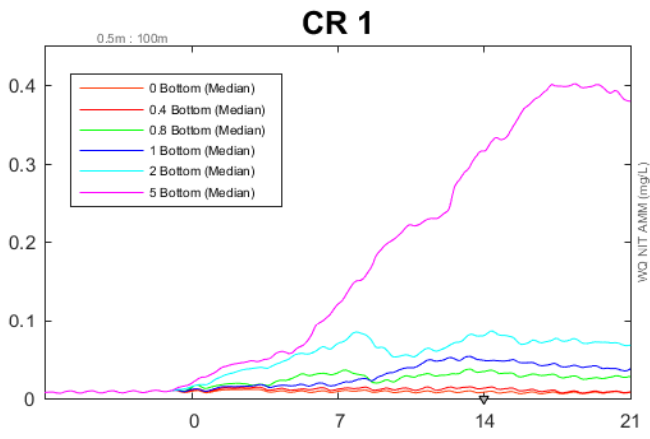
As in the previous section, we also analysed nutrient release for the 30 sub-regions (Appendix B), though only selected sites are presented as plots (Figure 24; sites in order from north to south). The rate of accumulation of NH_4 was much more notable than NO_3 , even though considerable nitrification was occurring over the simulation period. The peak NH_4 values were generally within acceptable ranges for most sites even at high biomass values, though note the presented time-series only cover the deeper water. Some shallow water regions did show high levels of DN accumulation, though this was only in the complex Chowilla domain (see Figure 26, referred to below).

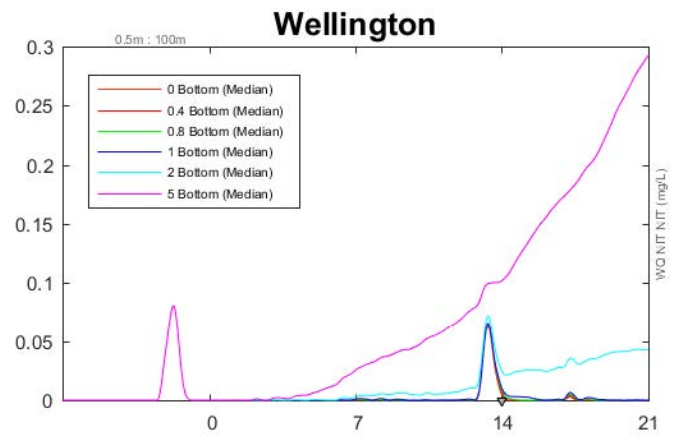
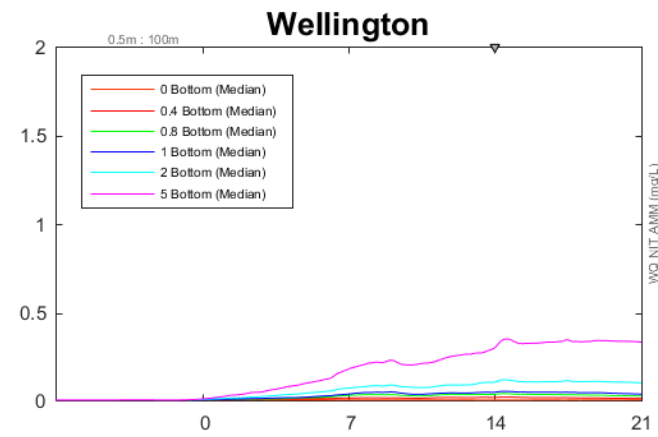
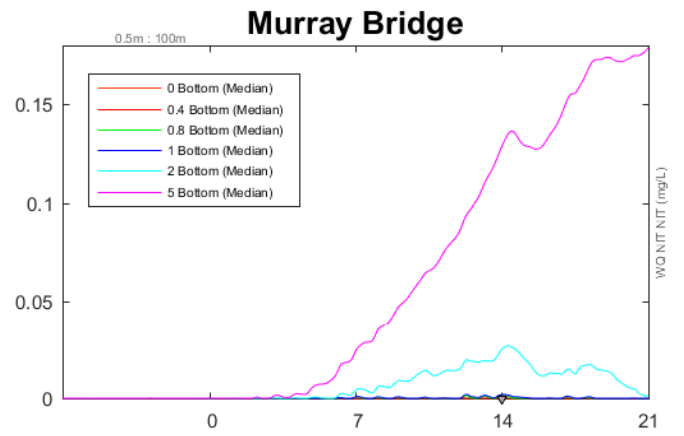
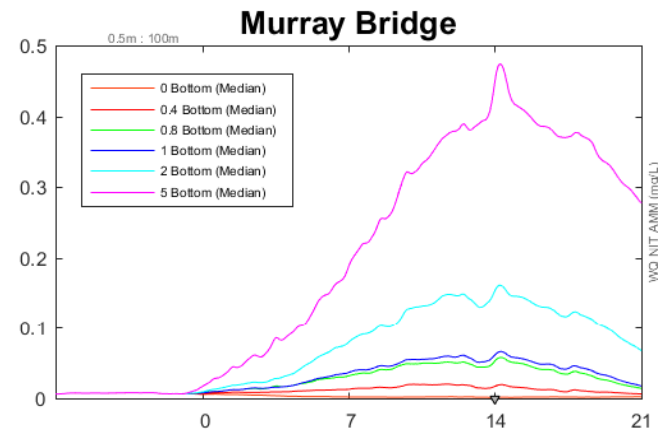
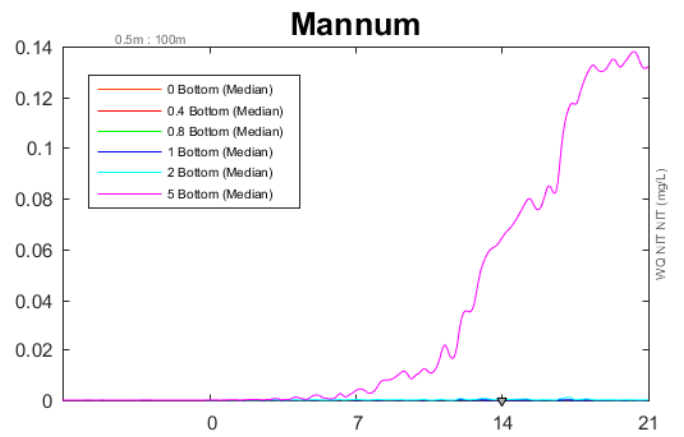
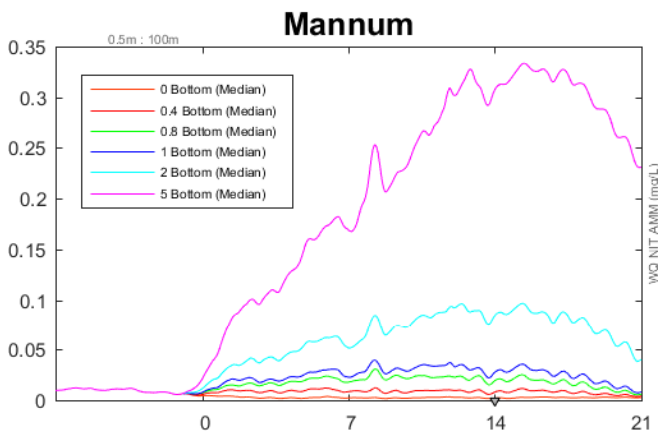
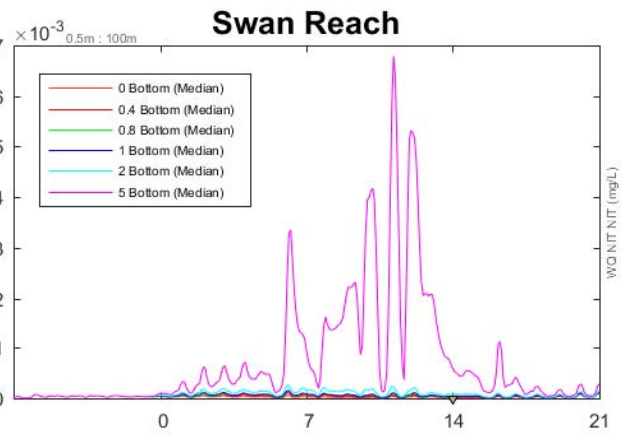
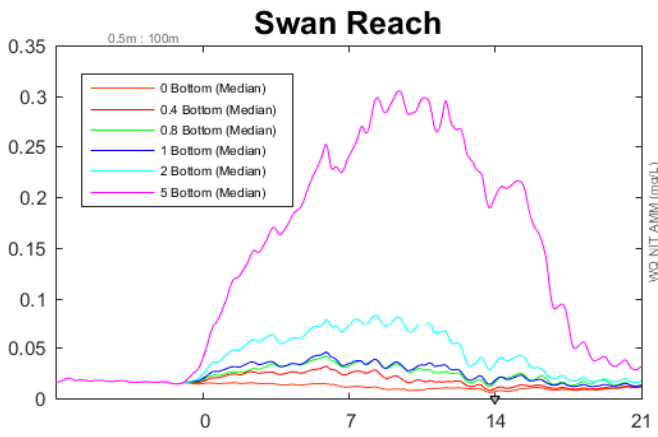
The PO_4 trends matched that for NH_4 , consistent with the high concentrations assumed to be released during breakdown. DOC was also simulated to increase by modest amounts, except in some of the disconnected sites in the Chowilla domain (e.g., Lake 2) where very high accumulation occurred. The DOC is relatively slow to react so this accumulation could act as a longer driver of oxygen demand.

Therefore, as with oxygen, there are regions with excessive nutrients, but overall the accumulation of nutrients is modest even at biomass values higher than the anticipated mortality rate. Unlike oxygen, the nutrient values do persist within the ecosystem and are not “reset” by reaeration; therefore they do present an ongoing risk contributing to long-term cyanobacterial productivity.

Figure 24 (overpage): Time series of NH_4 (left) and NO_3 (right) concentrations from the 1-month DCP simulations assessing carp biomass loading from day 0. Legend entries refer to the biomass loading factor, where 1× is the biomass according to Stuart et al. (2019). Selected sites are presented from the four domains in order from north to south (see Appendix B).







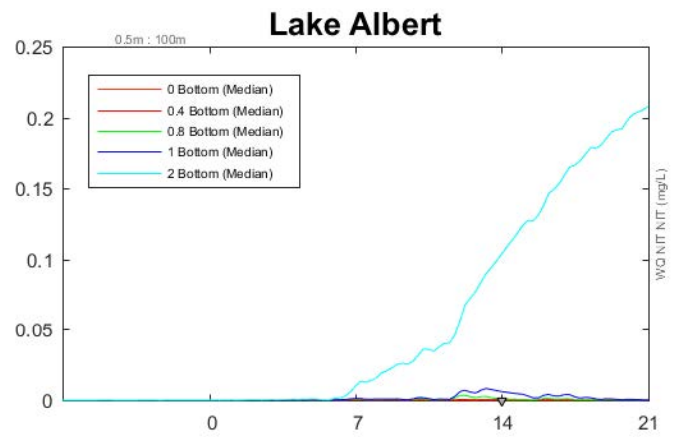
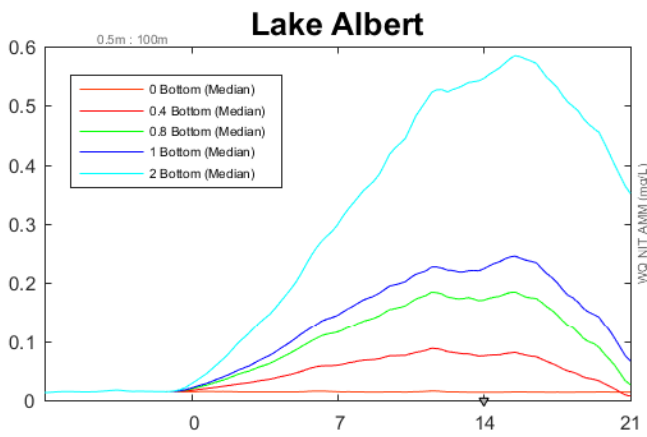
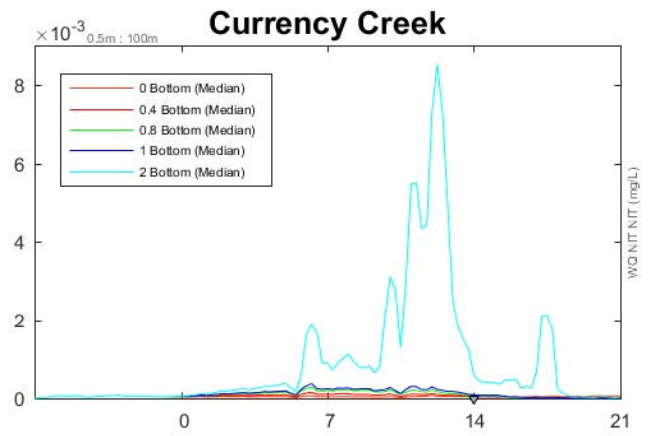
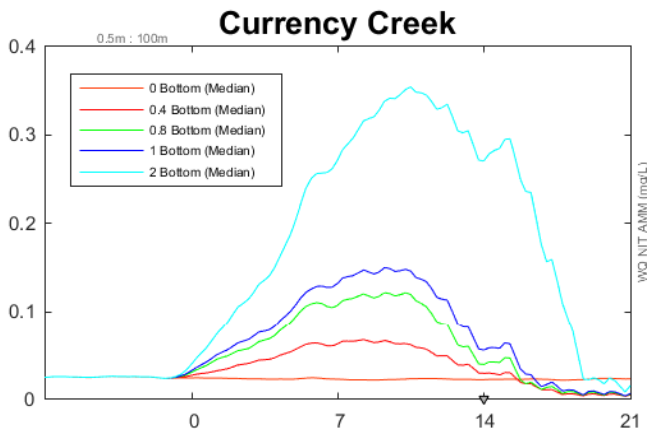
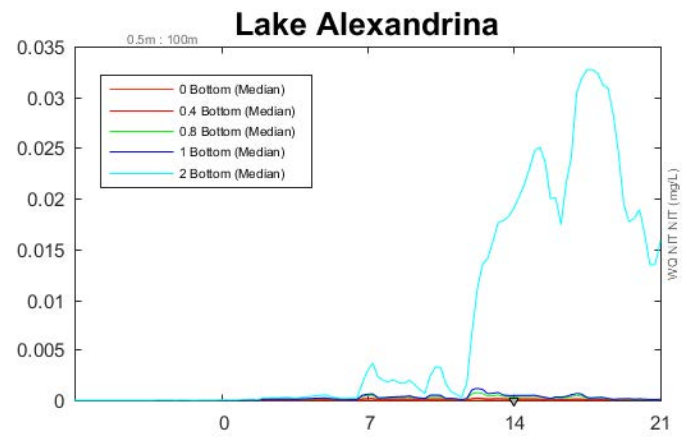
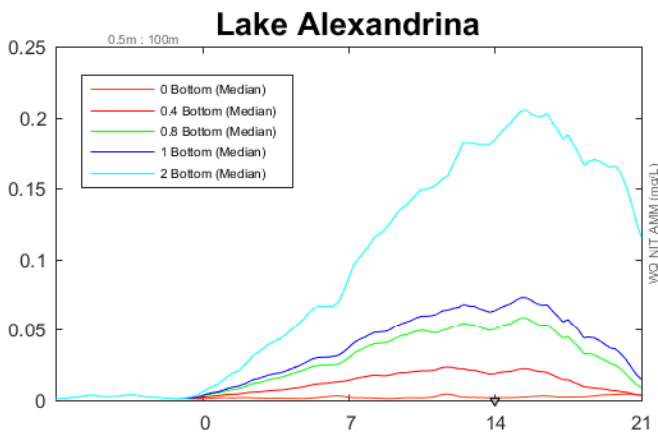
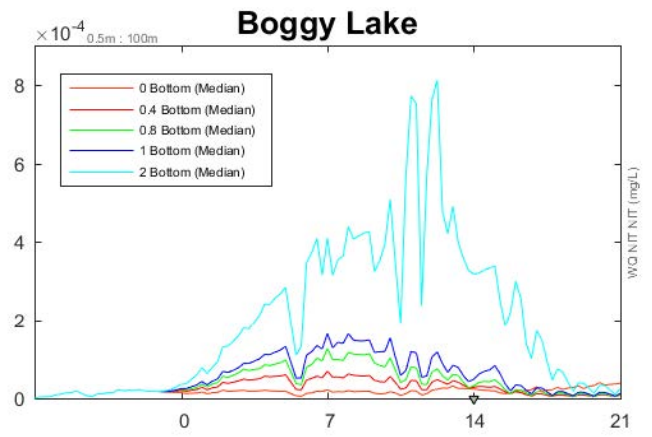
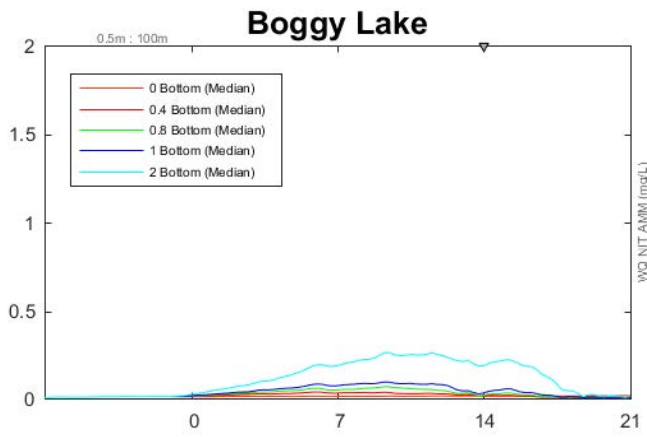
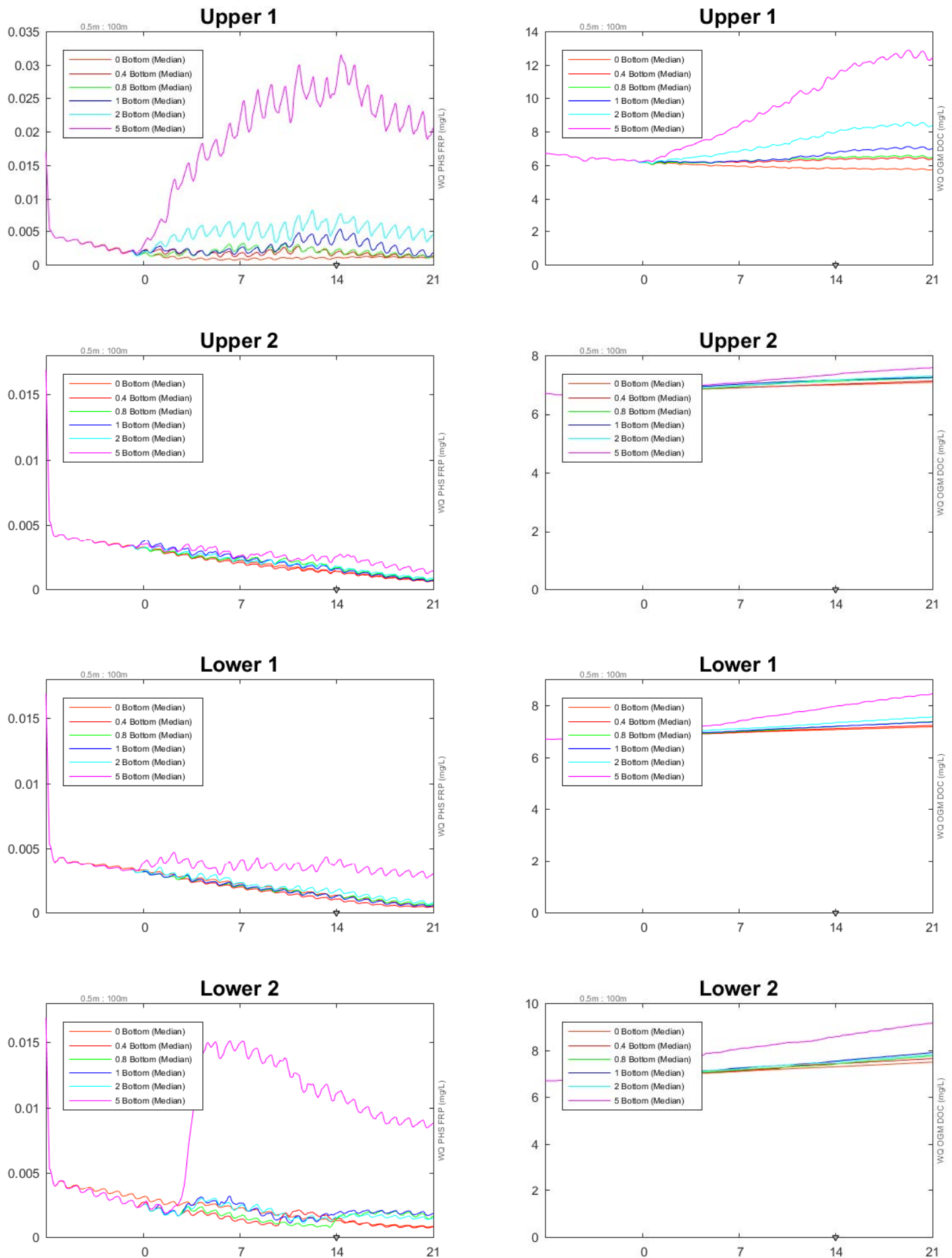
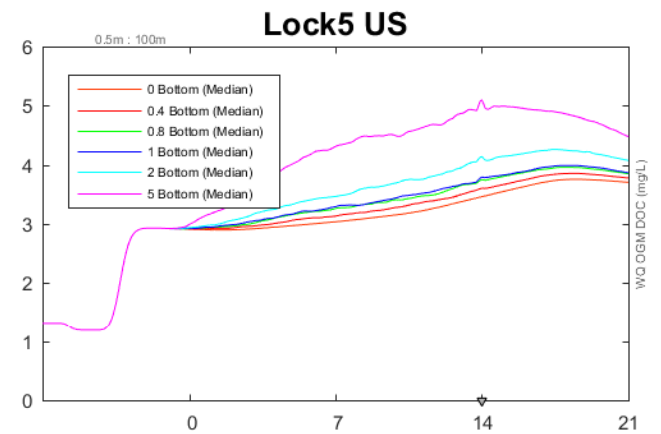
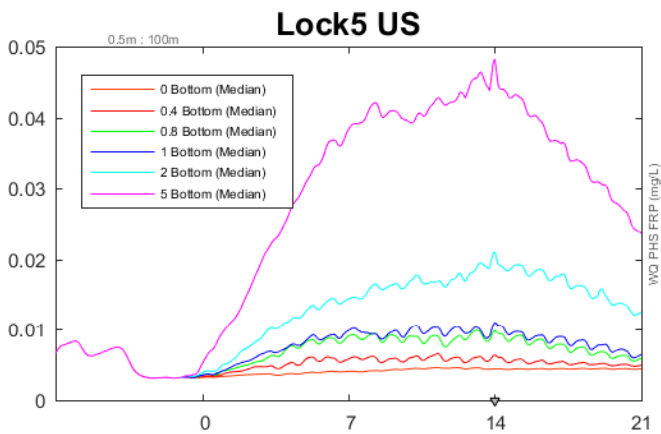
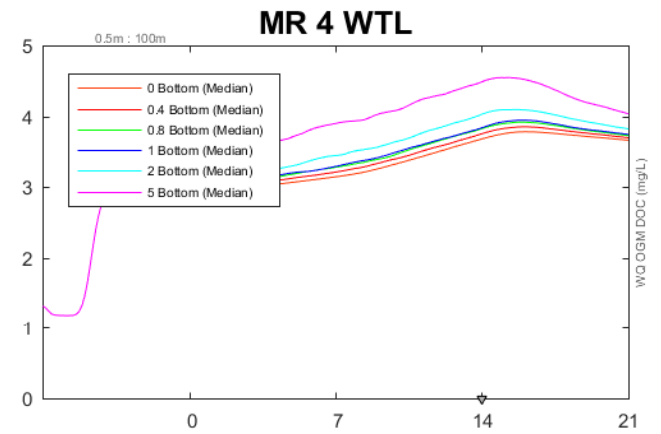
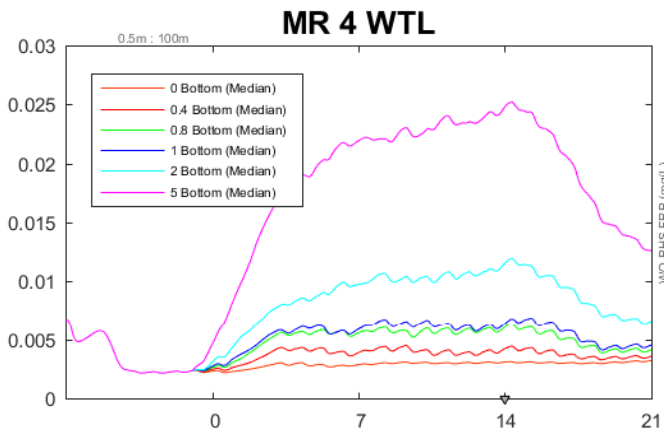
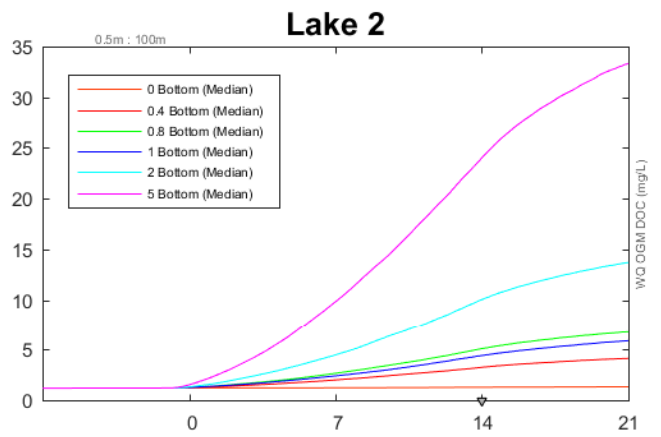
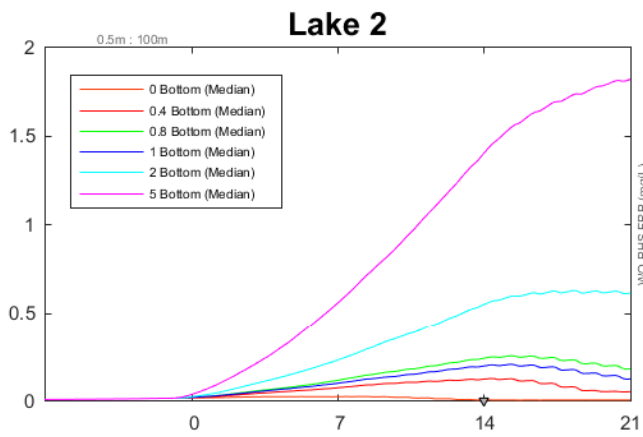
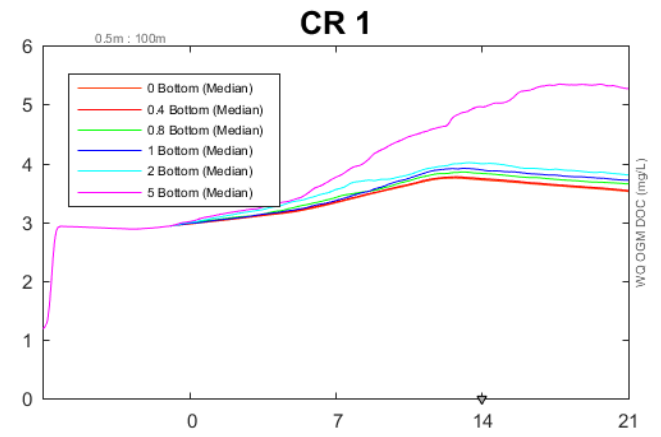
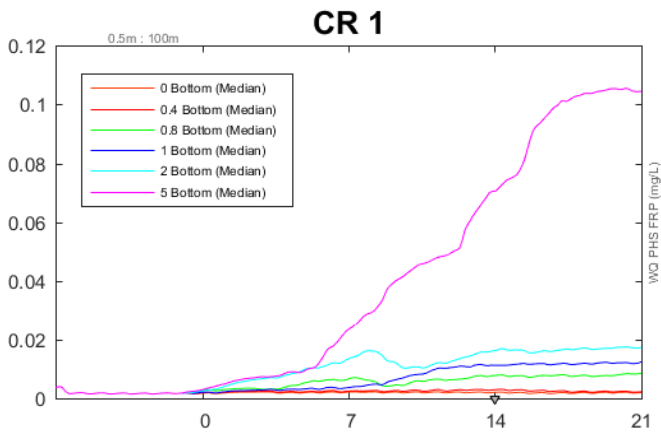
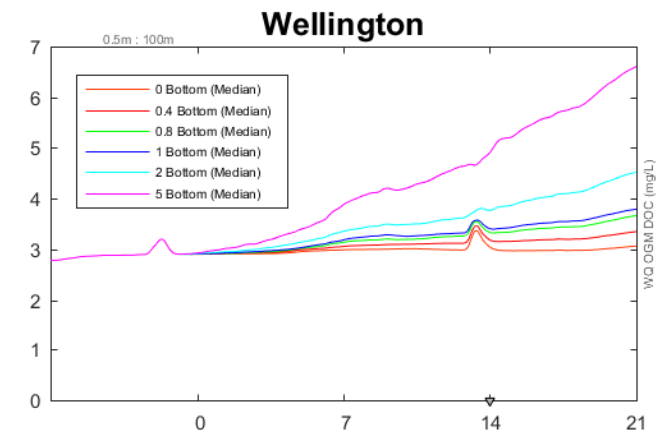
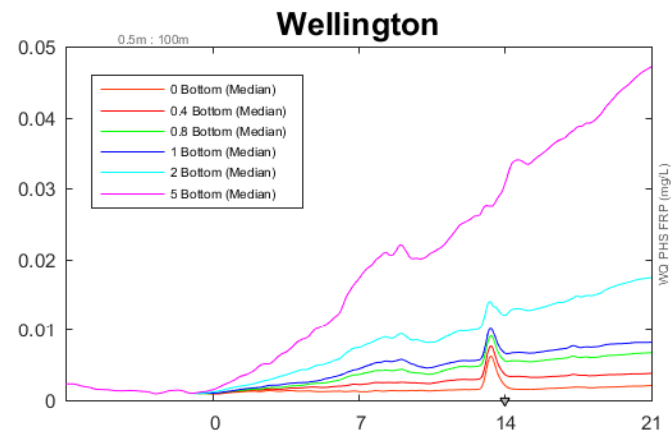
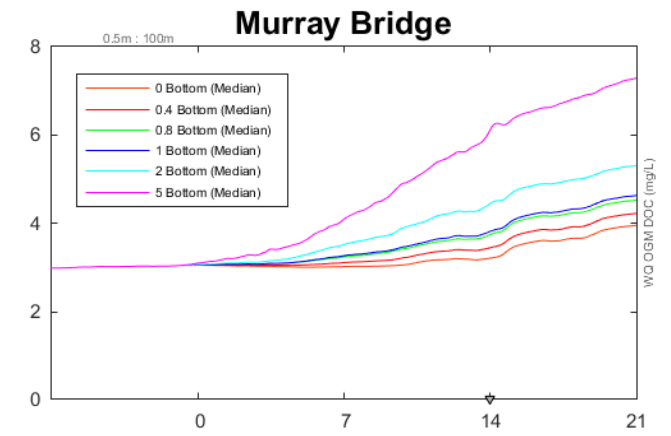
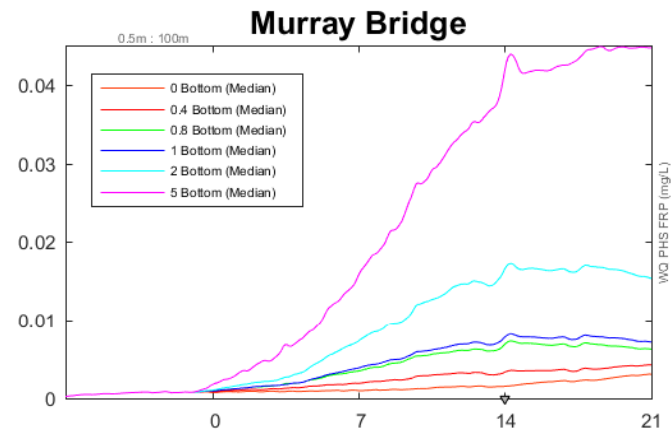
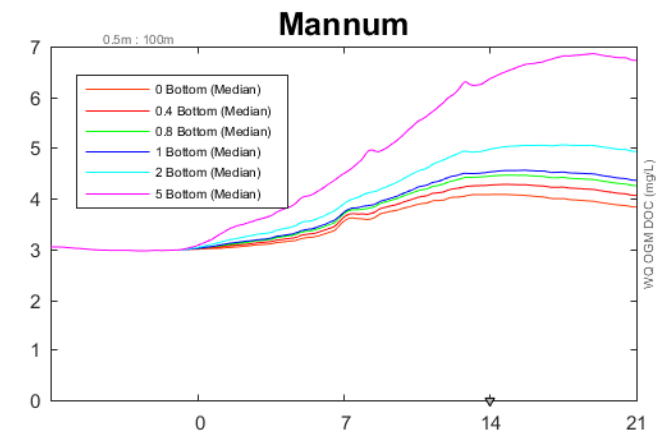
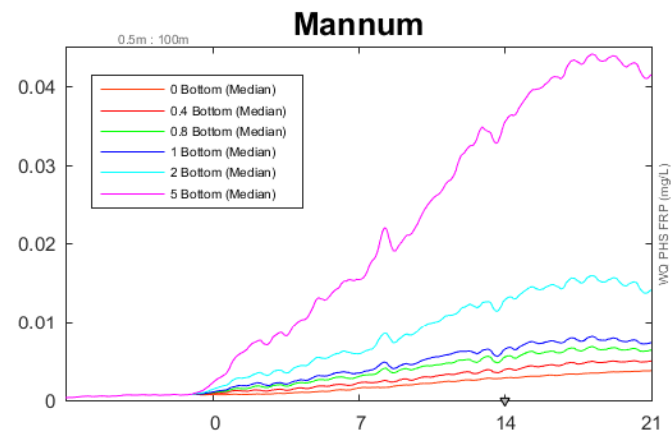
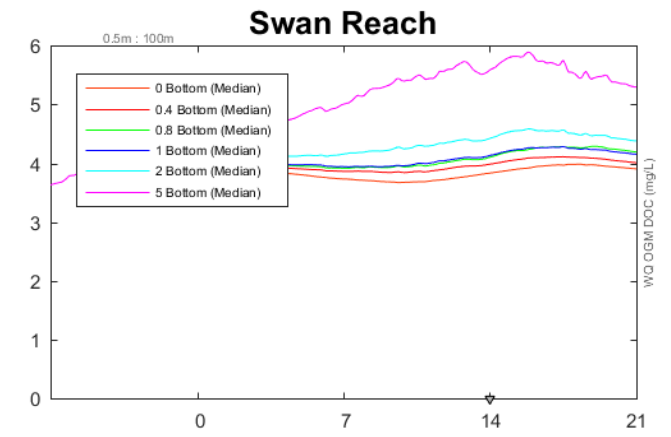
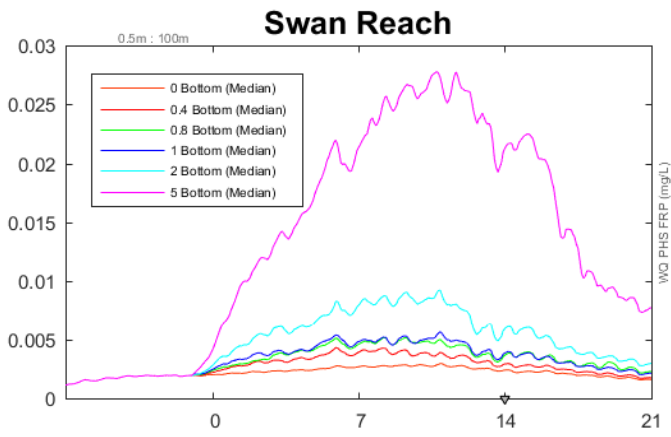


Figure 25 (continues overpage): Time series of PO4 (left) and DOC (right) concentrations from the 1-month DCP simulations assessing carp biomass loading from day 0. Results for flow factor 1x are shown. Legend entries refer to the biomass loading factor, where 1x is the biomass according to Stuart et al. (2019).







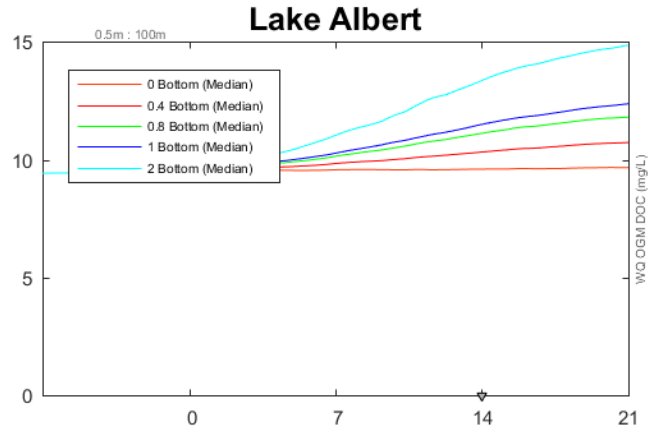
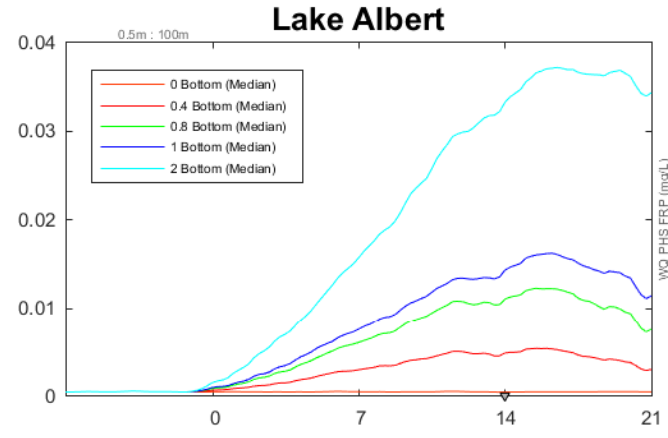
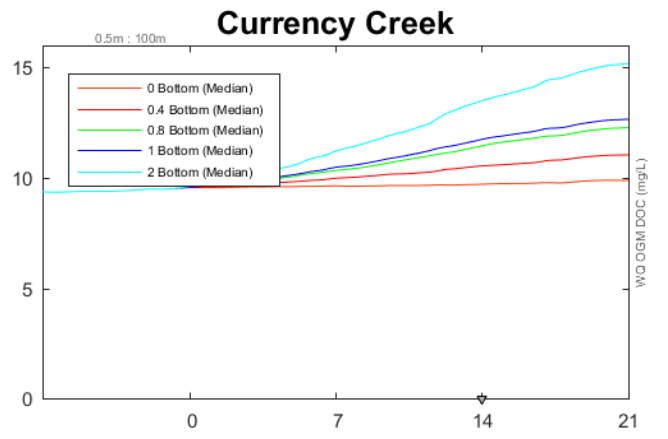
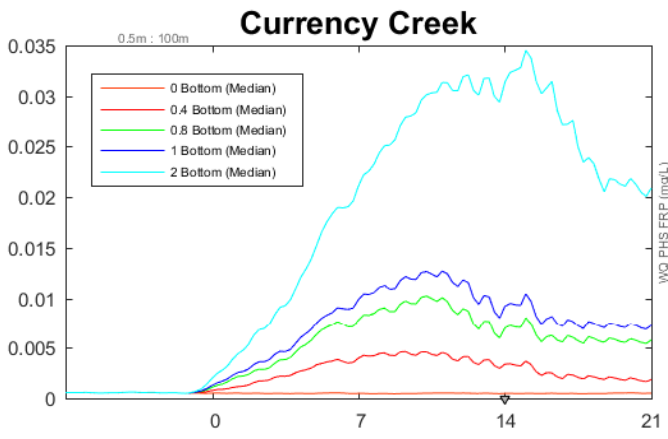
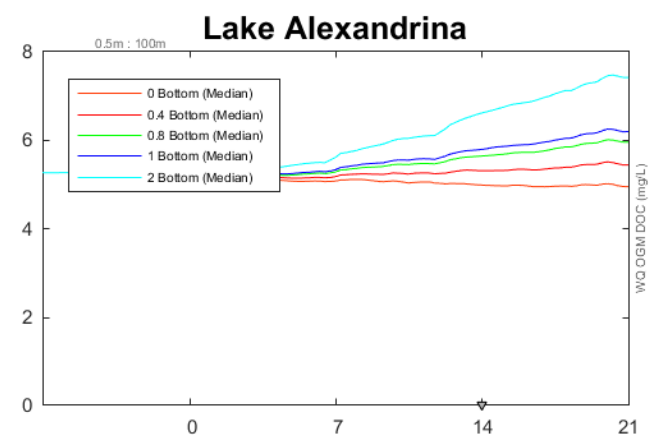
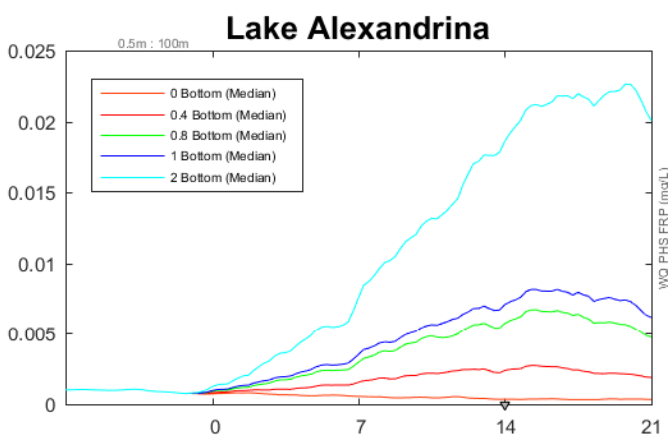
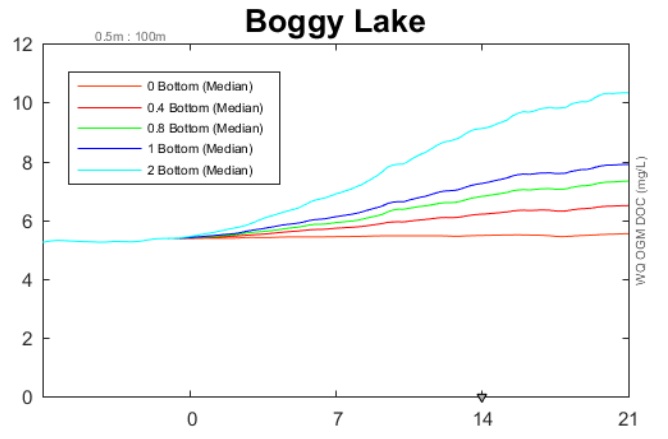
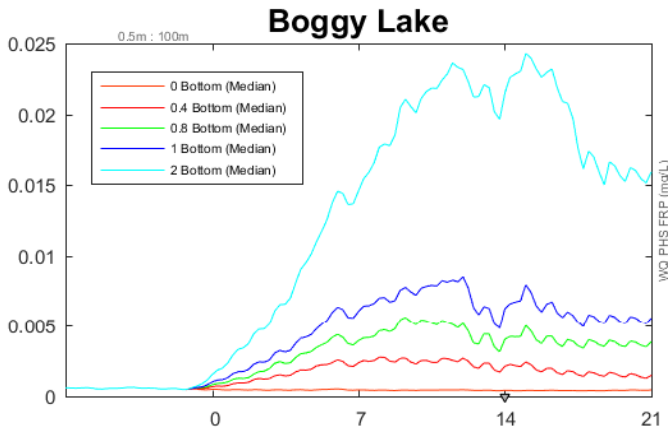
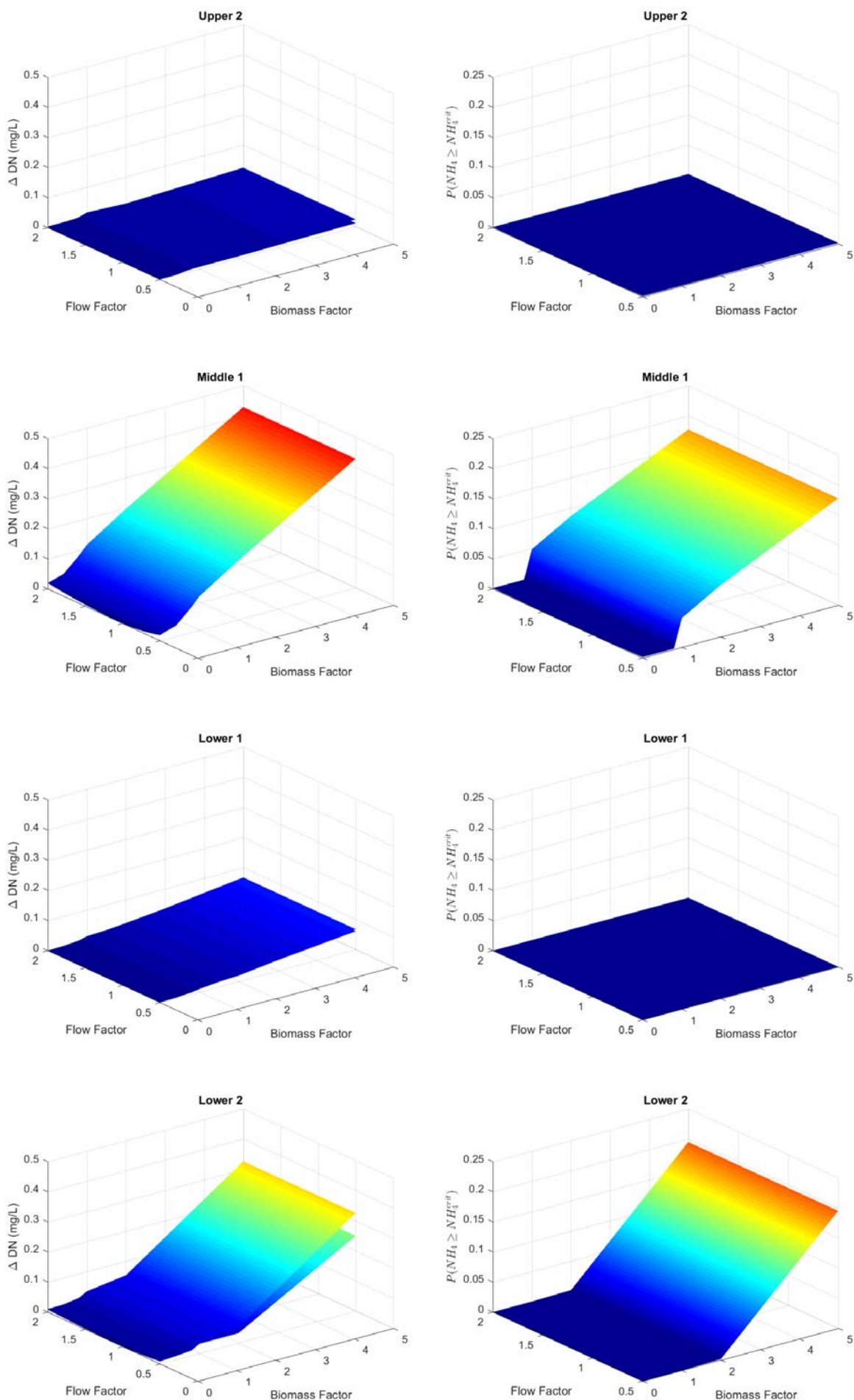
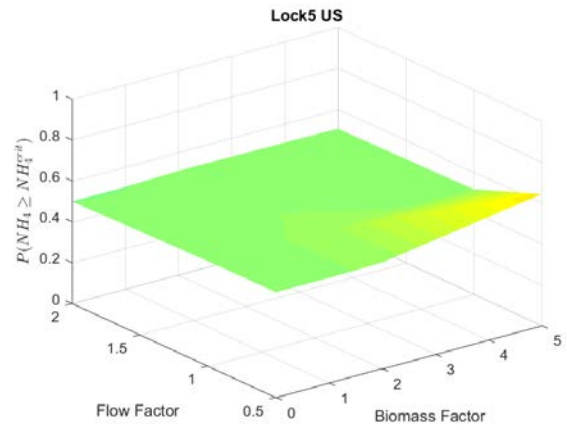
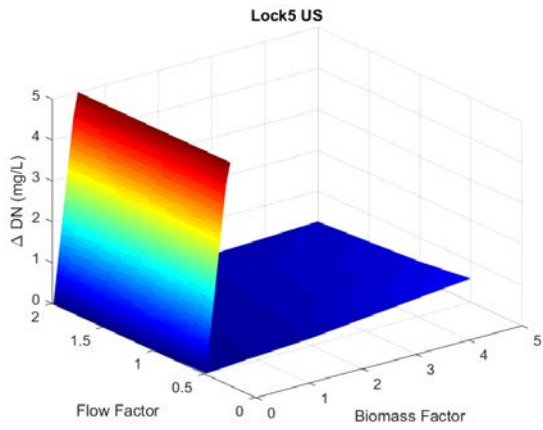
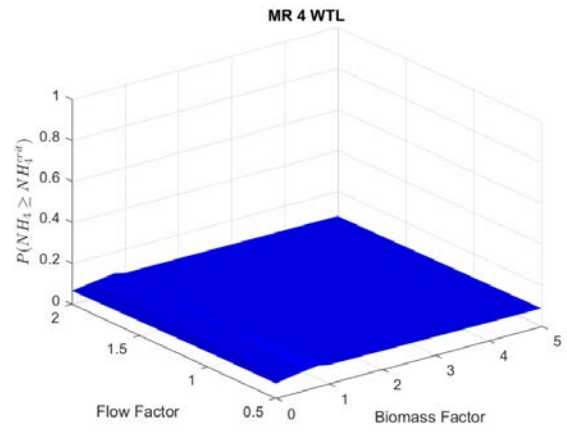
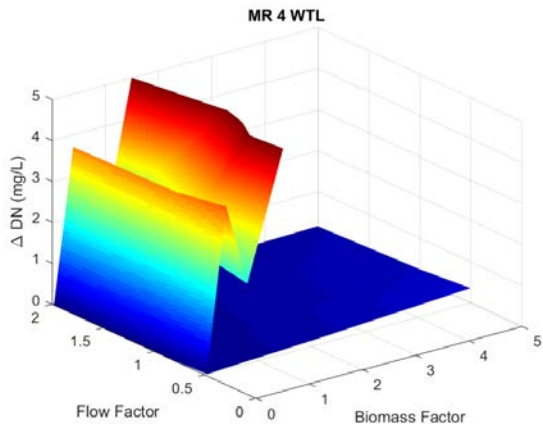
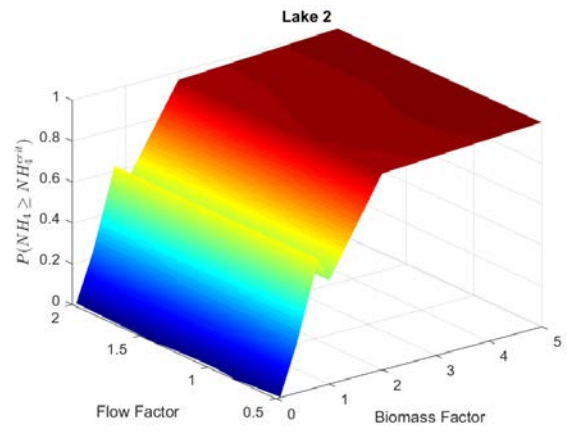
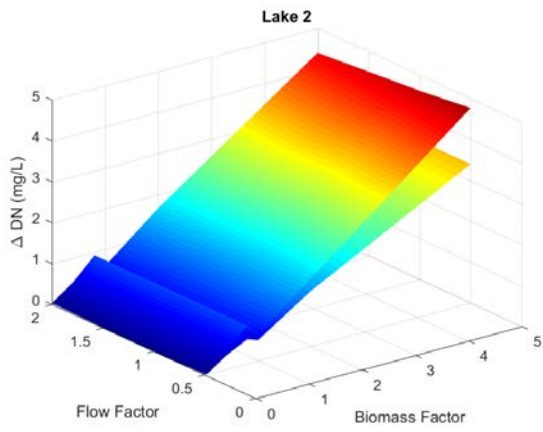
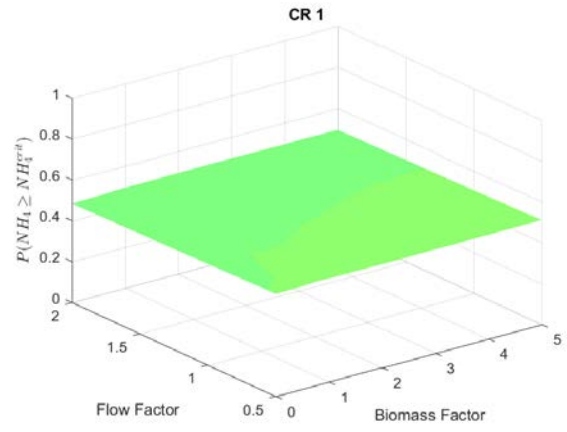
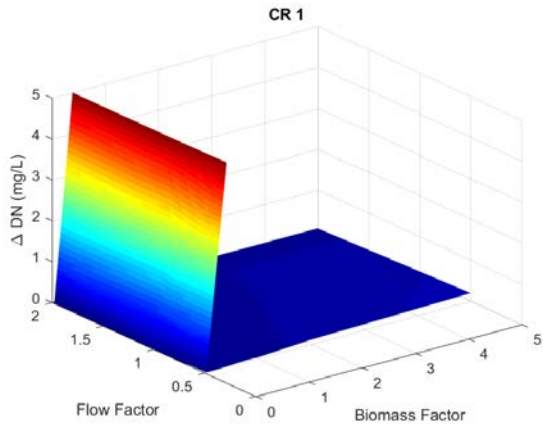
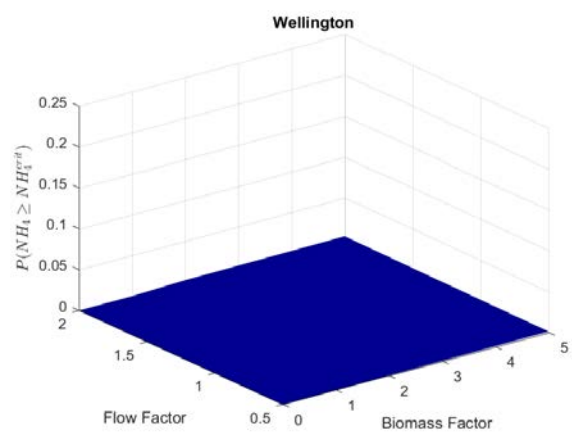
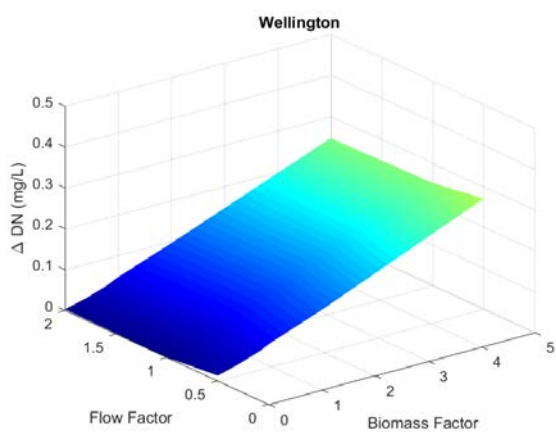
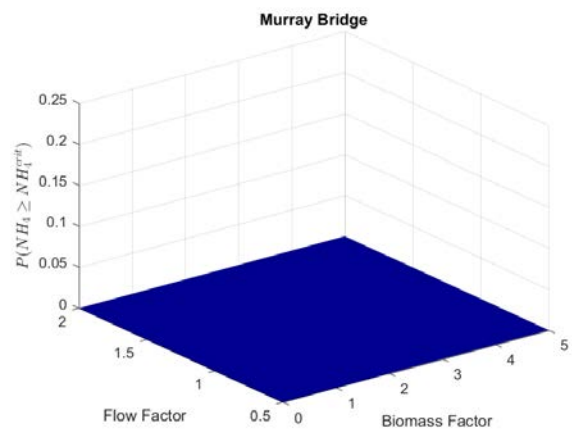
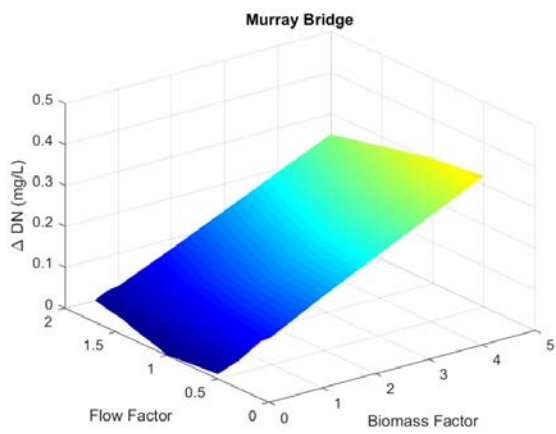
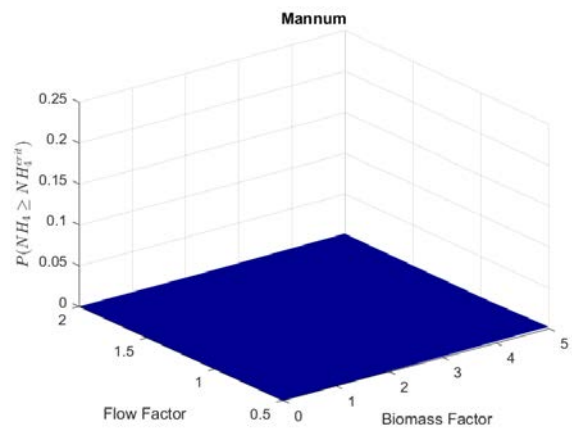
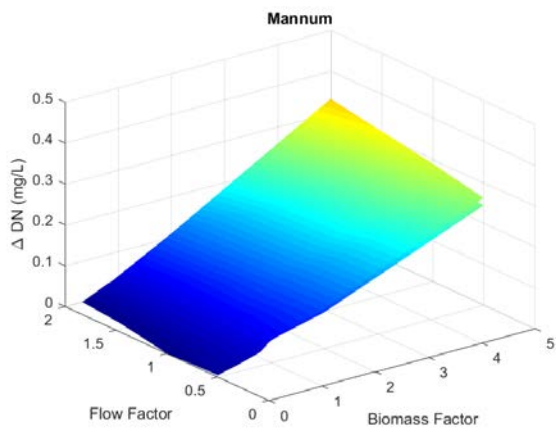
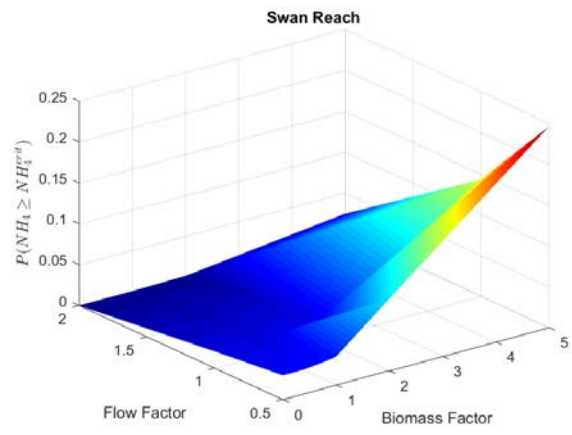
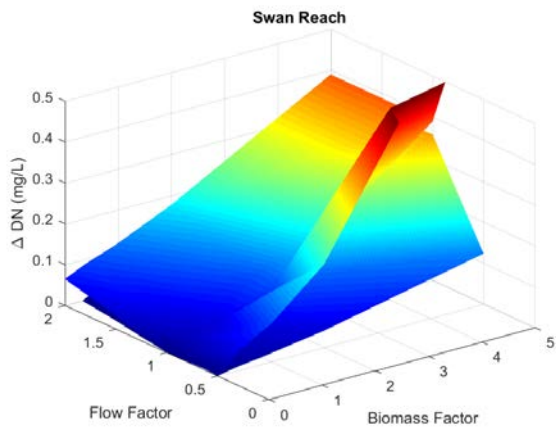


Figure 26 (continues overpage): Response surfaces of dissolved nitrogen (DN) accumulation (left) and ammonium toxicity risk (right) caused by carp mortality (DCP), for different flow conditions and biomass loading factors. The biomass factor of 1 represents the biomass values reported in Stuart et al., (2019), and a flow factor of 1 is as in Figure 20. For panels with 2 surfaces, the upper layer reflects water less than 50cm deep.







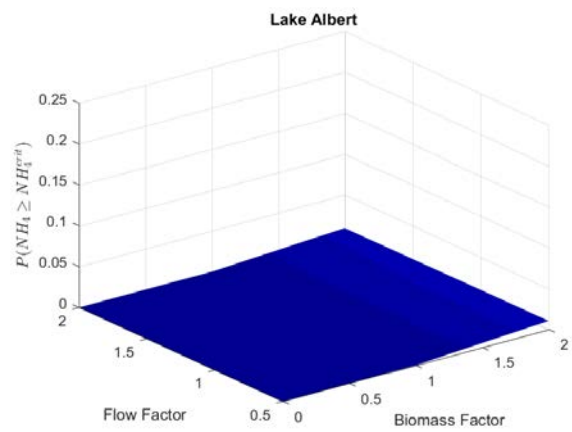
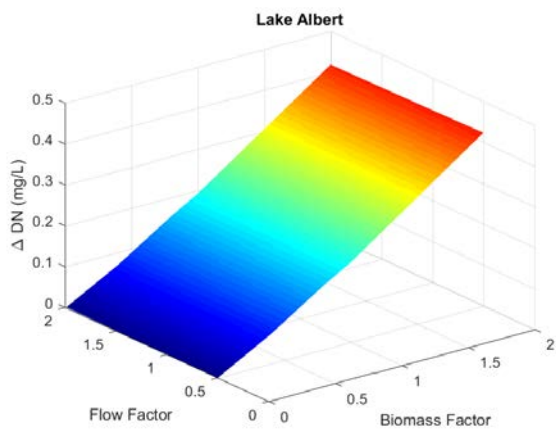
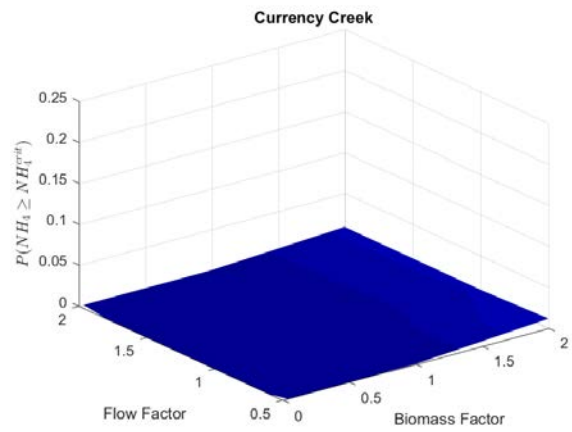
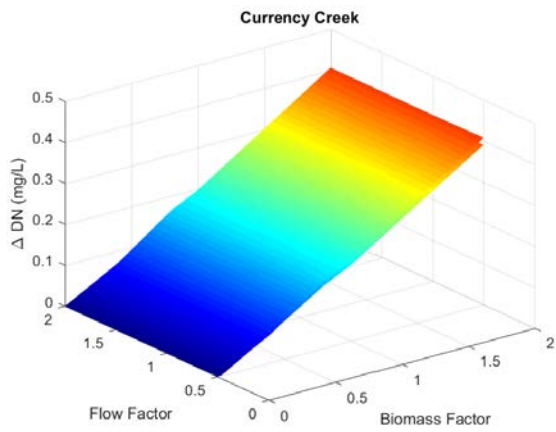
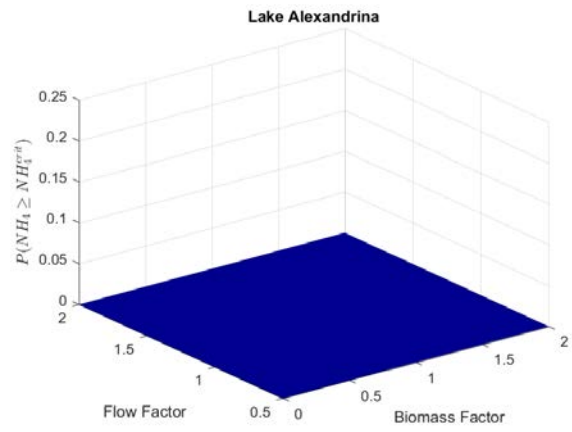
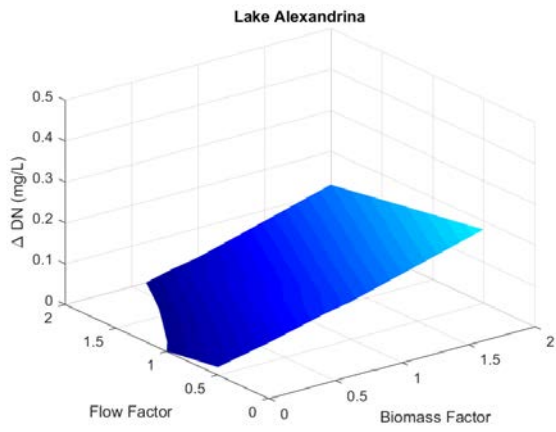
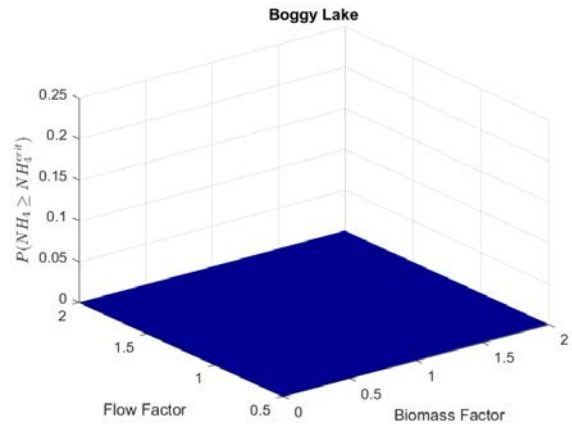
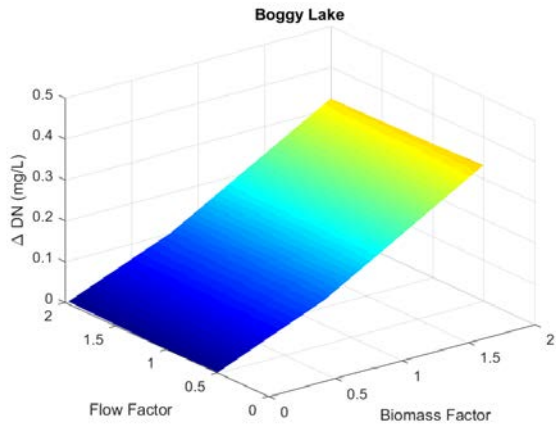
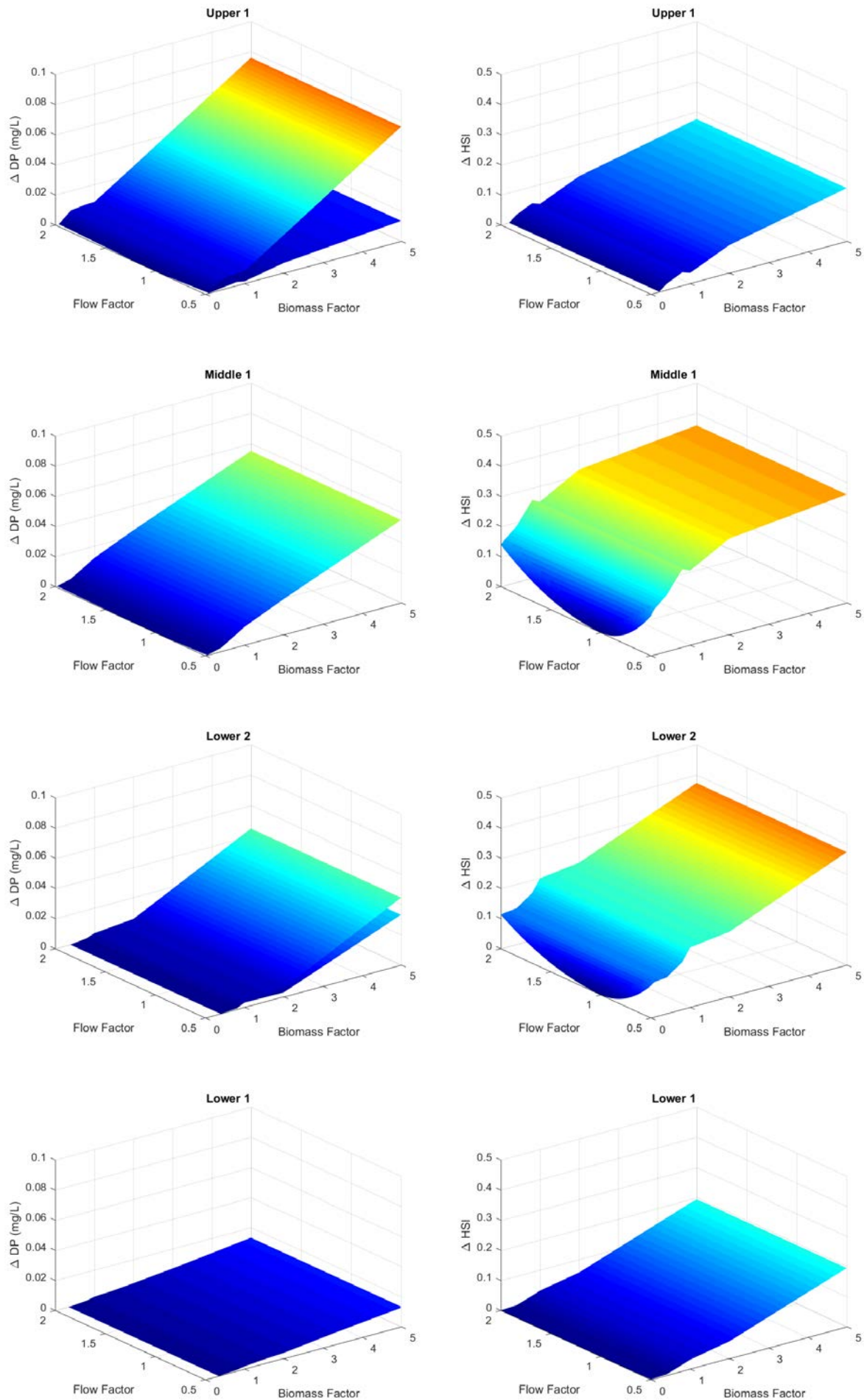
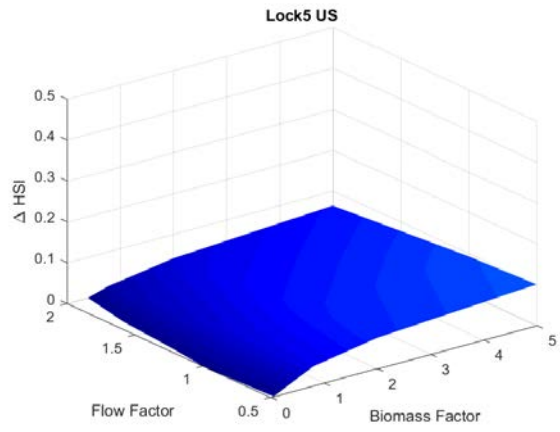
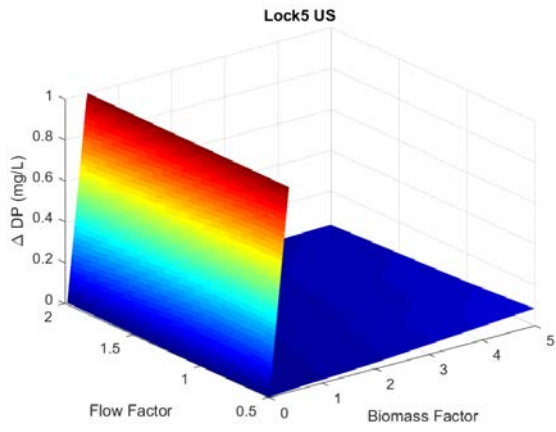
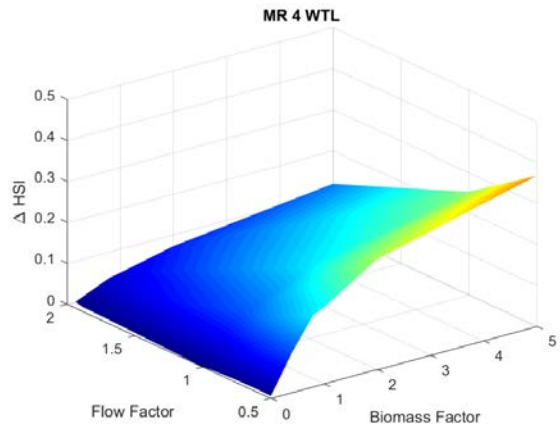
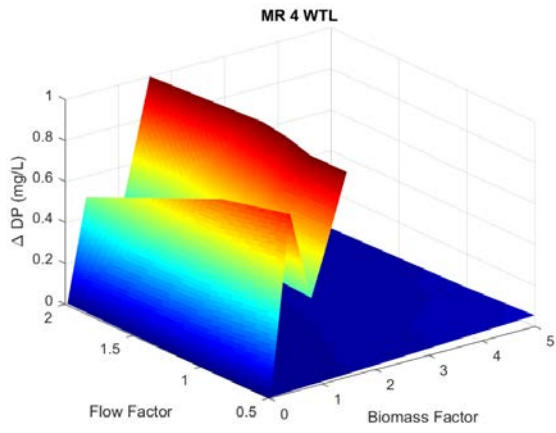
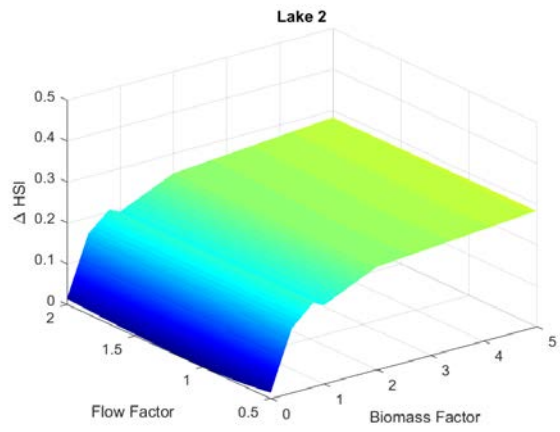
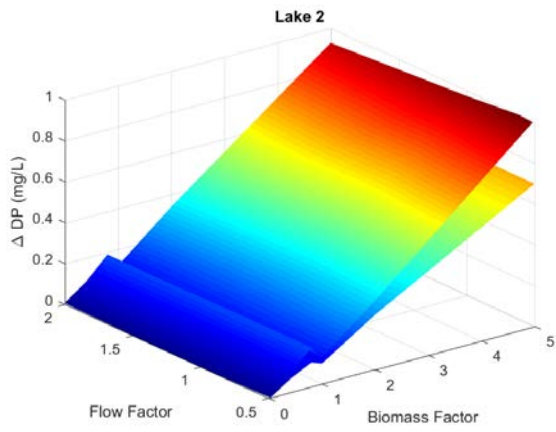
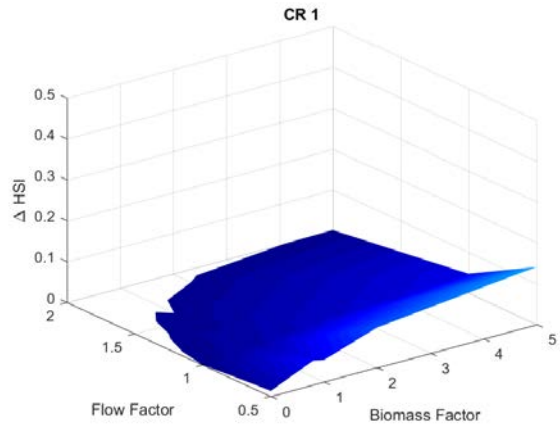
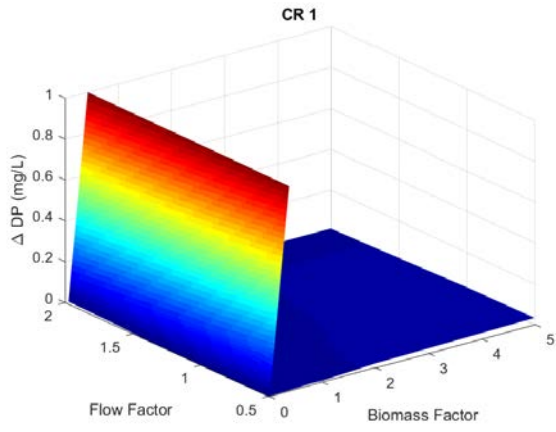
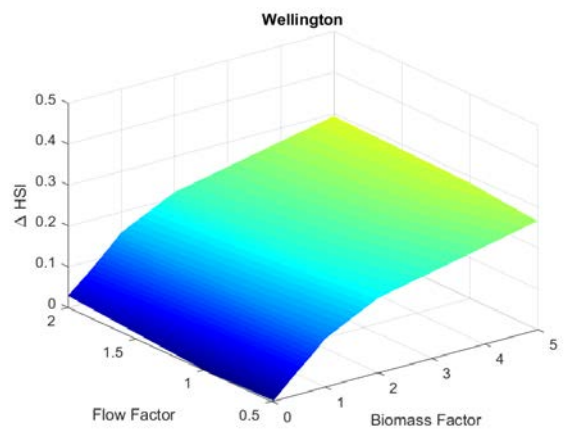
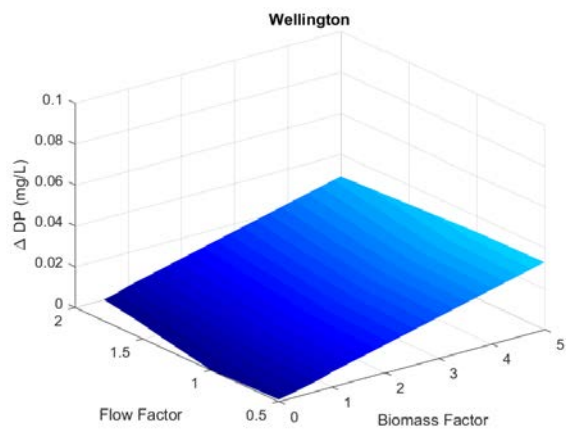
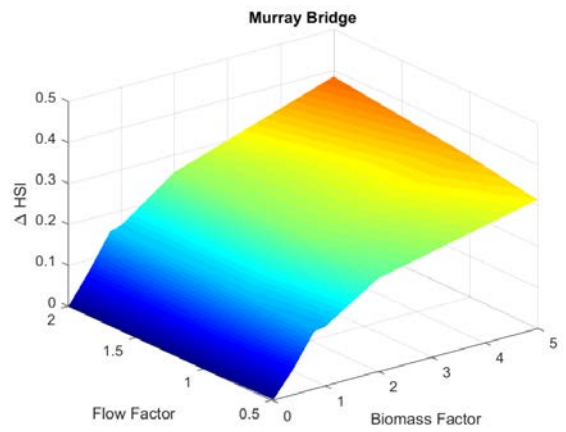
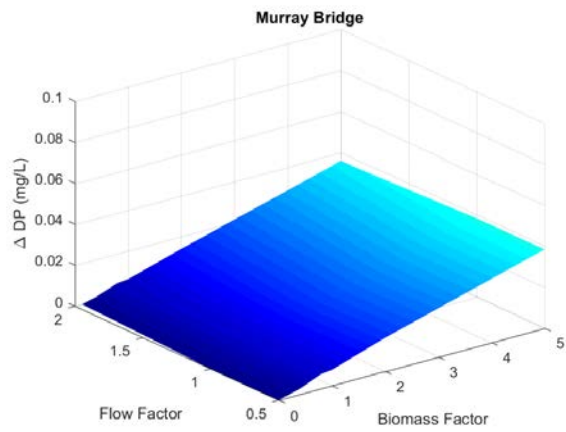
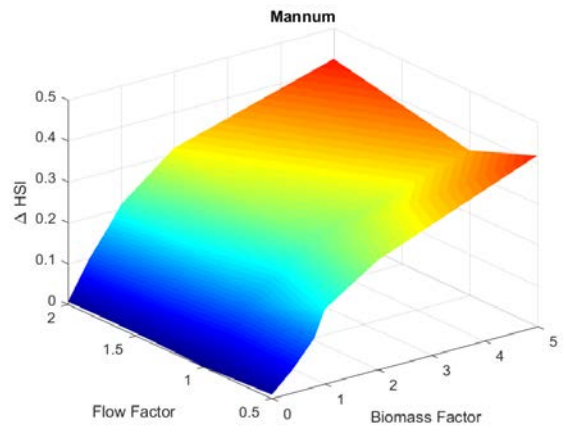
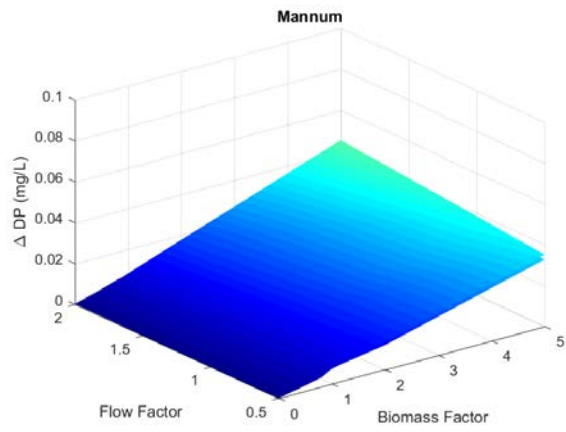
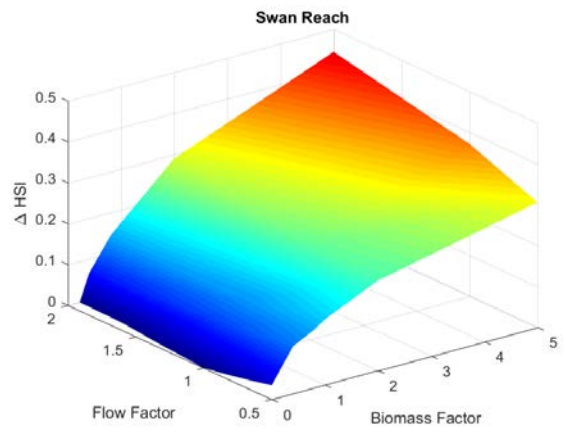
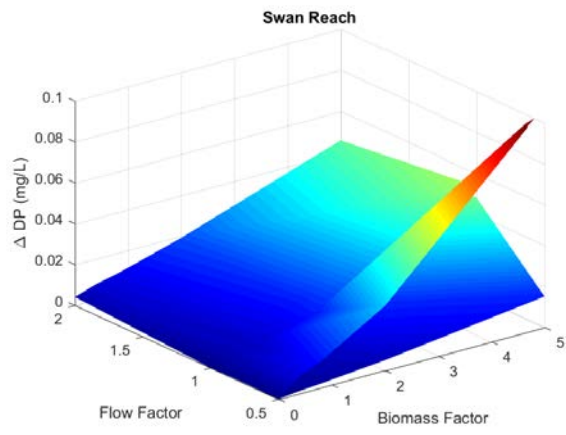
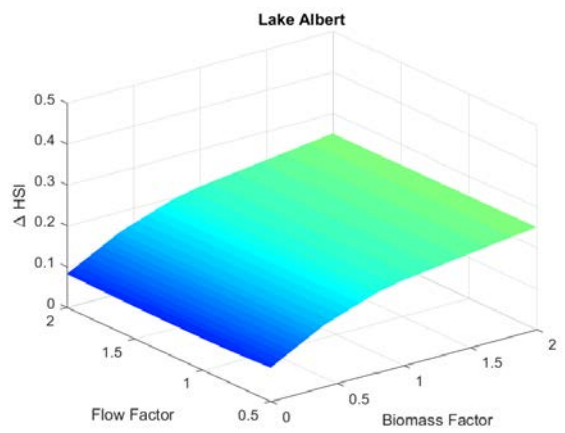
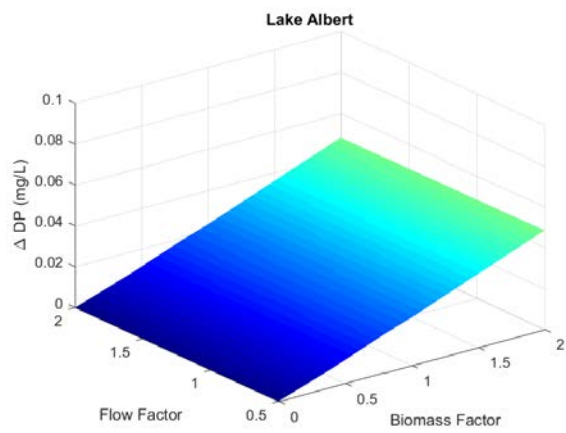
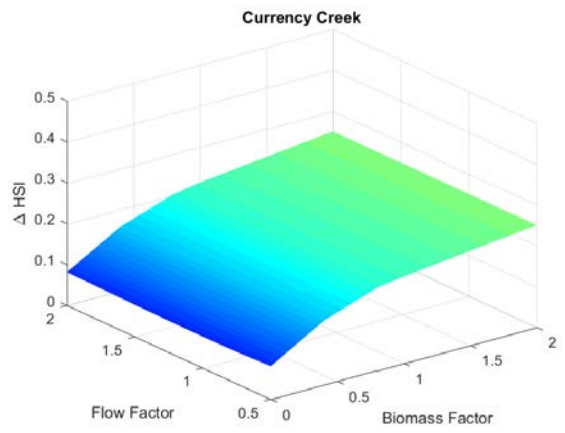
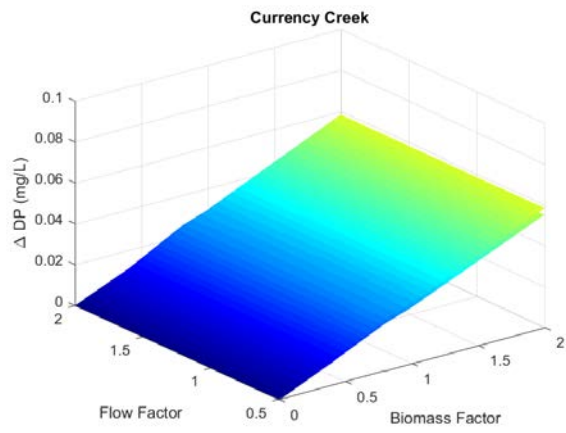
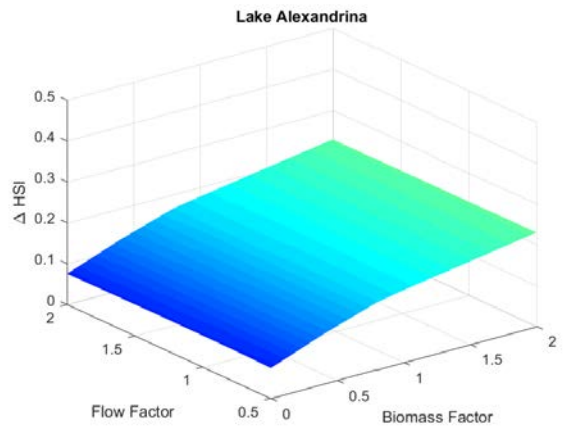
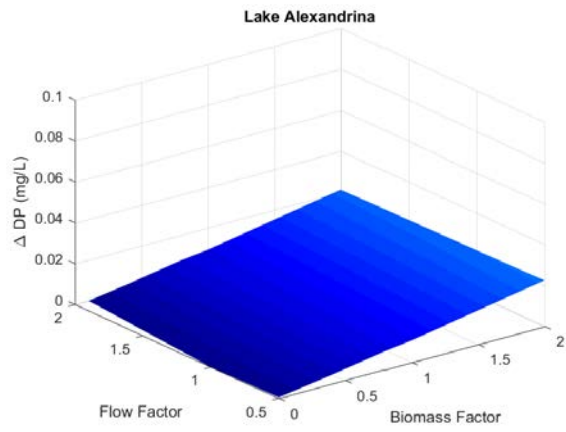
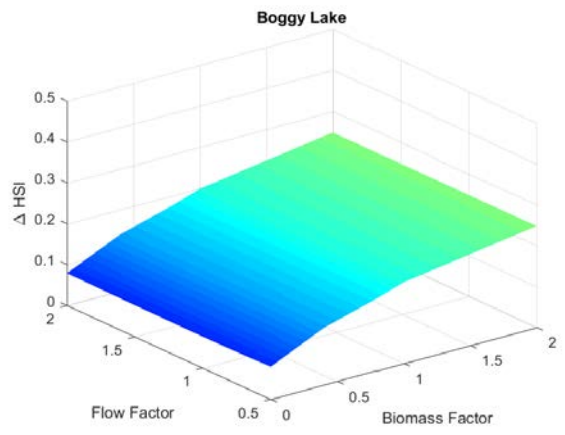
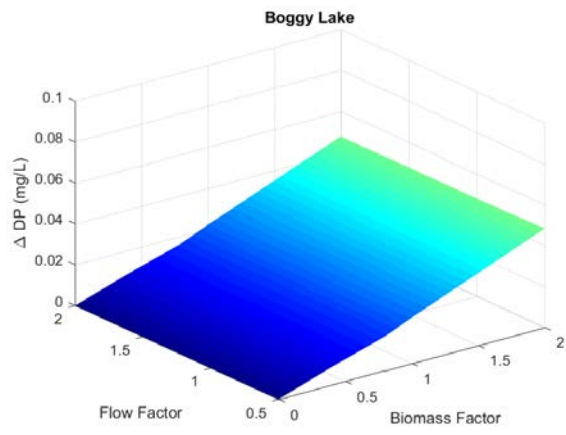


Figure 27 (continues overpage): Response surfaces of dissolved phosphorus (DP) accumulation (left) and cyanobacteria risk increase (right) caused by carp mortality (DCP), for different flow conditions and biomass loading factors. The biomass factor of 1 represents the biomass values reported in Stuart et al., (2019), and a flow factor of 1 is as in Figure 20. For panels with 2 surfaces, the upper layer reflects water less than 50cm deep.







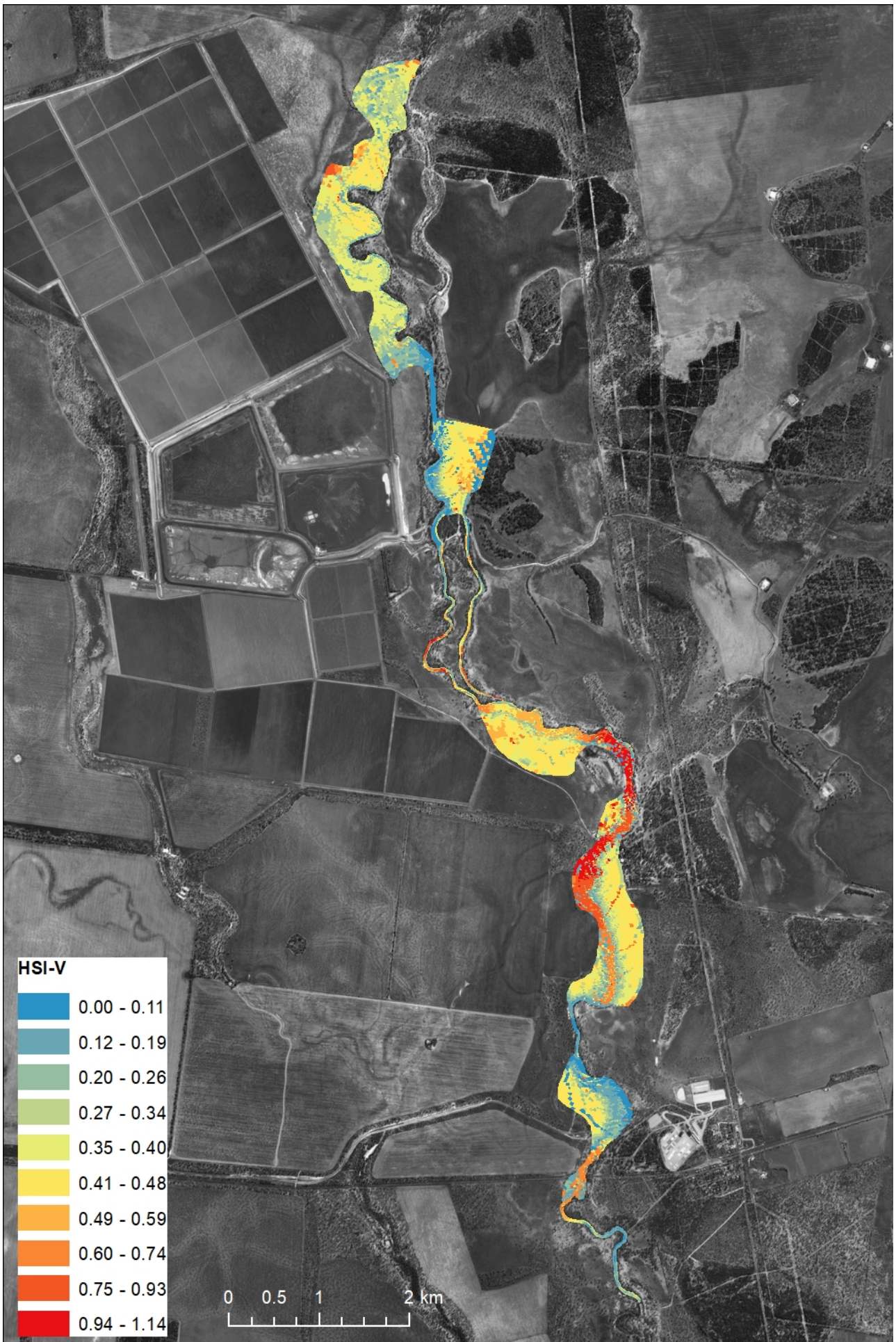


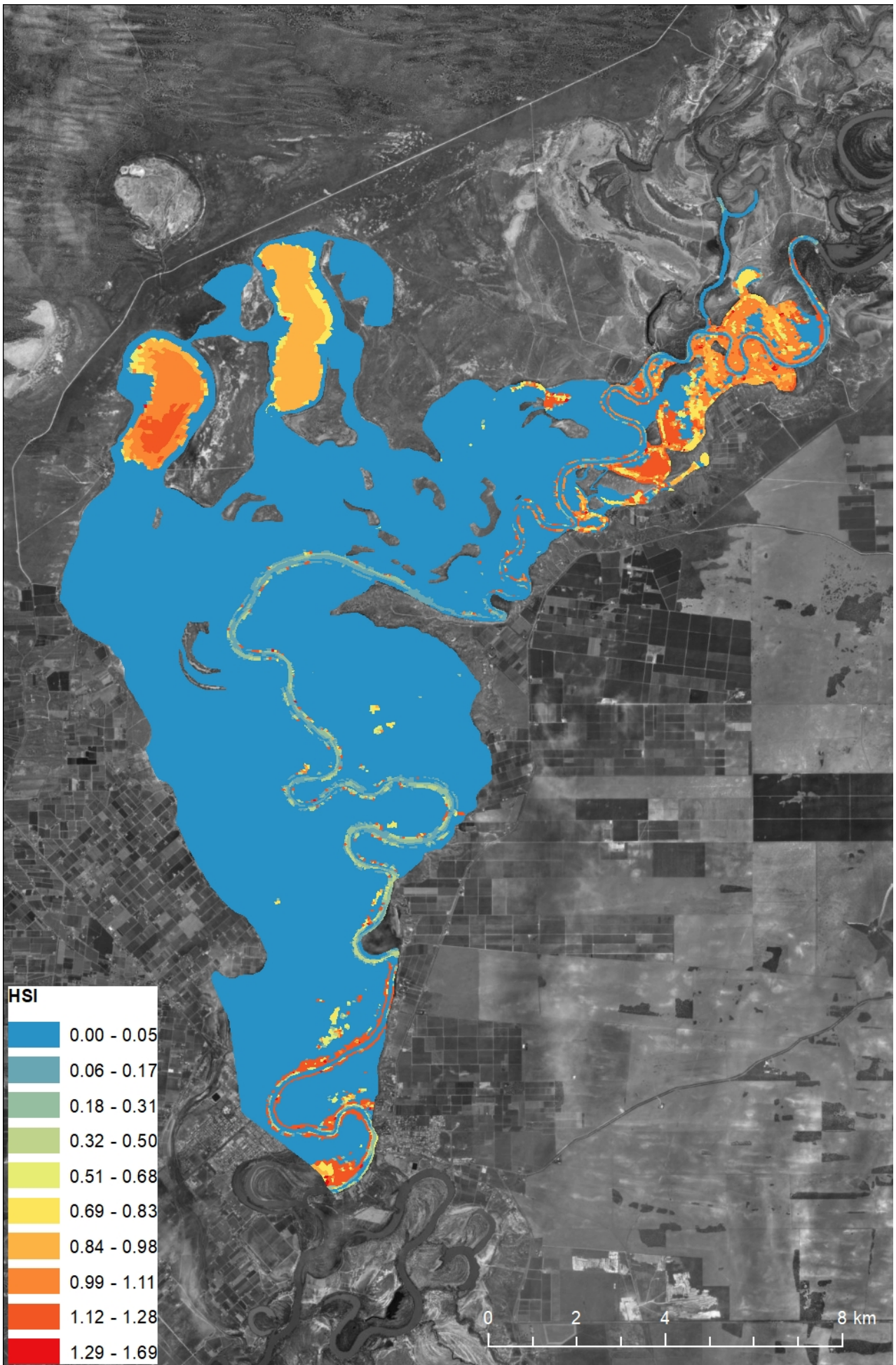
Cyanobacteria assessment

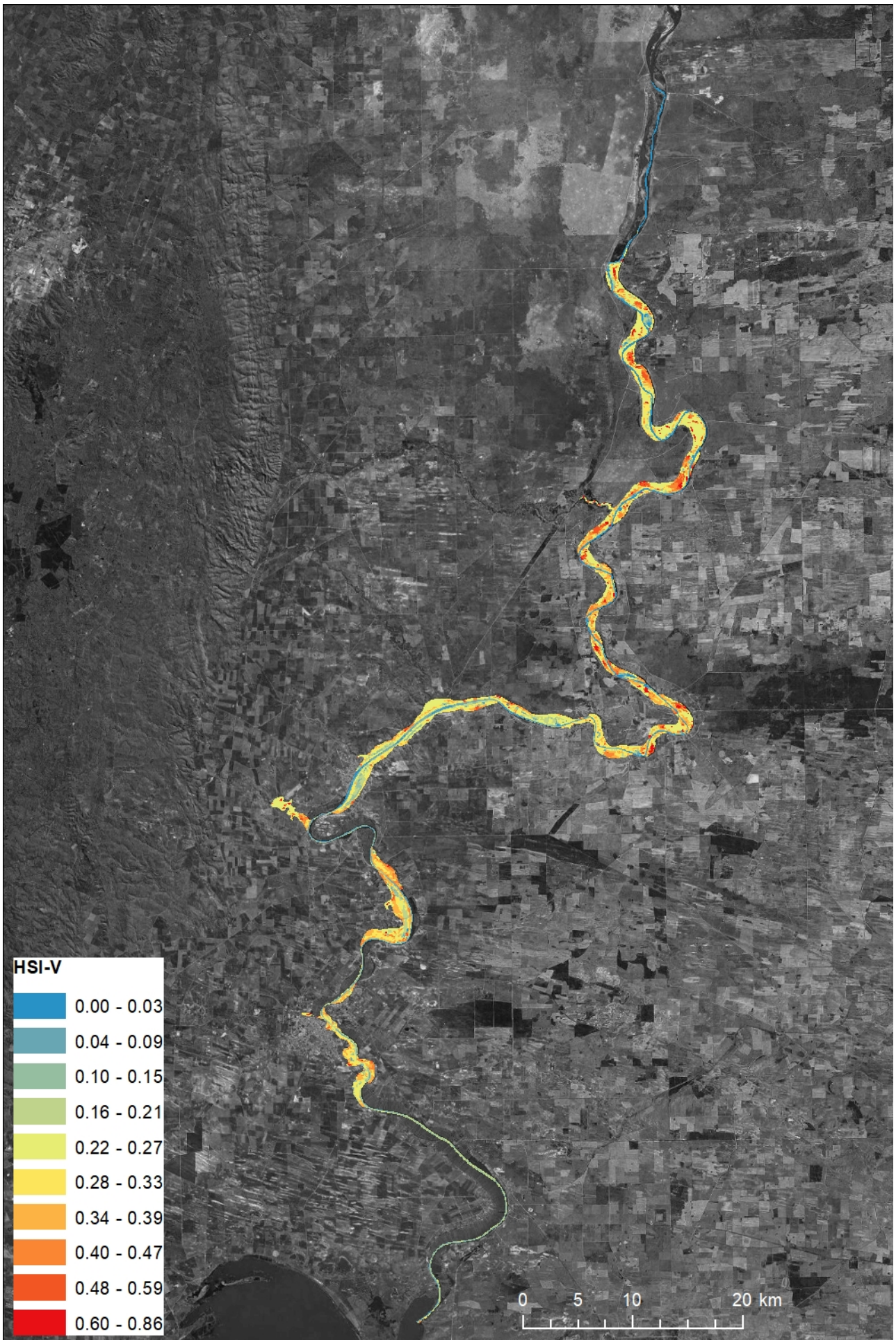
Response surfaces for the cyanobacteria risk calculation (Δ HSI) are shown alongside PO_4 in Figure 27 (above). Generally, the HSI is sensitive to carp biomass, linked to the high values of NH_4 and PO_4 being released into the water. The HSI increase, relative to base conditions, is most notable in the Lower Murray and Chowilla. Values are summarised in Appendix C.

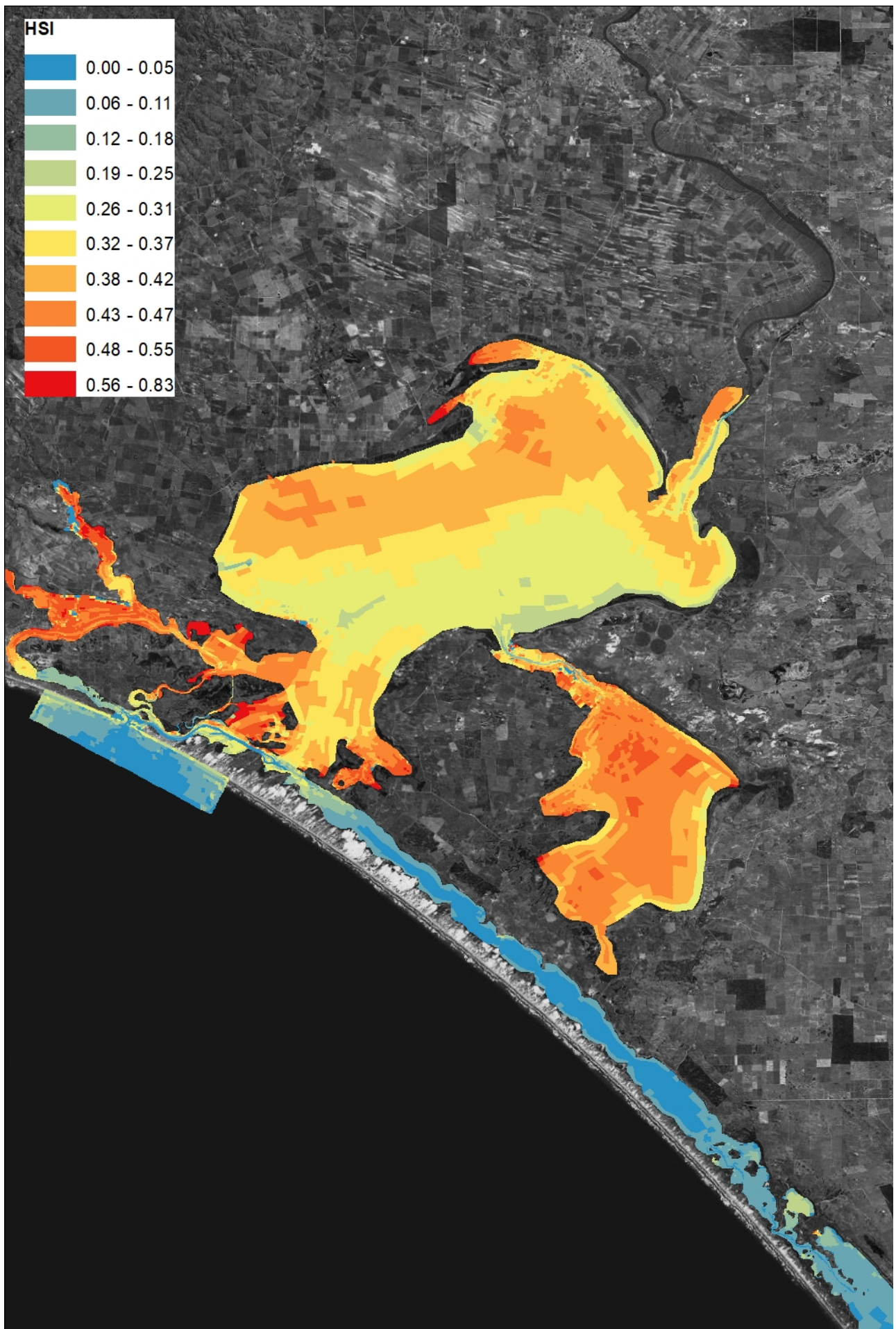
Maps showing areas of heightened HAB growth potential are shown in Figure 28 for the four domains.

Figure 28 (overpage): Average of the HAB suitability index (HSI, -) in the four simulated domains, assuming 100% carp biomass mortality over the simulation period (and no upstream carp inputs).









Discussion

The model approach is a first to be able to explore, at high resolution, the potential manifestation of carp mortality events due to the spread of the CyHV-3 after its introduction. Whilst there is a diversity of environments and hydrologic conditions that span the MDB and other Australian waterways, the analysis has highlighted that the risk of water quality decline can be assessed by considering the local balance of hydrologic flushing vs. biomass loading. The main simulated regions assessed in this study have together captured a range of conditions spanning a gradient of water flow and connectivity, and we have attempted to generalise from these sites by finding biomass loading thresholds relevant across the continuum of water body connectivity.

The lowest risk to water quality is when the carp biomass is evenly distributed over the system when mortality occurs, but due to preferred habitats and aggregation behaviour it is likely biomass will be unevenly distributed. By comparing the HC and DCP simulation approach we can gain insights into the significance of carp transport and accumulation, relative to an even spread of the biomass over the entire waterbody. Generally, the water quality effects of the dynamic particles implementation was comparable to the HC approach, particularly at the regional scale, however, individual sites did show differences. The spatial patterns of accumulation of carp biomass were compared across shallow and deep water environments and lakes, wetlands and rivers. As expected, the results did highlight accumulation “hotspots” are likely to occur and that there will be areas of concentrated water quality risk in poorly connected embayments, downwind areas, flow impediments, and “dead-end” flow paths with poor or partial connectivity to the main flow; carp densities in these regions became disproportionately higher than elsewhere.

At the biomass levels reported for these sites (Stuart et al., 2019), as supplied to this analysis, and considering the peak knock-down rates estimated of the epidemiological modelling (Davis et al., 2019), the risks to water quality within most sites and sub-regions of the simulated domains were manageable and not catastrophic. For oxygen, there tended to be modest oxygen sag’s; this was attributable to the re-aeration effects at the water surface buffering water column oxygen levels. There was some minor sensitivity to flow, but generally the extent of oxygen sag responded linearly to biomass loading. The length of impact was also co-incident with the time period over which the biomass entered, though DOC levels did increase and were not as fast to recover, thereby leading to a legacy oxygen demand. This was, however, generally within the levels of observed variability in DOC due to hydrologic variability. A limitation of the study is that we ran a relatively short period of hydro-meteorological conditions, and so periods of very still conditions, for example, may further exacerbate the effects reported here.

Of the systems studied, anticipated biomass levels in the Moonie River study domain were the lowest of all tested and as a result showed minimal impacts compared to other sites. This is somewhat counter-intuitive

give the risk within dryland rivers is different relative to the wetter rivers, and concerns about trapping of biomass during low flows between storm events and the potential for pool disconnection. Currently these pools already exhibit high risk to water quality due to poor flow, periods of stratification, and high nutrient concentrations that lead to cyanobacterial blooms (AAS, 2019). It is worth noting however, that the period tested for carp mortality was April-September, as this is when ambient water temperatures were considered to be most relevant to a virus outbreak. Previous cyanobacteria blooms have occurred in this period, but the high risks of algal blooms are in summer when stratification and warm water temperatures favours algal biomass growth and surface scum development. Nonetheless, further analyses of particular pools or reaches thought to be at high risk are recommended under low to zero flow conditions, noting however that virus transmission is likely to be sporadic without flow driving pool connectivity.

Even in these sites where oxygen sag was minimal, the dissolved nutrients did climb to problematic levels in some cases and the HAB risk also is increased. The levels of nutrient accumulation were more notable due to the high levels of bioavailable N and P released by carp biomass on decay, and the lack of a mechanism for short-term nutrient removal. Increases in levels of PO_4 , NO_3 and NH_4 were all predicted, though in most areas this was within the range of observed variability in these parameters for the anticipated (1×) biomass levels. As for oxygen, there were some exceptions to this with build-up of PO_4 in particular in shallow and poorly connected lakes and wetlands. In most sites, NH_4 build-up did not exceed thresholds associated with ammonium toxicity, except in some areas of the highest-biomass domain (Chowilla), where shallow waters and lake environments started to display very high levels that did not dissipate over the month-long simulation time scale.

Cyanobacterial bloom formation relies on the coalescence of favourable conditions, not just high nutrients but also warm temperatures and generally still (low flow) hydrodynamic conditions. Nonetheless, in line with the above findings, the cyanobacterial risk also followed trends described above for oxygen and nutrients, and the nutrient addition will exacerbate existing risks experienced by Australian waterways.

Of course, there is significant uncertainty in the biomass estimate (e.g., whether the densities apply equally under different hydrologic conditions), and in the estimate of virus transmission and the dynamics of carp population mortality. There is also uncertainty in the decay rate and transport dynamics assumptions used in this modelling. For this reason, 2× and 5× carp biomass alternatives for each domain and each flow setting were also assessed, to be able to more holistically see at what biomass water quality impacts manifest more significantly. Simulations run to test (hypothetical) higher biomass loading did begin to display more pronounced levels of oxygen sag. For sites with anticipated biomass amounts of 250 kg/Ha, once the decaying biomass levels exceeded this by 2-5×, periods of low oxygen were predicted to become more prominent, lasting for periods of weeks. In some cases, this did lead to more complete deoxygenation consistent with the wetland experiment reported in Chapter 1. At these levels the notable

decline in water quality was predicted, particularly in the Chowilla domain, which had the highest base carp densities of all the domains.

When biomasses that were by 2-5× higher than the anticipated amount were simulated, very high accumulations of PO₄ and NH₄ were reported in some sites that would be difficult to manage and would promote cyanobacteria bloom formation. The maximum concentrations detected in simulations exceeded the relevant freshwater trigger values outlined the Australia and New Zealand Guidelines for Fresh and Marine Water Quality (Australian and New Zealand Environment and Conservation Council and Agriculture and Resource Management Council of Australia and New Zealand 2000). Because the nutrient would likely enter the water at cool to medium temperatures, this may offset the increased risk, due to cyanobacteria preference for warmer waters, thereby providing time for flushing and dissipation of nutrients before highly favourable bloom conditions.

This analysis may still underestimate the extent of the biomass focusing into hotspots prior to decay, and this should be considered. The higher, hypothetical, biomass simulations can be used as a guide for what may be expected at these sites of high biomass focusing.

Implications

At the biomass levels anticipated based on the NCCP biomass and epidemiological projects, and under the hydro-climatological conditions tested, the likelihood of water quality impacts emerging appear to be modest at the broad-scale. Areas of biomass > 300 kg/Ha are predicted to show signs of decline, particularly in area with poor hydrologic connectivity, though they are relatively short lived when considered in the context of existing water quality conditions and periods of blackwater that the system already experiences. We highlight though that cumulative risk of poor water quality developing with increasing distance downstream has not been assessed in this study. If we consider the impacts on water departing the Chowilla domain and entering the Lower Murray at Lock 1, then it is foreseeable that the oxygen sags predicted here would be further increased.

This suggests that river hydrologic conditions should be considered in any release strategy, not just from the point of view of virus epidemiology, but as an important lever to mitigate the emergence of water quality risks. Hydrologic conditions suitable for virus transmission are potentially in tension with hydrologic conditions required to mitigate the subsequent water quality impacts, since higher flows reduce transmission effectiveness (Davis et al., 2019; Graham et al., 2019), but are beneficial for water quality management (e.g. Stewardson and Skinner, 2018). It is recommended high flows following a mortality event should be considered to enhance river flushing, to dilute biomass, and to prevent poorly connected areas becoming hotspots of biomass accumulation. CEWO (2017) have recently undertaken a review on approaches to manage naturally occurring blackwater events, which can help inform specific strategies for environmental watering options following a mortality event.

Whilst oxygen conditions can recover over reasonable time-frames due to reaeration, or potentially assisted through environmental watering, the long-term accumulation and persistence of nutrients will lead to a longer-term management challenge if not dealt with. The nutrients from decomposing carp are highly bioavailable and will fuel considerable algal growth, but the species of algae may vary depending upon the season and prevailing hydrodynamics. The pool of nutrients currently in carp in Australian waterways is considerable and, upon carp mortality, will be incorporated into algal biomass and contribute to an accumulation of nutrients in the sediment. These legacy nutrients may be available to support algal growth for a considerable period following any mass mortality event. Therefore, it is recommended that the release strategy also consider enhancing downstream (and ultimately oceanic) nutrient export by planning for a post-release hydrological conditions.

To prevent the cumulative risks of nutrient accumulation emerging, an effective approach would be to coordinate a clean-up program to remove fish carcasses prior to nutrient leaching. The study has highlighted that accumulation hotspots will occur, in downwind and poorly connected areas, including on the shallow margin, and therefore this suggests clean-up attempts could feasibly reduce nutrient inputs if removal was undertaken promptly (within a few days).

References

- Australian Academy of Science (2019). Investigation of the causes of mass fish kills in the Menindee Region NSW over the summer of 2018–2019
- Australian and New Zealand Environment and Conservation Council, Agriculture and Resource Management Council of Australia and New Zealand (2000) Australian and New Zealand guidelines for fresh and marine water quality. *Australian and New Zealand Environment and Conservation Council and Agriculture and Resource Management Council of Australia and New Zealand, Canberra* 1-103.
- Baker, PD, Brookes, JD, Burch, MD, Maier, HR, Ganf, GG (2000) Advection, growth and nutrient status of phytoplankton populations in the lower River Murray, South Australia. *Regulated Rivers: Research & Management* **16**, 327-344.
- Bormans, M, Maier, H, Burch, M, Baker, P (1997) Temperature stratification in the lower River Murray, Australia: implication for cyanobacterial bloom development. *Marine and Freshwater Research* **48**, 647-654.
- Bormans, M, Webster, IT (1997) A mixing criterion for turbid rivers. *Environmental modelling & software* **12**, 329-333.
- Bligh, EG, Dyer, WJ (1959) A rapid method of total lipid extraction and purification. *Canadian journal of biochemistry and physiology* **37**, 911-917.
- CEWO (2017) Blackwater Review - Environmental water used to moderate low dissolved oxygen levels in the southern Murray Darling Basin during 2016/17.
- Chorus, I, Bartram, J (1999) Toxic cyanobacteria in water: a guide to their public health consequences, monitoring and management. CRC Press
- Clunie, P, Koehn, J (1997) Recovery plans for silver perch and catfish. *RJ Banens and R. Lehane (eds)* 13-24.
- Correll, DL (1998) The role of phosphorus in the eutrophication of receiving waters: A review. *Journal of Environmental Quality* **27**, 261-266.
- Croome, R, Wheaton, L, Henderson, B, Oliver, R, Vilizzi, L, Paul, W, McInerney, P (2011) River Murray water quality monitoring program: phytoplankton data trend analysis 1980–2008. *MDFRC Publication* **6**, 2011.
- Davis, S, Hopf, J, Arakala, A, Graham, K, McColl, KA, Durr, PA (2019) The predicted impact of Cyprinid herpesvirus 3 as a potential biocontrol agent for controlling invasive common carp (*Cyprinus carpio*) in Australia, Unpublished report for Fisheries Research and Development Corporation, Canberra, ACT.
- Dean, TL, Richardson, J (1999) Responses of seven species of native freshwater fish and a shrimp to low levels of dissolved oxygen. *New Zealand Journal of Marine and Freshwater Research* **33**, 99-106.
- Driver, P, D., Harris, JH, Norris, RH, P., CG (1997) The role of the natural environment and human impacts in determining biomass densities of common carp in New South Wales rivers. *Fish and Rivers in Stress: The NSW Rivers Survey. NSW Fisheries Office of Conservation and the Cooperative Research Centre for Freshwater Ecology, Cronulla* 298
- Driver, PD, Harris, JH, Closs, GP, Koen, TB (2005) Effects of flow regulation on carp (*Cyprinus carpio* L.) recruitment in the Murray-Darling basin, Australia. *River Research and Applications* **21**, 327-335.
- Gehrke, PC (1988) Response-surface analysis of teleost cardiorespiratory responses to temperature and dissolved oxygen. *Comparative Biochemistry and Physiology a-Physiology* **89**, 587-592.
- Gehrke, PC, Brown, P, Schiller, CB, Moffatt, DB, Bruce, AM (1995) River regulation and fish communities in the Murray-Darling river system, Australia. *Regulated Rivers-Research & Management* **11**, 363-375.
- Gehrke, PC, Revell, MB, Philbey, AW (1993) Effects of river red gum, *Eucalyptus camadulensis*, litter on Golden perch, *Macquaria ambigua*. *Journal of Fish Biology* **43**, 265-279.
- Gehrke, PC, St Pierre, S, Matveev, V, Clake, M (2010) Ecosystem responses to carp population reduction in the Murray-Darling Basin. *Project MD923 Final Report to the Murray-Darling Basin Authority. Murray-Darling Basin Authority, Commonwealth of Australia*
- Gilmore, KL, Doubleday, ZA, Gillanders, BM (2015) Effects of hypoxia on fish: a metabolic approach. *Southern Seas Ecology Laboratories, School of Biological Sciences and Environment Institute, University of Adelaide, SA 5005, Australia*
- Gotesman, M, Kattlun, J, Bergmann, SM, El-Matbouli, M (2013) CyHV-3: the third cyprinid herpesvirus. *Diseases of Aquatic Organisms* **105**, 163-174.

- Graham, K, McColl, KA, Chen, Y, Sengupta, A, Joehnk, K, van Klinken, RD, Brown, P, Gilligan, D, Durr, PA, (2019). Spatio-temporal habitat suitability modelling of common carp (*Cyprinus carpio*) in south-eastern Australia for the planning of the potential release of the biocontrol agent, Cyprinid herpesvirus 3 (CyHV-3), Unpublished report for Fisheries Research and Development Corporation, Canberra, ACT
- Guo, X, Liu, F, Wang, F (2018) Carbon, nitrogen, and phosphorus stoichiometry of three freshwater cultured fishes in growth stage. *Turkish Journal of Fisheries and Aquatic Sciences* 18: 239-245.
- Hara, H, Aikawa, H, Usui, K, Nakanishi, T (2006) Outbreaks of koi herpesvirus disease in rivers of Kanagawa Prefecture. *Fish Pathology* 41, 81-83.
- Harris, JH, Gehrke, PC (1997) 'Fish and rivers in stress: the New South Wales Rivers survey.' (New South Wales Fisheries Office of Conservation, Cronulla, New South Wales, Australia:
- Hodges, B (1998) Heat budget and thermodynamics at a free surface: some theory and numerical implementation (revision 1.0 c) ED 1300 BH. *Center for Water Research, University of Western Australia* 14,
- Hipsey, MR, Boon, C, Paraska, D, Bruce, LC, and Huang, P (2019). 'AquaticEcoDynamics/libaed2: v1.3.0-rc2, Aquatic EcoDynamics (AED) Model Library & Science Manual', 1–34, doi:10.5281/zenodo.2538495.
- Howitt, JA, Baldwin, DS, Rees, GN, Williams, JL (2007) Modelling blackwater: Predicting water quality during flooding of lowland river forests. *Ecological Modelling* 203, 229-242.
- Jones, G (1993) 'Toxic blue-green algae: predicting and controlling toxic blooms.' (CSIRO, Division of Water Resources:
- Killberg-Thoreson, L, Sipler, RE, Heil, CA, Garrett, MJ, Roberts, QN, Bronk, DA (2014) Nutrients released from decaying fish support microbial growth in the eastern Gulf of Mexico. *Harmful Algae* 38, 40-49.
- Kimball, B, Idso, S, Aase, J (1982) A model of thermal radiation from partly cloudy and overcast skies. *Water resources research* 18, 931-936.
- King, AJ, Robertson, AI, Healey, MR (1997) Experimental manipulations of the biomass of introduced carp (*Cyprinus carpio*) in billabongs. 1. Impacts on water-column properties. *Marine and Freshwater Research* 48, 435-443.
- King, AJ, Tonkin, Z, Lieshcke, J (2012) Short-term effects of a prolonged blackwater event on aquatic fauna in the Murray River, Australia: considerations for future events. *Marine and Freshwater Research* 63, 576-586.
- Koehn, JD, Brumley, A, Gehrke, PC (2000) 'Managing the impacts of carp.'
- Koehn, JD (2004) Carp (*Cyprinus carpio*) as a powerful invader in Australian waterways. *Freshwater Biology* 49, 882-894.
- Lampert, W (1987) Laboratory studies on zooplankton-cyanobacteria interactions. *New Zealand Journal of Marine and Freshwater Research* 21, 483-490.
- Landsberg, JH (2002) The effects of harmful algal blooms on aquatic organisms. *Reviews in Fisheries Science* 10, 113-390.
- Lewis, WM (1970) Morphological adaptations of cyprinodontoids for inhabiting oxygen deficient waters. *Copeia* 319-326.
- Linden, LG, Lewis, DM, Burch, MD, Brookes, JD (2004) Interannual variability in rainfall and its impact on nutrient load and phytoplankton in Myponga Reservoir, South Australia. *International Journal of River Basin Management* 2, 169-179.
- Mackereth, FJH, Heron, J, Talling, JF, Association, FB (1978) Water analysis: some revised methods for limnologists.
- Maier, HR, Burch, MD, Bormans, M (2001) Flow management strategies to control blooms of the cyanobacterium, *Anabaena circinalis*, in the River Murray at Morgan, South Australia. *River Research and Applications* 17, 637-650.
- McCarthy, B, Zukowski, S, Whiterod, N, Vilizzi, L, Beesley, L, King, A (2014) Hypoxic blackwater event severely impacts Murray crayfish (*Euastacus armatus*) populations in the Murray River, Australia. *Austral Ecology* 39, 491-500.
- McKinnon, LJ (1995) Emersion of Murray crayfish, *Euastacus armatus* (Decapoda: Parastacidae), from the Murray River due to post-flood water quality. *Royal Society of Victoria Proceedings* 107, 31-38.
- McMaster, D, Bond, N (2008) A field and experimental study on the tolerances of fish to *Eucalyptus camaldulensis* leachate and low dissolved oxygen concentrations. *Marine and Freshwater Research* 59, 177-185.
- Mitrovic, S, Oliver, R, Rees, C, Bowling, L, Buckney, R (2003) Critical flow velocities for the growth and dominance of *Anabaena circinalis* in some turbid freshwater rivers. *Freshwater Biology* 48, 164-174.

- Monaghan, KA, Milner, A (2008) Salmon carcass retention in recently formed stream habitat. *Fundamental and Applied Limnology/Archiv für Hydrobiologie* **170**, 281-289.
- Murray Darling Basin Authority (2016) How Blue Green Algae Blooms Are Handled. At: www.mdba.gov.au/managing-water/water-quality/how-blue-green-algae-blooms-are-handled
- Oliver, RL, Ganf, GG (2000) Freshwater blooms. In 'The ecology of cyanobacteria.' pp. 149-194. (Springer:
- Paerl, H (2008) Nutrient and other environmental controls of harmful cyanobacterial blooms along the freshwater-marine continuum. In 'Cyanobacterial harmful algal blooms: state of the science and research needs.' pp. 217-237. (Springer:
- Paerl, HW, Fulton, RS, Moisander, PH, Dyble, J (2001) Harmful freshwater algal blooms, with an emphasis on cyanobacteria. *The Scientific World Journal* **1**, 76-113.
- Randall, D, Tsui, T (2002) Ammonia toxicity in fish. *Marine pollution bulletin* **45**, 17-23.
- Reid, D, Harris, J, Chapman, DJ (1997) 'NSW inland commercial fishery data analysis.' (Fisheries Research & Development Corporation:
- Schoenebeck, CW, Brown, ML, Chipps, SR, German, DR (2012) Nutrient and algal responses to winterkilled fish-derived nutrient subsidies in eutrophic lakes. *Lake and Reservoir Management* **28**, 189-199.
- Sherman, BS, Webster, IT, Jones, GJ, Oliver, RL (1998) Transitions between Aulacoseira and Anabaena dominance in a turbid river weir pool. *Limnology and Oceanography* **43**, 1902-1915.
- Small, K, Kopf, RK, Watts, RJ, Howitt, J (2014) Hypoxia, Blackwater and Fish Kills: Experimental Lethal Oxygen Thresholds in Juvenile Predatory Lowland River Fishes. *Plos One* **9**, 10.
- Stephan, CE, Mount, DI, Hansen, DJ, Gentile, J, Chapman, GA, Brungs, WA (1985) 'Guidelines for deriving numerical national water quality criteria for the protection of aquatic organisms and their uses.' (US Environmental Protection Agency Duluth, MN:
- Stevenson, C, Childers, DL (2004) Hydroperiod and seasonal effects on fish decomposition in an oligotrophic everglades marsh. *Wetlands* **24**, 529-537.
- Stewardson, MJ, Skinner, D (2018) Evaluating use of environmental flows to aerate streams by modelling the counterfactual case. *Environmental Management* **61**(3), 390-397.
- Stuart, I, Fanson, B, Lyon, J, Stocks, J, Brooks, S, Norris, A, Thwaites, L, Beitzel, M, Hutchison, M, Ye, Q, Koehn, J and Bennett A (2019) A national carp biomass estimate for Australia. Unpublished Client Report for the Fisheries Research and Development Corporation. Arthur Rylah Institute for Environmental Research, Department of Environment, Land, Water and Planning, Heidelberg, Victoria
- Thwaites, L, Fleer, D, Smith, B (2010) Estimating the biomass of adult common carp in Lake Albert, South Australia: a progress report for Biosecurity SA. South Australian Research and Development Institute (Aquatic Sciences), Adelaide. SARDI Publication Number F2010/000681-1. *SARDI Research Report Series*
- Usio, N, Townsend, CR (2004) Roles of crayfish: consequences of predation and bioturbation for stream invertebrates. *Ecology* **85**, 807-822.
- Vilizzi, L, Thwaites, LA, Smith, BB, Nicol, JM, Madden, CP (2014) Ecological effects of common carp (*Cyprinus carpio*) in a semi-arid floodplain wetland. *Marine and Freshwater Research* **65**, 802-817.
- Wasson, B, Banens, B, Davies, P, Maher, W, Robinson, S, Volker, R, Tait, D, Watson-Brown, S (1996) Inland waters.
- Water Environmental Federation, American Public Health Association (2005) Standard methods for the examination of water and wastewater. *American Public Health Association (APHA): Washington, DC, USA*
- Whitworth, KL, Baldwin, DS, Kerr, JL (2014) The effect of temperature on leaching and subsequent decomposition of dissolved carbon from inundated floodplain litter: implications for the generation of hypoxic blackwater in lowland floodplain rivers. *Chemistry and Ecology* **30**, 491-500.
- World Health Organization (2003) Cyanobacterial Toxins: Microcystin-LR in Drinking Water. *Geneva, World Health Organization*
- World Health Organization (2011) Guidelines for drinking-water quality, 4th edition. *WHO chronicle* **38**, 104-8.

Appendix A: Model setup information

Table A1: Summary of simulation setup details for the four domains, indicating data sources.

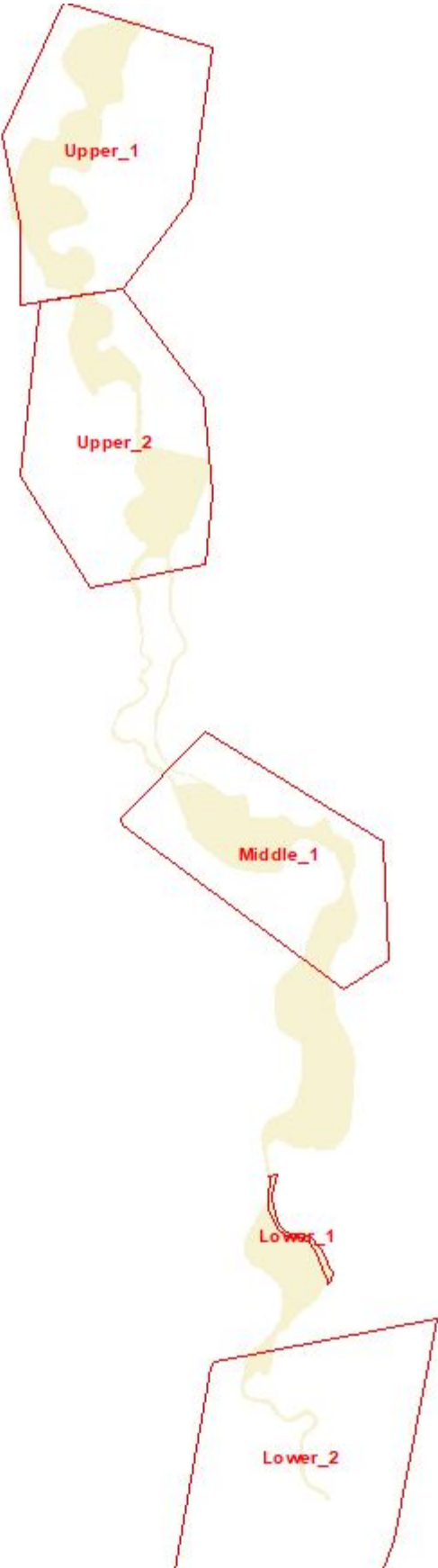
Site Name	Calibration/ Validation	Model Period	Inflows	Data Agencies	Outflows	Data Agencies	Weather Data Agencies
Lowerlakes	2008-2013	01/10/2015 - 01/11/2015	Wellington	SA DEW, SA EPA	N/A		SA DEW, BOM
			Tide	SA DEW, SA EPA	N/A		
			Salt Creek	SA DEW, SA EPA	N/A		
			Angus River	SA DEW, SA EPA	N/A		
			Bremer River	SA DEW, SA EPA	N/A		
			Currency Creek	SA DEW, SA EPA	N/A		
			Finniss River	SA DEW, SA EPA	N/A		
Murray River	2008-2013	01/10/2015 - 01/11/2015	Lock1	SA DEW, SA Water	MALP Offtake	SA DEW, SA EPA, SA Water	SA DEW, BOM
			Wellington	SA DEW, SA EPA, SA Water	MBO Offtake	SA DEW, SA EPA, SA Water	
					SR Offtake	SA DEW, SA EPA, SA Water	
					SRS Offtake	SA DEW, SA EPA, SA Water	
					TB Offtake	SA DEW, SA EPA, SA Water	
Chowilla	N/A	01/04/2016- 01/05/2016	Lock6	SA DEW, SA Water	N/A		BOM
			Lock5	SA DEW, SA Water	N/A		
			Chowilla Creek	SA DEW, SA Water	N/A		
Moonie River	N/A	01/04/2016- 01/05/2016	cf417201B		N/A		BOM
			cf417204A		N/A		

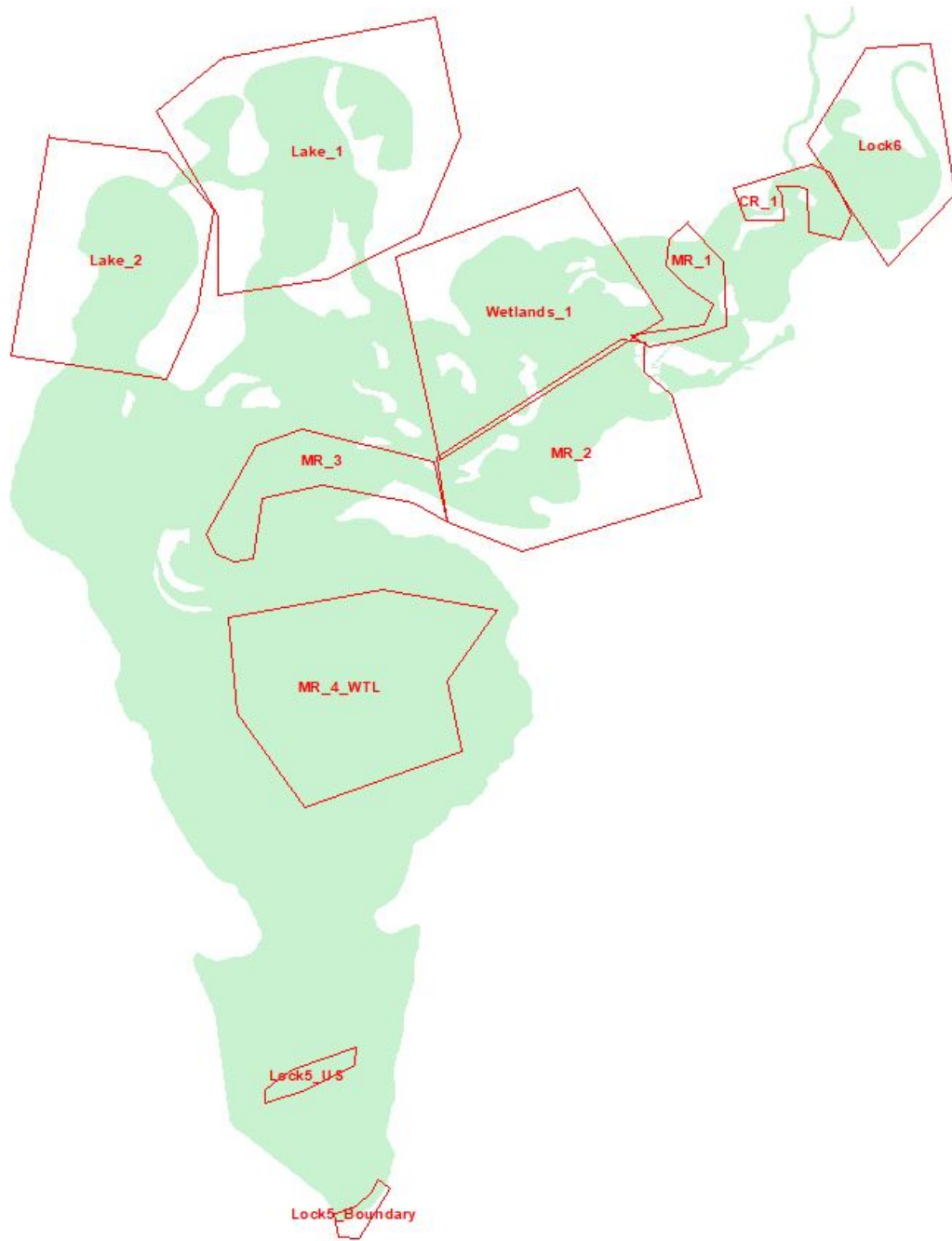
Table A2 (overpage): Summary of inflow water flow and water quality data sources for model inputs.

Variable	Lower Lakes Domain										Murray River Domain						Chowilla Domain		Moonie Domain	
	Wellington	Angus River	Bremer River	Currency Creek	Finniss River	Salt Creek	Wellington	Lock1	MALP_Offtake	MBO_Offtake	SR_Offtake	SRS_Offtake	TB_Offtake	Lock5	Lock6	cf41 720 720 4A	cf41 720 720 4A			
Flow/Height	A4260575 (2008)/A4 261159(2 009 onwards)	A4260503	A4261219	A4261099	A4261208	A2390568	A4260575 (2008)/A4 261159(2 009 onwards)	A4260903	Monthly Extraction from 2015-2016 Data	Monthly Extraction from 2015-2016 Data	A4260512	A4260511	cf41 720 720 4A	cf41 720 720 4A						
SAL	A4261159	A4261101	A4261219	EPA2014_Currency_Creek_US_of_Narrows	EPA2014_Finniss_River_US1	A2390568	A4261159	A4260903	EPA2014_LMRI A_Plume_Burdett	SAW_Mypolon ga_Surface	SAW_Swan_Reach_Town	EPA2014_LMRIA_Plume_Jervois_Woods_Point	A4260512	A4260510	cf41 720 720 4A	cf41 720 720 4A				
TEMP	A4261159	A4261101	A4261219	EPA2014_Currency_Creek_US_of_Narrows	EPA2014_Finniss_River_US1	A2390568	A4261159	SAW_Swan_Reach_SP	EPA2014_LMRI A_Plume_Burdett	SAW_Mypolon ga_Surface	SAW_Swan_Reach_Town	EPA2014_LMRIA_Plume_Jervois_Woods_Point	A4260512	A4260510	cf41 720 720 4A	cf41 720 720 4A				
TRACE_1	No Site	No Site	No Site	No Site	No Site	No Site	No Site	No Site	No Site	No Site	No Site	No Site	No Site	No Site	Assu med	Assu med				
WQ_TR C_SS1	No Site	EPA2014_Finniss_River_US1	SAW_Milang	EPA2014_Currency_Creek_US_of_Narrows	EPA2014_Finniss_River_US1	EPA_Salt_Creek_Flow	No Site	SAW_Swan_Reach_SP	EPA2014_LMRI A_Plume_Burdett	SAW_Mypolon ga_Surface	SAW_Swan_Reach_Town	EPA2014_LMRIA_Plume_Jervois_Woods_Point	SAW_Lock5	SAW_DS_lock6_8km	Assu med	Assu med				
WQ_TR C_RET	SAW_Tail em_Bend	No Site	No Site	No Site	No Site	No Site	SAW_Tail em_Bend	No Site	No Site	No Site	No Site	No Site	No Site	No Site	Assu med	Assu med				
WQ_OX Y_OXY	SAW_Tail em_Bend	EPA2014_Finniss_River_US1	EPA2014_Milang	EPA2014_Currency_Creek_US_of_Narrows	EPA2014_Finniss_River_US1	EPA2014_Morella_Basin_South_Salt_Creek	SAW_Tail em_Bend	SAW_Swan_Reach_SP	SAW_Murray_Bridge_SP	SAW_Mypolon ga_Surface	SAW_Swan_Reach_Town	SAW_Tail em_Bend	SAW_Remark_Su rface	SAW_Remark_Su rface	Assu med	Assu med				
WQ_SIL _RSI	SAW_Tail em_Bend	EPA2014_Milang	EPA2014_Milang	EPA2014_Currency_Creek_US_of_Narrows	EPA2014_Finniss_River_US1	EPA_Salt_Creek_Flow	SAW_Tail em_Bend	SAW_Swan_Reach_SP	EPA2014_LMRI A_Plume_Burdett	SAW_Murray_Bridge_SP	SAW_Swan_Reach_Town	EPA2014_LMRIA_Plume_Jervois_Woods_Point	SAW_Lock5	SAW_Remark_Su rface	Assu med	Assu med				
WQ_NIT _AMM	No Site	EPA2014_Finniss_River_US1	EPA2014_Milang	EPA2014_Currency_Creek_US_of_Narrows	EPA2014_Finniss_River_US1	EPA_Salt_Creek	No Site	EPA2014_LMRI A_Plume_Mobilong	EPA2014_LMRI A_Plume_Mobilong	EPA2014_LMRI A_Plume_Mobilong	EPA2014_LMRI A_Plume_Mobilong	EPA2014_LMRIA_Plume_Jervois_Woods_Point	EPA2014_LMRIA_Plume_Westbrook_Park	EPA2014_LMRIA_Plume_Westbrook_Park	Assu med	Assu med				

WQ_INT_INT	SAW_Tail em_Bend	EPA2014_Coorong_Ewe_Island_Barage	EPA2014_Finnisss_River_US1	EPA2014_Currency_Creek_US_of_Narrows	EPA2014_Finnisss_River_US1	EPA_Salt_Creek	SAW_Tail em_Bend	SAW_Swan_Re ach_SP	SAW_Mannum	EPA2014_LMRI A_Plume_Mobilong	SAW_Mypolonga_Surface	SAW_Swan_Re ach_SP	EPA2014_LMRIA_Plume_Jervois_Woods_Point	SAW_Benchmark_Price	SAW_DS_lock6_8k m	Assu med
WQ_PH S_FRP	SAW_Tail em_Bend	EPA2014_Coorong_Ewe_Island_Barage	EPA2014_Finnisss_River_US1	EPA2014_Currency_Creek_US_of_Narrows	EPA2014_Finnisss_River_US1	EPA_Salt_Creek	SAW_Tail em_Bend	SAW_Swan_Re ach_SP	SAW_Mannum	EPA2014_LMRI A_Plume_Mobilong	SAW_Mypolonga_Surface	SAW_Swan_Re ach_SP	EPA2014_LMRIA_Plume_Jervois_Woods_Point	SAW_Locks	SAW_DS_lock6_8k m	Assu med
WQ_PH S_FRP_A DS	SAW_Tail em_Bend	EPA2014_Coorong_Murray_Mouth	EPA2014_Finnisss_River_US1	EPA2014_Currency_Creek_US_of_Narrows	EPA2014_Finnisss_River_US1	EPA_Salt_Creek	SAW_Tail em_Bend	SAW_Swan_Re ach_SP	SAW_Mannum	EPA2014_LMRI A_Plume_Mobilong	SAW_Mypolonga_Surface	SAW_Swan_Re ach_SP	EPA2014_LMRIA_Plume_Jervois_Woods_Point	SAW_Locks	SAW_DS_lock6_8k m	Assu med
WQ_OG M_DOC	SAW_Tail em_Bend	EPA2014_Lake_Alexandrina_Clayton_east_of_regulator	EPA2014_Milang	EPA2014_Currency_Creek_US_of_Narrows	EPA2014_Finnisss_River_US1	EPA_Salt_Creek	SAW_Tail em_Bend	SAW_Swan_Re ach_SP	SAW_Mannum	EPA2014_LMRI A_Plume_Burdett	SAW_Mypolonga_Surface	SAW_Swan_Re ach_Town	EPA2014_LMRIA_Plume_Jervois_Woods_Point	SAW_Locks	SAW_DS_lock6_8k m	Assu med
WQ_OG M_POC	SAW_Tail em_Bend	Lock1	No Site	No Site	No Site	No Site	SAW_Tail em_Bend	Lock1	Lock1	Lock1	Lock1	Lock1	Lock1	Lock1	Lock1	Assu med
WQ_OG M_DON	SAW_Tail em_Bend	EPA2014_Coorong_Murray_Mouth	EPA2014_Finnisss_River_US1	EPA2014_Currency_Creek_US_of_Narrows	EPA2014_Finnisss_River_US1	EPA_Salt_Creek	SAW_Tail em_Bend	EPA2014_Lake_Alexandrina_To p	EPA2014_Lake_Alexandrina_Opening	EPA2014_Lake_Alexandrina_Opening	EPA2014_Lake_Alexandrina_Opening	Assu med				
WQ_OG M_PON	SAW_Tail em_Bend	EPA2014_Coorong_Murray_Mouth	EPA2014_Finnisss_River_US1	EPA2014_Currency_Creek_US_of_Narrows	EPA2014_Finnisss_River_US1	EPA_Salt_Creek	SAW_Tail em_Bend	EPA2014_Lake_Alexandrina_To p	EPA2014_Lake_Alexandrina_To p	EPA2014_Lake_Alexandrina_To p	SAW_Mypolonga_Surface	SAW_Swan_Re ach_SP	EPA2014_Lake_Alexandrina_Opening	SAW_Locks	SAW_DS_lock6_8k m	Assu med
WQ_OG M_POP	SAW_Tail em_Bend	EPA2014_Coorong_Murray_Mouth	EPA2014_Finnisss_River_US1	EPA2014_Currency_Creek_US_of_Narrows	EPA2014_Finnisss_River_US1	EPA_Salt_Creek	SAW_Tail em_Bend	SAW_Swan_Re ach_SP	SAW_Mannum	SAW_Murray_Bridge_SP	SAW_Mypolonga_Surface	SAW_Swan_Re ach_SP	SAW_Tallem_Bend	SAW_Locks	SAW_DS_lock6_8k m	Assu med
WQ_PH Y_GRN	SAW_Tail em_Bend	EPA2014_Coorong_Murray_Mouth	EPA2014_Milang	EPA_Currency_Creek_US_of_Narrows	EPA2014_Finnisss_River_US1	EPA_Salt_Creek	SAW_Tail em_Bend	SAW_Swan_Re ach_SP	SAW_Mannum	SAW_Tallem_Bend	SAW_Tallem_Bend	SAW_Morgana	SAW_Tallem_Bend	SAW_Morgana	SAW_Morgana	Assu med

Appendix B : Domain sub-regions







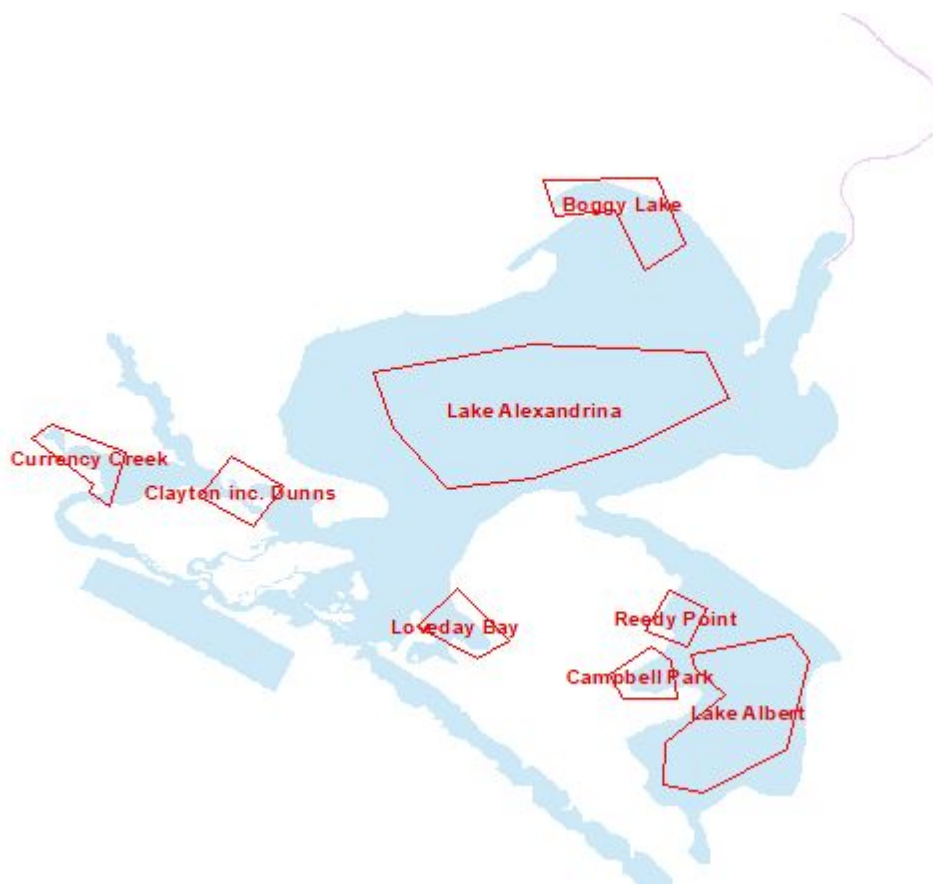


Table B1: Carp density used in the biomass zones in Figure 15; data from Stuart et al. (2019).

Zone Name	Biomass Zone	Density (kg/ha)
Moonie 1	1	30.563
Moonie 2	2	42.283
SA Wetland 1	3	250.4587
SA Wetland 2	4	301.9826
Lake Alexandrina	5	326.7548
Lake Albert	6	388.3837
Lowerlakes Misc	7	300
Ocean / Coorong	8	0
Murray Wetland 1	9	301.9826
River Murray (inc. Chowilla Domain)	10	482.0369
Chowilla Wetland	11	301.9826
Mooney River	12	123.7007
Mooney Wetland	13	42.283

Appendix C : Model simulation output summary

Table C1: Region summary values for oxygen sag (left) and hypoxia risk (right), organised from north to south.

Domain	Analysis region	Flow	delDO (mg/L)							DO risk (-)							
			Biomass Factor							Biomass							
			0	0.1	0.4	0.8	1	2	5	0	0.1	0.4	0.8	1	2	5	
Moonie	Upper_1	0.5		0.01	-0.03	-0.02	-0.01	-0.13	-0.07			0.00	0.00	0.00	0.00	0.00	0.00
		1.0	0.0 0	0.01	-0.03	-0.02	-0.01	-0.13	-0.07		0.00	0.00	0.00	0.00	0.00	0.00	0.00
		2.0		0.01	-0.03	-0.02	-0.01	-0.13	-0.07			0.00	0.00	0.00	0.00	0.00	0.00
	Upper_2	0.5		-0.01	-0.01	-0.01	-0.01	-0.01	-0.02			0.00	0.00	0.00	0.00	0.00	0.00
		1.0	0.0 0	-0.01	-0.01	-0.01	-0.01	-0.01	-0.02		0.00	0.00	0.00	0.00	0.00	0.00	0.00
		2.0		-0.01	-0.01	-0.01	-0.01	-0.01	-0.02			0.00	0.00	0.00	0.00	0.00	0.00
	Moonie	Middle_1	0.5									0.00	0.00	0.00	0.00	0.00	0.00
			1.0									0.00	0.00	0.00	0.00	0.00	0.00
			2.0									0.00	0.00	0.00	0.00	0.00	0.00
Moonie	Lower_2	0.5		-0.05	-0.04	-0.03	-0.07	-0.07	-0.04			0.00	0.00	0.00	0.00	0.00	0.00
		1.0	0.0 0	-0.05	-0.04	-0.03	-0.07	-0.07	-0.04		0.00	0.00	0.00	0.00	0.00	0.00	0.00
		2.0		-0.05	-0.04	-0.03	-0.07	-0.07	-0.04			0.00	0.00	0.00	0.00	0.00	0.00
Moonie	Lower_1	0.5		0.00	-0.01	-0.02	-0.01	-0.01	-0.10			0.00	0.00	0.00	0.00	0.00	0.00
		1.0	0.0 0	0.00	-0.01	-0.02	-0.01	-0.01	-0.10		0.00	0.00	0.00	0.00	0.00	0.00	0.00
		2.0		0.00	-0.01	-0.02	-0.01	-0.01	-0.10			0.00	0.00	0.00	0.00	0.00	0.00
Chowilla	Lock6	0.5		0.23	0.44	0.70	0.54	0.87	1.18			0.22	0.23	0.25	0.25	0.27	0.26
		1.0	0.0 0	0.07	0.25	0.44	0.33	0.46	0.52		0.20	0.22	0.23	0.25	0.25	0.27	0.25
		2.0		-0.02	0.16	0.33	0.20	0.30	0.24			0.22	0.23	0.25	0.25	0.27	0.25
	MR_1	0.5		0.13	0.21	0.35	0.29	0.64	1.33			0.12	0.13	0.13	0.13	0.14	0.16
		1.0	0.0 0	0.02	0.07	0.16	0.12	0.34	0.78		0.11	0.11	0.12	0.13	0.13	0.14	0.16
		2.0		-0.12	-0.09	-0.04	-0.06	0.04	0.24			0.11	0.11	0.12	0.12	0.13	0.14
	CR_1	0.5		0.30	0.41	0.61	0.55	1.20	2.32			0.14	0.15	0.17	0.17	0.17	0.24
		1.0	0.0 0	0.02	0.06	0.15	0.13	0.39	0.86		0.14	0.14	0.15	0.16	0.16	0.17	0.19
		2.0		-0.16	-0.15	-0.10	-0.11	-0.03	0.10			0.14	0.15	0.16	0.16	0.16	0.18
Wetlands_1	0.5		0.27	0.35	0.47	0.42	1.74	1.30			0.21	0.21	0.22	0.23	0.30	0.23	
	1.0	0.0 0	0.02	0.06	0.14	0.11	1.00	0.67		0.20	0.21	0.21	0.22	0.23	0.28	0.23	
	2.0		0.06	0.04	0.14	0.12	0.61	0.36			0.20	0.21	0.22	0.23	0.27	0.23	
Lake_1	0.5		0.58	1.35	3.24	3.36	4.27	5.93			0.18	0.29	0.38	0.42	0.54	0.78	
	1.0	0.0 0	0.55	1.72	3.04	2.96	4.28	5.82		0.12	0.18	0.29	0.38	0.42	0.54	0.78	
	2.0		0.82	1.87	3.39	3.60	4.56	5.84			0.18	0.29	0.39	0.42	0.54	0.78	
Lake_2	0.5		0.29	1.25	1.79	1.60	2.60	3.32			0.56	0.65	0.74	0.71	0.83	0.89	
	1.0	0.0 0	0.29	1.25	1.83	1.56	2.64	3.38		0.51	0.56	0.65	0.73	0.70	0.83	0.89	
	2.0		0.28	1.25	1.81	1.62	2.64	3.40			0.56	0.65	0.73	0.71	0.83	0.89	
MR_2	0.5		0.19	0.32	0.50	0.46	0.88	1.97			0.08	0.09	0.10	0.10	0.10	0.11	
	1.0	0.0 0	0.03	0.12	0.25	0.23	0.50	1.27		0.07	0.08	0.09	0.10	0.10	0.10	0.11	
	2.0		-0.16	-0.10	-0.03	-0.03	0.11	0.56			0.08	0.08	0.09	0.10	0.10	0.11	
MR_3	0.5		0.27	0.50	0.79	0.81	1.48	3.44			0.02	0.02	0.02	0.03	0.03	0.42	
	1.0	0.0 0	0.03	0.20	0.38	0.42	0.85	2.17		0.01	0.01	0.02	0.02	0.02	0.02	0.03	
	2.0		-0.24	-0.13	-0.03	-0.01	0.24	1.01			0.01	0.01	0.02	0.02	0.02	0.02	

Chowilla	MR_4_WTL	0.5		0.32	0.63	1.11	1.21	2.25	5.34			0.02	0.03	0.04	0.03	0.06	0.91	
		1.0	0.0 0	0.05	0.27	0.61	0.70	1.42	3.68		0.02	0.02	0.03	0.03	0.03	0.03	0.04	0.62
		2.0		-0.28	-0.14	0.06	0.13	0.55	1.91			0.02	0.03	0.03	0.03	0.03	0.03	0.05
Chowilla	Lock5_US	0.5		0.50	0.86	1.60	1.76	3.07	6.24			0.16	0.17	0.18	0.19	0.48	0.66	
		1.0	0.0 0	0.06	0.35	0.94	1.06	2.10	5.83		0.16	0.16	0.17	0.18	0.19	0.23	0.67	
		2.0		-0.31	-0.12	0.25	0.34	1.02	3.55			0.16	0.17	0.17	0.18	0.20	0.60	
Chowilla	Lock5_Boundary	0.5		0.60	1.04	1.74	1.94	3.30	6.32			0.06	0.08	0.08	0.08	0.56	0.82	
		1.0	0.0 0	0.09	0.47	1.08	1.23	2.37	5.98		0.06	0.06	0.08	0.08	0.08	0.29	0.83	
		2.0		-0.31	-0.06	0.35	0.45	1.21	3.90			0.04	0.06	0.07	0.07	0.07	0.69	
Murray	Wellington	0.5		0.07	0.20	0.43	0.59	1.18	3.02			0.00	0.00	0.00	0.00	0.00	0.27	
		1.0	0.0 0	0.03	0.16	0.39	0.56	1.15	2.98		0.00	0.00	0.00	0.00	0.00	0.00	0.26	
		2.0		-0.08	0.04	0.27	0.43	1.04	2.81			0.00	0.00	0.00	0.00	0.00	0.27	
Murray	Swan Reach	0.5		-0.01	0.07	0.14	0.19	0.42	1.35			0.00	0.00	0.00	0.00	0.01	0.07	
		1.0	0.0 0	0.03	0.11	0.20	0.23	0.57	1.98		0.00	0.00	0.00	0.00	0.00	0.00	0.05	
		2.0		0.09	0.24	0.42	0.47	0.96	2.89			0.00	0.00	0.00	0.00	0.00	0.13	
Murray	Mannum	0.5		-0.05	-0.01	0.08	0.20	0.47	1.57			0.00	0.00	0.00	0.00	0.00	0.01	
		1.0	0.0 0	0.01	0.06	0.18	0.26	0.63	1.94		0.00	0.00	0.00	0.00	0.00	0.00	0.00	
		2.0		0.05	0.16	0.33	0.46	1.02	2.65			0.00	0.00	0.00	0.00	0.00	0.14	
Murray	Walkers Flat	0.5		-0.06	0.06	0.21	0.29	0.78	2.26			0.00	0.00	0.00	0.00	0.00	0.01	
		1.0	0.0 0	0.04	0.16	0.32	0.41	1.00	2.64		0.00	0.00	0.00	0.00	0.00	0.00	0.01	
		2.0		0.19	0.32	0.53	0.65	1.33	3.36			0.00	0.00	0.00	0.00	0.00	0.20	
Murray	Murray Bridge	0.5		0.02	0.13	0.40	0.43	0.99	2.51			0.00	0.00	0.00	0.00	0.00	0.07	
		1.0	0.0 0	0.02	0.15	0.42	0.47	1.05	2.62		0.00	0.00	0.00	0.00	0.00	0.00	0.08	
		2.0		0.01	0.13	0.37	0.39	0.90	2.53			0.00	0.00	0.00	0.00	0.00	0.03	
Murray	Wood Point	0.5		0.03	0.14	0.33	0.44	0.88	2.54			0.00	0.00	0.00	0.00	0.00	0.09	
		1.0	0.0 0	0.02	0.13	0.31	0.43	0.84	2.50		0.00	0.00	0.00	0.00	0.00	0.00	0.08	
		2.0		-0.06	0.03	0.24	0.34	0.74	2.55			0.00	0.00	0.00	0.00	0.00	0.14	
Lowerlakes	Boggy Lake	0.5		0.02	0.09	0.19	0.30	0.87			0.00	0.00	0.00	0.00	0.00	0.00		
		1.0	0.0 0	0.02	0.09	0.20	0.30	0.87		0.00	0.00	0.00	0.00	0.00	0.00	0.00		
		2.0		0.02	0.09	0.20	0.30	0.88			0.00	0.00	0.00	0.00	0.00	0.00		
Lowerlakes	Loveday Bay	0.5		0.02	0.05	0.15	0.39	0.59			0.01	0.01	0.01	0.01	0.01	0.01		
		1.0	0.0 0	0.02	0.06	0.16	0.40	0.60		0.01	0.01	0.01	0.01	0.01	0.01	0.01		
		2.0		0.02	0.07	0.17	0.41	0.63			0.00	0.00	0.00	0.00	0.00	0.00		
Lowerlakes	Currency Creek	0.5		0.02	0.13	0.25	0.34	0.87			0.00	0.00	0.00	0.00	0.00	0.01		
		1.0	0.0 0	0.02	0.13	0.24	0.35	0.89		0.00	0.00	0.00	0.00	0.00	0.00	0.01		
		2.0		0.02	0.13	0.25	0.36	0.87			0.00	0.00	0.00	0.00	0.00	0.01		
Lowerlakes	Clayton inc. Dunns	0.5		0.05	0.11	0.32	0.56	1.62			0.00	0.00	0.00	0.00	0.00	0.00		
		1.0	0.0 0	0.04	0.12	0.32	0.55	1.63		0.00	0.00	0.00	0.00	0.00	0.00	0.00		
		2.0		0.04	0.11	0.32	0.56	1.59			0.00	0.00	0.00	0.00	0.00	0.00		
Lowerlakes	Reedy Point	0.5		0.04	0.22	0.53	0.76	1.79			0.00	0.00	0.00	0.00	0.00	0.01		
		1.0	0.0 0	0.04	0.22	0.54	0.76	1.79		0.00	0.00	0.00	0.00	0.00	0.00	0.01		
		2.0		0.04	0.22	0.54	0.76	1.78			0.00	0.00	0.00	0.00	0.00	0.01		
Lowerlakes	Lake Alexandrina	0.5		0.02	0.13	0.33	0.40	0.99			0.00	0.00	0.00	0.00	0.00			

Lowerlakes
Lowerlakes

Campbell Park

Lake Albert

1.0	0.0 0	0.02	0.13	0.33	0.40	0.99			0.00	0.00	0.00	0.00	0.00	0.00
2.0		0.01	0.12	0.33	0.40	1.00				0.00	0.00	0.00	0.00	0.00
0.5		0.05	0.17	0.41	0.63	1.44				0.00	0.00	0.00	0.00	0.00
1.0	0.0 0	0.05	0.17	0.41	0.63	1.45			0.00	0.00	0.00	0.00	0.00	0.01
2.0		0.05	0.17	0.41	0.63	1.43				0.00	0.00	0.00	0.00	0.01
0.5		0.06	0.28	0.67	0.84	1.89				0.00	0.00	0.00	0.00	0.00
1.0	0.0 0	0.06	0.28	0.67	0.84	1.89			0.00	0.00	0.00	0.00	0.00	0.00
2.0		0.06	0.28	0.66	0.84	1.89				0.00	0.00	0.00	0.00	0.00

Table C2: Region summary values for DN (left) and ammonium risk (right), organised from north to south.

Domain	Analysis region	Flow	delDN (mg/L)							NH4 risk (-)							
			Biomass Factor							Biomass							
			0	0.1	0.4	0.8	1	2	5	0	0.1	0.4	0.8	1	2	5	
Moonie	Upper_1	0.5		0.00	0.03	0.04	0.04	0.13	0.42		0.00	0.00	0.01	0.00	0.01	0.01	
		1.0	0.00	0.00	0.03	0.04	0.04	0.13	0.42	0.00	0.00	0.00	0.01	0.00	0.01	0.01	
		2.0		0.00	0.03	0.04	0.04	0.13	0.42		0.00	0.00	0.01	0.00	0.01	0.01	
	Upper_2	0.5		0.00	0.00	0.01	0.02	0.01	0.02		0.00	0.00	0.00	0.00	0.00	0.00	
		1.0	0.00	0.00	0.00	0.01	0.02	0.01	0.02	0.00	0.00	0.00	0.00	0.00	0.00	0.00	
		2.0		0.00	0.00	0.01	0.02	0.01	0.02		0.00	0.00	0.00	0.00	0.00	0.00	
	Moonie	Middle_1	0.5		NaN	NaN	NaN	NaN	NaN	NaN		0.00	0.00	0.00	0.05	0.09	0.18
			1.0	NaN	0.00	0.00	0.00	0.00	0.05	0.09	0.18						
			2.0		NaN	NaN	NaN	NaN	NaN	NaN		0.00	0.00	0.00	0.05	0.09	0.18
Moonie	Lower_2	0.5		0.01	0.01	0.02	0.03	0.03	0.25		0.00	0.00	0.00	0.00	0.00	0.19	
		1.0	0.00	0.01	0.01	0.02	0.03	0.03	0.25	0.00	0.00	0.00	0.00	0.00	0.00	0.19	
		2.0		0.01	0.01	0.02	0.03	0.03	0.25		0.00	0.00	0.00	0.00	0.00	0.19	
Moonie	Lower_1	0.5		0.00	0.00	0.01	0.01	0.02	0.06		0.00	0.00	0.00	0.00	0.00	0.00	
		1.0	0.00	0.00	0.00	0.01	0.01	0.02	0.06	0.00	0.00	0.00	0.00	0.00	0.00	0.00	
		2.0		0.00	0.00	0.01	0.01	0.02	0.06		0.00	0.00	0.00	0.00	0.00	0.00	
Chowilla	Lock6	0.5		0.01	0.08	0.20	0.10	0.21	0.39		0.51	0.55	0.56	0.60	0.63	0.56	
		1.0	0.00	0.01	0.09	0.18	0.10	0.18	0.33	0.50	0.51	0.54	0.56	0.61	0.62	0.56	
		2.0		0.02	0.08	0.17	0.09	0.18	0.37		0.51	0.54	0.55	0.60	0.61	0.55	
	Chowilla	MR_1	0.5		0.00	0.01	0.02	0.01	0.03	0.08		0.39	0.39	0.39	0.40	0.40	0.40
			1.0	0.00	0.00	0.00	0.01	0.01	0.02	0.05	0.38	0.38	0.38	0.38	0.38	0.38	0.38
			2.0		0.00	0.00	0.01	0.01	0.01	0.03		0.35	0.35	0.35	0.35	0.35	0.35
	Chowilla	CR_1	0.5		0.00	0.01	0.04	0.03	0.11	0.19		0.50	0.50	0.51	0.51	0.51	0.51
			1.0	0.00	0.00	0.00	0.02	0.02	0.07	0.15	0.49	0.50	0.50	0.50	0.50	0.50	0.50
			2.0		0.00	0.00	0.02	0.02	0.05	0.06		0.48	0.49	0.49	0.49	0.49	0.49
Chowilla	Wetlands_1	0.5		0.00	0.00	0.01	0.01	1.55	0.07		0.60	0.60	0.60	0.61	0.71	0.61	
		1.0	0.00	0.00	0.00	0.01	0.01	0.44	0.04	0.59	0.61	0.61	0.61	0.61	0.71	0.61	
		2.0		0.00	0.00	0.01	0.01	0.93	0.03		0.62	0.62	0.62	0.62	0.74	0.63	
Chowilla	Lake_1	0.5		0.10	0.30	0.86	0.98	1.80	4.92		0.01	0.23	0.71	0.86	0.96	0.97	
		1.0	0.00	0.09	0.33	0.79	0.85	1.76	4.76	0.01	0.01	0.23	0.71	0.86	0.96	0.97	
		2.0		0.11	0.34	0.84	0.92	1.84	4.68		0.01	0.24	0.72	0.86	0.96	0.97	
Chowilla	Lake_2	0.5		0.05	0.33	0.59	0.49	1.35	3.39		0.01	0.24	0.62	0.51	0.96	1.00	
		1.0	0.00	0.06	0.32	0.60	0.49	1.37	3.40	0.01	0.01	0.24	0.62	0.51	0.97	1.00	
		2.0		0.06	0.33	0.60	0.50	1.36	3.39		0.01	0.23	0.62	0.52	0.96	1.00	
Chowilla	MR_2	0.5		0.00	0.01	0.03	0.03	0.05	0.14		0.23	0.24	0.24	0.25	0.25	0.25	
		1.0	0.00	0.00	0.01	0.02	0.02	0.04	0.10	0.22	0.23	0.23	0.24	0.25	0.24	0.24	
		2.0		0.00	0.01	0.02	0.02	0.03	0.06		0.22	0.22	0.23	0.24	0.23	0.24	
Chowilla	MR_3	0.5		0.00	0.02	0.04	0.04	0.08	0.22		0.05	0.05	0.05	0.05	0.06	0.06	
		1.0	0.00	0.00	0.01	0.03	0.03	0.06	0.14	0.05	0.05	0.05	0.05	0.05	0.05	0.05	
		2.0		0.00	0.01	0.02	0.02	0.04	0.09		0.04	0.04	0.04	0.04	0.04	0.04	
Chowilla	MR_4_WTL	0.5		0.00	0.02	0.05	0.06	0.12	0.35		0.08	0.09	0.10	0.09	0.09	0.09	
		1.0	0.00	0.00	0.02	0.04	0.04	0.09	0.24	0.07	0.07	0.09	0.10	0.09	0.09	0.08	
		2.0		0.00	0.01	0.03	0.03	0.06	0.15		0.07	0.08	0.09	0.08	0.08	0.08	
Chowilla	Lock5_US	0.5		0.00	0.03	0.07	0.08	0.17	0.57		0.51	0.51	0.51	0.51	0.52	0.64	
		1.0	0.00	0.00	0.02	0.06	0.07	0.13	0.42	0.51	0.51	0.51	0.51	0.51	0.52	0.51	

Chowilla	Lock5_Boundary	2.0		0.01	0.02	0.04	0.05	0.09	0.25			0.50	0.50	0.50	0.50	0.51	0.50	
		0.5		0.01	0.04	0.09	0.10	0.21	0.69				0.18	0.18	0.19	0.19	0.19	0.49
		1.0	0.00	0.01	0.03	0.08	0.09	0.18	0.57		0.17	0.17	0.17	0.18	0.18	0.18	0.18	0.21
		2.0		0.01	0.02	0.05	0.06	0.12	0.33			0.12	0.12	0.12	0.12	0.13	0.14	
Murray	Wellington	0.5		0.02	0.03	0.05	0.06	0.11	0.27			0.00	0.00	0.00	0.00	0.00	0.00	
		1.0	0.00	0.00	0.01	0.03	0.05	0.09	0.25		0.00	0.00	0.00	0.00	0.00	0.00	0.00	
		2.0		0.01	0.02	0.03	0.05	0.09	0.25			0.00	0.00	0.00	0.00	0.00	0.00	
Murray	Swan Reach	0.5		0.00	0.01	0.02	0.02	0.04	0.12			0.03	0.03	0.03	0.03	0.09	0.25	
		1.0	0.00	0.01	0.03	0.04	0.05	0.10	0.36		0.02	0.02	0.02	0.02	0.02	0.02	0.14	
		2.0		-0.02	0.01	0.03	0.03	0.10	0.34			0.00	0.00	0.00	0.00	0.00	0.00	
Murray	Mannum	0.5		0.01	0.02	0.04	0.05	0.10	0.26			0.00	0.00	0.00	0.00	0.00	0.00	
		1.0	0.00	0.00	0.02	0.04	0.05	0.10	0.29		0.00	0.00	0.00	0.00	0.00	0.00	0.00	
		2.0		-0.01	0.00	0.02	0.04	0.11	0.33			0.00	0.00	0.00	0.00	0.00	0.00	
Murray	Walkers Flat	0.5		0.01	0.02	0.04	0.05	0.10	0.28			0.01	0.01	0.01	0.01	0.03	0.06	
		1.0	0.00	0.01	0.02	0.04	0.05	0.13	0.33		0.00	0.00	0.00	0.00	0.00	0.01	0.00	
		2.0		0.00	0.02	0.04	0.06	0.13	0.38			0.00	0.00	0.00	0.00	0.00	0.00	
Murray	Murray Bridge	0.5		0.02	0.03	0.06	0.07	0.13	0.32			0.00	0.00	0.00	0.00	0.00	0.00	
		1.0	0.00	0.00	0.02	0.05	0.05	0.12	0.31		0.00	0.00	0.00	0.00	0.00	0.00	0.00	
		2.0		-0.02	-0.01	0.02	0.02	0.07	0.25			0.00	0.00	0.00	0.00	0.00	0.00	
Murray	Wood Point	0.5		0.02	0.03	0.05	0.06	0.11	0.30			0.00	0.00	0.00	0.00	0.00	0.00	
		1.0	0.00	0.00	0.02	0.04	0.05	0.09	0.27		0.00	0.00	0.00	0.00	0.00	0.00	0.00	
		2.0		-0.02	-0.01	0.01	0.02	0.06	0.25			0.00	0.00	0.00	0.00	0.00	0.00	
Lowerlakes	Boggy Lake	0.5		0.01	0.05	0.11	0.14	0.33				0.00	0.00	0.00	0.00	0.00		
		1.0	0.00	0.01	0.05	0.10	0.14	0.33		0.00	0.00	0.00	0.00	0.00	0.00	0.00		
		2.0		0.01	0.05	0.10	0.14	0.32				0.00	0.00	0.00	0.00	0.00		
Lowerlakes	Loveday Bay	0.5		0.02	0.05	0.10	0.20	0.30				0.00	0.00	0.00	0.00	0.01		
		1.0	0.00	0.02	0.05	0.10	0.19	0.29		0.00	0.00	0.00	0.00	0.00	0.00	0.01		
		2.0		0.01	0.04	0.09	0.18	0.28				0.00	0.00	0.00	0.00	0.01		
Lowerlakes	Currency Creek	0.5		0.01	0.07	0.15	0.18	0.39				0.00	0.00	0.00	0.00	0.01		
		1.0	0.00	0.01	0.07	0.15	0.18	0.39		0.00	0.00	0.00	0.00	0.00	0.00	0.01		
		2.0		0.01	0.07	0.15	0.19	0.39				0.00	0.00	0.00	0.00	0.01		
Lowerlakes	Clayton inc. Dunns	0.5		0.01	0.04	0.10	0.15	0.34				0.00	0.00	0.00	0.00	0.00		
		1.0	0.00	0.01	0.04	0.10	0.15	0.34		0.00	0.00	0.00	0.00	0.00	0.00	0.00		
		2.0		0.01	0.04	0.10	0.15	0.34				0.00	0.00	0.00	0.00	0.00		
Lowerlakes	Reedy Point	0.5		0.02	0.08	0.17	0.23	0.52				0.00	0.00	0.00	0.00	0.09		
		1.0	0.00	0.02	0.08	0.17	0.23	0.52		0.00	0.00	0.00	0.00	0.00	0.00	0.08		
		2.0		0.02	0.08	0.17	0.22	0.51				0.00	0.00	0.00	0.00	0.00	0.07	
Lowerlakes	Lake Alexandrina	0.5		0.03	0.05	0.08	0.09	0.18				0.00	0.00	0.00	0.00	0.00		
		1.0	0.00	0.01	0.03	0.06	0.07	0.16		0.00	0.00	0.00	0.00	0.00	0.00	0.00		
		2.0		-0.04	-0.02	0.02	0.03	0.12				0.00	0.00	0.00	0.00	0.00		
Lowerlakes	Campbell Park	0.5		0.02	0.08	0.17	0.22	0.49				0.00	0.00	0.00	0.00	0.07		
		1.0	0.00	0.02	0.07	0.17	0.22	0.49		0.00	0.00	0.00	0.00	0.00	0.00	0.07		
		2.0		0.02	0.07	0.17	0.22	0.48				0.00	0.00	0.00	0.00	0.00	0.06	
Lowerlakes	Lake Albert	0.5		0.02	0.07	0.16	0.19	0.42				0.00	0.00	0.00	0.00	0.01		
		1.0	0.00	0.02	0.07	0.16	0.19	0.42		0.00	0.00	0.00	0.00	0.00	0.00	0.01		
		2.0		0.02	0.07	0.15	0.19	0.42				0.00	0.00	0.00	0.00	0.01		

Table C3: Region summary values for DP increase (left) and HAB risk (right), organised from north to south.

Domain	Analysis region	Flow	delDP (mg/L)						HAB risk (-)							
			Biomass Factor						Biomass							
			0	0.1	0.4	0.8	1	2	5	0	0.1	0.4	0.8	1	2	5
Moonie	Upper_1	0.5		0.00	0.01	0.01	0.01	0.03	0.08		-0.01	0.02	0.04	0.04	0.09	0.18
		1.0	0.00	0.00	0.01	0.01	0.01	0.03	0.08	0.00	-0.01	0.02	0.04	0.04	0.09	0.18
		2.0		0.00	0.01	0.01	0.01	0.03	0.08		-0.01	0.02	0.04	0.04	0.09	0.18
	Upper_2	0.5		0.00	0.00	0.00	0.00	0.00	0.00		0.00	0.00	0.01	0.02	0.01	0.03
		1.0	0.00	0.00	0.00	0.00	0.00	0.00	0.00	0.00	0.00	0.00	0.01	0.02	0.01	0.03
		2.0		0.00	0.00	0.00	0.00	0.00	0.00		0.00	0.00	0.01	0.02	0.01	0.03
	Middle_1	0.5		NaN	NaN	NaN	NaN	NaN	NaN		0.15	0.19	0.26	0.25	0.32	0.36
		1.0	NaN	NaN	NaN	NaN	NaN	NaN	NaN	0.00	0.15	0.19	0.26	0.25	0.32	0.36
		2.0		NaN	NaN	NaN	NaN	NaN	NaN		0.15	0.19	0.26	0.25	0.32	0.36
Lower_2	0.5		0.00	0.00	0.00	0.00	0.00	0.03		0.12	0.12	0.16	0.20	0.21	0.37	
	1.0	0.00	0.00	0.00	0.00	0.00	0.00	0.03	0.00	0.12	0.12	0.16	0.20	0.21	0.37	
	2.0		0.00	0.00	0.00	0.00	0.00	0.03		0.12	0.12	0.16	0.20	0.21	0.37	
Lower_1	0.5		0.00	0.00	0.00	0.00	0.00	0.01		0.00	0.00	0.02	0.03	0.06	0.19	
	1.0	0.00	0.00	0.00	0.00	0.00	0.00	0.01	0.00	0.00	0.00	0.02	0.03	0.06	0.19	
	2.0		0.00	0.00	0.00	0.00	0.00	0.01		0.00	0.00	0.02	0.03	0.06	0.19	
Chowilla	Lock6	0.5		0.00	0.02	0.04	0.02	0.04	0.08		0.03	0.04	0.06	0.06	0.09	0.10
		1.0	0.00	0.00	0.02	0.04	0.02	0.04	0.07	0.00	0.01	0.02	0.04	0.04	0.05	0.04
		2.0		0.00	0.02	0.04	0.02	0.04	0.08		0.00	0.01	0.03	0.03	0.03	0.02
	MR_1	0.5		0.00	0.00	0.00	0.00	0.01	0.01		0.01	0.02	0.03	0.03	0.05	0.07
		1.0	0.00	0.00	0.00	0.00	0.00	0.00	0.01	0.00	0.00	0.01	0.01	0.01	0.02	0.04
		2.0		0.00	0.00	0.00	0.00	0.00	0.00		-0.03	-0.03	-0.03	-0.03	-0.02	-0.01
	CR_1	0.5		0.00	0.00	0.01	0.01	0.02	0.03		0.02	0.04	0.06	0.05	0.10	0.14
		1.0	0.00	0.00	0.00	0.00	0.00	0.01	0.03	0.00	0.00	0.01	0.01	0.01	0.03	0.05
		2.0		0.00	0.00	0.00	0.00	0.01	0.01		-0.01	-0.01	-0.01	-0.01	0.00	0.00
Wetlands_1	0.5		0.00	0.00	0.00	0.00	0.34	0.01		0.00	0.00	0.00	0.00	0.03	0.01	
	1.0	0.00	0.00	0.00	0.00	0.10	0.01	0.01	0.00	0.01	0.01	0.01	0.01	0.03	0.01	
	2.0		0.00	0.00	0.00	0.00	0.21	0.00		-0.01	-0.01	-0.01	-0.01	0.02	-0.01	
Lake_1	0.5		0.02	0.07	0.19	0.21	0.37	1.02		0.06	0.14	0.19	0.20	0.23	0.25	
	1.0	0.00	0.02	0.08	0.17	0.19	0.37	0.98	0.00	0.06	0.14	0.19	0.20	0.23	0.25	
	2.0		0.03	0.08	0.18	0.20	0.38	0.96		0.06	0.14	0.19	0.20	0.23	0.25	
Lake_2	0.5		0.01	0.07	0.12	0.10	0.27	0.70		0.05	0.16	0.21	0.19	0.25	0.28	
	1.0	0.00	0.01	0.07	0.12	0.10	0.27	0.70	0.00	0.05	0.16	0.20	0.19	0.25	0.28	
	2.0		0.01	0.07	0.12	0.10	0.27	0.70		0.05	0.16	0.20	0.19	0.25	0.28	
MR_2	0.5		0.00	0.00	0.00	0.01	0.01	0.02		0.02	0.03	0.05	0.05	0.08	0.12	
	1.0	0.00	0.00	0.00	0.00	0.00	0.01	0.01	0.00	0.01	0.01	0.03	0.03	0.04	0.07	
	2.0		0.00	0.00	0.00	0.00	0.00	0.01		-0.01	0.00	0.00	0.01	0.01	0.03	
MR_3	0.5		0.00	0.00	0.01	0.01	0.01	0.03		0.03	0.10	0.17	0.17	0.28	0.40	
	1.0	0.00	0.00	0.00	0.00	0.00	0.01	0.02	0.00	0.01	0.05	0.09	0.10	0.17	0.27	
	2.0		0.00	0.00	0.00	0.00	0.00	0.01		-0.01	0.01	0.02	0.03	0.06	0.11	
MR_4_WTL	0.5		0.00	0.00	0.01	0.01	0.02	0.05		0.03	0.10	0.17	0.19	0.27	0.37	
	1.0	0.00	0.00	0.00	0.01	0.01	0.01	0.04	0.00	0.01	0.05	0.10	0.11	0.17	0.25	
	2.0		0.00	0.00	0.00	0.00	0.01	0.02		0.00	0.01	0.04	0.04	0.07	0.12	
Lock5_US	0.5		0.00	0.01	0.01	0.01	0.03	0.08		0.00	0.02	0.05	0.05	0.07	0.10	
	1.0	0.00	0.00	0.00	0.01	0.01	0.02	0.06	0.00	0.00	0.02	0.04	0.05	0.07	0.09	
	2.0		0.00	0.00	0.01	0.01	0.01	0.04		-0.01	0.00	0.02	0.02	0.04	0.06	

Chowilla	Lock5_Boundary	0.5		0.00	0.01	0.02	0.02	0.04	0.11		0.02	0.08	0.14	0.16	0.21	0.28	
		1.0	0.00	0.00	0.01	0.01	0.02	0.03	0.09		0.00	0.01	0.05	0.10	0.11	0.15	0.21
		2.0		0.00	0.00	0.01	0.01	0.02	0.05			-0.04	-0.02	0.01	0.02	0.05	0.10
Murray	Wellington	0.5		0.00	0.00	0.01	0.01	0.01	0.03		0.01	0.05	0.09	0.12	0.18	0.26	
		1.0	0.00	0.00	0.00	0.00	0.01	0.01	0.03	0.00	0.01	0.05	0.10	0.13	0.19	0.28	
		2.0		0.00	0.00	0.00	0.00	0.01	0.03			0.04	0.07	0.12	0.15	0.21	0.29
Murray	Swan Reach	0.5		0.00	0.00	0.00	0.00	0.01	0.02		0.06	0.12	0.14	0.16	0.22	0.31	
		1.0	0.00	0.00	0.00	0.01	0.01	0.01	0.05	0.00	0.03	0.09	0.13	0.14	0.23	0.37	
		2.0		0.00	0.00	0.00	0.00	0.01	0.04			-0.04	0.07	0.14	0.17	0.29	0.44
Murray	Mannum	0.5		0.00	0.00	0.01	0.01	0.01	0.04		0.02	0.06	0.12	0.18	0.27	0.42	
		1.0	0.00	0.00	0.00	0.01	0.01	0.01	0.04	0.00	0.01	0.05	0.11	0.14	0.23	0.35	
		2.0		0.00	0.00	0.01	0.01	0.02	0.05			0.03	0.10	0.17	0.21	0.31	0.43
Murray	Walkers Flat	0.5		0.00	0.00	0.01	0.01	0.01	0.04		0.05	0.08	0.11	0.12	0.20	0.27	
		1.0	0.00	0.00	0.00	0.01	0.01	0.02	0.04	0.00	0.02	0.06	0.10	0.12	0.23	0.32	
		2.0		0.00	0.00	0.01	0.01	0.02	0.05			-0.03	0.02	0.09	0.11	0.21	0.32
Murray	Murray Bridge	0.5		0.00	0.00	0.01	0.01	0.02	0.04		0.01	0.06	0.14	0.14	0.23	0.31	
		1.0	0.00	0.00	0.00	0.01	0.01	0.02	0.04	0.00	0.02	0.07	0.15	0.16	0.25	0.34	
		2.0		0.00	0.00	0.01	0.01	0.01	0.04			0.02	0.07	0.16	0.16	0.26	0.38
Murray	Wood Point	0.5		0.00	0.00	0.01	0.01	0.01	0.04		0.02	0.07	0.13	0.15	0.23	0.33	
		1.0	0.00	0.00	0.00	0.01	0.01	0.01	0.03	0.00	0.02	0.07	0.13	0.16	0.23	0.35	
		2.0		0.00	0.00	0.00	0.00	0.01	0.03			0.01	0.06	0.13	0.15	0.23	0.36
Lowerlakes	Boggy Lake	0.5		0.00	0.01	0.02	0.02	0.05			0.09	0.14	0.18	0.20	0.25		
		1.0	0.00	0.00	0.01	0.02	0.02	0.05		0.08	0.09	0.14	0.18	0.20	0.25		
		2.0		0.00	0.01	0.02	0.02	0.05				0.09	0.14	0.18	0.20	0.25	
Lowerlakes	Loveday Bay	0.5		0.00	0.01	0.02	0.03	0.04			0.10	0.13	0.17	0.20	0.23		
		1.0	0.00	0.00	0.01	0.02	0.03	0.04		0.08	0.10	0.13	0.17	0.20	0.23		
		2.0		0.00	0.01	0.02	0.03	0.04				0.10	0.13	0.17	0.21	0.23	
Lowerlakes	Currency Creek	0.5		0.00	0.01	0.02	0.03	0.06			0.10	0.16	0.20	0.21	0.25		
		1.0	0.00	0.00	0.01	0.02	0.03	0.06		0.08	0.10	0.16	0.20	0.21	0.25		
		2.0		0.00	0.01	0.02	0.03	0.05				0.10	0.16	0.20	0.21	0.25	
Lowerlakes	Clayton inc. Dunns	0.5		0.00	0.01	0.02	0.02	0.05			0.10	0.13	0.18	0.21	0.25		
		1.0	0.00	0.00	0.01	0.02	0.02	0.05		0.08	0.10	0.13	0.18	0.21	0.25		
		2.0		0.00	0.01	0.02	0.02	0.05				0.10	0.13	0.18	0.20	0.25	
Lowerlakes	Reedy Point	0.5		0.00	0.01	0.02	0.03	0.06			0.09	0.14	0.18	0.19	0.23		
		1.0	0.00	0.00	0.01	0.02	0.03	0.06		0.08	0.09	0.14	0.18	0.19	0.23		
		2.0		0.00	0.01	0.02	0.03	0.06				0.09	0.14	0.18	0.19	0.23	
Lowerlakes	Lake Alexandrina	0.5		0.00	0.00	0.01	0.01	0.02			0.09	0.12	0.16	0.18	0.23		
		1.0	0.00	0.00	0.00	0.01	0.01	0.02		0.08	0.09	0.12	0.16	0.18	0.23		
		2.0		0.00	0.00	0.01	0.01	0.02				0.09	0.12	0.16	0.18	0.23	
Lowerlakes	Campbell Park	0.5		0.00	0.01	0.02	0.03	0.06			0.10	0.14	0.19	0.20	0.24		
		1.0	0.00	0.00	0.01	0.02	0.03	0.06		0.08	0.10	0.14	0.19	0.20	0.24		
		2.0		0.00	0.01	0.02	0.03	0.06				0.10	0.14	0.19	0.20	0.24	
Lowerlakes	Lake Albert	0.5		0.00	0.01	0.02	0.02	0.05			0.10	0.15	0.20	0.21	0.25		
		1.0	0.00	0.00	0.01	0.02	0.02	0.05		0.08	0.10	0.15	0.20	0.21	0.25		
		2.0		0.00	0.01	0.02	0.02	0.05				0.10	0.15	0.19	0.21	0.25	